

**MOLECULAR ANALYSIS OF THE DOMAIN WITH NO  
NAME (DWNN)/RBBP6 IN HUMAN CANCERS**

**By**

**Zukile Mbita**

**Student number: 0217846Y**



**FACULTY OF SCIENCE**

**A thesis submitted to the Faculty of Science, School of Anatomical Sciences  
University of the Witwatersrand, in fulfilment of the requirements for the  
degree of Doctor of Philosophy**

**Johannesburg, 2012**

**Supervisor:** Prof. Margot Hosie

**Co-supervisors:** Prof. Zodwa Dlamini and Dr. Jasper Rees

## DECLARATION

I, (Zukile Mbita), declare that this thesis is my own work and where use was made of the work of others it has been duly acknowledged. It is being submitted for the degree of Doctor of Philosophy in the University of the Witwatersrand, Johannesburg. It has not been submitted before for any degree or examination in any other University.



.....  
(Signature of the candidate)

.....24<sup>th</sup>.....Day of.....April.....2012

## PUBLICATIONS

1. Dlamini, Z., Mbita, Z., and Ledwaba, T. (2005) Can targeting apoptosis resolve the cancer saga? *Future Oncology* 1 (3); 351-361.
2. Zukile Mbita, Mervin Meyer, Amanda Skepu, Margot Hosie, Jasper Rees and Zodwa Dlamini (2012) De-regulation of the RBBP6 isoform 3/DWNN in human cancers. *Mol Cell Biochem* 362 (1-2): 249-62.

### Published Proceedings

1. Mbita, Z., and Dlamini, Z. (2006) Molecular analysis of the RBBP6 in hepatocellular carcinoma. 97<sup>th</sup> *AACR Cancer Research* 47: 30.
2. Dlamini, Z., and Mbita, Z. (2007) Increased levels of RBBP6 suggest an involvement in the tumourigenesis of breast cancer. *Centennial AACR Cancer Research* 48: 481.
3. Mbita, Z., and Dlamini, Z. (2007) Expression pattern of the RBBP6 in uterine cervix squamous cell carcinoma. *Centennial AACR Cancer Research* 48: 1110.
4. Mbita, Z and Dlamini, Z. (2005) Elevated levels and cytoplasmic accumulation of RbBP6 in human cancers. 96<sup>th</sup> *AACR Cancer Research* 46: 828.
5. Motadi, L., Dlamini, Z., Mbita, Z., Kanti Bhoola (2005) Involvement of RBBP6 gene and apoptosis in the pathogenesis of lung cancer. 96<sup>th</sup> *AACR Cancer Research* 46: 857.
6. Dlamini, Z., Mbita, Z., Rupnarain, Z., Ledwaba, T., Motadi, L. (2005) RBBP6 gene expression in cancers. 96<sup>th</sup> *AACR Cancer Research* 46: 1289.

## ABSTRACT

Retinoblastoma binding protein 6 (RBBP6) is a nuclear protein, previously implicated in the regulation of cell cycle and apoptosis. It is a multi-domain protein containing a Zinc finger, a RING finger, an Rb binding domain, a p53 binding domain and a novel N-terminal protein domain, the so called, Domain With No Name or DWNN. The *RBBP6* gene encodes three isoforms of this particular protein. A common feature of all three isoforms of RBBP6 is the presence of the N-terminal DWNN domain. RBBP6 isoform 3 is comprised of the DWNN domain only. The DWNN itself has a ubiquitin-like fold, sharing 22% similarity with ubiquitin. It is likely that DWNN regulates intracellular levels of the two tumour suppressors, Rb and p53 through the ubiquitin-proteasome pathway and as such, DWNN may therefore play a role in the deregulation of cell cycle control in cancer cells. A mouse homologue, P2P-R of the gene has been implicated in mitotic apoptosis.

The expression of DWNN, RBBP6 and their roles in the cell cycle, apoptosis and human cancer were investigated. RT-PCR and real-time PCR were used to determine the gene expression of DWNN and RBBP6 variants in human cancer cells. An anti-human DWNN antibody was characterized using both Western Blotting analysis and MALDI-TOF mass spectroscopy to determine whether the antibody specifically recognizes DWNN and RBBP6 isoforms, or if it recognizes other proteins. Western blotting was also used to determine the nature of the DWNN in human cell lines. A DWNN probe and the characterized anti-human antibody were used to localize DWNN and RBBP6 gene products at the mRNA and protein levels using ISH/FISH and Immunohistochemistry respectively. Cell

labelling was also performed using this antibody to localize RBBP6 products in human cell lines. RNA interference and over-expression of DWNN and RBBP6 gene products was carried out to further investigate the role of RBBP6 products in the cell cycle, apoptosis and carcinogenesis.

Cloned RT-PCR products of RBBP6 binding domains, the RING finger domain, pRb-binding and p53-binding domains in human cancers cell lines (Hek 293T, MCF7, HeLa and HepG2 cells) showed no mutations, but MCF-7 cells showed the lowest expression of the RBBP6. Real-time PCR and Western blotting analysis confirmed that MCF-7 cells express very little DWNN (RBBP6 isoform 3) and RBBP6 gene products when compared to Hek 293T, HeLa and HepG2 cells. It was also shown that the anti-human DWNN antibody recognizes the DWNN domain (RBBP6 isoform 3) and the larger RBBP6 isoforms. Using 2D gel electrophoresis and MALDI-TOF spectrometry, it was also found that DWNN is associated with other proteins namely, Recoverin and a hypothetical protein XP\_002342450. This result suggested that DWNN may be a ubiquitin-like protein, which may be specific to these proteins in human cells. FISH and IHC demonstrated that the DWNN domain and its relatives are down-regulated in human cancers at both mRNA and protein levels, respectively. In contrast, however, cell staining showed that the expression of the DWNN gene products was high during the G2/Mitosis transition. Knocking-down the DWNN domain or over-expressing it did not sensitise the Hek 293T cells to Camptothecin (CPT)-induced apoptosis but rather slowed down cell growth.

These results strongly suggest that the *DWNN* gene is likely to be involved in cell cycle control. Up-regulation in mitotic cells and down-regulation in cancers also implies that RBBP6 gene products may additionally be involved in cell cycle arrest. Moreover, down-regulation in human cancers particularly indicates that the loss of its function which correlates with loss of cell cycle control in this disease may be involved in the pathogenesis of cancer. This was confirmed by up-regulation of the *DWNN* in arsenic trioxide induced cell cycle arrested cells specifically at G2/M phase where a p53-dependent cell cycle arrest ensued. It is thus proposed that the *DWNN* may be implicated both as a p53 stabilizer and additionally as a G2/M progression regulator.

## **DEDICATION**

This work is dedicated to all the orphans and families of those who succumbed to cancer. It is also dedicated to my family who supported me through smooth and rough times during the duration of my studies.

## ACKNOWLEDGEMENTS

- ❖ My greatest gratitude goes to Dr. Meyer (UWC) for all his help, with antibody characterization and apoptosis inductions. His help is appreciated, thank you!
- ❖ I declare my greatest appreciation to Dr. Clem Penny for the help he provided when this thesis was prepared.
- ❖ I would like to thank my supervisors, Prof. Margot Hosie, Prof. Zodwa Dlamini and Prof. Jasper Rees (UWC) for all their help.
- ❖ My appreciation goes to the Proteomics Laboratory (UWC) under the guidance of Prof. Bongani Ndimba for their help with the 2D work. I want to send my appreciation to Dr. Sharath and Mr. Lizex Hasselman for their help with the MALDI-TOF Spectrometry.
- ❖ I would like to thank Mr. Faghri February (UWC) with his help with RNA interference.
- ❖ Mr. Andrew Faro (UWC) for his help with recombinant protein expression and pull-downs assays.
- ❖ I would also like to acknowledge the late, Dr. Stonath Kanyenda (UWC) for his help with cell culture and FACS.
- ❖ I would also like to take this opportunity to express my sincere gratitude to Dr. Amanda Skepu for her undivided general help.
- ❖ My silly colleagues who made my stay at the University of the Witwatersrand full of fun.
- ❖ I would like to thank everyone at the Biochemistry laboratory (UWC).
- ❖ My sincere gratitude goes to The National Research Foundation (NRF), The Council for Scientific and Industrial Research (CSIR), The Medical Research Council of South Africa, The Department of Labour for the funding and the Wits financial Aid.
- ❖ The last but foremost important, my family and my better half (Nomso Charmaine Hintsho) who stood by me in times of hardness and sadness.

## TABLE OF CONTENTS

<b>DECLARATION</b> .....	<b>I</b>
<b>PUBLICATIONS</b> .....	<b>II</b>
<b>ABSTRACT</b> .....	<b>III</b>
<b>DEDICATION</b> .....	<b>VI</b>
<b>ACKNOWLEDGEMENTS</b> .....	<b>VII</b>
<b>TABLE OF CONTENTS</b> .....	<b>VIII</b>
<b>LIST OF TABLES</b> .....	<b>XV</b>
<b>LIST OF FIGURES</b> .....	<b>XVI</b>
<b>ABBREVIATIONS</b> .....	<b>XVIII</b>
<b>CHAPTER ONE: INTRODUCTION</b> .....	<b>1</b>
1. Introduction .....	1
1.1 Genes and carcinogenesis .....	1
1.1.1 Examples of gene regulations in specific cancers.....	2
1.1.1.1 Hepatocellular carcinoma (HCC) .....	2
1.1.1.2 Breast cancer.....	4
1.1.1.3 Cervical carcinoma.....	6
1.1.1.4 Research motivation .....	7
1.2 Hypothesis.....	9
1.3 Broad Objectives.....	9
1.4 Specific Objectives .....	9
1.5 Organisation of the Thesis.....	11
<b>CHAPTER TWO: LITERATURE REVIEW</b> .....	<b>15</b>
2.1. Retinoblastoma binding protein 6 (RBBP6).....	15
2.2 Interaction of RBBP6 with tumour suppressor proteins (pRb and p53) .....	20
2.3 The role of RBBP6 in human cells.....	20
2.4 RBBP6 homologues and their functions .....	21
2.5 Possible role of the RBBP6 in apoptosis.....	21
2.6 Tumour suppressors pRb and p53 .....	22

2.6.1 Retinoblastoma protein (pRb) in cancers .....	25
2.6.2 p53 Family of tumour suppressors .....	26
2.6.2.1 p53 as a tumour suppressor .....	26
2.7 Ubiquitin-proteasome pathway (UPP).....	27
2.7.1 6S Proteasome pathway: Ubiquitin ligases (ULs) .....	28
2.7.2 The role of ubiquitin ligases in the regulation of apoptosis .....	30
2.8 Apoptosis and its pathways.....	34
2.8.1. Apoptosis.....	34
2.8.1.2 Mitochondrion-mediated apoptotic pathway .....	38
2.8.1.3 Caspase-independent apoptotic pathway.....	42
2.8.1.4 The potential of using apoptotic pathways for cancer therapy .....	42
2.8.1.5 Apoptosis: A prospect for cancer therapy .....	43
2.9 Apoptosis Inhibition.....	44
<b>CHAPTER THREE: MATERIALS AND METHODS .....</b>	<b>47</b>
3.1 Introduction .....	47
3.2 Materials.....	47
3.2.1 Ethics Approval .....	47
3.2.2 Sample Materials.....	47
3.2.3 Primers .....	47
3.2.3.1 RBBP6 Iso3 forward and reverse primers .....	48
3.2.3.2 Iso2&1 Real-Time PCR forward and reverse primers.....	48
3.2.3.3 RING finger reverse and forward primers.....	48
3.2.3.4 Rb-binding domain forward and reverse primers.....	49
3.2.3.5 p53-binding domain forward and reverse primers .....	49
3.2.3.6 RNAi colony PCR forward and reverse primers.....	49
3.2.3.7 RNAi Oligos .....	49

3.2.4 Antibodies .....	50
3.2.5 Cloning Vectors .....	50
3.3 Methods.....	51
3.3.1 Cell culture .....	51
3.3.1.1 Preparation of complete cell culture medium .....	51
3.3.1.2 Cell culture.....	51
3.3.1.3 Trypsinization .....	51
3.3.2 RNA extraction .....	52
3.3.2.1 RNA Gel electrophoresis .....	53
3.3.2.2 Preparation of RNA agarose 1% gel .....	53
3.3.2.3 Quantification .....	53
3.3.3 Reverse transcription (RT).....	53
3.3.4 Polymerase Chain Reaction (PCR).....	54
3.3.5 Agarose gel electrophoresis of DNA .....	55
3.3.6 Cloning of PCR products into pGEM-T-Easy vector.....	55
3.3.6.1 DNA Ligation .....	55
3.3.6.2 Preparation of competent cells (Super competent protocol) .....	56
3.3.6.3 Transformation.....	57
3.3.6.4 Screening for positive clones using colony Polymerase Chain Reaction .....	57
3.3.6.5 Mini-preparation Plasmid DNA extraction .....	58
3.3.6.6 Restriction digestion of plasmid DNA .....	58
3.3.7 Sequencing analysis .....	58
3.3.8 Real-time polymerase chain reaction (real-time PCR).....	58
3.3.8.1 Real-time efficiency by hHPRT and DWNN standard amplification .....	58
3.3.8.3 Real-time quantification setup.....	59
3.3.8.4 Real-time PCR thermal conditions .....	59

3.3.9 Immunohistochemistry (IHC) .....	60
3.3.9.1 Colorimetric method.....	60
3.3.9.2 Cell staining: Immunocytochemistry (ICC) .....	61
3.3.10 <i>In situ</i> hybridization (ISH) .....	62
3.3.10.1 DWNN Probe preparation.....	63
3.3.10.2 DIG Labelling of the DWNN probes .....	63
3.3.10.3 Estimation of the concentration of the probes.....	64
3.3.10.4 <i>In situ</i> hybridization (ISH) and Fluorescence <i>ISH</i> (FISH).....	65
3.3.11 Ribonucleic acid interference (RNAi).....	66
3.3.11.1 RNAi vector digestion .....	66
3.3.11.2 Annealing RNAi oligos.....	67
3.3.11.3 RNAi oligos cloning into pEGFP-C1-U6 vector .....	67
3.3.11.4 Transfection of RNAi clones into human cells .....	67
3.3.11.4.1 Introduction.....	67
3.3.11.4.2 Transfection protocol .....	67
3.3.12 Western blot analysis.....	68
3.3.12.1 Total protein extraction.....	68
3.3.12.2 Sodium dodecyl sulphate – polyacrylamide gel electrophoresis (SDS PAGE).....	69
3.3.12.3 Protein quantification using a Bradford assay .....	69
3.3.12.4 Preparation of 12% SDS PAGE.....	69
3.3.12.3 Electroblothing.....	70
3.3.12.4 Probing the blot with antibodies .....	70
3.3.12.5 Detection and exposure.....	70
3.3.12.6 Blot stripping protocol .....	71
3.3.12.7 Two dimensional (2D) gel electrophoresis .....	71
3.3.12.8 Matrix-assisted laser desorption/ionization Time-of-flight (MALDI-TOF) Mass spectrometry (MS) .....	72

3.3.13 Detection of Apoptosis - Rationale.....	73
3.3.13.1 Apoptotic induction .....	74
3.3.13.2 APOPercentage Assay (Flow cytometry Method).....	75
3.3.14 Cell cycle analysis with Propidium iodide (PI) .....	76
3.3.15 MTT [3-(4, 5-dimethylthiazol-2-yl)-2, 5-diphenyltetrazolium bromide] assay.....	76
3.3.16 Statistical analysis .....	77
<b>CHAPTER FOUR: RBBP6 VARIANTS AND ISOFORMS IN HUMAN CELL LINES, CANCEROUS AND NON-CANCEROUS .....</b>	<b>78</b>
4.1 Mutational analysis of RBBP6 binding domains.....	79
4.2 Relative expressions of the RBBP6 transcripts in human cancer cell lines .....	82
4.3 The anti-human DWNN antibody recognizes DWNN proteins and unknown proteins .....	85
4.3 DWNN domain may bind and modify other proteins .....	89
4.3.1 DWNN domain may be endogenously associated with other protein products .....	90
4.3.2 Human cancer cell line 2D proteome establishment .....	93
4.3.3 Confirmation of non-specificity of the GST-contaminated anti-human DWNN antibody.....	94
4.3.4 Anti-DWNN antibody reacts with GST related proteins, DWNN and its related proteins .....	96
4.3.5 Identification of the unknown proteins detected by the anti-human DWNN using Mass Spectrometry .....	100
<b>CHAPTER FIVE: LOCALIZATION AND EXPRESSION OF THE DWNN IN HUMAN CANCERS .....</b>	<b>105</b>
5.1 Introduction .....	105
5.2 The generation and characterization of the labelled DWNN probe and specificity.....	105
5.3 Estimation of the DWNN probe.....	106
5.4 Expression pattern of the DWNN domain containing mRNAs in human cancers .....	106
5.4.1 RBBP6 mRNAs in breast carcinoma.....	109
5.4.2 RBBP6 mRNA in hepatocellular carcinoma (HCC).....	109
5.4.3 RBBP6 mRNAs in cervical carcinoma .....	112
5.4.4 Localization of RBBP6 mRNA in other cancers .....	112
5.4.5 Quantitative analysis of the expression of DWNN in human cancers .....	116

5.5 DWNN-containing proteins in human cancers.....	118
5.5.1 RBBP6 proteins in breast carcinoma .....	119
5.5.2 RBBP6 proteins in hepatocellular carcinoma (HCC).....	120
5.5.3 RBBP6 proteins in cervical carcinoma .....	120
5.5.4 Localization of the RBBP6 proteins in other human cancers .....	121
5.6 RBBP6 proteins in human cancer cell lines .....	126
5.6.1 RBBP6 proteins in CHO cells.....	126
5.6.2 RBBP6 proteins in the HeLa cell line.....	127
5.6.3 DWNN domain-containing proteins in MCF-7 cells .....	127
5.6.4 DWNN domain protein localization in HepG 2 cells.....	127
5.6.5 DWNN domain protein localization in Hek 293T cells .....	128
<b>CHAPTER SIX: THE ROLE OF THE DWNN IN APOPTOSIS AND CELL CYCLE.....</b>	<b>134</b>
6.1 Introduction .....	134
6.2 Functional studies: summary of the methods .....	134
6.3 The knock-down of the RBBP6 gene products .....	135
6.3 The effect of the RBBP6 knock-down in Hek 293T cells .....	138
6.4 Cell cycle analysis of the DWNN domain in human cells .....	142
6.5 Over-expression of the RBBP6 gene products in human cancer cells and related apoptosis .....	144
<b>CHAPTER SEVEN: GENERAL DISCUSSION .....</b>	<b>152</b>
7.1 Introduction .....	152
7.2 DWNN and its RBBP6 family relatives in human cancers .....	154
7.2.1 RBBP6 transcripts.....	154
7.2.2 RBBP6 isoforms .....	154
7.3 DWNN, a novel ubiquitin-like protein (UBL) .....	162
7.3.1 Recoverin.....	162
7.3.2 Immune system components.....	163

7.4 Localization of the DWNN and RBBP6 gene products .....	164
7.5 The role of the RBBP6 proteins in cell cycle and apoptosis.....	166
7.5.1 Arsenic trioxide in phosphorylation and DWNN function .....	167
7.6 Summary of the study.....	169
7.7 Conclusions .....	174
<b>CHAPTER EIGHT: LIST OF REFERENCES .....</b>	<b>177</b>
<b>APPENDICES .....</b>	<b>214</b>
Appendix A: Stock solutions recipes .....	214
Appendix A2: Reagents .....	216
Appendix A3: Equipment.....	217
Appendix B: Ethics clearance certificate .....	218
Appendix C, primer sets 1-6: Different primer sets, sequences, product sizes and pGEM T Easy vector .....	219
Appendix D: A table showing different RBBP6 RNAi oligos, annealing of oligos and RNAi vector .....	221
RNAi oligo designing .....	222
Appendix E: Vector maps 3-5 .....	223
Appendix F: Supporting tables .....	224
Appendix G: RBBP6 quantitative assessment of tissues on arrays .....	229
Appendix H: Method schedules.....	233
Appendix I: hHPRT1 and DWNN standard curve constructed with dilutions made from a Hek 293T cDNA.....	237
Appendix J: The GST-DWNN construct, an antigen for the generation of Anti-human DWNN antibody .....	239
Appendix K: Sequence alignment of RBBP6 domains versus reference sequence (NM006910).....	240
Appendix L1 An amplified DWNN fragment for probe labelling and sequence analysis.....	244
Appendix L2 - Dot plots for the estimation of the labelled probe concentrations .....	245
Appendix M: Summary of the results for the Column Analysis.....	246
Appendix O: Real-time PCR analysis .....	247

## LIST OF TABLES

Table 2.1: Different tumour suppressors and their functions with resultant cancers after loss of function.....	24
Table 2.1: A list of apoptosis Inhibitors that depend on the RING finger domain.....	31
Table 2.2: Table of Bcl-2 family of pro- and anti-apoptotic proteins.....	40
Table 4.1: Identification summary of the protein spots detected by the anti-human DWNN antibody.....	104
Table 7.1: Ubiquitin and ubiquitin-like proteins.....	157
Table 7.2: Ubiquitin-like protein modifiers, substrates and their functions.....	159
Table 1: RBBP6 RNAi oligos.....	221
Table 2: Cloning of the annealed RNAi oligos.....	222
Table 3: Template preparation for reverse transcription.....	224
Table 4: Cocktail of the reverse transcription (RT) mix.....	224
Table 5: Cocktail for Polymerase Chain Reaction.....	225
Table 6: Restriction digestion for <i>EcoR1</i> , <i>Pst I</i> and <i>ApaI</i> .....	225
Table 7: Real-time PCR setup.....	225
Table 8: Typical real-time conditions.....	226
Table 9: Linearization of pGEM-T Easy-DWNN plasmid DNA.....	226
Table 10: PCR mix for DIG labelling.....	226
Table 11: Dilutions for the estimation of the probes.....	227
Table 12: Preparation of the transfection mix.....	227
Table 13: Preparation of protein standards for the Bradford Assay.....	228
Table 14: Sample preparation for a Bradford Assay.....	228
Table 15: Relative expression of DWNN normalized using hHPRT1.....	238
Table 16: Relative expression of RBBP6 normalized using hHPRT1.....	238
Table 17: Relative knockdown of RBBP6 mRNAs normalized to hHPRT1 expression.....	247

## LIST OF FIGURES

Figure 2.1: – The gene structure of the RBBP6.....	16
Figure 1.2 - DWNN domain alignment from different organisms.....	18
Figure 2.2 - UPP pathway.....	29
Figure 2.3 – A network of the Akt, Mdm2 and p53.....	33
Figure 2.4 - Death receptor-mediated apoptotic pathway.....	37
Figure 2.5 - Schematic representation of the mitochondrial-mediated apoptotic pathway.....	41
Figure 2.6 - Apoptosis inhibition pathways.....	46
Figure 4.1 – Amplification of the RBBP6 domains.....	81
Figure 4.2 (A-D) – The expression of the RBBP6 transcripts in human cell lines.....	84
Figure 4.3 – The recognition of multiple proteins by the Anti-GST-DWNN antibody.....	86
Figure 4.4- Reaction of the DWNN polyclonal antibody with GST- and DWNN-related proteins.....	88
Figure 4.5 – A possible protein “DWNNylation”.....	92
Figure 4.6 – Non cancerous human embryonic kidney cell proteome and cancerous cell proteome.....	94
Figure 4.7 - 2D Western blot on Hek 293T and MCF-7 cells.....	95
Figure 4.8 – 2D Detection of the DWNN domain by partially purified anti-human DWNN antibody and GST- related antibodies by anti-GST antibody.....	97
Figure 4.9 - NetPhos 2.0 server prediction phosphorylation sites in the DWNN domain.....	99
Figure 4.10 - Glycosylation prediction using a NetGly 1.0 server in the DWNN domain.....	99
Figure 4.11 – Identification of proteins recognized by the anti-human DWNN antibody.....	102
Figure 4.12 – Mascot protein scores for protein identification.....	103
Figure 5.1 – Micrographs showing localization of the RBBP6 mRNAs in oesophageal carcinoma (Sense and antisense).....	108
Figure 5.2-Localisation of DWNN-containing RBBP6 mRNAs in Breast cancer.....	110
Figure 5.3 - Localisation of DWNN-containing mRNAs in HCC using FISH.....	111
Figure 5.4 - RBBP6 mRNA localization in cervical carcinoma using FISH.....	114
Figure 5.5 – Localization of the DWNN-containing mRNAs (RBBP6 mRNA) in different carcinomas.....	115
Figure 5.6 – Analysis of FISH results for DWNN mRNA using GraphPad PRISM 5.....	117
Figure 5.7 - Micrographs showing localization of the DWNN domain-containing RBBP6 proteins in breast.....	119
Figure 5.8 - Micrographs showing RBBP6 proteins in normal and HCC tissues.....	120
Figure 5.9 - Micrographs showing localization of RBBP6 proteins in cervical carcinoma.....	121
Figure 5.10 A – Localization of DWNN proteins in different carcinomas.....	123

Figure 5.10B - Localization of the DWNN in rectal and colon adenocarcinoma .....	124
Figure 5.10C - Localization of the DWNN proteins in ovarian papillary adenocarcinoma .....	125
Figure 5.11 - Localization of RBBP6 proteins in CHO cells .....	129
Figure - 5.12 - Localization of DWNN-containing proteins in HeLa cells .....	130
Figure 5.13 - Nuclear and cytoplasmic localization of RBBP6 in MCF-7 cells .....	131
Figure 5.14 - Immunostaining of the HepG2 cells with anti-human DWNN .....	132
Figure 5.15 – Micrograph showing localization of the DWNN in Hek 293T cells .....	133
Figure 6.1 – Confirmation of the DWNN and RBBP6 transcripts knockdown by RNAi .....	137
Figure 6.2 – RNAi transfections and efficacy in Hek 293T cells .....	139
Figure 6.3 – Effect of the RBBP6 knock-down in apoptosis .....	141
Figure 6.4 – DWNN involvement in Cell cycle regulation .....	143
Figure 6.5 – RBBP6 isoform 3, a p53 stabilizer .....	144
Figure 6.6 – Over-expression of the DWNN/Isoform 3 and RBBP6 proteins in MCF-7 cells .....	146
Figure 6.7 – The MTT viability assay in DWNN/Isoform 3 and RBBP6 isoform 1 expressing MCF-7 cells .....	147
Figure 6.8 – Apoptosis in the DWNN/Isoform 3 and RBBP6 isoform over-expressing MCF-7 cells .....	150
Figure 6.9 - The induction of the DWNN domain/Isoform 3 expression and Arsenic trioxide-induced apoptosis .....	151
Figure 7.1 – Structural and key amino acid similarities between ubiquitin and DWNN .....	158

## ABBREVIATIONS

<b>AD</b>	- Alzheimer's disease
<b>AIF</b>	- Apoptosis inducing factor
<b>Akt</b>	- Threonine/Serine kinase
<b>ALPS</b>	- Autoimmune lymphoproliferative syndrome
<b>Apaf-1</b>	- Apoptotic protease-activating factor-1
<b>APC</b>	- Antigen presenting cell
<b>APS</b>	- Ammonium persulphate
<b>ATP</b>	- Adenine triphosphate
<b>Bad</b>	- Bcl-X <sub>L</sub> /Bcl-2-associated death protein
<b>BARD1</b>	- BRCA1 associated RING domain 1
<b>Bak</b>	- Bcl-2 homologous antagonist killer
<b>Bax</b>	- Bcl-2-associated x protein
<b>Bcl-2</b>	- B cell leukemia-2
<b>BCRA1/2/3</b>	- Breast Cancer 1/2/3
<b>BH3</b>	- Bcl-2 Homologue 3
<b>BID</b>	- BH3 interacting domain
<b>BIR</b>	-Baculovirus IAP repeat
<b>BLAST</b>	- Basic sequence alignment search tool
<b>BLCAP</b>	- Bladder Cancer Associated protein
<b>bp</b>	- base pair
<b>BSA</b>	- Bovine serum albumin
<b>CAD</b>	- Caspase-3-activated deoxyribonuclease
<b>CARP</b>	- Caspase-8/10 associated RING domain protein
<b>Caspases</b>	- Cysteine aspartic-specific proteases
<b>cDNA</b>	- Complementary deoxyribonucleic acid
<b>cFLIP</b>	- FADD like interleukin –Beta converting enzyme-inhibitor
<b>CHO</b>	- Chinese Hamster Ovary
<b>cIAP</b>	- cellular inhibitor of apoptosis
<b>Dap3</b>	- Death associated protein 3
<b>DAPI</b>	- 4', 6'-Diamino-2-phenylindole

<b>DAXX</b>	- Death-Domain-Associated Protein 6
<b>DCC</b>	- Deleted in Colorectal Cancer
<b>DcR</b>	- Decoy receptor
<b>DD</b>	- Death domain
<b>DED</b>	- Death effector domain
<b>DEPC</b>	- Diethyl pyrocarbonate
<b>DISC</b>	- Death inducing signalling complex
<b>DMEM</b>	- Dulbecco's modified medium
<b>DMSO</b>	- Dimethyl sulfoxide
<b>DNA</b>	- Deoxyribonucleic acid
<b>dNTPs</b>	- Deoxyribonucleotides
<b>DPC4</b>	- Deleted in Pancreatic Cancer, locus 4
<b>DR</b>	- Death receptor
<b>DTT</b>	- Dithiothreitol
<b>DWNN</b>	- Domain with No Name
<b>EDTA</b>	- Ethylene diamine tetra acetic acid
<b>EGFP</b>	- Enhanced Green Fluorescent protein
<b>FACS</b>	- Fluorescence activated cell sorter
<b>FADD</b>	- Fas associated death domain
<b>Fas</b>	- Fibroblast-associated
<b>FasL</b>	- Fas ligand
<b>FBS</b>	- Foetal bovine serum
<b>FCS</b>	- Foetal calf serum
<b>FISH</b>	- Fluorescence <i>In situ</i> hybridization
<b>FITC</b>	- Flourescein isothiocyanate
<b>GAS</b>	- Growth Arrest-specific gene
<b>GPCR</b>	- G-protein coupled receptor
<b>HCC</b>	- Hepatocellular carcinoma
<b>hdm2</b>	- human double minute 2
<b>HER2</b>	- Human Epidermal growth factor Receptor 2
<b>hRF-1</b>	- host range factor 1
<b>IAP</b>	- Inhibitor of apoptosis protein

<b>ICAD</b>	- Inhibitor of caspase-3-activated DNase
<b>ICC</b>	- Immunocytochemistry
<b>IEF</b>	- Isoelectric focusing
<b>IKK</b>	- IκB Kinase complex
<b>IPTG</b>	- Isopropyl β-D-thiogalactopyranoside
<b>IRF-4</b>	- Interferon regulatory factor 4
<b>ISH</b>	- <i>In situ</i> hybridization
<b>IκB</b>	- Inhibitor of Kappa B
<b>Jade-1</b>	- Gene for Apoptosis and Differentiation in Epithelia
<b>JV18</b>	-Synonym for MADR2
<b>Kb</b>	- Kilobase
<b>kDa</b>	- Kilo dalton
<b>MAD</b>	- Mother against Decapentaplegic gene
<b>MADR2</b>	- MAD-regulated gene 2
<b>MALDI-TOF</b>	- Matrix-assisted laser desorption/ionization Time-of-flight
<b>MCS</b>	- Multiple cloning sites
<b>mdm2</b>	- Murine double minute 2
<b>MdmX</b>	-Murine double minute X
<b>MHC</b>	- Major Histocompatibility Complex
<b>ML-IAP</b>	- Melanoma associated IAP
<b>MMAC1</b>	- Mutated in Multiple cancers 1
<b>MOPS</b>	- 4-Morpholine propanesulphonic acid
<b>mRNA</b>	- messenger ribonucleic acid
<b>NF-κB</b>	- Nuclear Factor Kappa B
<b>NIAP</b>	- Neuronal apoptosis inhibitory protein
<b>NIK</b>	- NF- κB inducible kinase
<b>NLS</b>	- Nuclear localization signal
<b>P2P-R</b>	- Proliferation potential protein-related
<b>p53/TP53</b>	- protein 53/tumour protein 53
<b>p53BD</b>	- p53 binding domain
<b>p63 and 73</b>	- protein 63 and 73
<b>PAGE</b>	- polyacrylamide gel electrophoresis

<b>PBS</b>	- Phosphate buffer saline
<b>PCR</b>	- Polymerase chain reaction
<b>PI3K</b>	- Phosphatidylinositide 3'-hydroxyl kinase
<b>PKB</b>	- Protein kinase B
<b>PMSF</b>	- phenylmethylsulphonyl fluoride
<b>pRb</b>	- Retinoblastoma protein
<b>PTEN</b>	- Phosphatase and tensin homolog
<b>PTP</b>	- Permeability transition pore
<b>PUM2</b>	- Pumilio homolog 2
<b>PVDF</b>	- polyvinylidene difluoride
<b>RbBD</b>	- Retinoblastoma binding domain
<b>RBBP6</b>	- Retinoblastoma binding protein 6
<b>RbQ-1</b>	- Retinoblastoma-binding Q protein 1
<b>RbQ-3</b>	- Retinoblastoma-binding Q protein 3
<b>RFP</b>	- Red Fluorescent Protein
<b>RING</b>	- Really Interesting New Gene
<b>RIPA</b>	- Radio immunoprecipitation assay buffer
<b>RIP</b>	- Receptor interacting protein
<b>RNA</b>	- Ribonucleic acid
<b>RTK</b>	- receptor tyrosine kinase
<b>SCFA</b>	- Short chain fatty acids
<b>Smac/DIABLO</b>	- Second mitochondria derived activator of caspases
<b>SMAD2</b>	- Similar to MAD family member 2
<b>tBID</b>	- truncated BID
<b>TEMED</b>	- <i>N, N, N', N'</i> - Tetramethylethylenediamine
<b>TEP1</b>	- Telomerase-associated protein 1
<b>TNF</b>	- Tumour necrosis factor
<b>TNFR1</b>	- TNF receptor 1
<b>TNFRSF1A</b>	- Tumour necrosis factor receptor superfamily member 1A
<b>TRADD</b>	- TNFRSF1A-associated via death domain
<b>TRAF2</b>	- TNF receptor-associated factor 2
<b>TRAIL</b>	- TNF-related apoptosis-inducing ligand

<b>Tfb1&amp;2</b>	- Transformation buffer 1 and 2
<b>UBLs</b>	- Ubiquitin-like proteins
<b>UPP</b>	- Ubiquitin-Proteasome pathway
<b>VHL</b>	- Von-Hippel Lindau protein
<b>XIAP</b>	- X-linked IAP

**"Our greatest glory is not in never falling, but in rising every time we fall".**

## **Chapter one: Introduction**

---

### **1. Introduction**

Deregulation of apoptosis plays an important role in carcinogenesis. Many gene products, some of which are important regulators of apoptosis, are deregulated in cancers through mutations, post-translational modifications and other regulatory mechanisms, including for example promoter methylations (Gan et al., 2011, Kato et al., 2012). The list of genes that are involved in carcinogenesis is growing exponentially and some are tissue specific.

### **1.1 Genes and carcinogenesis**

Transformation of normal cells into cancer cells caused by mutations of the cell's genetic material is referred to as carcinogenesis. These mutations generally disturb the normal balance between cell proliferation and cell death resulting in uncontrolled cell division and tumour formation. Carcinogenesis requires more than one mutation in a number of genes that control cell division, DNA repair and apoptosis (Wickstrom et al., 2010). The gene types most likely to be affected in carcinogenesis include proto-oncogenes, tumour suppressors and key cell cycle regulating genes. Additionally, there are non-mutagenic carcinogens that are believed to encourage cancer initialization by stimulating high rates of cell division, which often results in high error rates with regard to the inherent DNA repair mechanisms. Viral infections may also play a crucial role in carcinogenesis, causing certain types of cancers, for example Human papillomavirus implicated in the development of cervical cancer (Mileo et al., 2009, Yoshida et al., 2008) and also causing a number of gene mutations (Wingo et al., 2009).

Although mutations are known to contribute to carcinogenesis, the cause of a specific cancer is not always known. However, there is a growing list of aetiological factors associated with the carcinogenic process, for example there appears to be a link between red and processed meat consumption and occurrence of cancer of the colon, indicating a complex aetiology (Cross et al., 2008, Sinha et al., 2009). So too is the list of genes implicated in cancer growing. The broad question that is addressed in this study is whether deregulation of the RBBP6 and DWNN is also involved in the process of carcinogenesis. In this regard the mouse homologue of the RBBP6, P2P-R was shown to be specifically expressed in murine oesophageal cancer cells in contrast to adjacent normal cells in mice suggesting a link to cancer (Yoshitake et al., 2004).

### **1.1.1 Examples of gene regulations in specific cancers**

#### **1.1.1.1 Hepatocellular carcinoma (HCC)**

Hepatocellular carcinoma is one of the most common abdominal cancers representing 80-90% of all liver malignancies worldwide. It is the fifth most common cancer and third most common cause of death from cancer globally (El-Serag and Rudolph, 2007, Gadelhak et al., 2009). Liver cancer often arises from metastasis from other organ cancers. Secondary epidemiological factors associated with liver cancer include infection with hepatitis B and C viruses and alcoholism (El-Serag et al., 2009, Invrios et al., 2008, Kumar et al., 2007). Liver cancer generally, is typified by de-regulation of hepatocyte division, often accompanied by de-regulation of apoptosis (Bai et al., 2010, Chang et al., 2010, Peroukides et al., 2010, Weber et al., 2009, Yu et al., 2008), making apoptotic-related genes very important in HCC. p53, known as the genome guardian is often

de-regulated in hepatocellular carcinoma, however in certain types of cancer therapy like chemotherapy and radiation therapy, p53 action is restored and cell cycle arrest and apoptosis are resumed (Song et al., 2009, Teoh et al., 2009, Zhu et al., 2009). In HCC, p53 has been documented to sensitize liver cancer cells to cell cycle arrest and apoptosis in response to heavy ion irradiation (Liu et al., 2008, Liu et al., 2007a).

Examples of agents that result in resumed apoptotic activity in HCC include an anti-tumour metabolite, 20-O-( $\beta$ -D-glucopyranosyl)-20(S)-protopanaxadiol (IH-901), a novel intestinal bacterial metabolite of ginseng protopanaxadiol saponins, which was found to inhibit HCC cells and induce apoptosis of other cells through the mitochondrial pathway (Cho et al., 2009, Lee et al., 2009a, Ming et al., 2007). It was shown that ginseng induces the intrinsic apoptotic pathway by up-regulation and activation of caspase-9 and caspase 3, Bax and p53 (Kumar et al., 2009). Other anticancer agents like *Spirulina platensis* C-phycoerythrin have been reported to induce apoptosis of hepatocellular carcinoma cells and other cells that are otherwise resistant to other anticancer agents (Chen and Wong, 2008b, Chen et al., 2009a, Roy et al., 2007).

Although p53 is not able to halt liver carcinogenesis, it does sensitize hepatocellular cancer cells to apoptosis during chemotherapy, at least with the use of irinotecan, a topoisomerase I inhibitor. Irinotecan activates p53 resulting in more p53-dependent apoptosis in hepatocellular carcinoma cells (Takeba et al., 2007a, Takeba et al., 2007b). There are other genetic factors that could contribute to desensitization of cells to apoptosis. Survivin has been documented to be over-

expressed in HCC and its over-expression may be involved in the inhibition of apoptosis (Duan et al., 2005, Li et al., 2009b, Pellerito et al., 2010, Zhang et al., 2009a).

### **1.1.1.2 Breast cancer**

Breast cancer is the most common cancer seen in women worldwide. It follows lung cancer as the leading cause of death from cancer (Wang et al., 2009c). Here too, the inhibition of apoptosis plays a role. Some types of breast cancer results from aberrations in pathways driving cellular proliferation and from the inhibition of apoptosis, which are both mediated by the phosphatidylinositol 3-kinase (PI3-K) induced activation of protein kinase B (PKB)/Akt (Pearson and Hunter, 2009, Siddiqua et al., 2008, Torbett et al., 2008, Vestey et al., 2005). Another cause of breast cancer arises from gene aberrations that inhibit the tumour suppressors, BRAC 1 and 2. BRAC 1 and 2 are the most researched tumour suppressor proteins in breast cancer, but there are other players like p53 and pRb proteins. Currently there is no literature linking the RBBP6 with breast cancer but P2P-R, a mouse homologue has been implicated in cell cycle regulation and apoptosis, while its interaction partners p53 and pRb have been implicated in breast cancer through their inactivation (Cao et al., 2009b, Elayat et al., 2009, Guo et al., 2007, Hedau et al., 2004, Henriquez-Hernandez et al., 2009, Macaluso et al., 2007).

It has been reported that the de-regulation of p53 and pRb leads to breast cancer due to the loss of cell cycle checkpoints and subsequent suppression of apoptosis (Heminger et al., 2009, Liu et al., 2009b, McGahren-Murray et al., 2006). Besides these tumour suppressors, caspases also play a role important in breast carcinoma

development as seen in the breast cancer cell line, MCF-7. These breast cancer cells were shown to be resistant to irradiation mediated-apoptosis because they do not express caspase-3 (Essmann et al., 2004), which is central to the apoptosis pathway. In an independent study (Cui et al., 2007), caspase-9 and p53 were also shown to play a role in apoptosis induction in breast cancer cells. Re-introduction of caspase-3 in MCF-7 cells enhanced the apoptotic response of these cells to apoptotic stimulus, for example after genistein-treatment (Ferenc et al., 2010, Li et al., 2009c, Yang et al., 2007).

Bcl-2 family members are also important in breast cancer development significantly Bcl2, Mcl-1 and Bcl-X<sub>L</sub>. The Bcl2 family of anti-apoptotic, pro-survival proteins have been reported to be up-regulated in primary breast tumours and breast cancer (Cao et al., 2009a, Valladares et al., 2006) with high expression levels of Bcl-2 resulting in the inhibition of apoptosis (Arakawa et al., 2009, Arun et al., 2003, Liu et al., 2009b). Over-expression of Mcl-1, an anti-apoptotic protein, in breast cancer is correlated with high grade tumours (Ding et al., 2007), normal expression of Mcl-1 can be achieved by the use of chemotherapeutic agents, for example taxol and tetraiodothyroacetic acid (Glinskii et al., 2009, Lu et al., 2009). Additionally herceptin antibody and granzyme B has also been reported to sensitize breast cancer cells to apoptosis by reducing the expression of Mcl-1 (Germain et al., 2008, Henson et al., 2006). Granzyme B was also reported to activate pro-caspase-3 through degradation of Mcl-1; freeing Bim from Mcl-1 sequestration, consequently resulting in “freed” Bim initiating mitochondrial-mediated apoptosis (Germain et al., 2008, Han et al., 2005).

### **1.1.1.3 Cervical carcinoma**

Cervical cancer is rated the second most common malignant tumour globally, and is aetiologically highly linked to the human papillomavirus [HPV] (Pisani et al., 2002, Stamataki et al., 2010). South Africa is reported to have the highest incidence of cervical cancer in the world. It is the most common cancer in Black (31.2%) and Coloured (22.9%) South African women (Denny, 2006, Gaym et al., 2007). The HPV viral genes in squamous cells prevent apoptosis by affecting p53 and pRb cellular functions and consequently lead to cancer of the cervix (Ganzenmueller et al., 2008, Liu et al., 2007b, Nees et al., 2000). It is noted that HPV infection may not be the sole aetiological factor leading to cervical carcinoma since cancer is a multi-aetiological disease.

The most studied tumour suppressor genes, p53 and pRb, are very important in cancer cell growth prevention. The hindered function of p53 and pRb is intrinsic in cervical cancer progression. The restoration of p53 and pRb function restores cell proliferation control and apoptosis induction (Liu et al., 2009a, Masamha and Benbrook, 2009). HPV's involvement in cervical carcinogenesis involves the reduction of p53 and pRb protein levels, which is reversible in SiHa cells. This can be achieved by using antisense RNA to target HPV's E6 and E7 genes, result in the increased expression of p53; accumulation of hypophosphorylated pRb (in SiHa cells) and possibly increased apoptosis of these cells (Morandell et al., 2008, Sima et al., 2007). These studies corroborate other studies, which demonstrated that repression of E6 and E7 proteins causes cellular senescence and apoptosis with a stabilized p53 expression (Bai et al., 2006, De Filippis et al., 2003, Liu et al., 2009a).

It is apparent that cervical carcinoma cells have altered apoptosis regulation accompanied by altered expression of apoptotic-related proteins as well as de-regulation of p53 and pRb tumour suppressor expressions and functions. Bcl-2 and other anti-apoptotic family members are very important in any carcinogenesis and cervical cancer is no exception. Two situations seem to exist in cervical cancer; either Bcl-2 is co-expressed with p53 in HPV positive cancer cases (used as a diagnostic marker for early cancer development) (Bhushan et al., 2009, Singh et al., 2009) or neither p53 nor Bcl-2 are present. This seems surprising as these proteins have opposing functions. An explanation for this situation would be that Bcl-2 both regulates and suppresses the p53-Bax pathway. Additionally, Bcl-2 over-expression not only suppresses apoptosis, but also promotes carcinogenesis in some other unknown way.

#### **1.1.1.4 Research motivation**

It was previously demonstrated that the loss of DWNN expression in Chinese Hamster Ovary (CHO) cells resulted in resistance to staurosporine-induced apoptosis (George, 1995, Pretorius, 2007). DWNN, which is both a standalone domain and associated with RBBP6 gene products, has so far not been implicated in apoptosis. This therefore raises a number of queries/questions, including: is DWNN another example of a gene that is deregulated in human cancers? Is the RBBP6 gene a potential candidate for tumour suppressor for de-regulation or is this gene an oncogene?

Human cancers are characterized by resistance to apoptosis and cell cycle deregulation (Chang et al., 2006, Lu et al., 2009, Poulsen et al., 2010). The

expression of cell cycle- and apoptosis-related gene products is crucial in cancer development and treatment. The relative expression of p53- and pRb-binding RBBP6 in human cancer cell lines has not been examined before. However, while RBBP6 has been detected in HeLa cells using a PACT antibody (Simons et al., 1997) and P2P-R has been over-expressed in MCF-7 cells (Gao and Scott, 2002), the existence of DWNN, the smallest member of the RBBP6 family of proteins has not so far been shown to be a human endogenous protein and further, has not been detected. Although it has also been previously reported that the recombinant DWNN domain has a ubiquitin-like fold (Pugh et al., 2006), its function is still un-elucidated. The research question asked here is; does DWNN tag other proteins in a similar fashion to ubiquitin in the human proteomes, in both cancerous and non-cancerous cells?

The up-regulation of the P2P-R, a murine RBBP6 homologue, in oesophageal carcinoma and a loss of the gene expression in the corresponding normal tissue has been reported (Yoshitake et al., 2004). The expression pattern of this gene suggests that it is involved in cancer, however, the role of RBBP6 in cancer is not understood and this study was aimed at further elucidating the role of this gene in cancer.

It was reported that RBBP6 binds p53 and pRb, two tumour suppressor proteins (Sakai et al., 1995, Simons et al., 1997). These tumour suppressor proteins both regulate the cell cycle. As the DWNN domain in RBBP6 has a ubiquitin-like fold and ubiquitin-like activity, it is queried here whether DWNN regulates p53 and pRb levels through ubiquitination? RBBP6 and DWNN may therefore be targets

of mutagenesis resulting in cancer. Moreover, does DWNN play a role in apoptosis or/and cell cycle regulation in human cancers?

The information currently available strongly suggests that DWNN and RBBP6 and its relatives are involved in protein stabilization, ubiquitination, cell cycle regulation and apoptosis.

## **1.2 Hypothesis**

The expression and regulation of DWNN/RBBP6 is targeted during carcinogenesis in human organs.

## **1.3 Broad objectives**

This research is aimed at determining a consensus of gene expression pattern of the RBBP6 in human cancers at both mRNA and protein levels using ISH/FISH; ICC, RT-PCR and Western blotting, with an emphasis on breast cancer, cervical cancer and liver cancer. It was also of interest to determine the involvement of RBBP6 in cell cycle regulation and apoptosis. The specific objectives were as follows:

## **1.4 Specific objectives**

- To investigate mutational status of RBBP6 using PCR, cloning and sequences in some selected human cancer cell lines, focussing on different coding regions of the gene, predominantly; the RING finger domain of the RBBP6, Retinoblastoma-binding domain and p53-binding domains.
- This study was also targeted at characterizing the anti-human DWNN antibody and testing the specificity of this antibody using one-dimensional, two-

dimensional gel electrophoretic and Western blot techniques to investigate the endogenous expression levels of RBBP6 iso3/DWNN in human cancer cells. MALDI-TOF mass spectrometry was used to confirm the identity of the protein spots obtained from the two-dimensional gel electrophoresis and were detected by the anti-human DWNN antibody. This was done to address the question of DWNN's ubiquitin-like activity.

- Determination of the expression pattern of the gene products at the mRNA level was also investigated. This was performed to determine whether there is RBBP6 expression in human cancer cells, to elucidate its expression status that is whether it is down- or up-regulated in the selected cancers. Since the mouse homologue has been shown to be highly expressed in oesophageal cancer, it was thought that the *RBBP6* gene products could be present in both cancer tissues and cancer cell lines (at the protein level).
- RNA interference was used to target RBBP6 transcripts in order to knockdown the expression of this gene in Hek 293T cells. This technique was used to evaluate the apoptotic response in Hek 293T cells with reduced levels of RBBP6. These knock-down derived cells were then treated with known apoptotic inducers, that is, camptothecin, arsenic trioxide and staurosporine and the extent of apoptosis was evaluated using the APOPercentage staining with the flow cell sorter (FACS). The percentage of apoptotic cells were analyzed using the CELL QUEST Pro software (Beckon Dickson, Biosystems, USA).
- Over-expression of the DWNN domain and RBBP6 was used in human cancer cells (MCF-7 and HepG2) to further investigate the function of the RBBP6 in

cell homeostasis particularly with regard to cell cycle and apoptosis regulation. The cell cycle analysis was done using the propidium iodide method that measures the DNA content and the percentages of cells in different phases of the cell cycle were analyzed using the CELL QUEST Pro software (Beckon Dickson, Biosystems, USA).

## **1.5 Organisation of the thesis**

The thesis is organized into seven chapters including this introductory chapter (**Chapter one**), and they are described as follows:

### **Chapter two**

This chapter covers the literature review addressing important information relevant to the study. This chapter also highlights the knowledge and the gaps that exist in our understanding of the role of RBBP6 and the mechanisms that it may play a role in.

### **Chapter three**

Chapter three covers the materials and methodology used in the study. This chapter is complemented by several appendices. Recipes for the solutions required for the methods are given in Appendix A1 and chemicals and their suppliers are given in Appendix A2. A list of the equipment used is given in Appendix A3. Several other method appendices are associated with this chapter.

### **Chapter four**

Chapter four describes the mutational analysis of the RBBP6 gene products and characterization of a novel anti-human DWNN uncharacterized antibody in human cancers. This anti-human DWNN polyclonal antibody (section 3.2.4) was

the only available reagent for staining and localization of the all RBBP6 gene products.

### **Chapter five**

In this chapter, expression pattern analysis of the DWNN and RBBP6 variants and isoforms was investigated using Fluorescent *in situ* hybridisation (FISH) (section 3.3.10), immunohistochemistry (IHC) and immunocytochemistry (section 3.3.9) to detect the RBBP6 transcripts and isoforms *in situ* respectively. A DWNN RNA probe (section 3.3.10.1-2) and purified DWNN antibodies were used to detect RBBP6 mRNA and protein respectively. The variant 3 (figure 2.1A) fragment of the DWNN cDNA was cloned into pGEM-T Easy vector and sequenced (Inqaba Biotech. Co, South Africa). The antibody that was characterized and purified as reported in chapter four was used in the immunohistochemistry and immunocytochemistry experiments. This chapter is complemented by Appendix G.

### **Chapter six**

In chapters four and five, it was demonstrated that the RBBP6 gene is expressed at both mRNA and protein levels in both human tissues and human cancer cell lines. There was differential expression and localization of the RBBP6 mRNAs and proteins between cancer and normal cells/tissues. The polymerase chain reaction coupled with the sequencing of the RBBP6 RING finger, RBBD and p53BD in chapters three, demonstrated that the full length RBBP6 transcripts and isoforms are expressed, with no evidence of mutations and truncations respectively. Western blotting analysis (chapter three) showed that RBBP6

isoforms 1 and 3 are expressed at very low levels in both non-cancerous and cancerous cells although Hek 293T, a non-cancerous cell line had higher expression levels than the cancerous cell lines (figure 4.4). Localization studies using Fluorescent *In Situ* Hybridization and immunocytochemistry (chapter 5) revealed a differential expression of RBBP6 between normal and cancerous cells. It was found that RBBP6 is down-regulated in cancers, while normal cells showed nuclear localization of RBBP6 mRNA and proteins. When immunolocalized, RBBP6 proteins (chapter five) were found to be up-regulated in mitotic cells, as well as apoptotic cells and this prompted an investigation of RBBP6 in normal cells. RNA knock-down technology was chosen to further elucidate the function of RBBP6 in cell homeostasis and RNA interference (3.3.11) was used to further investigate the role of RBBP6.

It has thus far been established that cancer cells when compared to normal cells, had down-regulated RBBP6 levels and therefore the following questions were addressed: (1) What would be the effect of RBBP6 knock-down in normal human cells (Hek 293T cells)? (2) What would be the effect of RBBP6 iso3 over-expression in human cancer cells that had been shown to have low expression of the RBBP6 isoforms 1 and 2 and 3? (3) Is there is a correlation between the expression of RBBP6, cell cycle and apoptosis induction in human cells?

Briefly, the RNAi oligos (Appendix F) were designed (section 3.3.11.1), annealed (section 3.3.11.3) and cloned into pEGFP-C1-U6 vector (Appendix E3). The colonies were screened by colony-PCR (section 3.3.6.4) using the RNA interference colony PCR primers (section 3.2.3.6) for plasmid containing the

annealed oligos (3.3.11.3). Plasmid DNA containing annealed oligos was purified (section 3.3.6.5) and subjected to sequence analysis (3.3.7). The purified plasmid DNA containing the RNAi annealed oligos (RNAi molecules) were used to transfect (section 3.3.11.5) Hek 293T cells. The effectiveness of gene knockdown was evaluated by PCR (section 3.3.4) and real-time PCR (section 3.3.8). Equal amounts of the cDNAs from the knock-downs and control samples were used. The effect of RBBP6 knock-down on apoptosis was investigated by inducing apoptosis with camptothecin, arsenic trioxide and staurosporine (Frese et al., 2009, Kang and Lee, 2008, Wang et al., 2009e) [section 3.3.13]. The levels of apoptosis were measured using the MTT assay (3.3.15) and the *APOPercentage* FACS technique (section 3.3.13.1). The chapter is complemented with two appendices, I1 and I2.

## **Chapter 7**

This chapter covers the general discussion and conclusion of the study. It also summarizes the core findings and areas that require further attention and investigation.

## **Chapter eight**

Chapter eight gives the list of scientific sources used in this thesis to support the scientific arguments used.

## Chapter Two: Literature review

---

### 2.1. Retinoblastoma binding protein 6 (RBBP6)

In humans, the retinoblastoma binding protein 6 (*RBBP6*) gene, localized on chromosome 16p12.2 codes for the RBBP6 protein products (Gao and Scott, 2002, Gao et al., 2002, Sakai et al., 1995), which bind two tumour suppressor proteins, retinoblastoma protein (pRb) and p53 (Simons et al., 1997, Witte and Scott, 1997). The *RBBP6* gene encodes three protein isoforms, 1, 2 and 3 that are from two mRNA transcripts, a 1.1 kb and 6.1 kb transcript. Isoform 1 is encoded by the 6.1 kb transcript, while alternative splicing of the 6.1 kb transcript results in isoform 2. Isoform 3 encoded by a 1.1 kb transcript is also known as a Domain With No Name (DWNN) (Pugh et al., 2006). The coding region of this gene is composed of 18 exons; isoform 1 is translated from all the 18 exons, while isoform 2 is coded for by 17 exons (exon 16 is absent, due to alternative splicing) and isoform 3 consists of only the first 3 exons (Figure 2.1A). These three exons that encode DWNN are the same first three exons found in transcripts 1 and 2. Consequently, all three RBBP6 isoforms share a common N-terminal domain, DWNN (figure 2.1B).

DWNN was first identified through genetic screening aimed at identifying novel components of the antigen processing and presentation pathway via major histocompatibility class I (MHC class I) molecules (George, 1995). This initial study showed that somatic cell mutants lacking DWNN were resistant to cytotoxic T cell killing (George, 1995). A more recent study demonstrated that mutant Chinese Hamster Ovary (CHO) cells lacking the DWNN protein product were also resistant

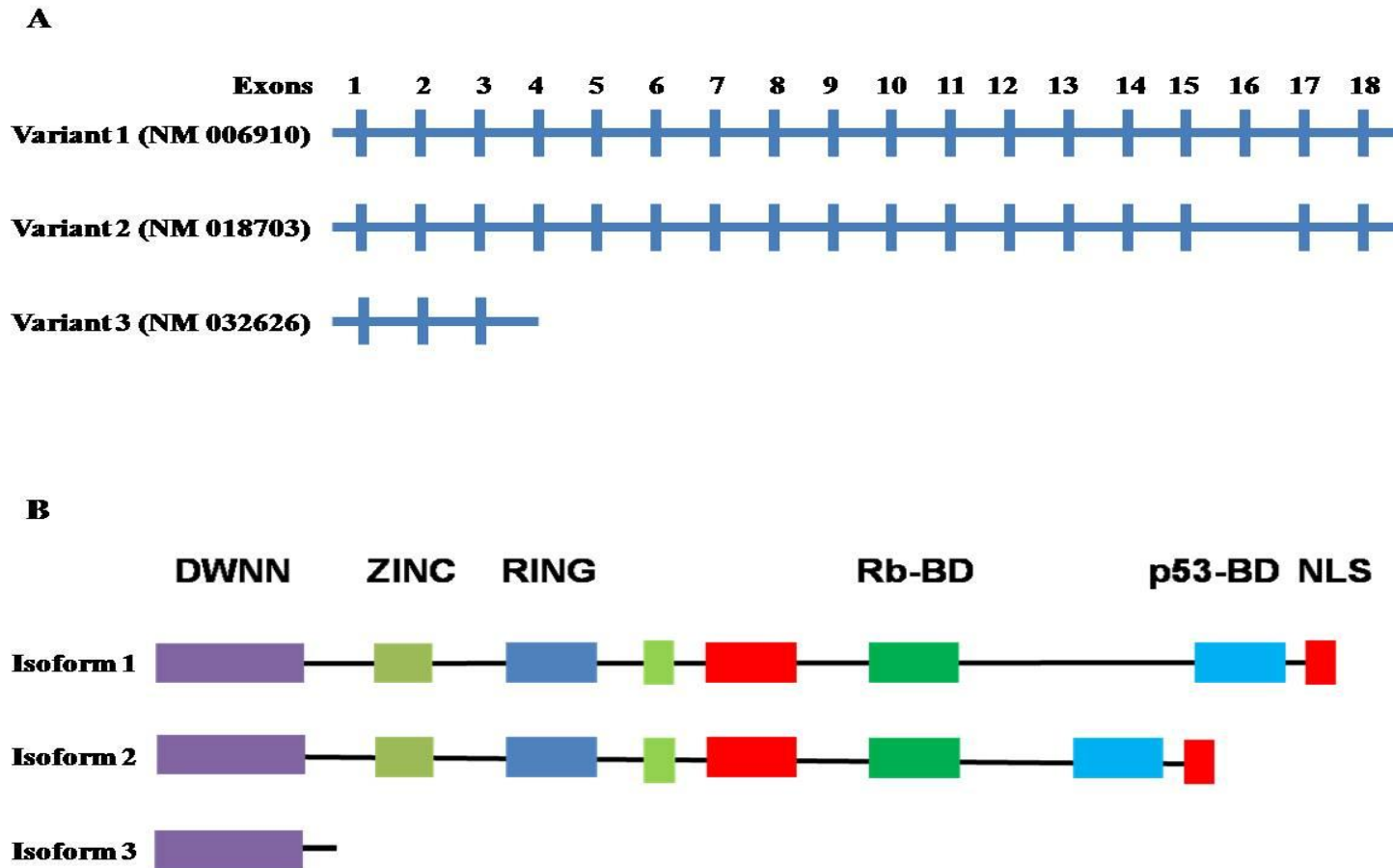


**Figure 2.1: – The gene structure of the RBBP6:** Figure 2.1A shows the differences between the three RBBP6 variants, 1, 2 and 3. Variant 3 is made up of the first 3 exons only (DWNN) while variant 1 has all the 18 exons and variant 2 has 17 exons, where exon 16 is missing. Figure 2.1B shows the domain arrangement of the three isoforms. Adapted from Altschul et al., 1997.

to staurosporine-induced apoptosis (Pretorius, 2007). Together, these studies reflect the importance of the DWNN protein in cell death.

The DWNN domain is a novel ubiquitin-like cell death-related protein, that only makes up RBBP6 isoform 3 (Pugh et al., 2006). RBBP6 isoform 1 and 2 also contain a zinc finger, RING (Really Interesting New Gene) finger, Rb-binding domain, p53-binding domain and Nuclear Localization Signal (NLS) downstream of the DWNN domain (figure 2.1B).

The DWNN domain is highly conserved across different species as shown in figure 2.2 (Pugh et al., 2006). For example, SNAMA is a fly homologue of the human RBBP6 and also contains the DWNN domain (Mather et al., 2005). However, unlike human RBBP6, a *Drosophila* SNAMA has so far been shown to have only a single gene product possessing E3 ubiquitin ligase activity (Antunes, 2009).

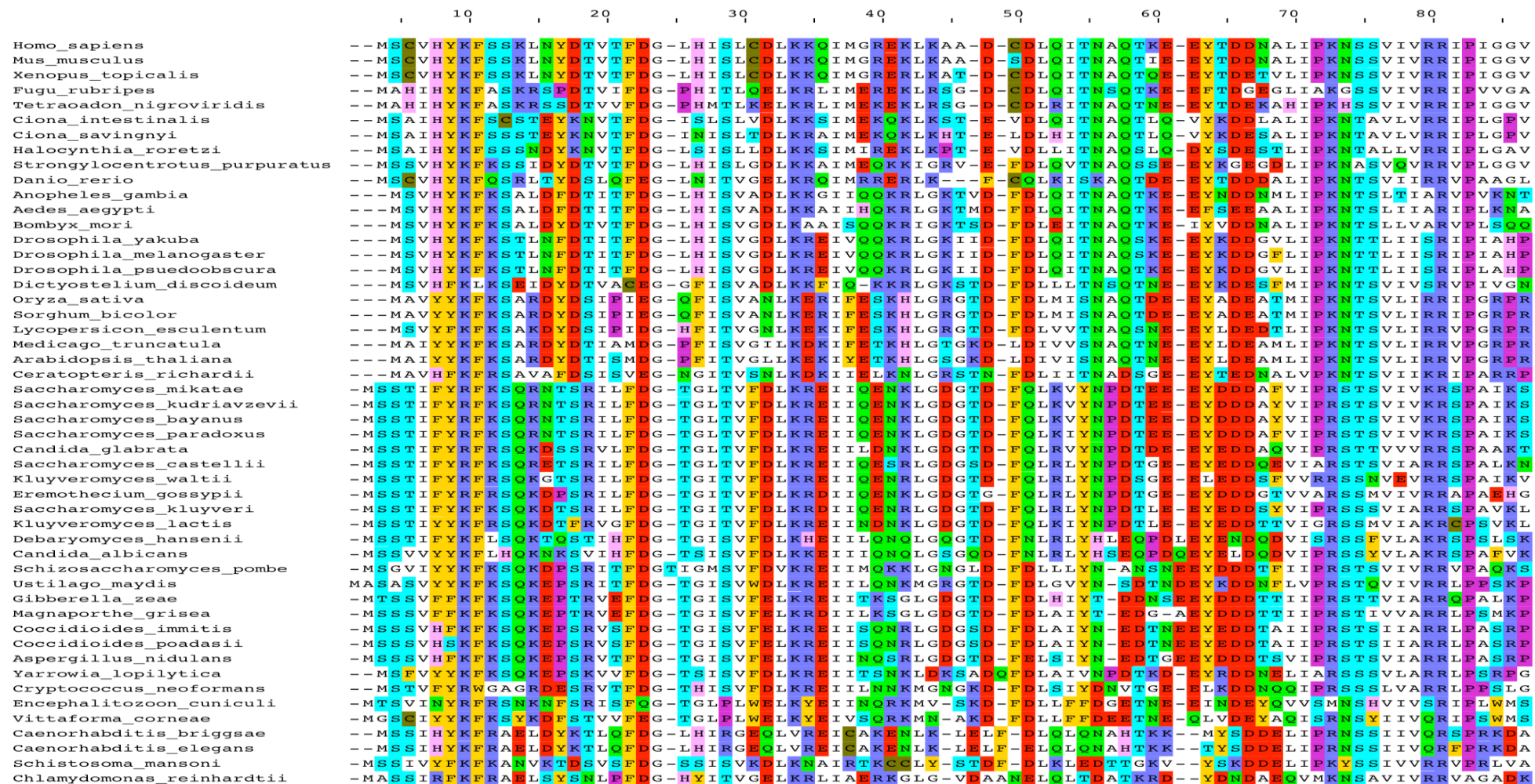


**Figure 7.2 - DWNN domain alignment from different organisms:** This figure shows the conservation of the RBBP6’s DWNN domain in different eukaryotic organisms and notes the high level of conservation seen in this domain (Pugh et al., 2006).

At present not much is known about the function of DWNN. However, RBBP6's DWNN domain has a ubiquitin-like fold and shares 22% similarity with ubiquitin, suggesting a function in regulating protein turn-over in the cell, and additionally, RBBP6 appears to be involved in both cell cycle regulation and camptothecin-induced apoptosis (Gao and Scott, 2003, Gao et al., 2002, Pretorius, 2007). Pretorius (2007) showed that when RNA interference technology was applied to mouse 3T3 cells, targeting RBBP6 transcript 1, the 3T3 cells appeared resistant to camptothecin-induced apoptosis. Equally in the study of Gao and Scott (2003), when P2P-R over-expression was induced, this sensitized the MCF-7 cells to camptothecin-induced apoptosis (Gao and Scott, 2003). Moreover, the presence of the ubiquitin-like fold in RBBP6 suggests a possible role similar to ubiquitin for RBBP6 and it may therefore be involved in ubiquitin ligase-like activities. Indeed, RBBP6 was reported to have ubiquitin ligase-like activity through its RING finger domain by ubiquitinating YB-1 protein, thereby reducing its transactivational ability (Chibi et al., 2008). Since RBBP6 binds to p53 and pRb (Sakai et al., 1995, Simons et al., 1997), it is likely that RBBP6 regulates the levels of these proteins in the cell through the DWNN.

The function of the three RBBP6 isoforms is not fully understood. This work explores some of the functions of this little known gene and its products, specifically isoform 3 and its role in the regulation of cell cycle, apoptosis and carcinogenesis.

## **2.2 Interaction of RBBP6 with tumour suppressor proteins (pRb and p53)**

RBBP6 can interact with both p53 and pRb. This has been documented by several research groups, where they have shown that P2P-R, a mouse homologue of RBBP6 lacking the N-terminal DWNN domain, can bind the two tumour suppressors, p53 and pRb (Sakai et al., 1995, Simons et al., 1997, Witte and Scott, 1997). Since p53 and pRb are known regulators of the cell cycle, it is thought that RBBP6 may be involved in the regulation of the cell cycle through its association with p53 and pRb and may therefore also play a role in regulating carcinogenesis. The role of p53 and pRb in cell cycle control and cancer is well known (Burkhardt et al., 2010, Lee et al., 2009b, Mukherjee et al., 2009, Ramzi et al., 2009, Seoane et al., 2008, Shangary et al., 2008, Zhang et al., 2010b). However, to elucidate the role of RBBP6 in cancer regulation, an understanding of the role of the two tumour suppressors that interact with RBBP6 is needed.

## **2.3 The role of RBBP6 in human cells**

RBBP6 has been reported to localize in the nucleus (Gao and Scott, 2002, Gao et al., 2002, Sakai et al., 1995). As a protein that interacts with two of the most studied and important tumour suppressors, pRb and p53, RBBP6 is hypothesized to play an important role in cell number homeostasis, that is, in cell cycle regulation, influencing/regulating both apoptosis and cell proliferation. In support of this view, Topors, a protein similar to RBBP6, binds p53 (Lin et al., 2005, Weger et al., 2002, Weger et al., 2005, Zhou et al., 1999) and RbQ-3 that interacts with pRb, preferentially when in an under-phosphorylated form (Saijo et al., 1995).

## **2.4 RBBP6 homologues and their functions**

Earlier studies erroneously described RBBP6 as being RbQ-1 (Sakai et al., 1995). RbQ-1 is described as consisting of a Zinc finger domain, Rb-binding domain (RbBD) and p53-binding domain (p53BD). These studies found a mouse homologue of RBBP6, called PACT that binds p53 (Simons et al. 1997). Witte and Scott (1997) reported a murine p53 and pRb interactor, P2P-R and subsequently a yeast homologue of the RBBP6, Mpe-1, was reported to be involved in RNA processing (Vo et al., 2001). No DWNN domain was reported in any of these molecules.

Of all these similar molecules, P2P-R has also been implicated in apoptosis and mitosis (Gao and Scott, 2003, Scott and Gao, 2002, Zhang et al., 2005a). *SNAMA*, a *Drosophila* RBBP6 gene homologue, is abundantly expressed in early embryogenesis where apoptosis is essential but surprisingly has not been demonstrated to interact with either p53 or pRb (Mather et al., 2005). However, *SNAMA* sequences notably do not show close homology to either the RbBD or p53BD. Li et al. (2007) linked murine RBBP6 to apoptosis and cell cycle regulation (Li et al., 2007a), suggesting that this homologue may play a role specifically, in apoptosis during embryonic development, similarly, *SNAMA*.

## **2.5 Possible role of the RBBP6 in apoptosis**

The literature indicates that RBBP6 may have multiple functions in cell homeostasis, including RNA processing (Simons et al., 1997, Vo et al., 2001), cell cycle regulation, apoptosis (Gao and Scott, 2002, Gao and Scott, 2003) and probably ubiquitin ligase activities (Chibi et al., 2008, Pugh et al., 2006). The role of RBBP6 in apoptosis and cancer is of particular interest. The main focus of this

study is aimed at gaining a better understanding the role of the human RBBP6 in apoptosis and cell cycle regulation in human cancer.

RBBP6's involvement in cancer is implied by its known role in oesophageal carcinoma cells where it is up-regulated when compared to normal oesophageal epithelial cells (Yoshitake et al., 2004). To date this is the only report of the involvement of the human RBBP6 in the development of cancers. It is postulated that the up-regulation of RBBP6 in oesophageal cancer is linked to overcoming the cancerous phenotype.

Although there are suggested functions for RBBP6 in mice where P2P-R regulates apoptosis and is possibly a player in regulating mitosis; and in drosophila where the SNAMA gene is thought to regulate apoptosis in early development. The function of the highly conserved DWNN domain in different organisms (figure 2.2) generally remains elusive, and therefore is the focus of this study.

## **2.6 Tumour suppressors pRb and p53**

Tumour suppressors balance the effect of oncogenes, and essentially function to modulate the cell cycle, providing a fine balance between cell proliferation and apoptosis. Oncogenes promote tumour cell proliferation resulting in undesirable conditions as manifested by human cancers. Conversely, tumour suppressors suppress cell growth when conditions are undesirable; for example, when DNA is damaged or when there are insufficient growth factors present, or if the cell division apparatus is faulty (Chatterjee et al., 2010, Coppé et al., 2008, Enari et al., 2006, Yuan et al., 2005).

There are many known tumour suppressor genes encoding proteins that inhibit the growth of potential cancerous cells by effecting cell cycle regulation and apoptosis (Gras et al., 2001, Liggett Jr and Sidransky, 1998, Rusan and Peifer, 2008, Scully, 2000, Tommasi et al., 2008, Toyooka, 1995). It is when tumour suppressors lose their ability to regulate the cell cycle that cancer can develop. Table 2.1 demonstrates the abundance of tumour suppressor genes identified in several different cancers. Of these genes, *Rb* and *p53* are the most studied and are often implicated in cancer progression.

*p53*, *pRb* and *p73* have been shown to be typical Knudson tumour suppressors, defined by a two-hit hypothesis, (while *p63* is not a typical Knudson tumour suppressor). The two-hit hypothesis requires that that both alleles that code for a particular gene must be affected before an effect is manifested (Akers et al., 2009, Meric-Bernstam, 2007, Segditsas et al., 2009).

**Table 2.1: Different tumour suppressors and their functions with resultant cancers after loss of function.**

Name	Function	Resultant cancer from loss of function	Reference
IRF-4	Inhibits cell growth through the cell cycle and apoptosis	B cell lymphoma	(Acquaviva et al., 2008, Hoefnagel et al., 2005)
BRCA3	Possible transcriptional regulation of DNA repair	Breast cancer and colorectal carcinoma	(Bergman et al., 2007, Seitz et al., 1997, Sivarajasingham et al., 2006)
BLCAP	Inhibits growth by inducing apoptosis. Transcription factor that regulates gene expression in BC	Bladder cancer (BC)	(Valleley et al., 2007, Zuo et al., 2006)
DCC	Controls cell growth, cell differentiation and development of metastases	Colorectal carcinoma, renal clear carcinoma	(Dekel et al., 2004, Lui Park et al., 2008)
DPC4	Mediates signalling from GF receptors Suppresses epithelial cell growth	Colorectal tumours Pancreatic Neoplasia	(Koliopanos et al., 2008, Wang et al., 2006a)
MARS2/JV18 (SMAD2)	Also mediates signalling from GF receptors	Colorectal tumours Lung cancer	(Riggins et al., 1996, Uchida, 1996)
BARD1	Involved in G1/S-phase check point, apoptosis after DNA damage	Breast and ovarian cancer	(Sauer and Andrulis, 2005, Shakya et al., 2008, Wu et al., 1996)
Jade-1	Promotes apoptosis	Renal cancer	(Chitalia et al., 2008, Zhou et al., 2005)
VHL	Transcriptional regulation of apoptosis Plays a role in mammalian oxygen-sensing pathway.	Renal clear cell carcinoma	(Kim and Kaelin, 2004, Linehan et al., 2009)
GAS1	Cell cycle regulator. Metastasis and tumour suppressor	Melanoma	(Gobeil et al., 2008, Lee et al., 2001, Sal et al., 1994)

## **2.6.1 Retinoblastoma protein (pRb) in cancers**

Retinoblastoma protein was the first protein to be identified as a tumour suppressor in humans in a study that demonstrated that loss of function of the protein leads to retinoblastoma in children (Friend et al., 1986). Additionally pRb's functional loss has also been implicated in other malignancies such as ovarian cancer (Armes et al., 2005, Li et al., 2007c, Masamha and Benbrook, 2009), head and neck squamous cell carcinoma (Golam Sabbir et al., 2006) and soft-tissue sarcoma (Pereira et al., 2009, Polsky et al., 2006). These findings suggest that pRb loss plays a pivotal role in the progression of a range of different cancers.

### **2.6.1.1 Retinoblastoma protein as a tumour suppressor**

The anti-cancer function of pRb involves the regulation of cell cycle progression through the inhibition of E2F activity. E2F transcription factors are proteins that regulate the cell cycle through repression or progression (Watabe et al., 2010). They are constantly under the control of pRb tumour suppressor, which controls their ability to activate cell cycle progression (Amato et al., 2009, Zhang et al., 2010a). Cell cycle progression or regression depends on levels and the status of the pRb tumour suppressor proteins that are either hyper- or hypophosphorylated. In its inactive state, the pRb proteins are hyperphosphorylated and cells are able to express genes that facilitate the progression from G1 to the S phase transition of the cell cycle. This process is facilitated by the release of E2F factors from pRb inhibition (Adams, 2001, Parisi et al., 2008, Xiao et al., 2003). In its active state, hypophosphorylated, pRb is able to halt cell cycle progression by binding E2F transcription factors rendering them incapable of directing transcription of the genes required for cell cycle progression from the G1 to the S phase (Arakawa et

al., 2008, Hu et al., 2008, Knudsen and Knudsen, 2006, Lin et al., 2009). pRb is thus a key regulator of the cell cycle and also a suppressor of cancer. The relationship between RBBP6 and p53 has not thus far been explored in human cells. Furthermore, it should be noted that genes that interact with p53 are potentially good targets for cancer research and novel cancer therapy.

## **2.6.2 p53 Family of tumour suppressors**

The apoptotic machinery in the cell is partly controlled by the p53 tumour suppressor, which is also involved in cell cycle control, in both the intrinsic and extrinsic apoptotic pathways (Baltaziak et al., 2009, Choi et al., 2010a, Kircelli et al., 2007). p53 was the first protein characterized in the p53 family of proteins that include p63 and p73 (Chatterjee et al., 2010, Sasaki et al., 2009). The other members of the p53 family have different splice variants and have mostly been shown to be involved in developmental and differentiation functions. Although, loss of function has also been indicated in the development of human cancers, for example bladder cancer and thus may also have a protective role against cancer (Guo et al., 2009, He et al., 2008, Urist et al., 2002).

### **2.6.2.1 p53 as a tumour suppressor**

Mutations to, or the silencing of the p53 gene is evident in more than half of human cancers, studied to date (Castedo et al., 2005, Ling et al., 2010a, Petitjean et al., 2007, Yamada et al., 2007). If p53 is silenced or mutated, cancerous cells either tend to evade cell cycle control, or fail to activate p53-dependent cell cycle arrest or apoptosis, resulting in the accumulation of cancer-causing mutations that can contribute ultimately towards tumour formation (Ling et al., 2010a). p53 is an important cellular tumour suppressor and responds mainly to different forms of

cellular stresses; for example, cellular stresses that include DNA damage and hypoxia, where p53 targets and activates genes involved in growth arrest in G0 or G2/M phase, cell cycle progression and cell death (Cheng et al., 2008, Choi et al., 2010a, Hahm and Singh, 2007). p53 suppresses tumour growth by modulating apoptosis and the cell cycle through the regulation of expression levels of its transcription targets (Ko et al., 2005, Ko et al., 2004, Lee et al., 2008, Sinha et al., 2010). p53 induces the expression of pro-apoptotic proteins of the bcl-2 family, resulting in the induction of apoptosis in cells that cannot be repaired (Achanta et al., 2001, Ismail et al., 2007, Ouyang et al., 2009, Woo et al., 2002, Yoda et al., 2008).

The p53 responses to damaged DNA (for example) are carried out by the transcription of various p53 response genes, including p21 and Bax (Schmidt et al., 2008, Steinbach and Weller, 2004). It should be noted that there are many different cellular pathways that regulate the expression and stability of tumour suppressors including the ubiquitin-proteasome pathway, which plays a key role in the life span of both pRb and p53. p53 is a target of 26S proteasomal degradation through E3 ligase-mediated ubiquitination. It has been suggested that p53 may be either protected against ubiquitin-proteasome pathway (UPP) or regulated by RBBP6, since RBBP6 is a potential ubiquitin ligase (Pugh et al., 2006). However, there is little evidence for this concept in the current literature.

## **2.7 Ubiquitin-proteasome pathway (UPP)**

The ubiquitin-proteasome pathway is crucial in controlling the levels of different proteins in order to maintain normal cell function (Girao and Pereira, 2007, Huang et al., 2009, Kaur et al., 2005). De-regulation of this system may result in

degradation of key proteins that maintain cell homeostasis. Imbalances of certain proteins due to the disruption of the UPP has been reported in some cancers, for example, in brain tumours and ovarian cancers (Berlingieri et al., 2006, Jiang et al., 2010b, Jiang et al., 2008, Okamoto et al., 2003), in Parkinson's Disease (Bedford et al., 2008, Ghee et al., 2005, McNaught and Jenner, 2001) and in Alzheimer's disease (AD) (Lopez Salon et al., 2000, Muñoz et al., 2008, Rosen et al., 2010). The E3 Ubiquitin ligases are fundamental elements of the UPP pathway and have been reported to play a role in tumourigenesis (Chitalia et al., 2008, Jin et al., 2009, Neil et al., 2009). The E3 ubiquitin ligases are sometimes over-expressed in cancers leading to the degradation of tumour suppressor proteins (Bromberg et al., 2007, Yen et al., 2006, Zhu et al., 2007). The ubiquitin ligases target a wide range of substrates for degradation, including regulators of the cell cycle, apoptosis and transcription, proto-oncogenes, transcription factors and tumour suppressors (Di Marcotullio et al., 2007, Glickman and Ciechanover, 2002, Munoz et al., 2007, Xu et al., 2007).

### **2.7.1 6S Proteasome pathway: Ubiquitin ligases (ULs)**

The core element of the UPP is the multi-subunit protease complex, 26S proteasome (Sato et al., 2009), which consists of a 20S core complex that is the catalytic region flanked by a 19S regulatory complex (Nickell et al., 2007). In order for the proteasome pathway to operate, enzymatic activities are necessary and E3 ubiquitin ligases are key elements in this process (Kim et al., 2007, Mastrandrea et al., 1999, Uchiki et al., 2009). The UPP (figure 2.3) has two steps involving firstly the conjugation of ubiquitin to the target protein, followed by the degradation of the target protein. The conjugation process makes use of the ubiquitin-activating enzyme (E1) which requires ATP. The activated ubiquitin is

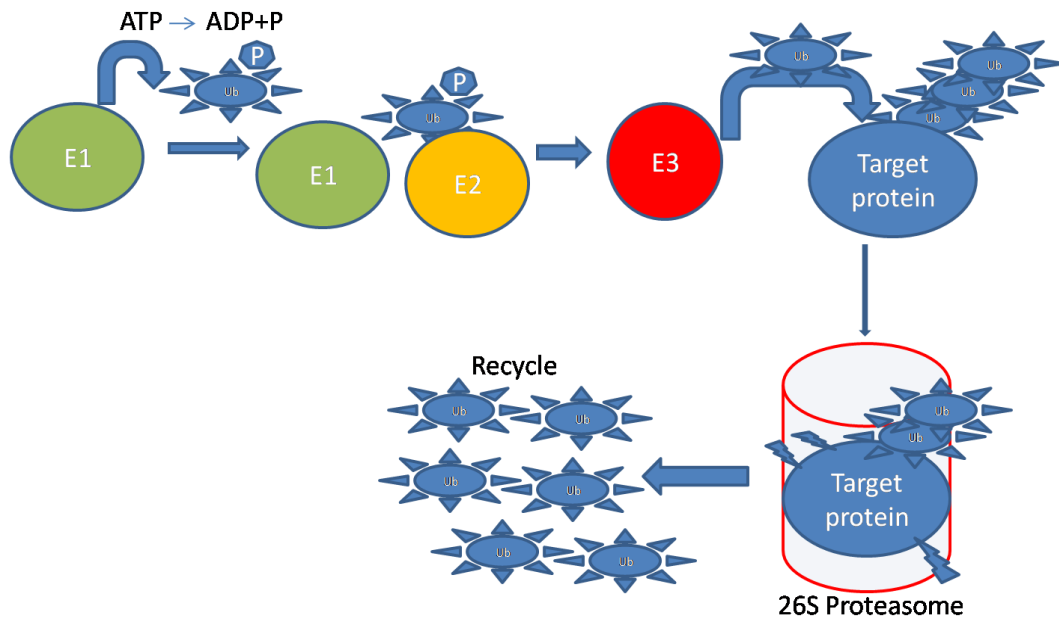


**Figure 2.8 - UPP pathway:** A complete UPP process requires the action of an enzymatic cascade of ubiquitin activating enzyme (E1), a ubiquitin conjugating enzyme (E2) and a ubiquitin ligase (E3). Free ubiquitin is recruited to E1 by thioester bond formation in a ATP-dependent manner. The activated ubiquitin is then transferred to E2 by the formation of a second thioester bond. E2 in conjunction with E3 transfers ubiquitin to a target protein. Several cycles of ubiquitinations lead to the target protein being recognized by 26S proteasome for subsequent degradation with ubiquitin molecules being recycled. Adapted from (Berke and Paulson, 2003, Glickman and Ciechanover, 2002).

then carried to ubiquitin ligase (E3) by a carrier protein (E2) that transfers the ubiquitin to the E3, which is then bound to the target protein. Several cycles of conjugation and ubiquitin transfer result in poly-ubiquitination. The poly-ubiquitin target protein is then recognized by 26S proteasome and the degradation process commences with ubiquitin being recycled (Ivantsiv et al., 2006, Leong et al., 2007, Ryu et al., 2008, Song et al., 2010). Many different cellular protein concentrations are regulated by this mechanism. Aberrations in the regulation of the UPP normally results in the pathogenesis of diseases like cancer (Choi et al., 2010b, Heriberto et al., 2010, Nikseresht et al., 2010, Zhao et al., 2010).

The most important and well documented UPP enzymes to date are the ubiquitin ligases that have been shown to influence cell fate by targeting key proteins for degradation. Ubiquitin ligases possess a RING finger domain that is essential for their function. This RING domain is necessary for the interaction between E2s and E3s (Kim et al., 2007, Uchiki et al., 2009, Van Wijk et al., 2009). Significantly, it has been reported that mutations in this domain abolish this interaction (Balastik et al., 2008, Das et al., 2009, Han et al., 2008, Makishima et al., 2009, Martinez-Noel et al., 2001).

Functionally, ubiquitin ligases can be divided into two major classes. These are homologous to the E6-AP C-terminus (HECT) family of ubiquitin ligases including the HECT-containing proteins; and the RING finger-containing proteins; the most well-known and frequently associated with diseases. The RING finger domains found in these ubiquitin ligases are classified into C3H2C3; C3HC4 and least abundant C2H2C4 (Beitel et al., 2002, Furukawa et al., 2002, Furukawa and Xiong, 2005, Kostic et al., 2006, Stone et al., 2005, Wawrzynow et al., 2009).

### **2.7.2 The role of ubiquitin ligases in the regulation of apoptosis**

Ubiquitin ligases can regulate apoptosis either negatively or positively. Their negative effect in terms of cancer, is exerted by targeting tumour suppressors and cell cycle regulators for degradation, leading to the down-regulation of apoptosis and cell cycle checks (Abe et al., 2008, Privette et al., 2008). The degradation of tumour suppressors (p53 and pRb) by ubiquitin promotes cell survival and cell growth which can lead to tumourigenesis (Min et al., 2010, Min et al., 2009, Zhang et al., 2005b). Their positive effect is exerted by targeting proliferation

signal proteins for degradation thus leading to down-regulated proliferation (Makki et al., 2008). Most ubiquitin ligases exert their effect via their RING finger domain. The number of documented ubiquitin ligases is growing and a new family of ULs has been described and includes Caspase-8/-10 associated RING domain proteins (CARP) (Yang and El-Deiry, 2007). These proteins are also associated with apoptosis inhibition. Table 2.2 shows some of the known inhibitors of apoptosis that depend on their RING finger domains for their ubiquitin ligase activities.

**Table 2.3: A list of apoptosis Inhibitors that depend on the RING finger domain.**

<b>Apoptosis Inhibitor</b>	<b>Presence/Absence of a RING finger domain</b>	<b>Number of RING fingers</b>
<b>Survivin</b>	<b>No</b>	<b>-</b>
<b>XIAP</b>	<b>Yes</b>	<b>1</b>
<b>cIAP1</b>	<b>Yes</b>	<b>1</b>
<b>cIAP2</b>	<b>Yes</b>	<b>1</b>
<b>NIAP</b>	<b>No</b>	<b>-</b>
<b>ML-IAP</b>	<b>Yes</b>	<b>1</b>
<b>Bruce</b>	<b>No</b>	<b>-</b>
<b>ILP2</b>	<b>Yes</b>	<b>1</b>

Mdm2, an E3 Ubiquitin ligase, provides a good example of ubiquitin ligase involvement in cancer progression. Figure 2.4 demonstrates how the PI3K/Akt pathway stabilizes Mdm2 and destabilizes p53 and thus apoptosis. Degradation of tumour suppressor proteins mediated by E3 ligases such as Mdm2, always inhibit apoptosis and promote cell survival leading for example, to hypertrophy in cardiomyocytes (Foo et al., 2007, Toth et al., 2006). In one study, Mdm2 demonstrated protection against cell death of ischemic or endogenous cardiomyocytes, suggesting that this E3 ubiquitin ligase may be involved in cancer development and cancer progression (Abe et al., 2008, Li et al., 2007b, Toth et al., 2006, Zhang and Zhang, 2008). Mdm2 is protected from degradation by the 26S proteasome pathway through the phosphatidylinositide 3'-hydroxyl kinase/protein kinase B (PKB) Akt pathway (Feng et al., 2004, Gama et al., 2009, Shankar et al., 2008) through mdm2 phosphorylation at serine 166 and 188. These phosphorylations protect Mdm2 from self-ubiquitination which results in increased accumulation of Mdm2 and consequently results in an increased p53 degradation and reduced apoptosis (Feng et al., 2004). Recently, however, it has been shown that Mdm2 poly-ubiquitination of p53 is inhibited by ATM (Cheng and Chen, 2010, Cheng et al., 2009). Evidence suggests that Mdm2 also promotes cell cycle progression, whereby Mdm2 antagonists are able to restore normal cell cycle regulation (Ambrosini et al., 2007, Carvajal et al., 2005, Van Maerken et al., 2009). This suggests that mdm2 promotes cancer progression by not only targeting tumour suppressors for degradation and subsequently inhibiting apoptosis, but also by promoting cell proliferation which results in carcinogenesis. Although Mdm2 is one example, there are many other emerging E3 Ubiquitin ligases that regulate tumour suppressors, targeting mainly p53 and pRb.

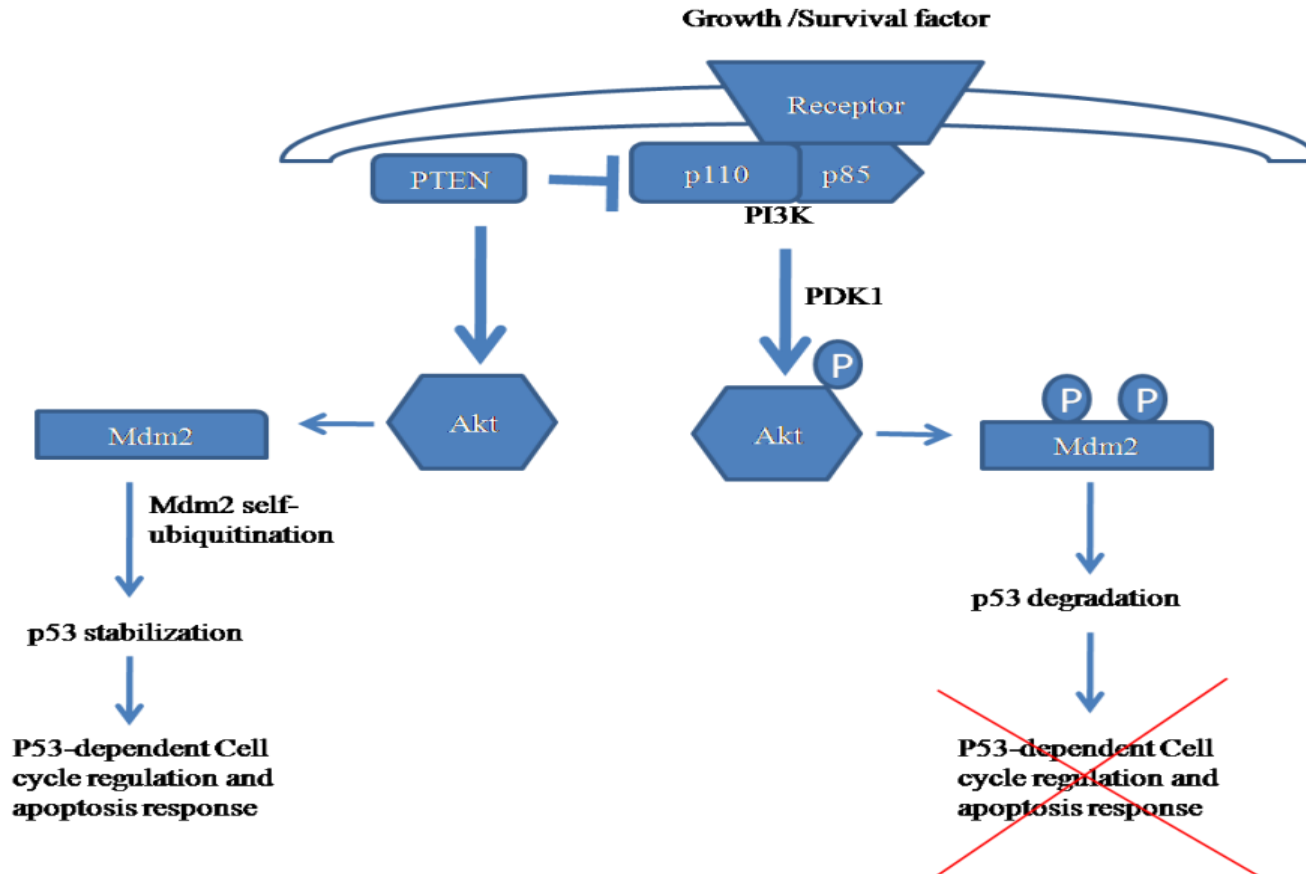


**Figure 2.9 – A network of the Akt, Mdm2 and p53:** This figure shows the survival pathway mediated by phosphatidylinositol 3-kinase (PI3K). PI3K phosphorylates Akt, a process inhibited by PTEN; Akt phosphorylates mdm2, which prevents its self-ubiquitination. The stabilized mdm2 promotes p53 ubiquitination and subsequent degradation that result in the abolition of p53-dependent cell cycle responses and apoptosis. PTEN inhibition of PI3K resulting in mdm2 self-ubiquitination, which restores p53-dependent responses. Adapted from Mayo and Donner, 2002.

These include MdmX (Mancini et al., 2009), which binds pRb and protects it from ubiquitination and its subsequent degradation through the 26S proteasome pathway (Uchida et al., 2006). MdmX is a positive co-factor for p53 degradation and inhibits p53 transcriptional activities (Mancini et al., 2009, Okamoto et al., 2009, Uchida et al., 2006, Zhang et al., 2009b). Another E3 ubiquitin ligase involved in p53 and pRb regulation through degradation is gankyrin. Although its role in p53 and pRb degradation and consequent tumourigenesis (Qiu et al., 2008) is poorly understood, it is however especially prominent in hepatocyte proliferation (Iwai et al., 2003, Shan et al., 2006).

Mdm2 has a similar domain composition to RBBP6, where they both have RING finger domains and pRb and p53 binding domains. The question that arises is whether RBBP6 also regulates cell cycle and apoptosis through p53 and pRb.

## **2.8 Apoptosis and its pathways**

As apoptosis research is a very broad field, this section will focus on apoptosis and the role it plays in cancer development and progression. Apoptosis pathways and their involvement in cancer manifestation and prevention will also be discussed.

### **2.8.1. Apoptosis**

Apoptosis is widely defined as programmed cell death, which is a regulatory mechanism for the deletion of unwanted, aged, damaged or dysfunctional cells (Doonan and Cotter, 2008, Fadeel and Orrenius, 2005, Kerr, 2002, Kerr et al., 1972). In the past this mechanism was seen as simply cell shrinkage. In the 1970's it was defined as a series of predetermined events resulting in what is now defined

as apoptosis. In some diseases, a high or elevated level of apoptosis may result in the development of harmful effects, while in other cases low levels of this process may also be detrimental (Bohsali et al., 2010, Dupont-Versteegden, 2005). Various cell homeostasis mechanisms for example, may detect certain cells to be threatening to the body and employ apoptosis for the destruction of those cells. An imbalance between cell proliferation and cell death may also give rise to cancer (Koster et al., 2010, Mazan-Mamczarz et al., 2008, Oh et al., 2010, Subauste et al., 2009), this being the focus of this section.

A hallmark of cancer cells is their resistance to apoptosis (Fulda, 2009, Peter et al., 1997). Other important features seen in cancer include chromosome abnormalities for example, deletions and/or other alterations (Carén et al., 2008, Debernardi et al., 2004, Weigel et al., 1998). Apoptosis usually plays a very important role in the prevention of cancer progression by targeting these damaged pro-cancerous cells. The manipulation of apoptotic cell death pathways is a prospective therapeutic strategy to treat cancer. Possible ways of achieving this include relieving apoptosis inhibition by apoptosis inhibitors (Arora et al., 2007, Crnkovic-Mertens et al., 2010, Crnkovic-Mertens et al., 2007, Tomicic et al., 2010). Examples of some compounds that are used to activate apoptotic pathways include Camptothecin (Frese et al., 2009, Hsu et al., 2009, Jimenez-Lara et al., 2010, Wang et al., 2009a), staurosporine (Gregory-Bass et al., 2008, Wang et al., 2009e) and arsenic trioxide (Ge-ping et al., 2009, Kang and Lee, 2008, Li et al., 2009a). These compounds are able to induce either the receptor-mediated apoptotic pathway or the mitochondrial-mediated pathway (Antonsson and Persson, 2009, Du et al., 2009, Lunghi et al., 2008, Nakamura-López et al., 2009,

Uo et al., 2009, Wang et al., 2009d). The discovery of new genes that are involved in the apoptotic pathways induced by these compounds can almost certainly improve therapeutic strategies.

### **2.8.1.1 The receptor-mediated pathway**

Signalling of apoptosis by many members of the death receptor subfamily appears to follow common basic rules that are initiated in a sequential manner (Amrán et al., 2007, Cai et al., 2010a, Muppidi et al., 2006) as figure 2.5 demonstrates. Ligand binding initiates the cascades, often followed by receptor trimerization and subsequent formation of the death inducing signalling complex (DISC). When DISC is formed it attracts and is joined by the adaptor molecule, FADD (Fas-associated death domain). The DISC-FADD complex then associates with procaspase-8, with the resultant autocatalytic cleavage of pro-caspase-8 to form an active caspase-8. The active caspase-8 then activates downstream executioner caspases that cleave cellular death substrates, resulting in morphological and biochemical changes that are often observed in apoptotic cells (Liu et al., 2005, Nohara et al., 2007, Sohn et al., 2005), including cell blebbing, cell shrinkage, chromatin condensation, DNA fragmentation and formation of apoptotic bodies. These changes constitute the morphological hallmarks of apoptosis (Chaube et al., 2005, Giri et al., 2006, Reich III and Pisetsky, 2009).

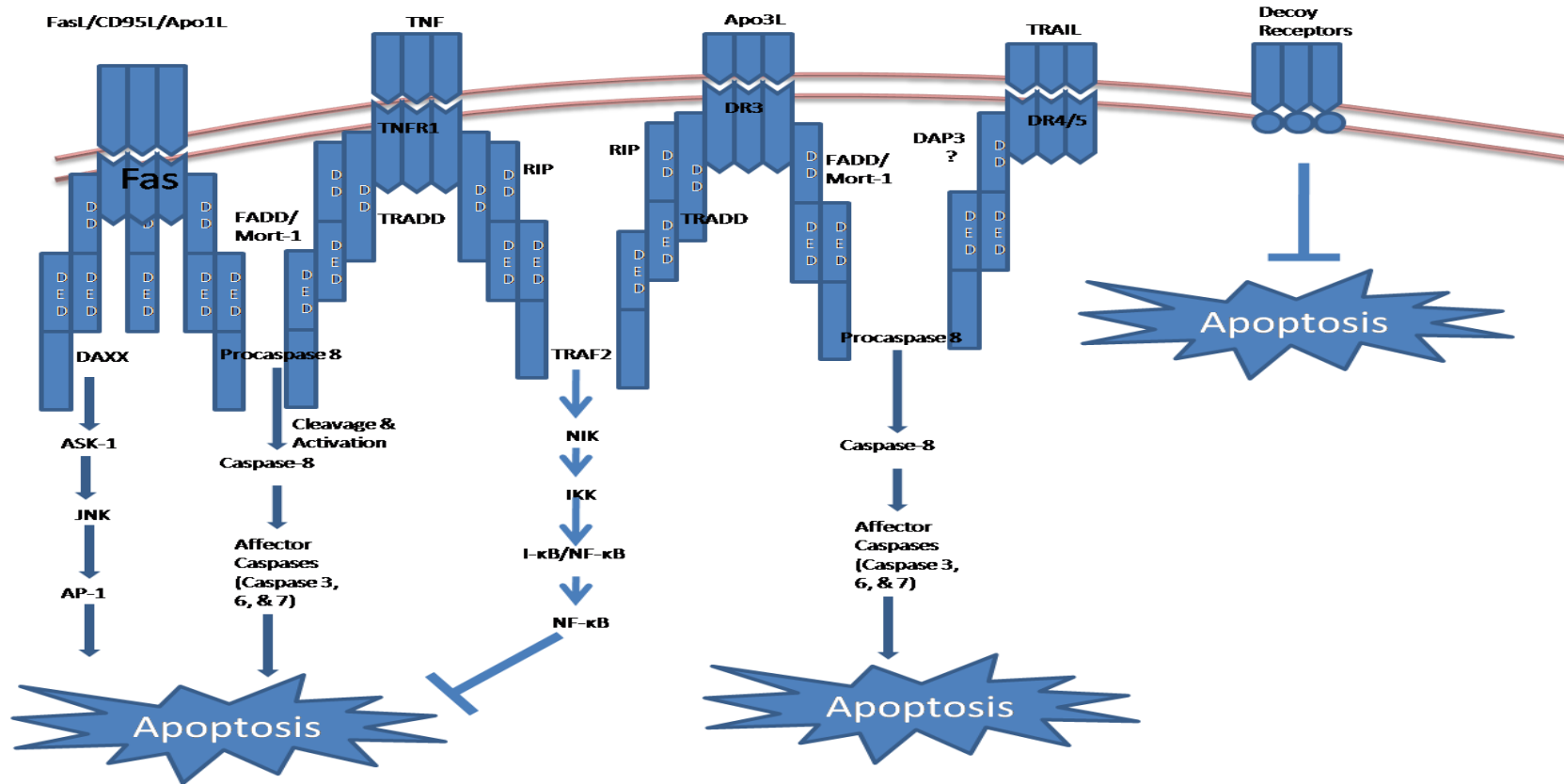


**Figure 2.10 - Death receptor-mediated apoptotic pathway:** This figure shows the death receptor-mediated apoptotic pathway initiated by the binding of different death ligands to their respective death receptors. Upon ligand binding to the death receptor, an interaction between the death domain of the receptor and that of the adaptor protein, that is, Daxx, Fadd, Tradd, Dap3, etc; is formed. This results in information being passed through to the intracellular mechanisms such as caspase activation, leading to apoptosis or signal regulating kinase pathways and that leads to apoptosis inhibition, for example, the NF-κB apoptotic inhibition signalling pathway. Adapted from (Ashkenazi and Dixit, 1998, Ashkenazi and Herbst, 2008).

The death receptors initiate apoptosis by linking, through their cytosolic death domains (DD) to adaptor proteins such as FADD, which in turn bind through their death effector domain (DEDs) to initiator caspases (-8 and -10) that contain DEDs in their N-terminal pro-domains. Death domains seem to be the key for the death receptors to direct cells to the apoptotic pathway. Downstream effector caspases such as caspase-3, -6, and -7 are then activated through their cleavage by activated initiator caspases (Kumar et al., 2008, Kuribayashi et al., 2006). These downstream effector caspases next cleave and activate enzymes that cause morphological and molecular changes observed in apoptotic cells (Kawai *et al.*, 2007). These proteins (which include ICAD and acinus) have been shown to be associated with both biochemical and morphological changes that characterize apoptosis (Joselin et al., 2006, Kovacsovics et al., 2002, Wu et al., 2004). However in some instances they may interact with molecules that have non-apoptotic functions (Chen et al., 2009b). This property is demonstrated by the receptor interacting protein (RIP) [which also has the death domain] that stimulates the pathways that lead to activation of NF- $\kappa$ B and an inhibition of apoptosis (Krieg et al., 2009, Palacios et al., 2010, Thakar et al., 2006, Wang et al., 2007).

### **2.8.1.2 Mitochondrion-mediated apoptotic pathway**

The death receptor-mediated apoptotic pathway is not the sole means of cellular apoptosis, there is also the mitochondrial or intrinsic pathway. The mitochondrion harbours a family of pro-apoptotic proteins that play a very significant role in the demise of the cell. These pro-apoptotic proteins include cytochrome c, Smac (Second mitochondria-derived activator of caspases) and AIF (Apoptosis-

inducing factor) (Brustovetsky et al., 2005, Engel et al., 2010, Li et al., 2010a). AIF is believed to play a pivotal role in caspase-independent apoptosis (Lo et al., 2010, Mahmud et al., 2009, Zhang et al., 2009c). Although the intrinsic pathway also makes use of apoptotic executioner caspases, it is triggered primarily by the release of cytochrome *c*, which in turn is dependent on the Bcl-2 family of pro-apoptotic proteins (Li et al., 2010b, Wu et al., 2010, Yun et al., 2009). This apoptotic pathway is predominant in cases of cellular stresses and in development and its first step is thought to be the translocation of the pro-apoptotic Bcl-2 family members, such as Bax to the mitochondrion (Paschen et al., 2007, Salvesen and Duckett, 2002, Zhang et al., 2007).

Mitochondrial DNA mutations are especially prevalent in human cancers and are associated with mitochondrial dysfunction (Jakupciak et al., 2008, Tseng et al., 2006, Wallace, 2005). Mitochondrial dysfunctions may be linked to deregulation of apoptosis in cancer cells, therefore targeting the mitochondrion for drug development is a step in a logical step towards the treatment of cancer. Indeed some studies have shown that some drugs can induce cytochrome *c* release from the mitochondria in cancer cells, so triggering the intrinsic apoptotic pathway (Kim et al., 2008, Yan et al., 2007).

The release of cytochrome *c* and Smac, both pro-apoptotic molecules, is caused by the induction of the mitochondrial permeability transition, which is associated with the disruption of mitochondrial inner transmembrane potential ( $\Delta\psi_m$ ) and then the disruption of the outer membrane (Li et al., 2008, Pastorino et al., 1998, Tafani et al., 2002). This event is controlled by members of the Bcl-2 family of proteins and is central to initiating the intrinsic pathway where they control the

release of pro-apoptotic molecules in the mitochondria. There are several Bcl-2 family members of pro-apoptotic proteins with their anti-apoptotic counterparts as shown in table 2.3. The pro-apoptotic family members are divided into two sets; the Bcl-2-homologue (BH) 123 multi-domain proteins, for example, Bax and the second set, proteins with the BH3-only domains, for example, Bid. The mitochondrial permeability transition pore (PTP) that results in the release of cytochrome *c*, is regulated by Bax expression (Birbes et al., 2005, Li et al., 2008, Pastorino et al., 1999) and conversely Bcl-2 inhibits the release of cytochrome *c*. Upon cytochrome *c* release, the apoptosome complex is formed by cytochrome *c*, caspase-9 and apaf-1 as shown in figure 2.6. It is the apoptosome that activates effector caspases (Liu et al., 2005).

**Table 2.4: Table of Bcl-2 family of pro- and anti-apoptotic proteins.**

Pro-apoptotic members	Anti-apoptotic members
Bax, Bak, Bnip3, Hrk and BH3 only (Bad, Noxa, Puma, Bid, Bim)	Bcl-2, Bcl-X <sub>L</sub> , Mcl-1, A1, Bcl-W

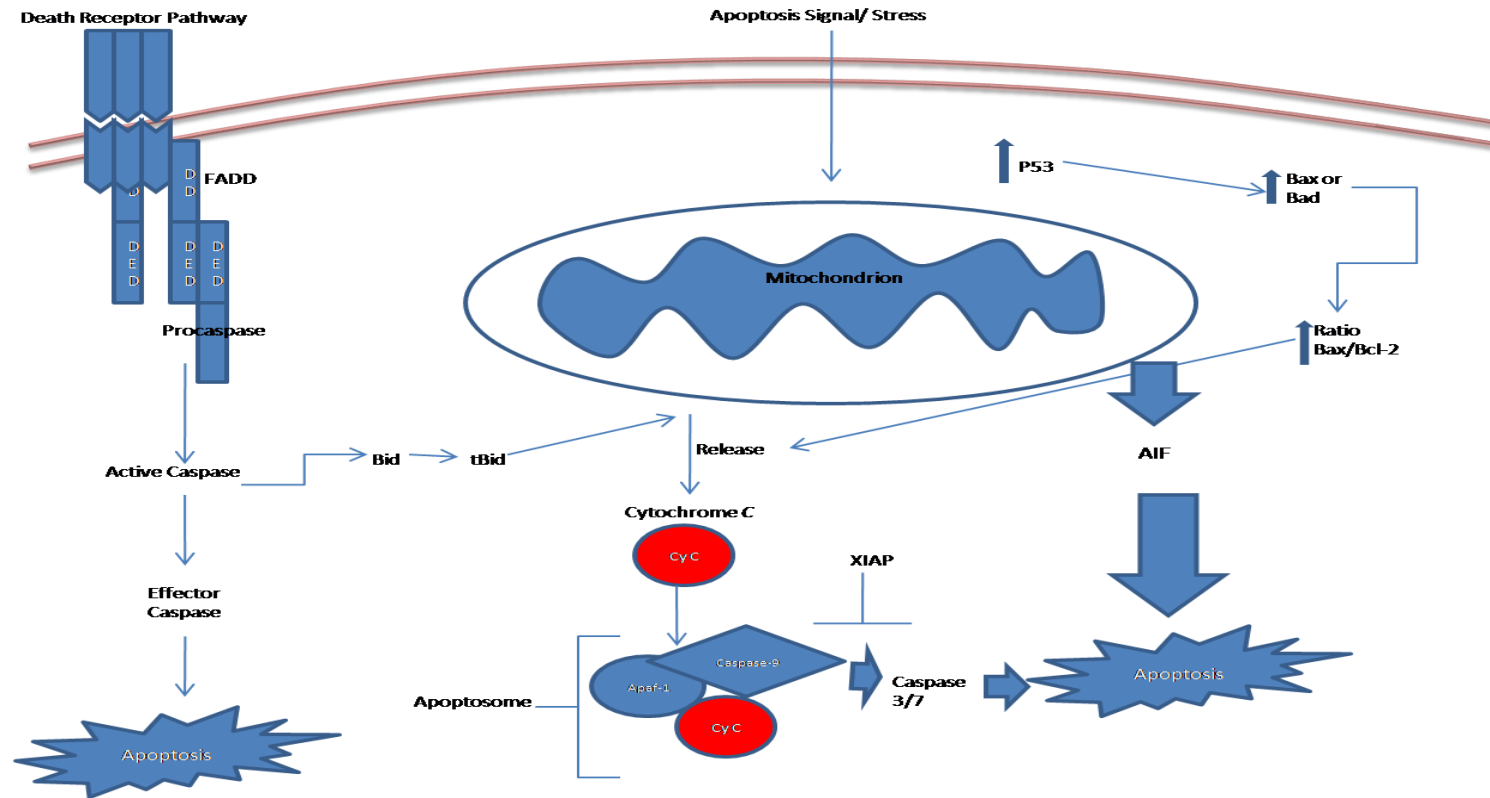


**Figure 2.11 - Schematic representation of the mitochondrial-mediated apoptotic pathway:** Upon apoptotic stimulus, the mitochondrial permeability transition pore is formed, resulting in the release of the cytochrome *c*, Smac/Diablo and apoptosis inducing factor (AIF). AIF induces the caspase independent pathway while cytochrome *c* and Smac are involved in the caspase-dependent apoptosis pathway. The release of these pro-apoptotic molecules is controlled by the Bcl-2 family of pro-apoptotic members. When pro-apoptosis Bcl-2 proteins (Bax and Bad) are expressed in excess of Bcl-2 anti-apoptosis proteins (Bcl-2 and Bcl<sub>XL</sub>), mitochondrial pore formation occurs and cytochrome *c* is released. Receptor-mediated apoptosis can enhance this pathway through Bid cleavage by caspase-8, enhancing the cytochrome *c* release from the mitochondria. This process has been discussed in a review based on targeting apoptosis as a therapeutic strategy. Adapted from (Dlamini *et al.*, 2005).

### **2.8.1.3 Caspase-independent apoptotic pathway**

Caspase-independent cell death through the mitochondrial pathway occurs when an apoptosis inducing factor (AIF) is released to the cytosol and the nucleus. AIF is the main mediator of caspase-independent apoptosis and this mitochondrial flavoprotein is associated with chromatin condensation and DNA fragmentation (Krantic et al., 2007). This apoptosis inducer is synthesized in the cytoplasm and remains in an inactive state until it is imported into the mitochondrial intermembrane space where it is activated. Activation of the AIF is achieved by the removal of an amino terminal mitochondrial targeting sequence, and the attachment of a flavin adenine dinucleotide group (Daugas et al., 2000). Upon apoptosis induction, AIF translocates from the mitochondria back to the cytosol and the nucleus causing chromatin condensation and DNA fragmentation, hallmarks of the caspase-independent apoptosis (Candé et al., 2002). AIF, therefore has the potential to be used as a therapeutic target (Lorenzo and Susin, 2007). It has also been reported that AIF is involved in the induction of apoptosis in many diseases including cancer (Scharstuhl et al., 2009, Vittar et al., 2010), Alzheimer's disease (Landshamer et al., 2008, Polser et al., 2005, Slemmer et al., 2008) and HIV infections (Bellet et al., 2004).

### **2.8.1.4 The potential of using apoptotic pathways for cancer therapy**

The cancer research community is showing an increasing interest in compounds or agents that induce apoptosis through both extrinsic and intrinsic pathways (Chen and Wong, 2008a). Regulation of apoptosis and its own pathway regulators are prominent in the fight against cancer. Understanding cell death pathways that result in apoptosis may contribute to the eradication of diseases, such as cancer where apoptosis is inhibited. There is a growing body of literature describing how

anticancer compounds eliminate tumour cells by inducing the death-receptor mediated pathway (Kang et al., 2006, Raja et al., 2008, Scholz et al., 2005). The mechanism of how this occurs is varied and may be due to the up-regulation of the death receptors themselves or of downstream components of this extrinsic pathway. Chemical or herbal compounds or natural products are known to be able to induce extrinsic apoptosis by modulating protein function (Lo et al., 2010, Wang et al., 2006b, Zaidman et al., 2007).

Any drug that is able to induce any of the apoptotic pathways at an effective point either within the intrinsic or extrinsic pathway, can potentially be used to reverse most cancerous phenotypes (Fetz et al., 2009, Puca et al., 2008).

There is crosstalk between these two main pathways, that is, the induction of one can lead to the activation of the other. This is exemplified by the induction of cytochrome *c* release through the activation of Bid, a pro-apoptotic Bcl-2 family protein. Bid is cleaved by caspase-8 bound to the adaptor protein, FADD, linked to the death receptor. The active Bid then translocates to the mitochondria where it causes the release of cytochrome *c*, which then leads to activation of intrinsic apoptotic cell death (Oh et al., 2004, Tang et al., 2000, Wu et al., 2005). These apoptotic pathways are often inactivated by apoptosis inhibitors. Targeting these apoptosis inhibitors for drug development could potentially be used to reactivate apoptosis in cancer cells (Ashkenazi and Herbst, 2008, Dlamini et al., 2005).

#### **2.8.1.5 Apoptosis: A prospect for cancer therapy**

From the few cancers that have been described above, there is a consistent pattern demonstrating the inhibition of apoptosis and deregulation of cell and tissue

homeostasis in carcinogenesis. There is a growing body of literature implicating apoptosis and different apoptosis-related genes and their products in cancer development. It is hoped that the elucidation of the apoptotic pathways in cancer progression and their inhibition in carcinogenesis may lead to a better understanding of the mechanics of cancer development. Currently, chemotherapy and radiation-mediated cancer therapy involve apoptosis induction in their mode of action against cancer development and progression and p53 is involved in the induction of apoptosis in both these treatments (Han et al., 2009, Holownia et al., 2003). The present study investigated if RBBP6 therapy or DWNN could enhance p53 activity in apoptosis induction and cell cycle regulation.

Any method targeting the reversal of apoptosis inhibition and tumour suppressor proteins inhibition should in principle be able to restore cell cycle control and apoptosis. Down regulation of anti-apoptotic genes have been targeted for apoptosis induction (Cheung et al., 2009, Naderi et al., 2010). All these reports demonstrate that cancer results as a consequence of inhibited apoptosis and improper cell cycle regulation. Most of the bcl-2 family members are transcriptionally regulated by p53. This tumour suppressor is down-regulated in breast cancer (Kuo et al., 2009). This work specifically investigates if the DWNN domain is de-regulated in apoptosis and cell cycle and do these de-regulations contribute to carcinogenesis?

## **2.9 Apoptosis Inhibition**

Inhibition of apoptosis may be as a result of many factors that include tumour suppressor inactivation (Heminger et al., 2009, Lee et al., 2009c, Ling et al., 2010b, Santer et al., 2007, Tsao et al., 2008), oncogene activation (Costa et al.,

2010, Lowe et al., 2010, She et al., 2008), expression of inhibitors of apoptosis for example, survivin, NF- $\kappa$ B activation (Bian et al., 2002, Chow et al., 2010, Kang et al., 2009, Kim et al., 2010) and deregulation of kinase signalling pathways (Matallanas et al., 2007, Oka et al., 2008, Pang et al., 2010, Whittaker et al., 2004). Some proteins are highly expressed in cancers and exert an inhibitory effect on apoptosis. Survivin, a member of the inhibitor of apoptosis protein (IAP) family, is an example of proteins that are involved in the inhibition of apoptosis and manifestation of cancer (Tamm, 1998, Zhou et al., 2010). Other IAPs, that is, cIAP 1 and 2 and XIAP also inhibit apoptosis by exerting their influence through inhibiting caspase activation (Cillessen et al., 2008, Deveraux et al., 1999, Iijima et al., 2009, Sun et al., 2009, Takahashi et al., 1998, Wang et al., 2004). There are also other mechanisms that cancerous cells employ to evade elimination through apoptosis and these include NF- $\kappa$ B and Akt survival pathways shown in figure 2.7. Additionally, the action of IAPs can be reversed by inhibiting these proteins (Carter et al., 2005, Morioka et al., 2009, Wang et al., 2009b, Ziegler et al., 2008)

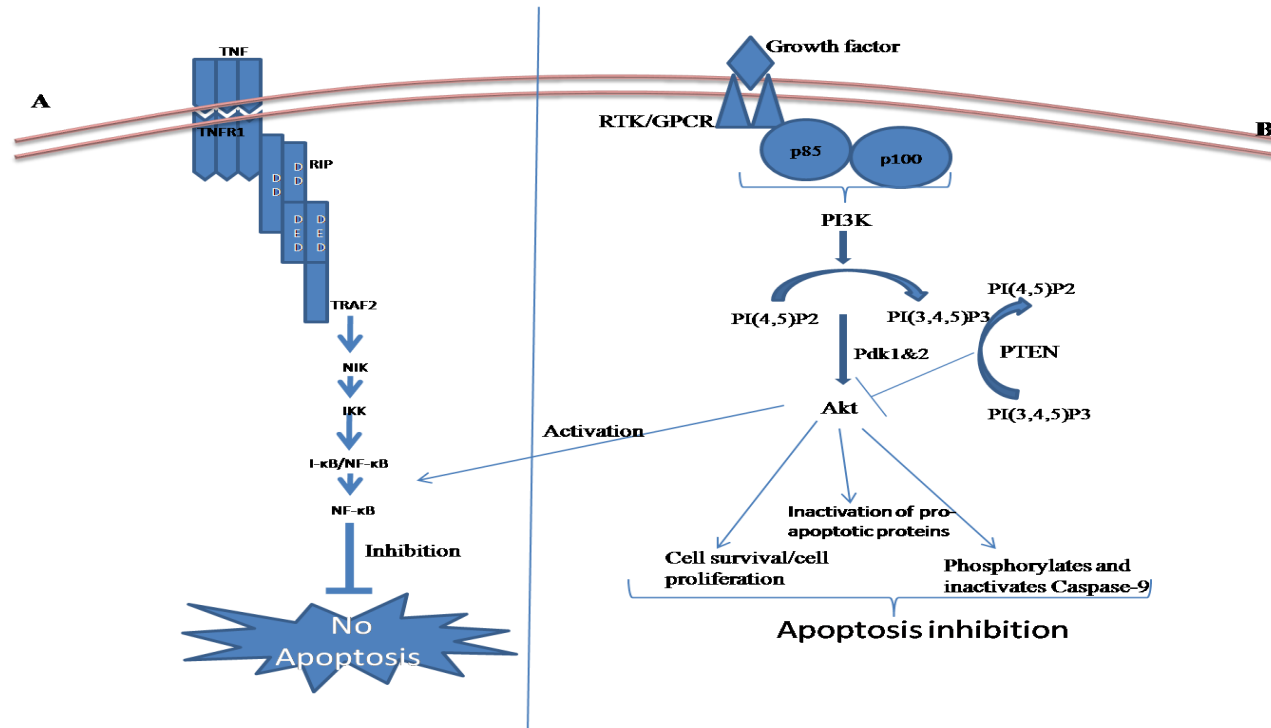


**Figure 2.12 - Apoptosis inhibition pathways:** NF-κB is generally retained in the cytoplasm with IκBs. Signals for example from Akt activity and TNFs, NF-κB are activated with concomitant phosphorylation of IκB and its subsequent degradation through the proteasome pathway. The TNF/TNFR1 complex recruits RIP which attracts TRAF2. This then recruits NF-κB-Inducible Kinase (NIK) that activates the IκB Kinase complex (IKK). IKK complex phosphorylates IκB exposing NF-κB's NLS after its degradation leading to NF-κB translocation to the nucleus where it activates its anti-apoptotic genes resulting in apoptosis inhibition. (B) Upon growth factors binding to their receptor tyrosine kinases (RTK) or G protein-coupled receptor (GPCR), initiating the phosphorylation of phosphatidylinositol 3-kinase (PI3K). This action then causes the conversion of phosphatidylinositol-4,5 biphosphate [PI(4,5)P2] to phosphatidylinositol-3,4,5 tri phosphate [PI(3,4,5)P3]. This product with PDK1&2, [PI (3, 4, 5) P3] phosphorylates Akt thereby activating it. An activated Akt is translocated to the cytoplasm and nucleus and phosphorylate a number of anti-apoptotic proteins, thus inactivating them i.e. Bad, Bax, FasL and Bim. This action is reversed by PTEN, which dephosphorylates [PI (3, 4, 5) P3] to [PI (4, 5) P2] thereby inhibiting the activation of Akt and thus prevents the inhibition of apoptosis. Adapted from (Wullaert et al., 2006).

## **Chapter Three: Materials and methods**

---

### **3.1 Introduction**

Recipes for the solutions required for the methods are given in Appendix A1 and chemicals and their suppliers are given in Appendix A2. A list of the equipment used is given in Appendix A3. Several other method appendices are associated with this chapter.

### **3.2 Materials**

#### **3.2.1 Ethics Approval**

Human Ethics approval was granted for use of the human tissues and arrays, Number R14/49 Mbita (Appendix B).

#### **3.2.2 Sample Materials**

The following cell lines: Hek 293T cell line (human embryonic kidney, transformed cells); HeLa cell line (cervical carcinoma); HepG2 (hepatocellular carcinoma) and MCF-7 (Breast cancer) were used in this study; for RNA extraction, RNA interference, over-expression experiments and to localize the DWNN/RBBP6 proteins. All the cell lines were originally sourced from ATCC and donated by Prof Rees' laboratory from the University of the Western Cape.

#### **3.2.3 Primers**

In this section, primers used in the analysis of the RBBP6 will be described so that in subsequent sections each primer set is just referred by its short name without describing what the primer should amplify. Appendix C (primer sets 1-7) summarizes the primer sequences and their product sizes in base pairs (bp). The primers were either designed manually or using the online Primer3plus software

([www.bioinformatics.nl/cgi-bin/primer3plus/primer3plus.cgi](http://www.bioinformatics.nl/cgi-bin/primer3plus/primer3plus.cgi)) and synthesized at Inqaba Biotech., South Africa.

### **3.2.3.1 RBBP6 Iso3 forward and reverse primers**

This set of primers (Appendix C, primer set 1) was designed to amplify a fragment of the translated region from the DWNN domain of the isoform 3 of the RBBP6. The fragment that these primers amplify is found in all three isoforms; therefore this primer set was used to amplify all the RBBP6 fragments from the three transcripts of this gene; for amplifying the fragment used for making probes for *in situ* hybridization; and for real-time quantitative PCR, to monitor the expression of all three RBBP6 transcripts. This set of primers was designed using the online Primer3Plus software and synthesized at Inqaba Biotech., South Africa.

### **3.2.3.2 Iso2&1 Real-Time PCR forward and reverse primers**

These primers (Appendix C, primer set 2) specifically amplify fragments in both variants 1 and 2 of the RBBP6 gene but not variant 3. They were used to differentiate RBBP6 variants 1 and 2 expressions from variant 3 expression. This primer set was designed using Primer3 software and synthesized at Inqaba Biotech., South Africa.

### **3.2.3.3 RING finger reverse and forward primers**

This primer set (Appendix C, primer set 3) was used to amplify the RING finger domain of the RBBP6 for cloning into pGEM T-Easy vector (see section 3.2.5, Appendix C, vector map 1) for sequencing and subsequently for mutational analysis. This primer set was designed manually and synthesized at Inqaba Biotech., South Africa.

#### **3.2.3.4 Rb-binding domain forward and reverse primers**

This primer set (Appendix C, primer set 4) was used to amplify the RbBD of the RBBP6 for cloning into pGEM T-Easy vector (see section 3.2.5, Appendix C, vector map 1) for sequencing and subsequently for mutational analysis. This primer set designed manually was synthesized at Inqaba Biotech., South Africa.

#### **3.2.3.5 p53-binding domain forward and reverse primers**

This set of primer (Appendix C, primer set 5) was used to amplify the p53BD of the RBBP6 for cloning into pGEM T-Easy vector (see section 3.2.5, Appendix C, vector map 1) for sequencing and subsequently for mutational analysis. This primer set was also designed manually and synthesized at Inqaba Biotech., South Africa.

#### **3.2.3.6 RNAi colony PCR forward and reverse primers**

These primers were used for screening of the RNAi clones. They were donated by Prof. Rees (Biotechnology Department, University of the Western Cape). The Primer sequences are given in Appendix C, primer set 6. This primer set was also manually designed in Prof. Rees' Laboratory and synthesized at Inqaba Biotech., South Africa.

#### **3.2.3.7 RNAi Oligos**

RNAi targets were generated by using the sequences for all 3 RBBP6 variants in the RNAi design engine:

([http://www.ambion.com/techlib/misc/siRNA\\_finder.html](http://www.ambion.com/techlib/misc/siRNA_finder.html)). Appendix D (table 1)

shows the single stranded RNAi oligos (forward and reverse) generated against the RBBP6 transcripts. The RNAi oligos were synthesized in such a manner that

when annealed (Appendix D, table 2) they could be cloned between the *Bgl* II site (Forward oligo) and the *Hind* III site (Reverse oligo) of the pEGFP-C1-U6 vector (Appendix D, vector map 2 from Pretorius, 2007).

### **3.2.4 Antibodies**

GST-RBBP6 fusion proteins were used to generate antibodies of different domains of RBBP6 in rabbits according to Bellstedt's method (Bellstedt *et al.*, 1987). Antibodies were raised against the DWNN domain as illustrated in figure 2.2 in Chapter Two. They were donated by Prof. Rees, Department of Biotechnology, and University of the Western Cape (UWC). This antibody had not been characterised previously so this study also focused on characterizing the specificity of the GST-DWNN antibody in both cell culture-derived protein lysates and the recombinant DWNN protein using Western blotting analysis on both one-dimensional (1D) and two-dimensional (2D) acrylamide gel electrophoresis. The anti-human-DWNN antibody was also used for localisation of the DWNN both *in situ* and in *in vitro* situations. The purified anti-human DWNN antibody was used for both immunohistochemistry; cell staining and Western blotting. Anti-human DWNN antibody detects all of the RBBP6 isoforms.

### **3.2.5 Cloning Vectors**

Different vectors were used in this study; pGEM T-Easy (Appendix C, vector map 1) and pGEX 6P-2 (Appendix E, vector map 3) were used for cloning and expression of RBBP6 fragments respectively. The pEGFP-C1-U6 vector (Appendix D, vector map 2) was used for RNA interference work and was a gift

from Professor Rees. The pGFP-DWNN-13 (Appendix E, vector map 4) and pDsRed1-C1-DWNN-200 (Appendix E, vector map 5) were used to over-express the DWNN domain and RBBP6 isoform 2 respectively in the human cell lines.

### **3.3 Methods**

#### **3.3.1 Cell culture**

##### **3.3.1.1 Preparation of complete cell culture medium**

The complete (Dulbecco's Modified Eagle's Medium) DMEM, Hams F-12 and RPMI 1640, 10% foetal calf serum (FCS), 1% Penicillin-Streptomycin and in RPMI 2 mM Glutamine was added. The media were then stored at 4°C and pre-warmed to 37°C before being added to the cell cultures. All the cell culture media and Dulbecco's buffered saline were purchased from Lonza Rockland Inc., USA.

##### **3.3.1.2 Cell culture**

The cells (section 3.2.2) were grown up to 60–70% confluence as a monolayer in Dulbecco's medium or RPMI 1640 (Jurkat cells) and Ham's F-12 (CHO cells) supplemented with 10% foetal calf serum and 1% Penicillin and streptomycin in an atmosphere of 5% CO<sub>2</sub>. The cells were cultured in 25 cm<sup>3</sup> flasks (Greiner Bio-One, Germany).

##### **3.3.1.3 Trypsinization**

Confluent 25 cm<sup>3</sup> flasks of cells were washed with 1X 0.1M phosphate buffered saline (PBS) pH 7.3 and trypsinized with 0.125% trypsin in PBS (Lonza Rockland Inc., USA). FCS-containing medium was added to deactivate the trypsin followed by centrifugation at 3000 rpm in a Sorvall TC6 centrifuge (American Instrument Exchange, Inc., USA) for four min. The supernatant was discarded and the cells

were resuspended in the desired media. These cells were either re-plated or frozen in complete medium containing 10% DMSO.

### **3.3.2 RNA extraction**

Total RNA was isolated from cultured cells using a High Pure RNA isolation Kit [11828 665001] (Roche Biochemicals, Germany). The manufacturer's instructions were followed. Briefly, cultured cells were detached by scrapping the cells off the cell culture flasks using a cell scraper (Greiner Bio-one, Germany). The cells were pelleted and resuspended in 1X PBS. Resuspended cells were then lysed in lysis-Binding Buffer (Roche Biochemicals, Germany) by vortexing for 15 seconds. A High Pure Filter tube + collection tube was assembled as described by the manufacturer. The entire sample was then transferred into the High Pure Filter tube-assembly and incubated for one min and then centrifuged for 15 seconds at 6720 x g at room temperature. The flow-through liquid was discarded and the High Pure Tube + collection tube were re-assembled. Wash buffer I (Roche Biochemicals, Germany) was added and centrifuged for 15 seconds at 6720 x g. The flow-through was then discarded and the High Pure Tube + collection tube was re-assembled and the washing was repeated with Wash Buffer II (Roche Biochemicals, Germany). A third wash was done with Wash Buffer II (Roche Biochemicals, Germany) followed by centrifugation at 11700 x g for two min. The collection tube was discarded and the High Pure Filter Tube was transferred into a sterile 1.5 ml micro centrifuge tube. RNA Elution Buffer (Roche Biochemicals, Germany) was added to this assembly to elute the total RNA and incubated for one min. The elution was carried out by centrifugation at 6720 x g for one min. The total RNA was then electrophoresed to assess the integrity and

the quality of RNA. The RNA was stored at -80°C in aliquots of 10 µl for future use.

### **3.3.2.1 RNA Gel electrophoresis**

#### **3.3.2.2 Preparation of RNA agarose 1% gel**

A 1% agarose solution was prepared in 1X MOPs (prepared in DEPC water), 0.6% (37% (v/v) formaldehyde), 0.3 µg/ml ethidium bromide (EtBr) (Promega, USA). The RNA sample (1µg) was mixed with an equal volume freshly prepared formaldehyde gel loading buffer. The mixture was heated at 65°C for five minutes, cooled on ice and then loaded onto a 1X MOPS equilibrated gel. The RNA was electrophoresed at 100 volts for one hour in 1X MOPS.

#### **3.3.2.3 Quantification**

Quantification of both RNA and cDNA was done using a Nanodrop spectrophotometer (NanoDrop technologies, USA). Readings were taken at 260 nm and 280 nm as described by the manufacturer. A 260/280 ratio of 1.8 or more was regarded as pure quality.

### **3.3.3 Reverse transcription (RT)**

Reverse transcription was performed using the ImProm-II-Reverse Transcription System (A3802) (Promega, USA). The manufacturer's instructions were followed. First, 1 µg of total RNA sample was mixed with either 0.5 µg/reaction oligo (dT)<sub>15</sub> or random primers and incubated at 70°C for five min in order to denature any secondary structures and to allow the primers to anneal. This was followed by chilling the template preparation on ice for five minutes. This preparation (Appendix F, table 3) was then mixed with the rest of the components

of the cDNA synthesis reaction (Appendix F, table 4). The samples were mixed and briefly centrifuged. Following this; the samples were incubated at 25°C for five minutes to allow the primers to anneal at their sites. This was followed by the incubation of the samples at 42°C for an hour to allow reverse transcription to occur. After this incubation the reverse transcriptase was inactivated by incubation at 70°C for five minutes and the samples were cooled on ice. The samples were either used immediately for Polymerase Chain Reaction (PCR) or Real-time PCR or stored at -20°C for later use.

### **3.3.4 Polymerase Chain Reaction (PCR)**

The cDNA obtained through reverse transcription was used as a DNA template using sequence specific primers for different fragments of the RbBBP6 gene. The PCR was performed using a master mix from Promega (USA) [50 units/ml of *Taq* DNA polymerase in a PCR reaction buffer; 400 µM dATP; 400 µM dGTP; 400 µM dCTP; 400 µM dTTP and 3mM MgCl<sub>2</sub>]; 1 pg-0.5 µg template DNA and nuclease-free water to make up to a required reaction volume. The reactions were then subjected to 30 cycles consisting of the three PCR steps (denaturation, annealing and extension), after the initial denaturation step and followed by a final extension step. The steps were as follows with some variation in annealing temperature and extension time depending on the nucleotide sequence of the gene of interest:

95°C for 3 min

94°C for 30 min

$T_m$ -5 for 0.5-1 min

72°C for 1 min

72°C for 10 min

25-30 cycles

**Note:** The actual temperature used was the calculated temperature ( $T_m$ ) minus 5°C.

The products were either stored at 4°C for further use or electrophoresed on 0.8-2% agarose gels.

### **3.3.5 Agarose gel electrophoresis of DNA**

The DNA samples were electrophoresed on 1% agarose gel containing 0.3µg/ml Ethidium bromide and then visualized using UV light. A 100 bp DNA molecular weight marker (Fermentas, USA) was used. Gels were then subjected to 70 Volts for one hr in 1X TBE buffer.

### **3.3.6 Cloning of PCR products into pGEM-T-Easy vector**

#### **3.3.6.1 DNA Ligation**

A ligaFast cloning system (Promega, USA) was used to clone PCR products in pGEM-T-Easy vector for both sequencing and probe synthesis. For the experimental ligation, ~ 3 ng PCR product was added to 2X Ligation buffer (60mM Tris pH7.8; 20mM MgCl<sub>2</sub>; 20mM DTT; 2mM ATP) to 1X final concentration; 10 ng of pGEM-T-Easy vector; 3 units of T4 DNA ligase and sterile distilled water. A background control (no insert/fragment DNA of interest)

was also run as well as a positive control supplied with the kit. The components were mixed and quickly centrifuged to collect all the components to the bottom of the tube. These ligations were incubated at room temperature for one hr, then transformed into an MC1061 (F<sup>-</sup>araD139 Δ (araA-leu) 7696 ΔlacX74 galK16 galE15 (GalS) λ<sup>-</sup> e14<sup>-</sup> mcrA0 relA1 rpsL150 (strR) spoT1 mcrB1 hsdR2) *Escherichia coli* (*E. coli*) cloning strain.

**Note:** Negative control was a transformation with no plasmid DNA transformed. Positive control (Promega Corp., USA) consisted of a DNA fragment that had been optimised to ligate to pGEM-T-Easy vector. The background control was a pGEM-T Easy vector with no insert (used to check if the vector would ligate to itself).

### 3.3.6.2 Preparation of competent cells (Super competent protocol)

Sixteen hours before preparing the competent cells, a desired strain (for example, an MC1061 strain of *E.coli* (for cloning) or a BL21 (DE) pLysS strain of *E.coli*) was streaked out on a nutrient agar plate containing 10 mM MgCl<sub>2</sub>. All glassware used in the preparation of competent cells was washed with concentrated HCl, rinsed with dH<sub>2</sub>O and autoclaved. A single fresh colony of the desired strain of *E.coli* was grown for two hrs in 20 ml TYM broth in a 200-500 ml flask shaken at 300 rpm, at 37°C up to an OD<sub>550</sub>= 0.2; then diluted five times with fresh TYM broth in a 2 litre flask. This was shaken for a further two to three hrs until the OD<sub>550</sub>= 0.2; then further diluted four times with a fresh TYM broth in a 2 litre flask. This was then shaken for a further two to three hrs until the OD<sub>550</sub>=0.4-0.6. The cells were then rapidly cooled in ice water with swirling and collected by centrifugation at 1380 x g for 10 min in polypropylene tubes. The medium was

drained and discarded and the cells were resuspended in 125 ml Tfb 1. The cells were then incubated for 30 min and centrifuged for 10 min at 4°C and gently resuspended in 50 ml Tfb 2, aliquoted in micro-centrifuge tubes and frozen on dry ice. The cells were then stored at -70°C.

### **3.3.6.3 Transformation**

Competent MC1061 *E. coli* cells were thawed on ice, then mixed with 1 ng of plasmid and incubated at 4°C for 30 minutes. This mixture was immediately incubated at 37°C for five minutes, and then incubated on ice for two min. Nine hundred millilitre Luria broth (LB) without ampicillin was added to the mixture. This was followed by incubation at 37°C for one hour to allow all the cells to grow. After one hour, a tenth of each transformation mix was plated on pre-warmed LB plates containing 100 µg/ml ampicillin. The plates were incubated at 37°C overnight.

### **3.3.6.4 Screening for positive clones using colony Polymerase Chain Reaction**

Individual colonies were picked from LB agar plates and resuspended in sterile water. A fraction of this mixture was then used as a template for a PCR reaction (Appendix F, table 5). The PCR conditions were dependent on the fragment of interest and the primers in question but generally universal primers (M13 universal primers) were used. Those colonies that showed the presence of the DNA fragment of the expected size were selected for the plasmid extraction procedure. The remainder of the colony mix was used as an inoculum for making an overnight culture for plasmid extraction.

### **3.3.6.5 Mini-preparation Plasmid DNA extraction**

In order to get high quality plasmid DNA for further experiments including, restriction digestion, sequencing and probe synthesis, plasmid DNA was extracted using the Wizard Plus SV Miniprep DNA Purification System (Promega, USA). Manufacturer's instructions were followed (Appendix H, schedule 1).

### **3.3.6.6 Restriction digestion of plasmid DNA**

Two restriction endonucleases (REN) were used for restriction analysis of the clones following the manufacturer's instructions. *Pst* I and *Apa* I were used to linearize the clones and *EcoR*I was used to release the insert. Five hundred nanograms of plasmid DNA of each clone was restriction digested with these three RENs. The restriction digests are tabulated in Appendix F-table 6.

### **3.3.7 Sequencing analysis**

The sequencing was done by Inqaba Biotech (Pretoria, South Africa). The sequences were analyzed using Sequencher DEMO ([www.genecodes.com](http://www.genecodes.com)) and BLAST basic alignment tool ([www.ncbi.nlm.nih.gov](http://www.ncbi.nlm.nih.gov)).

### **3.3.8 Real-time polymerase chain reaction (real-time PCR)**

#### **3.3.8.1 Real-time efficiency by hHPRT and DWNN standard amplification**

DNA of known concentration was serially diluted by a dilution factor of 10 to 1000. These dilutions were then used in the real-time PCR set up. Real-time efficiencies were obtained from the Roche Lightcycler 1.5 (Roche Diagnostics, Germany).

### **3.3.8.2. Real-time PCR quantification by standard curve analysis**

The house-keeping genes chosen were  $\beta$ -actin, GAPDH, 28S and hHPRT1 (Toegel et al., 2007).

There are 2 ways to quantify the real-time PCR results, either by using a standard curve, which is used as a reference for extrapolating quantitative information for target mRNAs of unknown quantities, or by the use of comparative cycle number cross point (Ct) method (Livak and Schmittgen, 2001). The later uses the comparison of the Ct values of the samples of interest with a control sample such as an untreated sample and the Ct values are then normalised to an appropriate house-keeping gene. Any of the two methods may be used and the results from both are comparable.

### **3.3.8.3 Real-time quantification setup**

cDNAs from different responses were quantified using a Nanodrop spectrophotometer (NanoDrop Technologies, USA). Concentrations of 200-500 ng of DNA were subjected to real-time reactions. The Sybr Green technology (Roche Applied Science, Germany) was used to quantify the results and the reactions were prepared as shown in Appendix F, table 7 in triplicates in three independent experiments.

### **3.3.8.4 Real-time PCR thermal conditions**

The LightCycler FastStart DNA Master SYBR Green I (Roche, Germany) was used in this study. It was used for the amplification, detection and quantification of the DNA or cDNA target. Recommendations from the manufacturer for

thermal conditions (Appendix F, table 8) were followed with minor adjustment depending on the primer sets used.

### **3.3.9 Immunohistochemistry (IHC)**

The anti-human-DWNN antibody that was used for this study was obtained from Prof. Rees' laboratory (Biotechnology Dept., University of the Western Cape). It was raised in rabbit against the recombinant GST-DWNN domain fusion and had not been characterized prior to this study. It was designed to localize to all three RBBP6 isoforms. In this study the antibody was first characterized prior to experimental use (Chapter 4).

To avoid repetition, the IHC procedure given below was used throughout for all the tissue arrays analysed, unless otherwise stated. Tissue arrays (US Biomax Incl. and Cybrd Tissue Array Tech, USA) were used to localize the RBBP6 proteins in different cancers. The cancers, six cases each (Listed in Appendix G) studied included Breast cancer, cervical cancer, and hepatocellular carcinoma; these were the ones of major interest. Also studied were oesophageal cancer, colon, stomach, rectum, lung, kidney and uterine cervix.

#### **3.3.9.1 Colorimetric method**

Immunohistochemical localization was carried out with the antibody for human DWNN. Tissue arrays (Cybrdi-CC00-11-001 and Biomax.us-BC 001111) from both cancer and normal tissue spots were used. The staining was performed using strep-avidin-anti-peroxidase-peroxidase method using an LSAB+ Kit peroxidase (DAKO, Denmark). Briefly, the tissue arrays were dewaxed (Appendix H-schedule 2) and antigen retrieval was performed using microwaving. The primary

antibody (0.2µg/µl) was applied and left overnight at 4°C. The next day the sections were washed in Tris buffered saline (TBS) buffer and the secondary antibody incubation (ready-to-use, DAKO, Denmark) was carried out at room temperature for 15 min, the colour was developed with Diaminobenzidine-DAB (DAKO, Denmark) and counterstained with haematoxylin. The tissue arrays were examined for DWNN reactivity in the tumour islands, non-cancerous and tumour associated areas. (See appendix H, schedule 2 for a detailed description of the procedure)

**NOTE:** Controls that were used were as follows:

- 1) Negative control: omitted primary antibody was replaced by PBST/TBST containing 1% BSA and pre-absorbed recombinant DWNN antibody.
- 2) The positive controls were a section from the normal testis tissue, which had been shown to express the DWNN (Mbita, 2004) and oesophageal carcinoma tissue, which was reported to express the murine P2P-R (Yoshitake et al., 2004). EST database analysis suggests that RBBP6 is highly expressed in this tissue and has been documented that this tissue has the highest expression of the PACT (Simons et al., 1997).
- 3) The secondary antibody did not show non-specific staining when the primary antibody was omitted.

### **3.3.9.2 Cell staining: Immunocytochemistry (ICC)**

The cells (HepG2, HeLa, MCF-7, and Hek 293T) were grown in Dulbecco's Essential Minimal Medium while CHO cells were grown in Ham's F-12 to a required confluence (80-90%) and then washed with 0.1M PBS, pH 7.4 at room temperature.

Briefly, cells were grown on cover slips in 6-well cell culture plates. After 24 hrs the cells were washed twice with PBS containing 0.5% BSA then fixed in 4% paraformaldehyde (PFA) in PBS at room temperature for 15 min. The cells were then washed three times with PBS before permeabilization in PBS containing 0.1% Triton X-100 for 10 min. The cells were again washed twice in PBS and non-specific binding was blocked with PBS containing 0.5% BSA for one hr at room temperature. The cells were then incubated with the DWNN antibody (1:10000 dilution in PBS containing 0.5% BSA) for one hr; washed twice in PBS-BSA and incubated (in the dark) at room temperature in the secondary antibody (Anti-rabbit IgG-AlexaRed) 1:1000 dilution for one hr. The cells were washed twice in 1X PBS and then mounted in vector shield mounting medium (Vector Laboratories Incl., USA), containing DAPI (a nuclear counterstain). The mounted cells were examined under the fluorescence microscope (Axioplan 2 imaging, Zeiss, Germany) using the excitation at 590 nm and emission at 617 nm or using a light filter.

The characterization of the DWNN antibody was carried out by using Western blotting techniques described in section 3.3.12 using both the 1D and 2D electrophoresis methods.

### **3.3.10 *In situ* hybridization (ISH)**

Tissue arrays (Appendix G) were used for the *in situ* hybridization (ISH). The Digoxigenin (DIG) labelling system from ROCHE, Germany, was used for labelling RNA probes for both ISH and Fluorescent *in situ* hybridization (FISH).

### **3.3.10.1 DWNN Probe preparation**

Different DWNN fragments were amplified and cloned into pGEM-T Easy vector. The clone for probe synthesis was then sequenced and linearized with appropriate enzymes to generate antisense and sense RNA probes as shown in Appendix F, table 9. The enzymes used to linearize the DWNN clones were *Pst* I and *Apa* I generating antisense and a sense probe respectively. The direction of cloning (5' to 3' or 3' to 5') was assessed from the sequence results. Based on these results, either T7 or Sp6 promoter was used to generate sense or antisense probes. The linearized clones were electrophoresed on a 0.8% agarose gel. The DNA bands of interest were visualized using a UV lamp and purified from the gel using a Promega Wizard SV gel and PCR clean-up system (Appendix H, Schedule 3).

### **3.3.10.2 DIG Labelling of the DWNN probes**

The linearized plasmids containing DWNN fragment were used as templates for the labelling reaction to generate antisense and sense DWNN RNA transcripts as tabulated in Appendix F, table 10. One microgram of linearized and purified plasmid containing the *DWNN* gene was incubated with a mixture containing DIG dUTP (deoxyuridine triphosphate) for two hrs at 37°C with T7 RNA polymerase or Sp6 RNA polymerase (Roche Diagnostics, Germany) to generate both antisense and sense probes, respectively. The specificity of the labelling reaction was determined by generating a DIG labelled control cRNA probe from DNA PSPT 18-Neo/Pvu II supplied in the labelling kit (Roche Diagnostics, Germany). The reaction mixture of DIG labelling of antisense, sense and control RNA probes was generated by adding the reagents as tabulated in Appendix F, table 10 into 1.5

ml micro-centrifuge tube. These mixtures were incubated in a thermocycler for two hr at 37°C. The reactions were then stopped with 0.2 M EDTA (pH 8.0). These were mixed and pulse-centrifuged to collect all the constituents at the bottom of the tubes. The precipitation of the labelled RNA probes was achieved by the addition of 1/10 volume 4 M Lithium chloride and 5 volumes cold absolute ethanol. These were mixed, pulse-centrifuged and incubated at -20°C for two hrs. The precipitate was pelleted by centrifugation at 7571 x g for 15 min at 4°C and decanting the supernatant. The pellet was washed with cold 70% ethanol and centrifuged at 11708 x g for 15 min at 4°C after which the supernatant was removed with a pipette to avoid dislodging the pellet. The pellet was dried in the laminar flow cabinet. It was then dissolved in 50 µl sterile DEPC treated water. This was left for one hr at 4°C to allow the pellet to completely dissolve. The DIG labelled probes were stored at -70°C in aliquots of 10 µl in 500 µl screw-capped tubes. The concentrations of the probes were then estimated using guidelines described in DIG user's guide (Roche, Germany).

**NOTE:** RNase inhibitor was not added because it requires high concentrations of DDT (dithiotretiol) which may affect Sp6 and T7 polymerase activity. DNase was not used either because there was no assurance that it was RNase free.

At the end of labelling there was approximately 0.2 µg/µl of probe.

### **3.3.10.3 Estimation of the concentration of the probes**

To estimate the probe concentration of the synthesized probes, dilutions were made as tabulated in Appendix F, table 11. Dilutions for control labelled RNA (supplied); antisense and sense DWNN RNA and DIG labelled cRNA to control

DNA pSPT-18-Neo. DIG user's guide was used (Roche Diagnostics). Spot points were marked lightly with a pencil on a nylon membrane (Hybond, Amersham, USA), and the manufacturer's instructions were followed (Appendix H, schedule 4).

#### **3.3.10.4 *In situ* hybridization (ISH) and Fluorescence ISH (FISH)**

Before starting the procedure, a fresh 4% paraformaldehyde (PFA) solution was prepared. The PFA was dissolved at 60°C with stirring, not allowing the temperature of the solution to exceed 60°C. Once the solution cleared, it was allowed to cool to room temperature.

The tissue arrays were dewaxed, rehydrated and pre-treated for *in situ* hybridization (Appendix H, schedule 5). Hybridization was performed with 100 pg/μl and 3 pg/μl antisense and sense DWNN RNA probes respectively and incubated overnight at 55°C in a Hybaid Omnislid Flat Block Humid Chamber (Hybaid, USA) containing 5X SSC (3M NaCl, 0.3 M Na-citrate, pH 7.0) buffer and 50% formamide. Hybridization was carried out in hybridization buffer (2 X SSC, 10% Dextran (v/v), 0.2% SDS (w/v), 50% formamide) containing 0.01 μg/μl Herring Sperm DNA. The hybridization buffer + HSD were used as a negative control for the sense probe. After hybridization the tissue arrays were subjected to a post-hybridization treatment (Appendix H, schedule 6). The probes were either visualized colorimetrically or fluorescently. Colorimetrically, the probes were visualized using with 5-bromo-4-chloro-3-indolyl phosphate/nitroblue tetrazolium [NBT/BCIP] (Roche Diagnostics, Germany), counterstained with haematoxylin (Sigma, Germany) and mounted with aqueous

mounting medium (Serotec, UK). For the fluorescence studies, the slides were incubated with anti-DIG conjugated with FITC (Roche Diagnostics, Germany) after the blocking step. The probes and the slides were then mounted with SlowFade Light AntiFade (Molecular Probes, USA). They were then viewed with a fluorescence microscope using a 490 nm excitation filter. A minimum of three images for each tissue was taken with 40X objective and were used for a quantitative analysis of the FISH results. Labelled cells were counted for the analysis. Statistical software (GraphPad Prism 5, USA) was used to analyze the FISH data from tumour associated tissues and islands of the tumours. A One-way ANOVA and non-parametric column analyses was used.

### **3.3.11 Ribonucleic acid interference (RNAi)**

The RNAi oligos were designed as shown in Appendix D under RNAi oligo design subheading.

#### **3.3.11.1 RNAi vector digestion**

Promega restriction enzymes were used and manufacturer's instructions were followed with optimisation where necessary. The pEGFP-C1-U6 vector (500ng) [Prof. Rees, Department of Biotechnology, University of the Western Cape]; shown in Appendix D, vector map 2 was digested with *Hind* III or *Bgl* II. A doubly digested vector was purified from agarose gel as described in Appendix H, schedule 3. The purified digested vector was quantified using a Nanodrop (Nanodrop Technologies, USA) and used in the cloning of annealed RNAi oligos into RNAi vector.

### **3.3.11.2 Annealing RNAi oligos**

Before cloning the RNAi oligos (Appendix D, table 1) into RNAi vectors, the two oligos (forward and reverse from Inqaba Biotech) were annealed. They were annealed by adding 4 pmoles of each oligo in 1X TE buffer and 0.05 M sodium chloride. This was subjected to the following thermal steps:

- Denature at 94 °C for 5 min
- Cool at room temperature for 4 hrs, or overnight
- Store at -20 °C or use for cloning step.

### **3.3.11.3 RNAi oligos cloning into pEGFP-C1-U6 vector**

Cloning was done as previously described with other fragments cloned in this study (section 3.3.6). The setup of the cloning reaction was described in Appendix H.

### **3.3.11.4 Transfection of RNAi clones into human cells**

#### **3.3.11.4.1 Introduction**

In this research a better and less toxic reagent, Metafectene Pro (Biontex, Germany) was used to transfect the RNAi constructs into Hek 293T cells and the RBBP6 constructs into MCF-7 cells.

#### **3.3.11.4.2 Transfection protocol**

Manufacturer's instructions were followed and the optimal DNA concentration was found to be 2 µg for each transfection, setup was done as shown in Appendix H, table 12. The tubes containing the DNA and transfection reagent were combined into 1 tube for each RNAi plasmid DNA. The addition was done in such a manner that the DNA tube constituents were added to transfection reagent

tube constituents drop by drop. The mixed samples were incubated at room temperature for 25 min. Cells were cultured in 6 well plates until approximately 60-80% confluent, washed with PBS and a serum-free medium was added. The transfection mixture was added drop-wise onto the cell cultures and after 4 hrs the medium was substituted with complete medium and the cells were left to grow for a further 24 or 48 hrs. For transient transfections, the cells were then assessed for the efficacy of the RNAi molecules.

### **3.3.12 Western blot analysis**

#### **3.3.12.1 Total protein extraction**

Total protein was extracted using RIPA and 9 M urea buffers with the latter used for 2D gel electrophoresis. Briefly, cultured cells were washed with 1X PBS and scrapped off the culture dishes with a scrapper (Greiner Bio One, Germany) and put into PBS containing protease inhibitors. Detached cells were then centrifuged at 1132 x *g* at room temperature, and then resuspended in (10X volume of the pellet) RIPA or 9M Urea buffer. The cells were then vortexed for 15 seconds and incubated on ice for 30 min with occasional vortexing. The samples were then centrifuged at 11708 x *g* at room temperature for 5 min. The centrifugation resulted in the soluble proteins from the cells being transferred to the supernatant which was then transferred to a new 1.5 ml centrifuge tube. The protein concentration was determined using the Bradford assay. The protein solution was then mixed with 2X sample buffer containing 10 mM DTT and stored at -70 °C until further use.

### **3.3.12.2 Sodium dodecyl sulphate – polyacrylamide gel electrophoresis (SDS PAGE)**

Protein samples were separated on a 12% separating PAGE gel. For the SDS PAGE gel, these samples were thawed and boiled, and 20-50 µg of protein was loaded onto a 12% SDS PAGE gel. The protein electrophoresis system was then set at a constant voltage of 120V and allowed to run for one hr in 1X SDS-PAGE running buffer.

### **3.3.12.3 Protein quantification using a Bradford assay**

The Bradford assay was used in this study to determine protein concentrations because it is a fast efficient and accurate method and uses very little sample. A Bovine Serum Albumin Fraction V was used as a standard.

The standards were prepared as tabulated in Appendix F, table 13 as described by the manufacturer with minor modifications. The preparation of the protein samples was done as shown in Appendix F, table 14.

### **3.3.12.4 Preparation of 12% SDS PAGE**

The SDS PAGE gel was prepared with 12% Acrylamide/Bis (40%-37:5:1), 0.375 M Tris-Cl (pH 8.8); 0.1% SDS; 0.1% ammonium persulphate (APS); 0.005 ml of TEMED and made up to the required volume with distilled water. This mixture was poured into the acrylamide gel casting apparatus (BioRAD, USA). It was then overlaid with water and after solidifying the water was discarded. A stacking gel (0.125 M Tris, pH 6.8; 0.5% Acrylamide/Bis (40%-37:5:1); 0.1% SDS; 0.1% APS; 0.005 ml TEMED) was made up to the required volume with distilled water and added on top of this separating gel.

### **3.3.12.3 Electroblotting**

An electro-blotting cassette (BioRAD, USA) was assembled according to the manufacturer's instructions to transfer proteins onto the polyvinylidene fluoride membrane (PVDF) [Sigma] in transfer buffer for two hrs. After the transfer the membrane was stained with Poncheau S stain (Sigma-Aldrich, Germany) to confirm the transfer. The stain was removed with several washes in water and TBST.

### **3.3.12.4 Probing the blot with antibodies**

Before probing with the primary antibody, the membrane was incubated in TBSMT overnight at 4°C or at room temperature for two hrs. Then the membrane was probed with anti-human DWNN primary antibody (1:5000 in TBSMT) and incubated for one hr on the shaker at room temperature. After an hour the membrane was washed three times, (10 min for each), with 1X PBS containing 0.1% Tween 20. After washing, the membrane was incubated in a secondary antibody (1:2000 in TBSMT), Anti-rabbit IgG peroxidase conjugated (DAKO) for one hr. This was followed by washing the membrane six times (10 min) with 1X PBS containing 0.1% Tween 20.

### **3.3.12.5 Detection and exposure**

Detection of the antibody binding was done using autoradiography. To visualize the bands that the primary antibody bound to, the membrane was immersed in a solution containing Super Signal West Pico Chemiluminescent Substrate (PIERCE, USA) for five min. The blot was then exposed to CL X-Posure film (Thermo Scientific, USA) for an appropriate period (30 seconds; one min; 10 min; 30 min and one hr). The x-ray film was then developed in the dark.

### **3.3.12.6 Blot stripping protocol**

In most instances a specific blot was stripped to be probed with a different antibody. Stripping was done by washing a membrane with dH<sub>2</sub>O for five min at room temperature. This was followed by washing with 0.2 M Sodium hydroxide for a further five min at room temperature. A stripping method was concluded with another five min-wash with distilled water. The membrane was then ready for blocking and detection using a different antibody.

### **3.3.12.7 Two dimensional (2D) gel electrophoresis**

A total of 1-2X 10<sup>7</sup> cells for each of the cell lines (Hek 293T, MCF-7 and HeLa, HepG2) were collected by trypsinization, then centrifugation and lysed in 2D gel lysis buffer (9M urea, 2M thiourea, 4% 3-[(3-Cholamidopropyl) dimethylammino]-1propanesulfonate (CHAPS) and a tablet of protease inhibitors cocktail (Roche, Germany). First dimension electrophoresis was performed using the Ettan IPGphor II (GE Healthcare, UK). Precast 7 cm immobilized pH gradient (IPG) with pH ranges from 3-10 and 4-7 were purchased from BioRad, USA. Cell lysates (100-500 µg) were thawed and mixed with rehydration buffer (9M, 2M thiourea, 4%CHAPS, 50 mM DDT, 2% Ampholytes and 0.01% Bromophenol blue). 200 µg of protein sample mixture was loaded to each of the IPG strips. The strips were rehydrated with the sample mixture and overlaid with a layer of mineral oil overnight (12-16 hours). Iso-electric focussing was carried out in three steps: 250 V for 15 min, 8000 V for 3 hours and 8000 V rapid ramp to achieve 10000 V-hours in 4 hours.

The second dimension was performed in the BioRad Protean II system (BioRad, USA). The IPG strips were equilibrated in 1% DTT equilibration buffer (6 M

Urea, 2% SDS, 0.05 M Tris pH 8.8 and 20% glycerol) for 10-15 min with shaking. Equilibration was repeated with 0.25 M iodoacetamide (BioRAD, USA) for a further 10-15 min on a stirrer. The strips were rinsed in 1X SDS running buffer and were placed on top of a 12-14% SDS gel. A protein marker filter paper was also placed on top of the gel. These were then sealed with 0.5% agarose solution containing 0.0001% bromophenol blue. This was then run as a normal SDS-PAGE at 50V increasing gradually to 120V. After the SDS PAGE was done, gels were either stained with coomassie brilliant blue or blotted for Western blotting. The spots that showed reaction to the DWNN antibody were located and analyzed by Mass spectroscopy.

#### **3.3.12.8 Matrix-assisted laser desorption/ionization Time-of-flight (MALDI-TOF) Mass spectrometry (MS)**

Spots of interest were picked from the 2D gels with sterile yellow tips and transferred to clean sterile 1.5 ml centrifuge tubes. The gel pieces were washed twice with 50 mM ammonium bicarbonate for 5 min each, discarding the wash solution after each wash. The washing was repeated with 50 mM ammonium bicarbonate for a further 30 min with occasional vortexing. The gel pieces were washed twice with 50% 50 mM ammonium bicarbonate/50% acetonitrile for 30 min each with occasional vortexing, discarding the wash solution at the end of each wash. The destaining of the gel pieces was completed by the addition of 100% acetonitrile and incubated for 5 min at room temperature. The gel pieces were dried completely in a speed vac for 10 min at a medium setting. The dried protein gel pieces were incubated with 10 $\mu$ g/ml trypsin solution in 25 mM

ammonium bicarbonate for 6 hours at 37°C. The digestion solution was then transferred to 4°C until the MALD-TOF MS analysis.

The trypsinized spots were mixed with the MS matrix and loaded onto an MS plate. In-between the samples, the calibration mix (Calmix 2 and the matrix) was loaded. These were allowed to dry on the MS plate for few min up to an hour. The MS plate was then loaded into the Voyager-DE Pro MALDI-TOF system (Applied Biosystems, UK). The peptide masses were measured with the MALDI-TOF and the protein identities were searched for from a Mascot server ([www.matrixscience.com/server.html](http://www.matrixscience.com/server.html)).

### **3.3.13 Detection of Apoptosis - Rationale**

Apoptosis was detected using different techniques depending on the sample that was used. Conventionally, DNA laddering was the chosen method for detecting apoptosis where DNA was extracted and electrophoresed on an agarose gel. DNA laddering/fragmentation is normally evident when the cells die as a result of apoptosis. There are commercially available kits that have been developed to detect this DNA laddering on both fixed tissue sections and cultured cells. One example of such kits is a Terminal deoxynucleotidyl Transferase Biotin-dUTP Nick End Labelling (TUNEL) kit available from many different companies (Promega Corp., USA; Roche Diagnostics, Germany). Alternatively, apoptosis can be detected using kits like ANNEXIN V (Sigma-Aldrich, Germany) and APOPercentage (Biocolor Ltd., UK) that use a different principle from TUNEL. While TUNEL detects DNA fragmentation, the latter two detect the externalization of phosphatidylserine (in the plasma membrane) seen in apoptotic

cells. In this project, *APOPercentage* assay using a FACScan (Becton Dickson, USA) was used to detect apoptosis in cultured cells, under controlled conditions and after apoptotic stimulus. The *APOPercentage* assay works by showing the cellular uptake of *APOPercentage* dye when a change in the asymmetric composition of the membrane phospholipids occurs. The asymmetric composition of the membrane phospholipids is essential in maintaining a 'viable' cell membrane and cell and is maintained and controlled by flippase. Flippase control is negated by the action of another enzyme; floppase or scramblase during apoptosis (Zhao et al., 1998). The *APOPercentage* Dye enters the cell once the phosphatidylserine residues, usually present only in the inner plasma membrane leaflet, are externalized to the outer membrane surface. The dye uptake continues until blebbing of the cell occurs after which no further dye can enter the apoptotic cell and the dye that has accumulated within the cell is retained. Dye-uptake can be visualised by transmission light microscopy. Apoptotic cells can also be quantified by flow cytometry (Keter et al., 2008). In this study flow cytometry was also used to quantify apoptosis.

### **3.3.13.1 Apoptotic induction**

Apoptosis was induced with Staurosporine, Camptothecin and Arsenic trioxide. These compounds have been shown to induce high levels of apoptosis (Charlot et al., 2006, Debret et al., 2008, Mei et al., 2007). Untreated cells grown for 24 hrs were used as the negative control. To make sure that equal numbers of cells were plated at the start of inductions, the numbers of cells plated were counted using a Fuchs haemocytometer.

### **3.3.13.2 APOPercentage Assay (Flow cytometry Method)**

The instructions of the manufacturer were followed with minor changes (Meyer et al., 2008). The assay was done as follows: The APOPercentage was diluted 1:160 in complete medium. From the culture plate or wells, the supernatant (SN) was removed and retained. The cells were washed with 1X PBS and trypsin (0.125%) was added to each well. The cells were washed off in trypsin and added to SN and PBS. These were centrifuged for three min at 7043 x g. The pellet was resuspended in APOPercentage dye (250 µl) and incubated at 37°C for 30 min. The cells were washed with 2ml PBS and centrifuged at 7043 x g for three min. The supernatant was removed and the pellet was solubilised in 300 µl FACS Flow liquid (BD Biosystems, USA). This was then used for analysis in the flow cytometer (Beckon Dickson, Biosystems, USA).

### **Flow Cytometry**

After APOPercentage staining (3.3.12.2), the cells were acquired and analysed on a FACScan instrument equipped with 488 nm Argon Laser as a light source immediately or within one hr. Acquisition was done by setting forward scatter (FSC) and side scatter (SSC) on a log scale Dot Plot to differentiate population of cells and cellular debris. On a linear histogram dot plot, APOPercentage (FL-3 channel) was measured against relative cell numbers. Negative control cells were used to set the cells in the negative quadrant before all samples were acquired and analysed using CELLQUEST Pro software (Beckon Dickson, Biosystems, USA).

### **3.3.14 Cell cycle analysis with Propidium iodide (PI)**

Cancer is a disease that is fundamentally characterized by the existence of too many cells. This may be due to ferocious cell cycles with a decrease in sensitivity to signals that indicate to a cell to adhere or differentiate or die (Collins et al., 1997). This process is gene-regulated and p53 plays a major role in this control. In this study, a cell cycle blocker, arsenic trioxide was used to investigate the role of the DWNN in cell cycle regulation.

Hek 293T, HeLa, HepG2 and MCF-7 cells were seeded at a density of  $2.5 \times 10^5$  cell per well in 6 well culture plates. After a further 24 hours, the cells were treated with  $12.5 \mu\text{M}$  arsenic trioxide. After 24 hours the cells were harvested by trypsinization and washed with 2 ml PBS. The cells were resuspended in 1 ml 1% (w/v) paraformaldehyde in PBS, pH 7.4. The cells were placed on ice for 30 minutes. 5ml PBS was added and the cells were pelleted by centrifugation at 4000 rpm for 10 minutes. The wash was repeated with PBS and the pellet was resuspended in residual PBS. 4 ml 70% ethanol was added slowly while mixing. Cells were placed at  $-20^\circ\text{C}$  for at least 48 hours up to several weeks prior to Propidium (PI) staining and flow cytometric analysis. Cells were pelleted at  $4000 \times g$  for 10 minutes, washed twice in PBS and were resuspended in 1 ml PI master mix and incubated at  $37^\circ\text{C}$  for 30 minutes. The cells were kept on ice until analysed by flow cytometry.

### **3.3.15 MTT [3-(4, 5-dimethylthiazol-2-yl)-2, 5-diphenyltetrazolium bromide] assay**

The cytotoxicity of the compounds (Arsenic trioxide, Staurosporine and Camptothecin) used in this study was measured using the MTT assay. Briefly, the

cells were seeded on 96 well polystyrene cell culture plates at a density of  $1 \times 10^4$  cells per well and allowed to attach overnight. Various dilutions of each compound and the blank controls were applied to the cells in triplicate for 24 hours. After the incubation time with the compounds the medium was removed and the cells were rinsed three times with 1X PBS. Cell viability was measured by the addition of 5mg/ml MTT solution and incubation for 4 hours at 37°C in the dark. The resultant crystals were dissolved by the addition of DMSO. The absorption wavelength of  $560 \pm 10\text{nm}$  of each well was read in a plate reader (Struers, Germany).

### **3.3.16 Statistical analysis**

The data from the real-time PCR, *in situ* hybridization, FACS and MTT assay presented in this study was analyzed using GraphPad Statistical software, USA and presented as mean  $\pm$  SD. A one-way ANOVA (analysis of variance) and non-parametric column tests were used.

## **Chapter Four: RBBP6 variants and isoforms in human cell lines, cancerous and non-cancerous**

---

An uncharacterized anti-human DWNN polyclonal antibody (section 3.2.4) was available for this study and the first part of the study was aimed at characterizing it. Before the uncharacterized antibody raised against the DWNN domain was used to label the different cell lines used in this project, it was important to confirm the genotype of the RBBP6, which was expected to be detected by this antibody. As some mutations can result in truncated protein products or higher molecular weight products, it was therefore important to determine the mutation status in the RBBP6 binding domains (section 4.1) before detecting protein products, in case unexpected bands were found.

Once the genotype status was established, the relative expression of RBBP6 (section 4.2) was conducted in order to choose appropriate cell lines that could be utilized for the characterization studies. The next question was whether the anti-human DWNN polyclonal antibody recognized the recombinant DWNN domain, endogenous DWNN and RBBP6 in low and higher expressing cell lines (sections 4.3) using Western Blotting analysis. Due to the recognition of multiple proteins from the human cell lines, it was of further importance to extensively investigate these proteins (section 4.4).

RT-PCR (section 3.3.3) was used to detect RBBP6 domains for mutational analysis in Hek 293T, HeLa, HepG2 and MCF-7 cell lines. This was performed to determine whether the cell lines used in this study have the expected RBBP6

transcripts. One (1D) and two (2D) dimensional polyacrylamide gel electrophoresis (sections 3.3.12.2 and 3.3.12.7 respectively) were used to separate total proteins extracted from the human cancer cell lines (MCF-7, HeLa and HepG2) and the normal Hek 293T cells. The total protein was extracted using both RIPA buffer and Urea buffer (Appendix A1) and Western blotting was carried out (section 3.3.12) on both 1D and 2D gels.

Four rabbits were immunised with a Glutathione S Transferase (GST)-DWNN recombinant protein as shown in Appendix J. It was expected that the sera from these animals would contain antibodies against the DWNN/RBBP6 proteins (figure 2.1). Western blotting demonstrated that the anti-human DWNN antibody recognises other unexpected proteins and Matrix-assisted laser desorption/ionization Time-of-flight (MALDI-TOF) mass spectrometry was carried out on these proteins to identify them.

#### **4.1 Mutational analysis of RBBP6 binding domains**

The cell lines that were used in this study were the Hek 293T, a normal cell line and the cancerous cell lines (HeLa, HepG2 and MCF-7); all expressed all three RBBP6 transcripts. This was evident when RBBP6 domains were amplified using PCR with specific primers to the four domains. Figures 4.1 (A-D) show PCR products of the DWNN, RING finger, Rb- and p53-binding domains of the *RBBP6* gene. These results suggest that in cancers, DWNN domain and its related RBBP6 products are expressed as full gene products. This also suggests that the DWNN domain (also known as RBBP6 isoform 3) may be found in the human proteome. According to NCBI nucleotide database (figure 2.1), the anti-human

DWNN antibody should detect both DWNN and its associated RBBP6 isoforms. Successful amplification of the first RBBP6 domain and the last three binding domains, as well as no detectable mutations, suggests that RBBP6 may exist as wild-type in these cancers. The amplification of the RING finger, RbBD+ and p53BD in MCF-7 cells was visible only after nested PCR. This result suggested that the *RBBP6* gene may be down-regulated in breast cancer cells, or at least, in MCF-7 cells. Lane 3 in figure 4.1 D shows a very faint PCR product in MCF-7 cells, which is better visualized when nested PCR is performed.

The DWNN domain, RING finger domain, RbBD and p53-binding domains were amplified from HepG2, HeLa and MCF-7 cells and the normal control Hek 293T cells were cloned into a pGEM T-Easy vector and sequenced. The sequencer demo software was used to assemble two sequences from the sequencing primers (Sp6 and T7) against the NCBI reference sequence (RBBP6- NM006910). The NCBI blast tool was also used to align the sequences from the cells against the reference sequence. The sequence alignments of the sequenced domains versus the reference sequence (APPENDIX K) showed that the RBBP6 domains had no mutations which suggested that RBBP6 transcripts were expressed as normal in the cell lines investigated unless mutations are in-between these domain sequences.

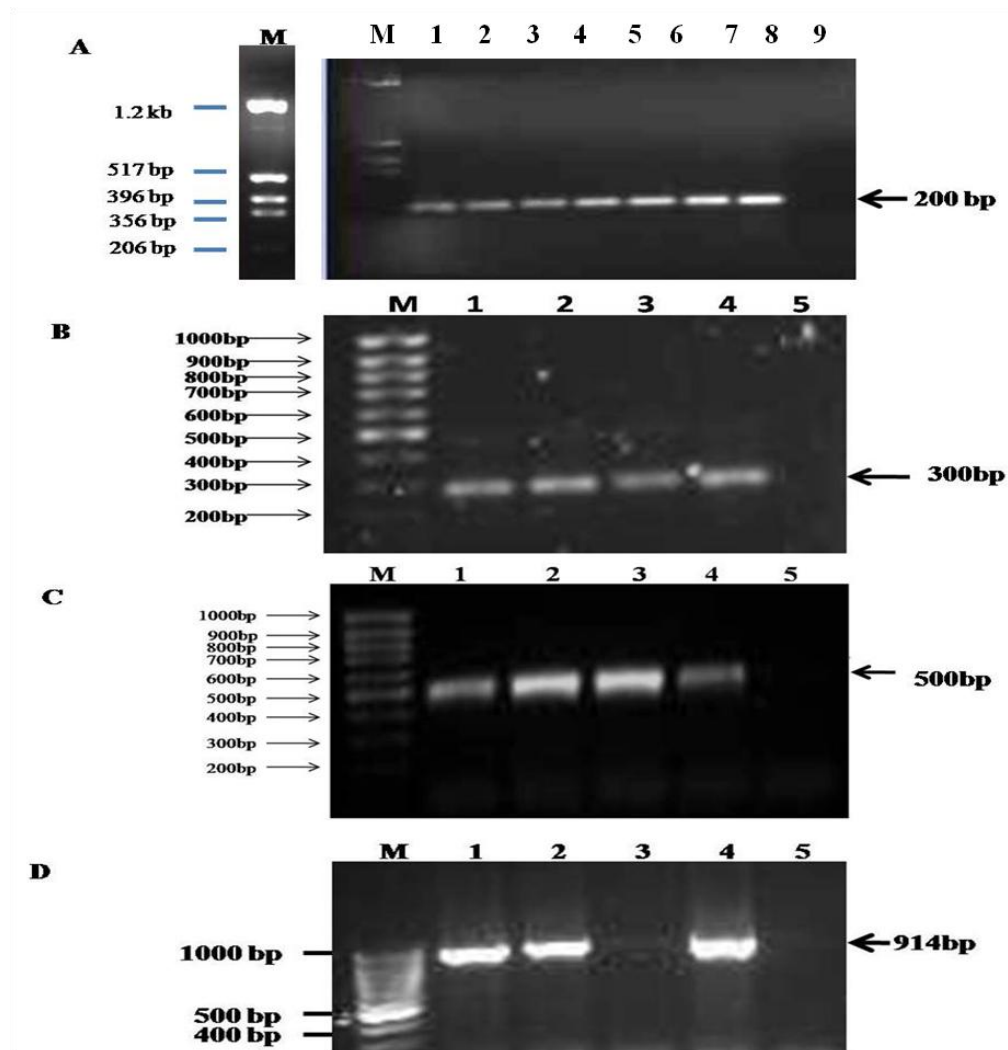


**Figure 4.1 – Amplification of the RBBP6 domains:** Agarose gel images showing the amplification of RBBP6 domain, that is, DWNN (A), RING finger (B), Rb-binding domain (C) and p53-binding domain (D). Figure 4.1A shows a marker (lane M), DWNN amplification in MCF-7 (lane 1), in HeLa (Lanes 2, 3), HepG2 (lane 4 and 5), WHCO (Lanes 6 and 7), Hek 293T (Lanes 8) and blank control (lane 9). Figure 4.1B shows the amplification of RING finger domain in HeLa (Lane 1), HepG2 (Lane 2), Hek 293T (Lane 3), MCF-7 (Lane 4), Blank control (Lane 5) and a molecular weight marker (Lane M). Figure 4.1C shows the amplification of RbBD in HeLa (lane 1), HepG2 (lane 2), MCF-7 (lane 3), Hek 293T (lane 4) and negative control (lane 5). Figure 4.1D shows p53BD amplification in HeLa (Lane 1), HepG2 (Lane 2), MCF-7 (Lane 3) where there was very little amplification and Hek 293T (Lane 4). Lane 5 represent a blank control where there was no template added.

## 4.2 Relative expressions of the RBBP6 transcripts in human cancer cell lines

For both characterization of the anti-human DWNN antibody and functional analysis of the DWNN and its RBBP6 family members, it was important to analyse the relative expression of the RBBP6 transcripts in different cell lines, so that an appropriate cell line could be used for knock-down analysis by RNA interference. This verification was also required to transfect the appropriate cell line with the DWNN and RBBP6 transcript 1 for over-expression studies (see chapter 6).

Relative Real-time PCR (section 3.3.8), using equal amounts of cDNA prepared from six cell lines as a starting template, showed that two cell lines, Hek 293T (non-cancerous kidney embryonic cells) and Jurkat cells (an immortalized line of T lymphocytes) had a higher expression of RBBP6 transcripts than the solid tumour cell lines investigated (HeLa, HepG2, MCF-7 and WHCO [an oesophageal carcinoma cell line]). The relative expression of DWNN and RBBP6 mRNAs was calculated using the comparative threshold cycle (Ct) method, a variation of Livak and Schmittgen's (2001) method. The relative expression formula:  $\text{Ratio (reference/target)} = 2^{\text{Ct (Reference)} - \text{Ct (Target)}}$  was used to normalize the expression using the reference housekeeping gene, hHPRT1. Table 15 (Appendix I) shows the average DWNN Ct values normalized with hHPRT1 and delta Ct for different cell lines. Table 16 (Appendix I) shows the average RBBP6 variants 1 and 2 Ct values normalized with average hHPRT1 Ct values for different cell lines. Figure 4.2 shows the calculated relative expressions comparing Hek 293T expression with the solid tumour cells; Hek 293T has a higher DWNN expression

than the solid tumour cell lines (figure 4.2A). Hek 293T also has a higher RBBP6 variant 1 expression than the solid tumour cell lines (figure 4.2B). Jurkats cells show a tenfold higher expression of both DWNN and RBBP6 variant 1 when compared to Hek 293T cells. Jurkats cells were the only cells that have a higher expression level of DWNN than the Hek 293T cells (figure 4.2C). Using GraphPad Prism (GraphPad Software, Inc., USA), a one way ANOVA was performed and the data was found to be statistically significantly different ( $P < 0.05$ ). The MCF-7 cells were found to have the lowest expression of DWNN and RBBP6 variant 1 and 2. The hHPRT1 primers were used as an internal control for these experiments. Raw data shows that hHPRT1 was expressed at similar levels in all the cell lines while the DWNN and RBBP6 demonstrated reduced levels consecutively in HeLa, HepG2, WHCO and MCF-7 cells. The WHCO cell line was also included as a positive control because the mouse RBBP6 homologue was reported to be highly expressed in oesophageal cancer (Yoshitake et al., 2004).

As this data suggest that DWNN and RBBP6 are down-regulated in human cancers at the mRNA level. The next logical query is whether DWNN and RBBP6 protein levels actually corroborate this?

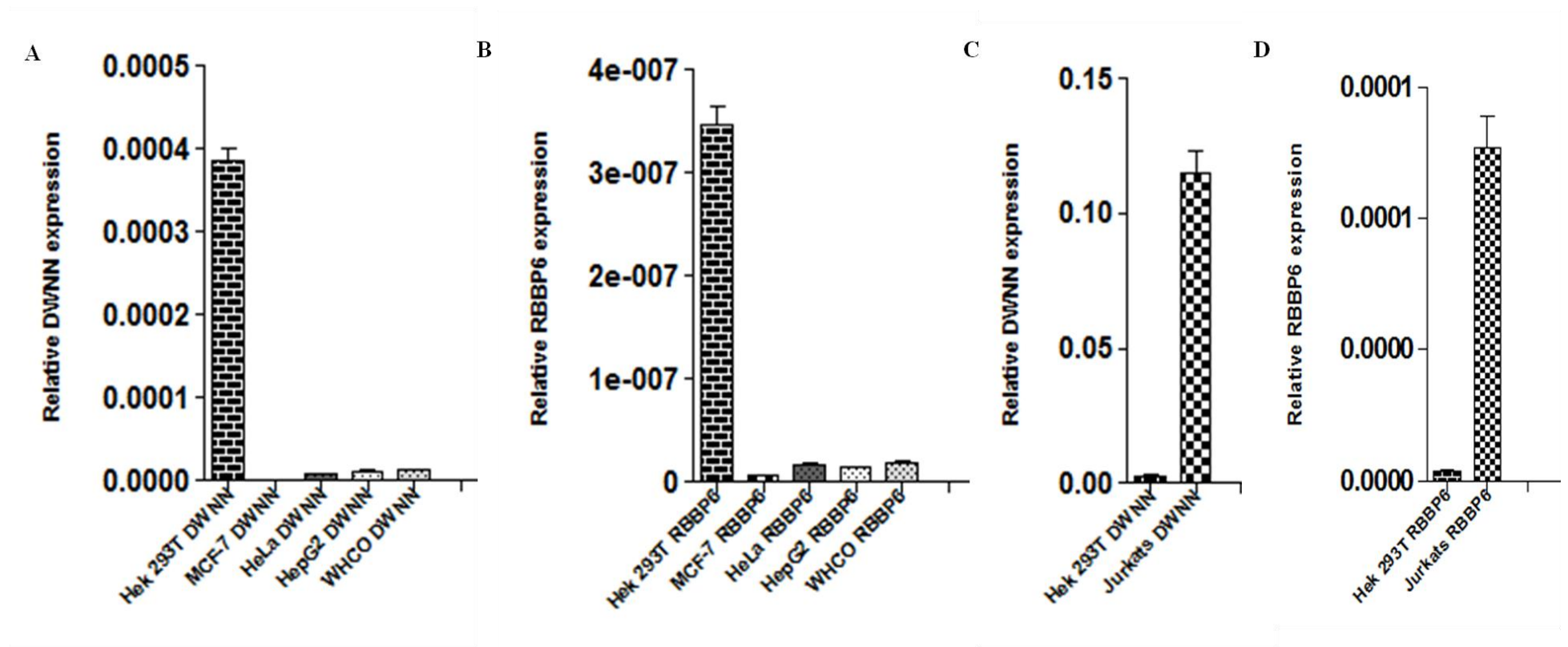


**Figure 4.2 (A-D) – The expression of the RBBP6 transcripts in human cell lines:** showing the relative expression of the DWNN and the RBBP6 transcript 1 using the optimised real-time PCR (Appendix I) in the different human cell lines used in this work in comparison to Hek 293T. The data was analyzed and presented in the graph as the mean  $\pm$  SD. A 1 way ANOVA test was performed and the data was found to be statistically significantly different ( $P < 0.05$ ) from three independent experiments. The DWNN and RBBP6 data was normalized to that of the house keeping gene, hHPRT1.

### **4.3 The anti-human DWNN antibody recognizes DWNN proteins and unknown proteins**

The DWNN polyclonal antibody was raised in rabbits against GST-DWNN fusion protein (Appendix J).

One dimensional gel electrophoresis and Western blotting showed that the anti-GST-DWNN antibody recognized the recombinant GST-DWNN protein (figure 4.3A) and the cleaved-off GST (figure 4.3B). The antibody additionally recognized a 15 kDa protein (thought to be the DWNN domain), and a ladder of bands that included a 120 kDa protein (unknown proteins) and 250 kDa protein bands (probably the RBBP6 isoforms 1 or 2). Figure 4.3C shows the absence of the 250 kDa protein in MCF-7 cells compared to Hek 293T cells. Figure 4.3D shows that equal quantities of the protein lysates were loaded. The ladder of bands could either be non-specific bands that may include human GST-related proteins or a DWNN domain attached or tagged to other protein products. The pre-immune serum did not show the DWNN domain, or the 120 kDa and the 250 kDa bands. This result suggested that the antibody was detecting the DWNN domain, the 120 kDa protein, possibly a GST-related or DWNN tagged protein and one of RBBP6's bigger isoforms. It is possible that the extra protein bands are due to the recognition of GST-related proteins. Figure 4.3B shows that the anti-GST-DWNN antibody recognized the cleaved GST tag suggesting that this antibody could also detect human GST-related proteins. To confirm this, a GST antibody (Santa Cruz Biotechnology, USA) was used on the human cell lysates to investigate whether it would recognize these GST-related antibodies.

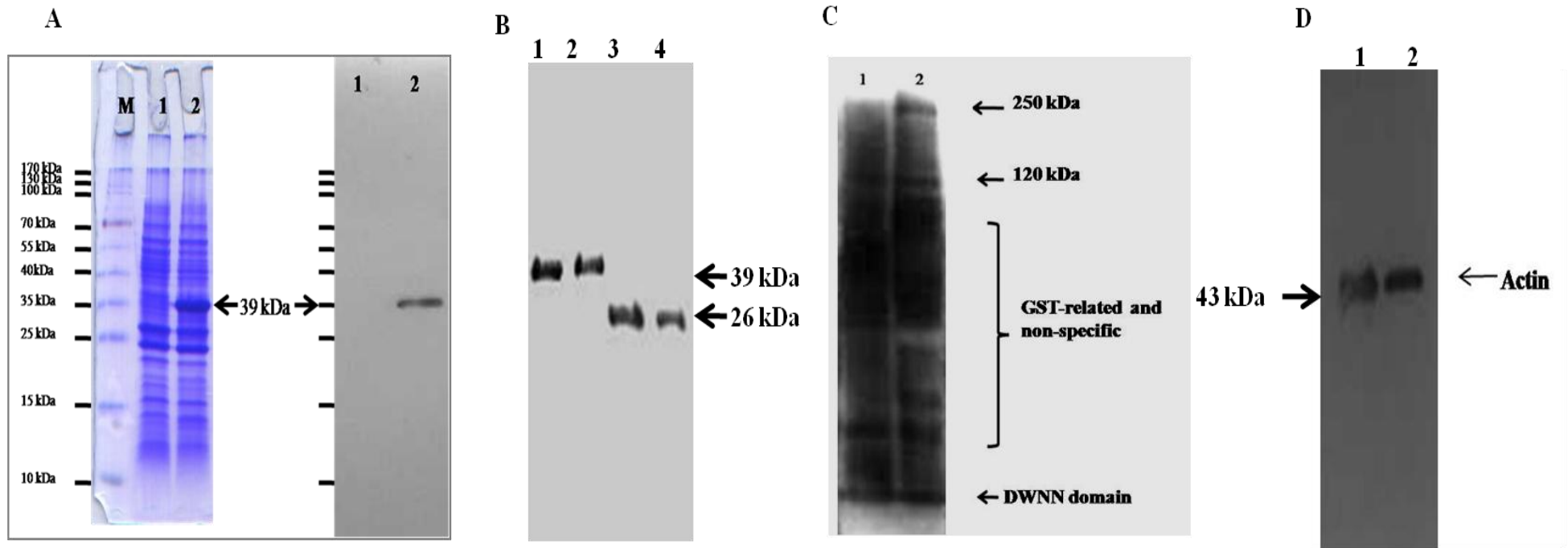


**Figure 4.3 – The recognition of multiple proteins by the Anti-GST-DWNN antibody:** Figure 4.3A shows the recombinant expression of the GST-DWNN (Lane 2) confirmed by Western blotting. Lane M represents a protein molecular weight marker. Lane 1 shows an uninduced bacterial total protein lysate and lane 2 shows an induced total bacterial lysate showing an induced protein band between 35 kDa and 40 kDa. Figure 4.3B shows Western blot with anti-human DWNN antibody on a 39 kDa GST-DWNN recombinant protein (lanes 1-2) and a 26 kDa recombinant GST protein (Lanes 3 and 4). Figure 4.3C shows a Western blot result with the anti-human DWNN antibody on MCF-7 cell lysate (Lane 1) and Hek 293T cell lysate (Lane 2). In both lanes there were either GST-related proteins or non-specifically bound proteins and in addition three proteins were detected in Hek i.e. 15 kDa; ~120 kDa and 250 kDa proteins. In lane 1 there was no 250 kDa protein detected. Figure 4.3D shows loading control using actin antibody.

A pre-absorbed antibody with GST-DWNN fusion protein served as a negative control. A second negative control was the use of pre-immune serum from all the rabbits immunised to raise this antibody. To determine whether the antibody detects GST-related proteins in human, an anti-GST antibody was used on MCF-7 and Hek 293T total protein lysates using a Western blot analysis. An identical Western blot was probed with anti-Human DWNN antibody. Figure 4.4A shows anti-human DWNN polyclonal antibody reactivity to two protein bands on one-dimensional SDS PAGE gel. One of these proteins is approximately 120 kDa and is most probably a DWNN domain associated protein, while the second protein is approximately 50 kDa and is most likely to be a human GSTs or GST related protein. Figure 4.4B also confirms that the 50 kDa protein is a mammalian GST-related protein as this band was labelled when an anti-GST antibody was used on the same cell line protein lysates. Pre-absorption of the polyclonal anti-human DWNN antibody with GST recombinant protein also confirmed that the smaller second band was a GST-related protein band as figure 4.4C showed that only the larger DWNN-associated protein band was labelled. All the RBBP6 isoforms contain the DWNN domain and should therefore be detected by the antibody against the DWNN domain. The RBBP6 isoforms have been both predicted to, and reported to give rise to 250 kDa proteins (Altschul et al., 1997, Simons et al., 1997), while the DWNN domain is predicted to be 13 kDa ([www.expasy.org](http://www.expasy.org)) as shown in figure 4.3 and most probably a 15 kDa protein due to post-translational modification of a 13 kDa DWNN domain. The results obtained were both expected and unexpected in the sense that the 15 kDa and approximately 250 kDa proteins were expected, while the suspected GST-related and the 120 kDa proteins

were unexpected. Figure 4.4 C confirms that the bigger protein detected contained DWNN, though the signal was weak because the GST-preabsorbed antibody could no longer detect the GST-related proteins while it could still detect the DWNN-associated proteins.

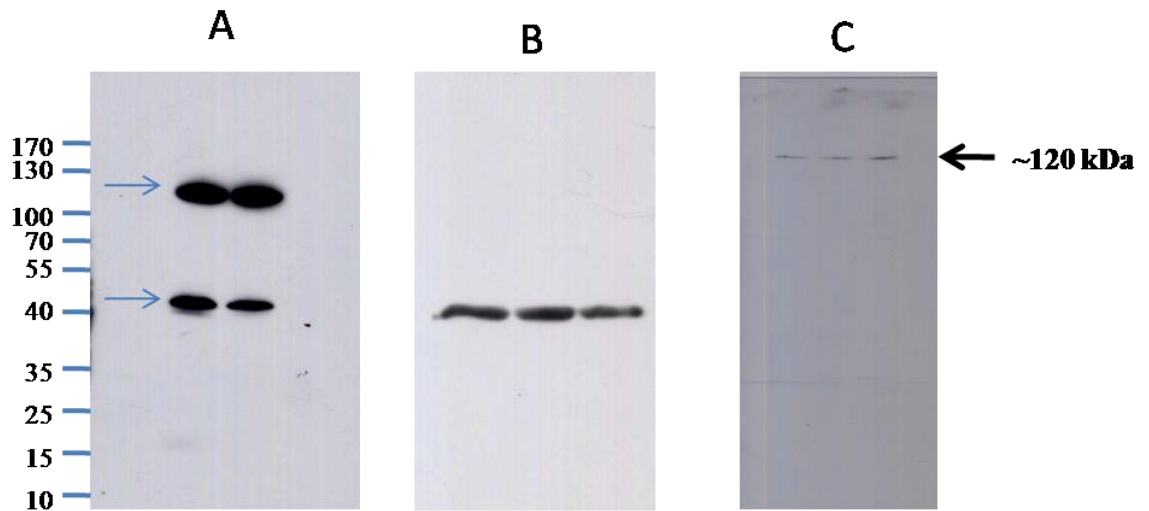


**Figure 4.4- Reaction of the DWNN polyclonal antibody with GST- and DWNN-related proteins:** This figure shows Western blot results using the anti-Human DWNN antibody on MCF-7 and Hek 293T cell lysates (A), an anti-GST antibody applied to MCF-7, HeLa and Hek 293T cell lysates (B) and a GST pre-absorbed anti-Human DWNN applied to the same lysates (C).

In all the human cancer cell lines used, a DWNN associated protein product was observed. The DWNN domain and its associated proteins were detectable with the GST-related band labelled in all of these cell lines. These included cervical carcinoma cells (HeLa), kidney embryonic epithelial (Hek 293T), breast cancer (MCF-7), hepatocellular carcinoma (HepG2) and acute T cell leukaemia (Jurkat) cell lines. These results suggested that a pure anti-DWNN antibody could be obtained by binding anti-GST isotopes to immobilised glutathione molecules. In

figure 4.4 (C) it was shown that the purification step reduces the signal of the DWNN associated protein. It is suggested that the DWNN associated protein labelled could be associated with the DWNN domain by attaching to these other proteins through the ubiquitination-like process, as the DWNN has a ubiquitin like fold (Pugh et al., 2006).

### **4.3 DWNN domain may bind and modify other proteins**

Ubiquitination plays a role in protein stability and stable proteins are important in the execution of different biological functions that are involved in cell homeostasis (Amemiya et al., 2008). Ubiquitin protein molecules are attached to ubiquitin proteasome targeted proteins for degradation (Schreiner et al., 2008). There are many other ubiquitin-like proteins that are also protein modifiers and play roles in either degradation or stabilization of proteins. These include Sumo-1 (Matic et al., 2008) and Nedd8 (Bornstein et al., 2006). It has also been suggested but never been shown, that the DWNN domain is a ubiquitin-like protein modifier (Chibi et al., 2008, Pugh et al., 2006). The detection of multiple bands (figure 4.3) suggested that this protein may either be tagged to other or posttranslationally modified. The purification of the antibody using affinity purification suggested that the 120 kDa protein (figure 4.4) may be posttranslationally modified RBBP6 isoform 3 (DWNN) or tagged to another protein. Using two dimensional gel electrophoresis, anti-DWNN antibody and MALDI-TOF Mass spectrometry, the possible DWNNylation (possible tagging of other protein with DWNN domain) was investigated.

### **4.3.1 DWNN domain may be endogenously associated with other protein products**

The purified anti-Human DWNN polyclonal antibody demonstrated that the DWNN exists in human cells and is either covalently attached to a bigger protein product or posttranslationally modified as well as a DWNN protein. It was expected that the anti-human DWNN antibody would detect the three RBBP6 isoforms as shown in figure 4.3C. As previously suggested that the DWNN domain shares a similar protein structure with ubiquitin, the possibility of the DWNN being tagged to and modifying other proteins was not discounted.

Two-dimensional gel electrophoresis coupled with Western blotting was used to determine whether this association could be further clarified, or alternatively, it was investigated whether denaturing conditions would release the DWNN domain from complexes postulated.

Using one dimensional SDS PAGE, figure 4.5 shows that the purified anti-human DWNN polyclonal antibody detected high molecular proteins in different cell line lysates extracted with 9M Urea buffer. In all the cell lines, the DWNN domain at the 15 kDa region and the higher molecular weight protein bands were also detected, which suggested that there might still be DWNN domain bound to a bigger protein or posttranslational modification protein. While the possibility of this higher molecular weight protein consisting of degradation products of the RBBP6 isoforms 1 and 2 was highly unlikely because this protein band seemed stable, with no visible smearing, suggestive of degradation. Urea denatures proteins and disassembles protein complexes. The use of 9M urea extraction buffer showed a size decrease of the 120 kDa proteins (seen with RIPA buffer) to

approximately 100 kDa as shown in figure 4.5A. This suggested that DWNN may be a covalent modifier of certain proteins and confirms that the high molecular protein band is an antibody reaction to DWNN associated with another protein or possible posttranslational modified DWNN. This result also suggested that this association could be with more than one DWNN associated protein molecule, because dissociation of the DWNN domain from the unknown protein should have resulted in the loss of signal altogether. Figure 4.5 shows that in all the cell lysates extracted with the urea buffer, the DWNN was observed and possibly had been released from protein complexes. This further suggested the attachment of the DWNN domain molecules to more than one protein.

Figure 4.5 shows that all the human cell lines express all the human RBBP6 proteins with a notable low expression in breast cancer cell line, MCF-7. Both the high percentage acrylamide gel (figure 4.5A) and the low percentage gel (figure 4.5C) showed a ladder of bands, with MCF-7 cells showing low expression of the RBBP6 proteins. Figures 4.5B and D shows an actin loading control. Together, this data suggests that the DWNN domain/RBBP6 is a ubiquitin-like modifier. Two dimensional gel electrophoresis was employed to attempt the identification of the possibly “DWNNylated” proteins.

Western blotting of the two dimensional protein gel confirmed that the anti-human DWNN protein detected other proteins besides the DWNN domain and RBBP6 bigger isoforms. The proteomes for the human cell lines were established and used to investigate the identity of the possibly “DWNNylated” proteins in the human cell lines.

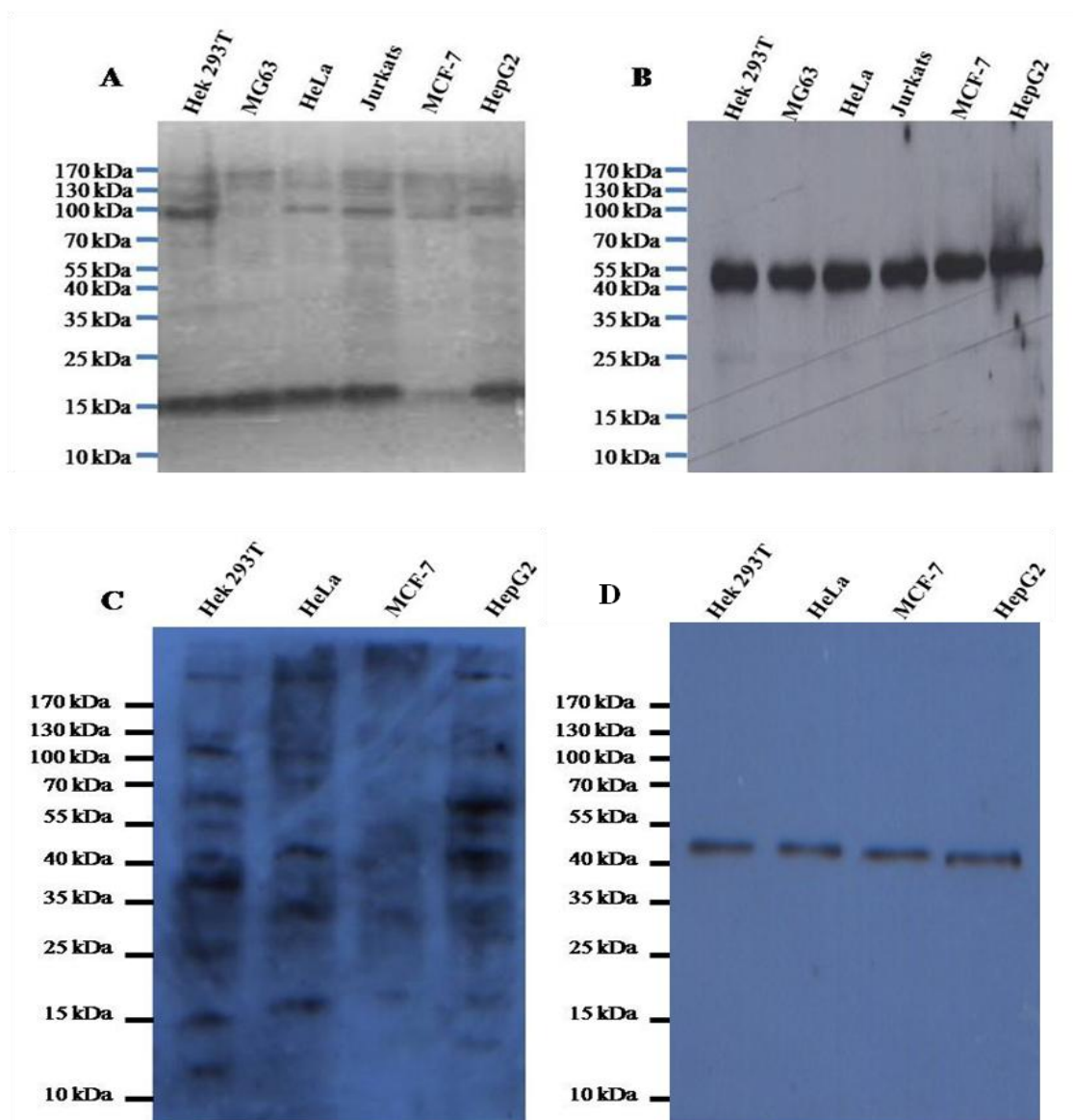


**Figure 4.5 – A possible protein “DWNNylation”:** This figure shows that the anti-human DWNN antibody recognizes all the RBBP6 isoforms. Figure 4.5A shows the detection of  $\pm 100$  kDa proteins and 15 kDa proteins in human cell lines on a high percentage acrylamide gel. Low expression of the DWNN domain and its associated protein were observed in MCF-7 cells by using an actin antibody loading control (figure 4.5B). The antibody (figure 4.5C) detected the 250 kDa RBBP6 protein and other proteins. Again MCF-7 showed low expression when compared to the actin antibody loading control (figure 4.5D).

### **4.3.2 Human cancer cell line 2D proteome establishment**

The observation that the DWNN domain/RBBP6 isoform 3 may be covalently linked to another protein or proteins instigated the more sensitive blotting of 2D gels, in order to determine which proteins the anti-human DWNN antibody detects. The cell lines used to extract proteins for Western blotting were Hek 293 cells (normal), HeLa cells (cancerous), HepG2 cells (cancerous) and MCF-7 cells (cancerous)

Figure 4.6 shows proteomes of a non-cancerous human embryonic kidney cell (Hek 293T) and that of a cancerous human cell (MCF-7) respectively. There was a noticeable difference between the two proteomes in respect to protein distribution. These may be different in terms of protein composition between proteomes, but Coomassie Blue and Flamingo Pink staining was not sensitive enough to detect the less abundant proteins. The proteins from these 2D gels were subjected to Western blotting to determine whether the anti-human DWNN antibody (both the GST-contaminated and purified) would react with more proteins or just the protein detected in the one dimensional gel electrophoresis and to further confirm non-specificity of the contaminated antibody.

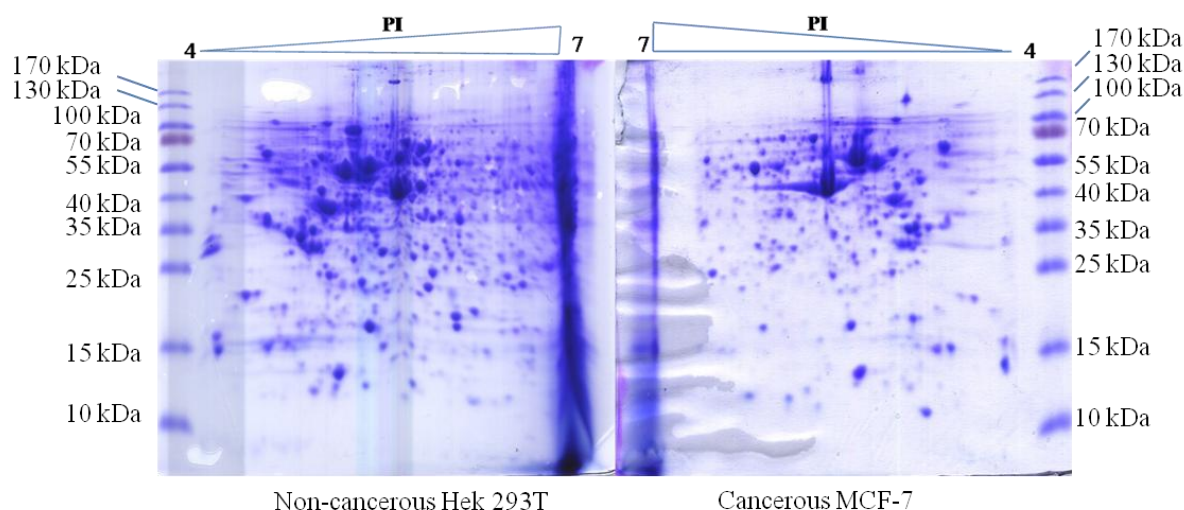


**Figure 4.6 – Non cancerous human embryonic kidney cell proteome and cancerous cell proteome:** This figure shows two proteomes of Hek 293T and MCF-7 cells.

#### **4.3.3 Confirmation of non-specificity of the GST-contaminated anti-human DWNN antibody**

For the purpose of determining whether the DWNN antibody detects more than one protein or just the DWNN proteins, a 2D gel technique (3.3.12.7) was used. The denaturing conditions of this method make it possible to separate proteins into individual protein spots for further characterization. The urea extraction buffer disrupts hydrogen and hydrophobic bonds denaturing proteins, producing suitable samples for isoelectric focussing and separating proteins according to their charges before the second dimension separation according to size. This method should make it possible to disrupt any protein complexes and results in isolated proteins (Chevalier et al., 2009, Ludvigsen et al., 2009). Figure 4.7 shows that the non-specific anti-Human DWNN antibody reacted with a number of proteins from non-cancerous Hek 293T cells and MCF-7 cells. Both results demonstrate a non-specific reaction. These results suggested that DWNN may be covalently linked or bound to other proteins in human cell systems and that the

contaminating GST antibodies results in non-specific reaction in both proteomes. The presence of more than two protein spots suggests that the DWNN domain may be a ubiquitin-like modifier and is tightly bound to other proteins. In both the Hek cells and the MCF-7 cells, there were two spots in the 15 kDa region. These spots may be two DWNN domain products with the larger one due to post-translational modifications, that is, phosphorylation or glycosylation, the two most common post-translational modifications (Liang et al., 2006, Yamakoshi et al., 2008). The anti-human DWNN antibody was raised against the GST-DWNN fusion protein and that is the reason it detects both DWNN-associated and GST-related proteins. Protein spots detected at the 15 kDa and 100 kDa regions could be DWNN-containing protein because the Western blot on 1D gel detected proteins at the same regions (figure 4.5).

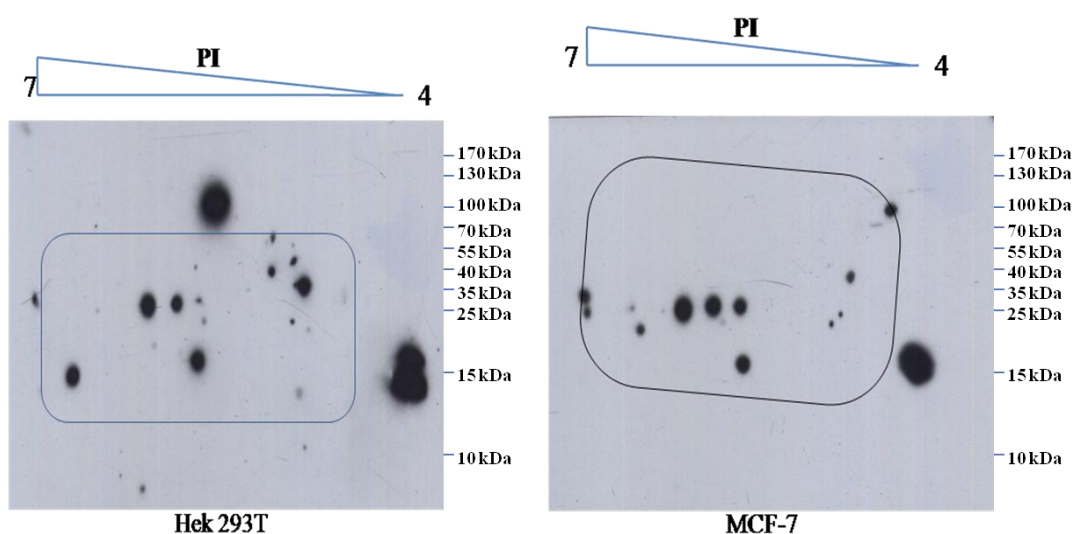


**Figure 4.7 - 2D Western blot on Hek 293T and MCF-7 cells:** These figures show a number of protein spots detected by anti-human DWNN antibody in both Hek 293T and MCF-7. The circled protein cluster shows what could be non-specific detection. At 15 and 100 kDa strong protein spots were detected by the anti-human DWNN antibody in Hek 293T cells while in MCF-7 cells the higher molecular weight protein at approximately 100 kDa shifted from the neutral to the more acidic pI.

#### **4.3.4 Anti-DWNN antibody reacts with GST related proteins, DWNN and its related proteins**

Purification of the anti-DWNN by GST pre-absorption resulted in a more specific antibody that reacted with fewer spots. Figure 4.8 shows anti-human DWNN reacting with two protein spots at the 15 kDa region at a PI of about 4.5; one spot at about 100 kDa at a PI of approximately 5 and a spot at approximately 40 kDa at a PI of 7. This procedure reduced the unidentified proteins detected by the contaminated un-purified antibody. This result suggested that the polyclonal anti-human DWNN antibody contained non-specific antibodies which were removed by pre-absorbing the antibody with GST.

It was observed that the anti-human DWNN antibody showed a reaction to GST related proteins as the use of an anti-GST antibody labelled most of the spots detected by the un-purified anti-human DWNN antibody. To confirm that the non-specific proteins were due to the effects of contaminating GSTs, an anti-GST antibody was used on Hek 293T proteome. Figure 4.8 also shows that most of the protein spots detected by the unpurified anti-human DWNN antibody were human GST-related proteins, thus demonstrating that the antibody was also reacting with GSTs and related proteins (compare with figure 4.7). Additionally, protein spots of approximately 50 kDa were detected with the anti-GST antibody further suggesting the non-specificity of the un-purified anti-human DWNN polyclonal antibody.

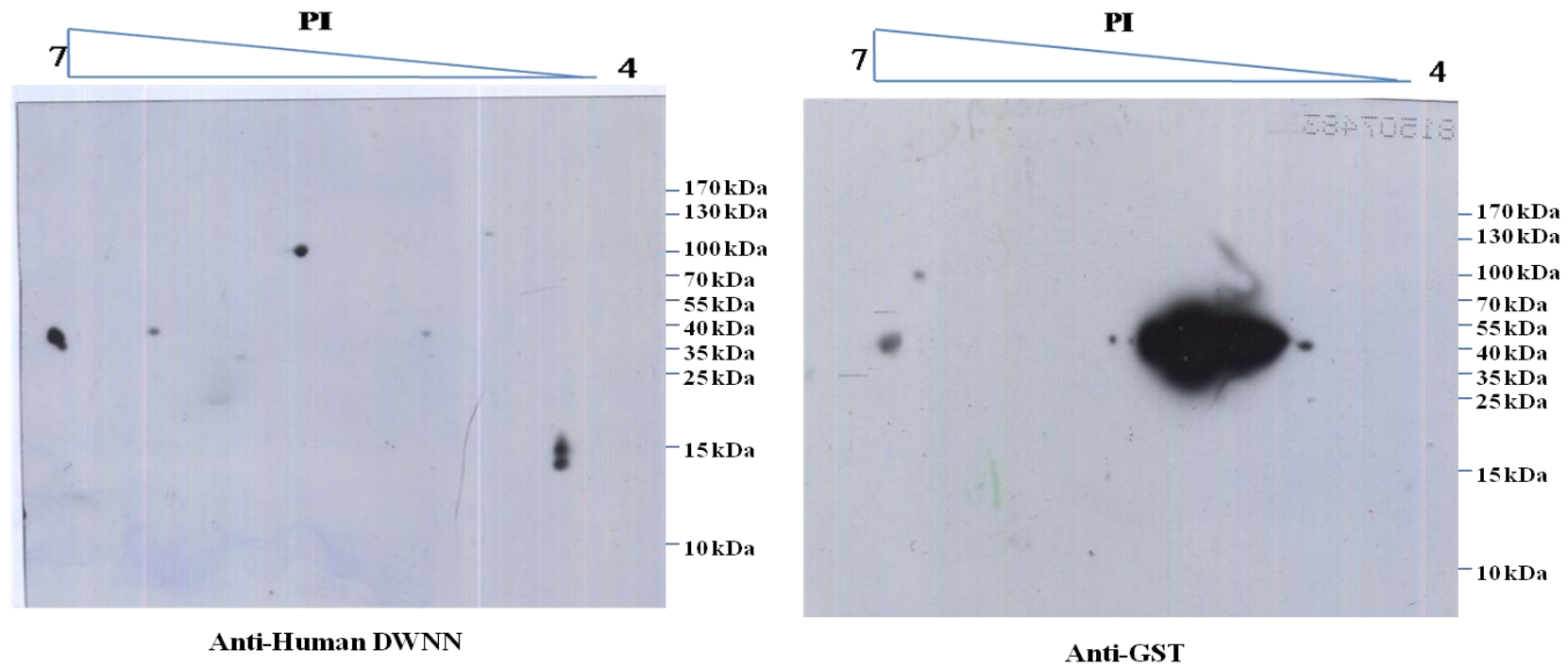


**Figure 4.8 – 2D Detection of the DWNN domain by partially purified anti-human DWNN antibody and GST-related antibodies by anti-GST antibody:** This figure shows that a partially purified anti-human DWNN antibody detects a few protein spots that include two spots, 1 of approximately 15kDa and the second one of just above 15kDa. The antibody also detected few protein spots between 35 kDa and 70 to 100 kDa range. The anti-GST antibody detects some of the spots detected with the DWNN antibody in Hek 293T cells.

In figure 4.8, the purified anti-human DWNN antibody detected two protein spots at the 15 kDa region where the DWNN was expected to be detected. There were two spots, with one just smaller than 15 kDa, suggesting that this 15 kDa spot could be a DWNN domain post-translationally modified. To investigate this, the DWNN-expressing plasmid was introduced into Hek 293T cells so that the DWNN protein would over-express, to determine if the same pattern of protein distribution would be evident, thus testing/assessing whether the over-expressed protein would have a similar pattern of electrophoretic migration to the two 15 kDa spots detected by the purified anti-human DWNN antibody.

Figure 4.8 shows that the DWNN domain was positive to anti-DWNN antibody. This figure also shows that the DWNN protein exists in two sizes of small difference that were migrating at the 15kDa range on the 2D gels. This result suggests that these spots were DWNN domain spots with one possibly phosphorylated (figure 4.9) or glycosylated (figure 4.10). This figure demonstrates that the anti-DWNN antibody does recognize the DWNN domain and its related proteins.

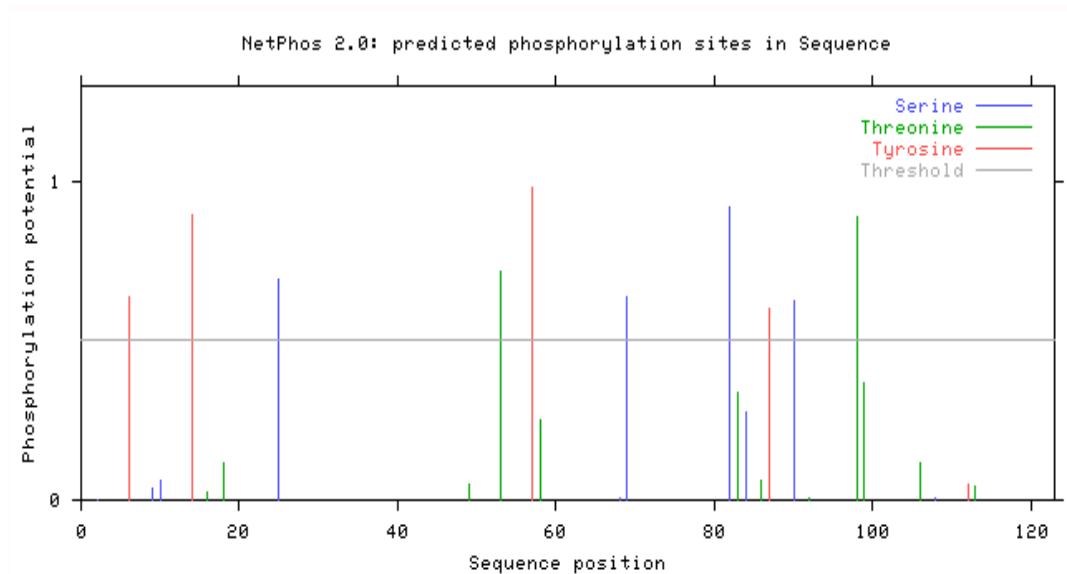


**Figure 4.9 - NetPhos 2.0 server prediction phosphorylation sites in the DWNN domain:** This figure shows that the DWNN has 10 hot phosphorylation sites as gauged by the threshold horizontal line. There are 4 serine, 2 threonine and 4 tyrosine phosphorylation sites, making up 10 phosphorylation sites.

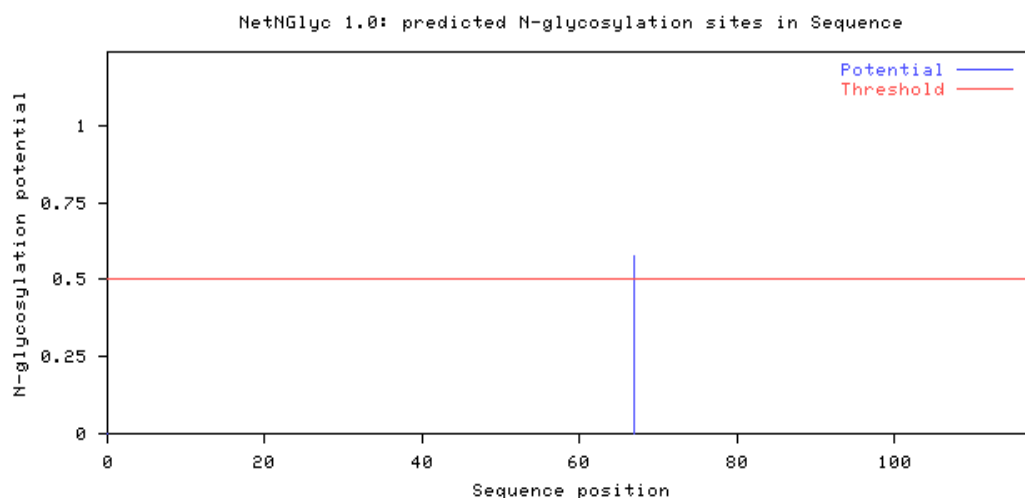


**Figure 4.10 - Glycosylation prediction using a NetGly 1.0 server in the DWNN domain:** This figure shows the single glycosylation site in the DWNN domain that is above the threshold for glycosylation.

#### **4.3.5 Identification of the unknown proteins detected by the anti-human DWNN using Mass Spectrometry**

The mass spectrometric techniques would have been easier if the spots recognized by the anti-DWNN antibody were visible on the 2D gels. The Matrix-assisted laser desorption/ionization top-of-flight (MALDI-TOF) mass spectrometer at the University of the Western Cape had been optimized for Coomassie Blue and Flamingo-Pink-stained gels and these were not sensitive enough to detect the smaller protein spots. The silver staining method, which is the most sensitive stain, could not be used as it was not compatible with the MALDI technique used. The protein spots stained with three gradient concentrations of Coomassie Blue (to increase visibility of faint protein spots) that were detected by anti-human DWNN antibody were excised from the 2D Western blotting. These spots were subjected to mass spectrometric analysis (section 3.3.12.8) and this technique was chosen to solve the identity of the protein spots unexpectedly detected by the anti-human DWNN antibody (figure 4.11).

After the protein spots were subjected to MALDI-TOF, peptide masses were obtained and were used to search the Mascot server for protein identities. Six spots were positively identified. The Mascot server uses Protein score as a  $-10 \cdot \log(P)$ , where P is the probability that the observed match is a random event and Protein scores greater than 67 are significant ( $p < 0.05$ ) [<http://www.matrixscience.com>]. Different spots (figure 4.11A and B) showed different results identifying different proteins (figure 4.12), suggesting that the DWNN domain may be forming complexes with different proteins and may be

either part of the immune system or reacting non-specifically with human IgGs.

The summary of proteins identified is given in table 4.1.

The MS data showed that the anti-human DWNN antibody may not be detecting human GST as suspected. These results suggest a very complex network of proteins that the DWNN domain may interact with. Some of the identified proteins are hypothetical proteins and some are unknown proteins. Recoverin and hypothetical protein XP were identified with the DWNN peptides. This result suggests either that the DWNN could be a modifier of these two proteins or these proteins are involved in DWNN regulation or there is covalent attachment of DWNN to these proteins.

The absence of DWNN peptides in spot 1, identified to contain peptides of Amyotrophic lateral sclerosis 2 chromosomal region candidate gene 11 protein isoform 4 and unnamed protein, suggests either that the DWNN could be modifying these proteins or the DWNN domain is regulated by these proteins, but could not identify its peptides may be because this technique is not sensitive enough for purposes of the present study. Another possibility is non-specificity on the other spots. These results therefore further suggest the possibility of the DWNN being a novel ubiquitin-like modifier of the above mentioned proteins.

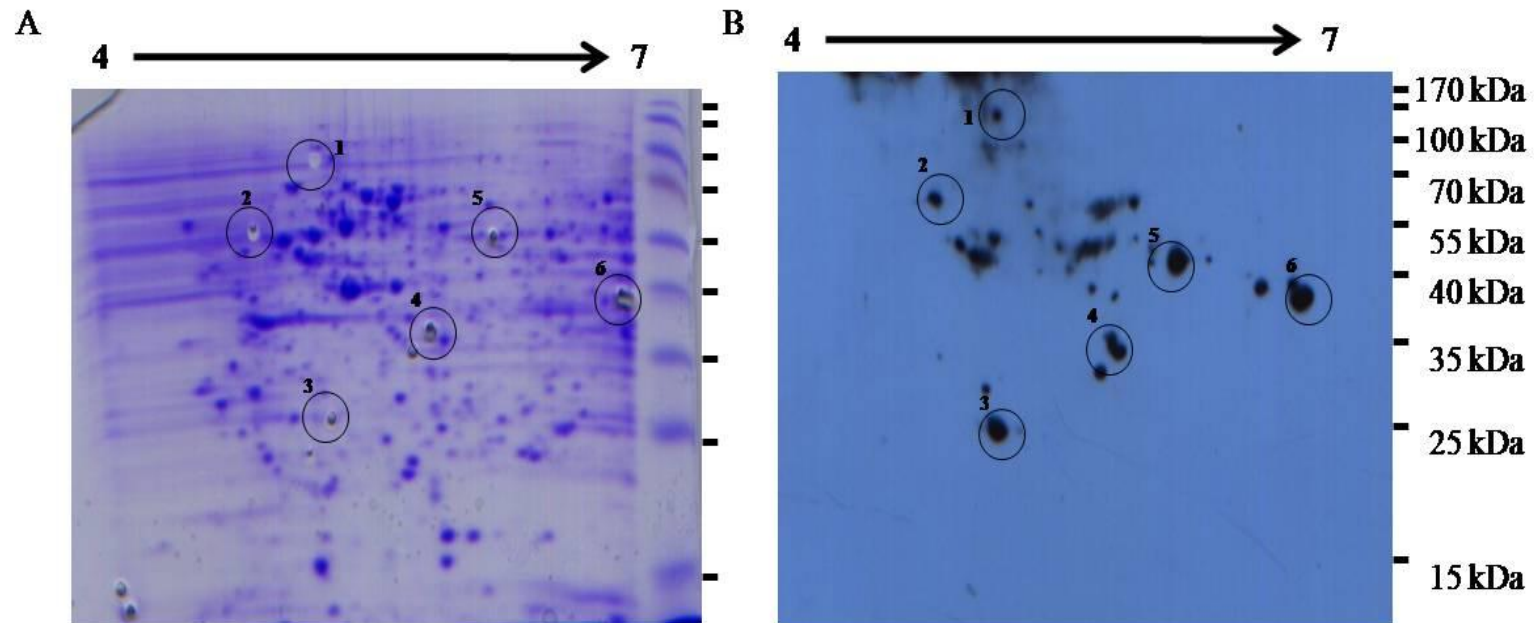


**Figure 4.11 – Identification of proteins recognized by the anti-human DWNN antibody:** This figure shows several prominent protein spots detected by the anti-human DWNN antibody. Figure A shows the number of spots that were subjected to MALDI-TOF because of their reaction with the antibody on figure B.

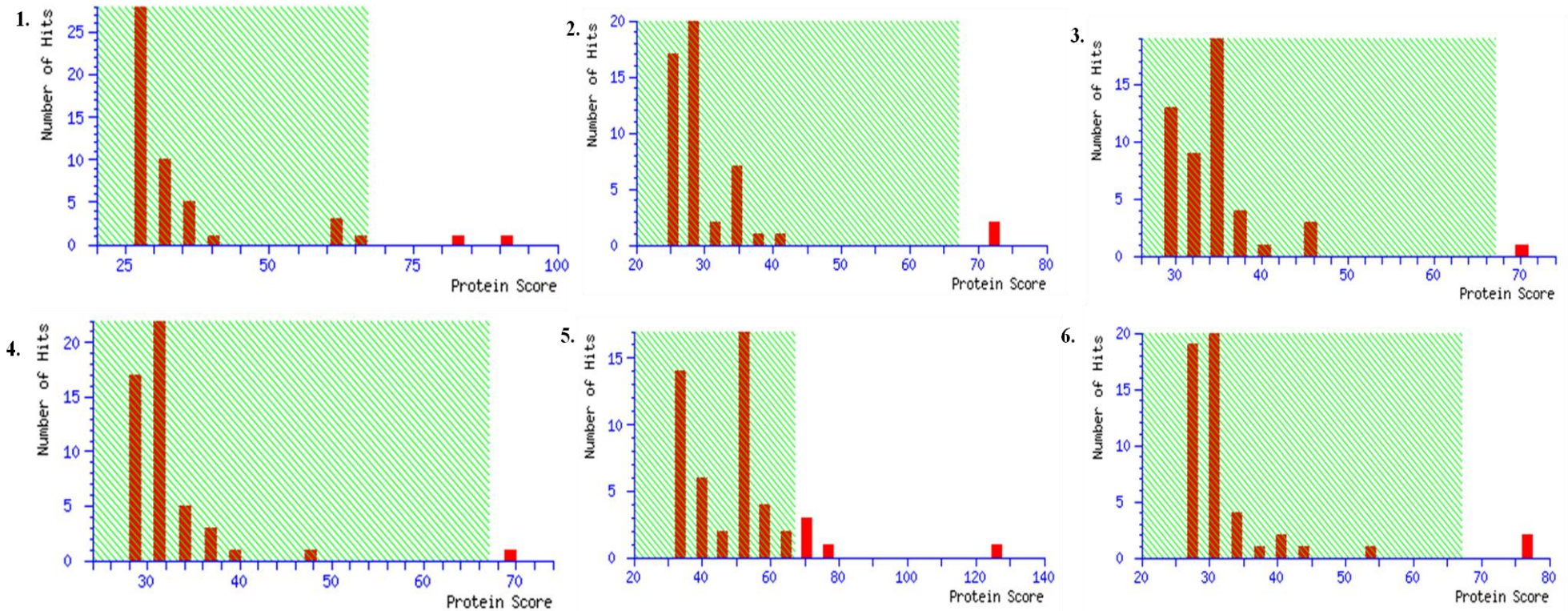


**Figure 4.12 – Mascot protein scores for protein identification:** Figures showing protein scores for the identification of protein identities from the MALDI-TOF mass spectrometry. The numbers next to each protein score correspond to spot ID given in figure 4.11 and table 4.1. Two significant protein scores for spot 1 were obtained, while spot 2 had 1 significant protein score and so forth.

**Table 4.1: Identification summary of the protein spots detected by the anti-human DWNN antibody.**

Spot ID	Accession No.	Protein Identification	Mowse score	Theoretical Mw	Theoretical pI	Expert error	Sequence coverage	No. Of matching peptides
1	NP_001161688	1. Amyotrophic lateral sclerosis 2 chromosomal region candidate gene 11 protein isoform 4	91	45198 Da	6.81	0.00019	49%	13
	<u>16554102</u>	2. Unnamed human protein	81	45189 Da	6.77	0.002	44%	12
	NP_116015	amyotrophic lateral sclerosis 2 chromosomal region candidate gene 11 protein isoform 3	66	62372	5.73	0.071	31%	12
2	<u>3293409</u>	Immunoglobulin heavy chain FW2-JH region	72	7725	8.07	0.015	52%	3
3	NP_116015	1. RBBP6 isoform 3	70	13227	9.08	0.034	48%	6
	XP_002342450	2. Hypothetical protein XP_002342450	46	28901	12.07	6.3	34%	4
4	<u>41393490</u>	Unknown protein	69	13516	6.20	0.029	58%	6
5	<u>6010164</u>	T-cell receptor delta chain	126	10686	8.59	6.3e-08	80%	7
	<u>221044630</u>	Unknown protein	68	15866	9.34	0.04	35%	5
6	RECO_HUMAN	Recoverin	77	23116	5.06	0.0054	38%	5
	NP_116015	RBBP6 isoform 3	43	13227	9.08	12	21%	4
BSA	<u>ABBOS</u>	Bovine serum albumin precursor	77	69225	5.78	0.026	19%	12

## **Chapter Five: Localization and Expression of the DWNN in human cancers**

---

### **5.1 Introduction**

In chapter three, it was demonstrated that DWNN and other RBBP6 variants and isoforms are expressed in different human cancer cell lines. In this chapter, expression pattern analysis of the DWNN and RBBP6 variants and isoforms was investigated using Fluorescent *in situ* hybridisation (FISH) (section 3.3.10), immunohistochemistry (IHC) and immunocytochemistry (section 3.3.9) to detect the RBBP6 transcripts and isoforms *in situ* respectively. A DWNN RNA probe (section 3.3.10.1-2) and purified DWNN antibodies were used to detect RBBP6 mRNA and protein respectively. The variant 3 (figure 2.1A) fragment of the DWNN cDNA was cloned into pGEM-T Easy vector and sequenced (Inqaba Biotech. Co, South Africa). The antibody that was characterized and purified as reported in chapter four was used in the immunohistochemistry and immunocytochemistry experiments.

A DWNN domain coding region was shown to have been successfully labelled with digoxigenin (DIG). This probe specifically detects the DWNN containing mRNAs. This data is based on BLAST analysis and was used to localize the RBBP6 mRNAs in breast cancer, cervical cancer, hepatocellular carcinoma and other neoplasias. An anti-human DWNN antibody was used to localize RBBP6 proteins containing the DWNN domain in these human cancers.

### **5.2 The generation and characterization of the labelled DWNN probe and specificity**

The DWNN domain coding region was successfully amplified by PCR (section 3.3.4), cloned into pGEM-T-Easy vector (section 3.3.6) and sequenced (section 3.3.7). The cloned DWNN fragment was prepared for DIG labelling as described in

section 3.3.10.1 and labelled with DIG as described in section 3.3.10.2. The labelled RNA probes were then used in both *in situ* hybridization techniques (ISH and FISH). Appendix I1 shows the purification of the DNA fragment that was used for preparing the DWNN probes (antisense and sense probes). Figure 5.1B shows the specificity of the probe by sequence alignment using BLAST. The sequence alignment shows a 100% identity to RBBP6 transcripts in the DWNN domain coding region.

### **5.3 Estimation of the DWNN probe**

The DWNN and control RNA probes were labelled with DIG as described in section 3.10.1-2 and the concentration of the labelled probes was estimated as described in section 3.10.3. Appendix I2 shows the detected probes labelled with anti-DIG Fab conjugated to alkaline phosphatase. The bound antibody was visualized with NBT/BCIP (purple colour precipitate on the nylon membrane). The labelled RNA probes were estimated by comparing the spot intensity to that of the control labelled probes (Appendix I2).

### **5.4 Expression pattern of the DWNN domain containing mRNAs in human cancers**

DIG labelled RNA probes were used for the detection of the RBBP6 mRNAs. After hybridization, these were then detected using anti-DIG-alkaline phosphatase or anti-DIG-Flourescein secondary antibodies. The alkaline phosphatase tag is visualised via hydrolysis of Nitro blue tetrazolium chloride/5-bromo-4chloro-indolyl phosphate, toluidine salt (NBT/BCIP) resulting in purple precipitate, thus indicating a probe-target hybrid. Using fluorescence microscopy, the anti-DIG-Flourescein is excited at a wavelength of 490 nm to emit a green fluorescence at the site of the probe-target hybrid.

A comparison between the different cancers tested (figures 5.1 to 5.6) shows that DWNN-containing mRNAs (RBBP6) are expressed only in small quantities in the solid tumours that have been investigated in the present study. This result was obtained with both ISH and FISH. ISH and FISH demonstrated little localization of RBBP6 mRNA in the cytoplasm and cell surface indicating the position of the DWNN mRNAs in these tumours. In the corresponding normal tissues however, the DWNN mRNA is expressed by few cells around the island of the tumour, showing nuclear staining, while the island of the tumours did not show any staining.

To address the issue of non-specific detection and to establish whether the antisense probe was specific, an RBBP6 sense probe was used to determine whether it would detect non-specific mRNAs as there was no fluorescent signal. Figure 5.1A shows that the sense probe did not detect any mRNA. In oesophageal carcinoma the RBBP6 gene products have been shown to be highly expressed when compared to normal oesophageal cells (Yoshitake et al., 2004). Figure 5.1A shows that there is no labelling of RBBP6 mRNAs in oesophageal carcinoma compared to the antisense probed oesophageal carcinoma (Fig 5.1B).

In oesophageal carcinoma tissue (a positive control in this study), RBBP6 has been reported to be expressed although it is not expressed in normal cells (Yoshitake et al., 2004). In the present study, RBBP6 mRNA was detected in some nuclei while other cells showed cytoplasmic localization of the RBBP6 mRNA; Figure 5.1B shows that the positive control had RBBP6 mRNA nuclear localization. This is clearly illustrated in figure 5.1B wherein the positive control has cells with nuclear localization of RBBP6 mRNA, and cells with cytoplasmic staining for this mRNA.

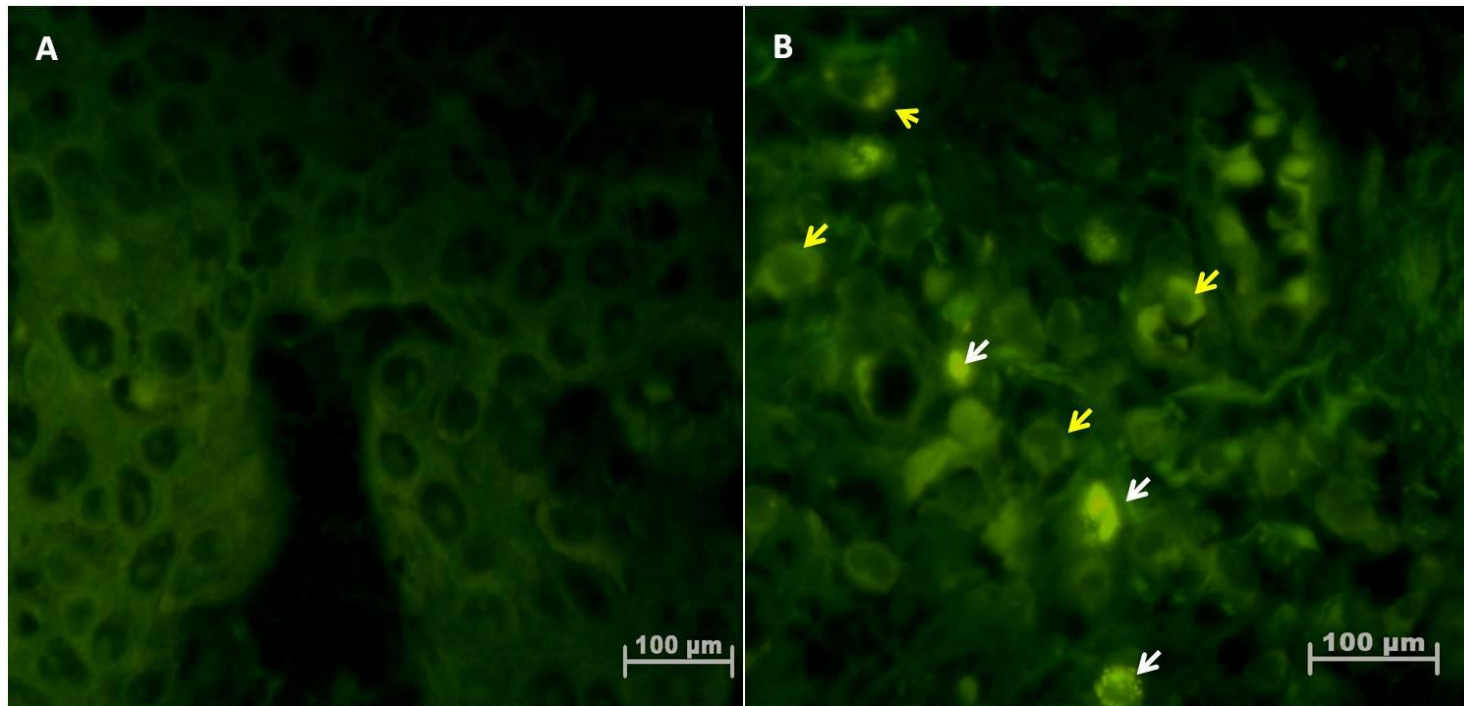


**Figure 5.1 – Micrographs showing localization of the RBBP6 mRNAs in oesophageal carcinoma (Sense and antisense):** Micrograph A shows a negative control with the sense probe showing no staining. Micrograph B shows the localization of the RBBP6 in oesophageal carcinoma where white arrows point to nuclear localization, while yellow arrows show cytoplasmic localization in the poorly differentiated tumour of the oesophagus. **Stain:** Fluorescein isothiocyanate (FITC) **Magnification:** 100X

#### **5.4.1 RBBP6 mRNAs in breast carcinoma**

In chapter four, MCF-7 cells were shown to express DWNN and DWNN-containing RBBP6 variant 1 and 2 mRNAs at low levels. This was also evident in breast tumour tissue using both ISH and FISH. With FISH, breast cancer showed very little accumulation of the RBBP6 mRNAs in the mass of tumours (Figure 5.2 C), in contrast to nuclear accumulation in normal fatty breast tissue (Figure 5.2 B), this with reference to sense probed breast tissue (5.2A). Qualitatively this suggests that in breast cancers the DWNN-associated RBBP6 mRNA products are down-regulated when compared to a normal tissue.

#### **5.4.2 RBBP6 mRNA in hepatocellular carcinoma (HCC)**

Liver tissues (both cancerous and non-cancerous) express the RBBP6 variants and its isoforms. In HCC tissue, RBBP6 mRNAs were detected in cellular areas between islands of tumours. Figure 5.3C shows that RBBP6 mRNAs were not localized in the tumour islands, while areas of tissue adjacent to the tumours show few cells localizing the RBBP6 mRNAs. In figure 5.3B some normal hepatocytes show both nuclear and cytoplasmic staining for RBBP6 mRNAs. This result contradicts previous reports that the liver lacks expression of the PP-R mRNA (Yoshitake et al., 2004), as well as PACT mRNA (Simons et al., 1997). It is suggested here that the localization of PACT is possibly more likely to be DWNN localization, as the PP-R was initially thought to lack the 5' DWNN. Colorimetric *in situ* hybridization and Fluorescence *in situ* hybridization can be used interchangeably. The latter has been reported to be more sensitive (Klinger, 1994) and was therefore used in this study. Figure 5.3A shows a negative control which was a HCC tissue probed. The negative controls clearly show no labelling.

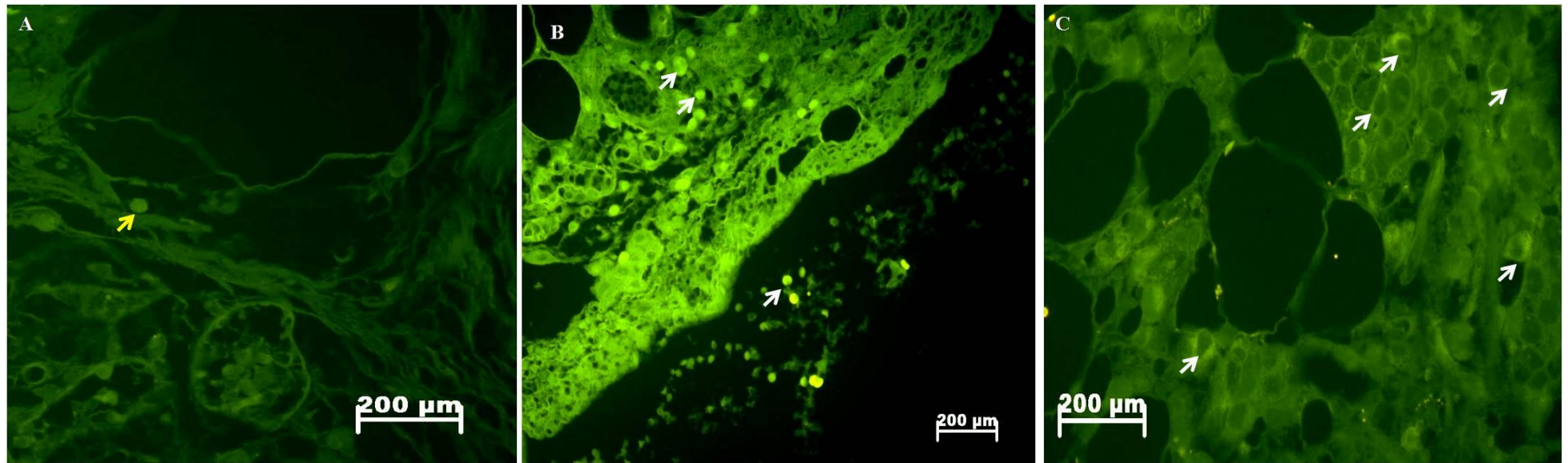


**Figure 5.2-Localisation of DWNN-containing RBBP6 mRNAs in Breast cancer:** Micrograph A shows the sense probe, which lacks labelling, there was only pale background. The two micrographs B and C show a difference in expression and localization of DWNN and RBBP6 mRNAs between normal tissue (B) and breast tumour tissue (C). Figure 5.2B shows that RBBP6 mRNAs are localized in the normal tissue. Figure 5.2C shows little cytoplasmic localization of the RBBP6 mRNAs. In both B and C, white arrows are pointing to labelling. **Stain:** Fluorescein isothiocyanate **Magnification:** 40X.

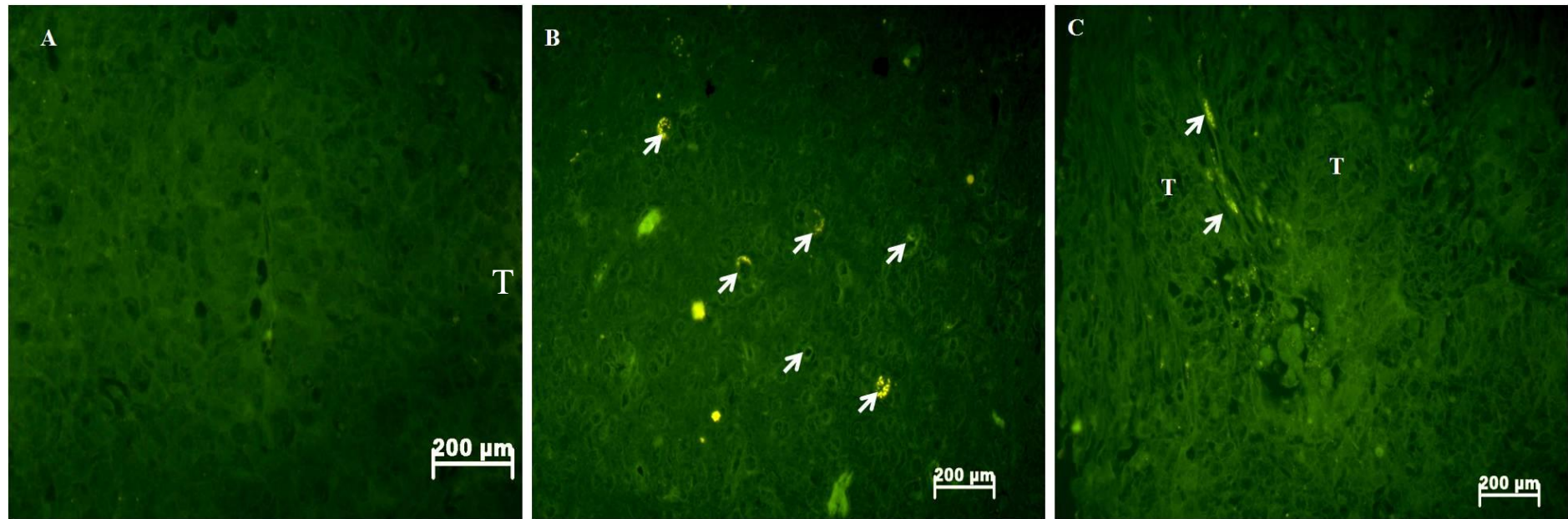


**Figure 5.3 - Localisation of DWNN-containing mRNAs in HCC using FISH:** The normal liver tissue was devoid of staining when a sense probe was used (Fig 5.3A). Micrograph B shows some hepatocytes staining positive for the DWNN-containing mRNAs. In contrast, hepatocellular tissue (C) some cells stained positively in the tissue adjacent to the island of tumours (T). **Magnification: 40X Stain: Fluorescein isothiocyanate.**

### **5.4.3 RBBP6 mRNAs in cervical carcinoma**

The pattern of DWNN-containing RBBP6 mRNAs in cervical carcinoma tissue reported previously demonstrated that this gene is down-regulated in cervical carcinoma (Ledwaba, 2005). In the present study, there was no detectable localization of the RBBP6 mRNAs in the tumour islands. The normal tissue (fig 5.4B) showed few labelled cells. This result is in agreement with prior studies which reported that cervix expresses low levels of RBBP6 (Yoshitake et al., 2004). In the cervical tumour (T) (figure 5.4C), although tumour cells lacked RBBP6 mRNA, some cells in tissue located between the tumour islands were positive.

### **5.4.4 Localization of RBBP6 mRNA in other cancers**

All the human carcinomas observed in this study showed cytoplasmic labelling in the normal tissues and normal tumour-associated tissue with no localization of the RBBP6 mRNAs in the tumour island itself, either nuclear or cytoplasmic. This trend was consistent in the tumours of the stomach, colon, rectum, ovary and kidney. Figure 5.5 summarizes the results from these tumours demonstrating a common pattern of RBBP6 localization.

The oesophageal tissue (fig 5.5A) showed RBBP6 mRNA localization in the normal tissue around the tumour (T) while the sense probed oesophageal tissue showed no staining. This was also observed for serous papillary adenocarcinoma (Fig 5.5B). In colon cancer most of the RBBP6 mRNAs localized in the infiltrating lymphocytes (arrows) situated in the lamina propria. The goblet cells and the absorptive cells within the tubular crypts/glands did not show any RBBP6 mRNA localization. There was no labelling in the tumour tissue (T) (Fig 5.5C). Similarly in rectal tissue, there was no labelling of the RBBP6 mRNAs in the

rectal adenocarcinoma for this gene. These results suggest that the infiltrating lymphocytes are over-expressing the DWNN and DWNN-containing mRNAs to aid the immune system in suppressing tumour formation.

Cancer cells are known to express gene products that enable them to evade detection by the immune system. Cancer cells are also known to express programmed death-1-ligand 1 (PD-L1) that promotes PD-L1-mediated T cell apoptosis, thus increasing their chances of survival (Zhang et al., 2008). Greater expression of the DWNN mRNAs in lymphocytes may be due to excessive death of these cells caused by PD-L1 expression in cancer cells. It was previously reported that DWNN-over-expressing infiltrating lymphocytes undergo excessive apoptosis, at least in human immunodeficiency virus associated nephropathy [HIVAN] kidney tissues (Mbita, 2004). These results and the previous work on HIVAN suggest that the lymphocytes may be expressing the DWNN mRNAs as part of the apoptotic mechanism that they undergo. Another possible explanation is that the DWNN domain could be part of the CTL mediated immune system, as the initial studies showed that the knockout of the DWNN resulted in CHO resistance to CTL killing (George, 1995).

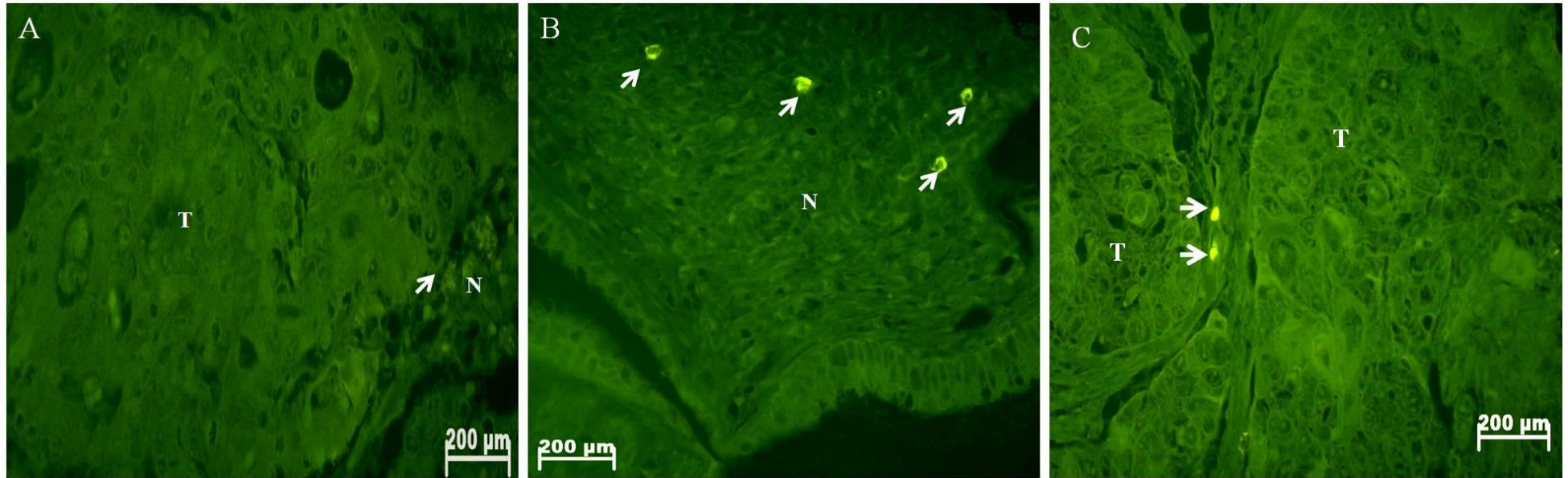


**Figure 5.4 - RBBP6 mRNA localization in cervical carcinoma using FISH:** This micrograph shows localization of the DWNN-containing RBBP6 mRNAs in cervical cancer. The sense control on cervical tissue in micrograph A shows no staining. The normal tissue in micrograph B shows a few positive cells staining. In cervical carcinoma (C), island of tumour (T) showed no nuclear localization in contrast to nuclear staining observed in cells found the normal tissue (arrows). **Magnification 40X Stain:** Fluorescein isothiocyanate.

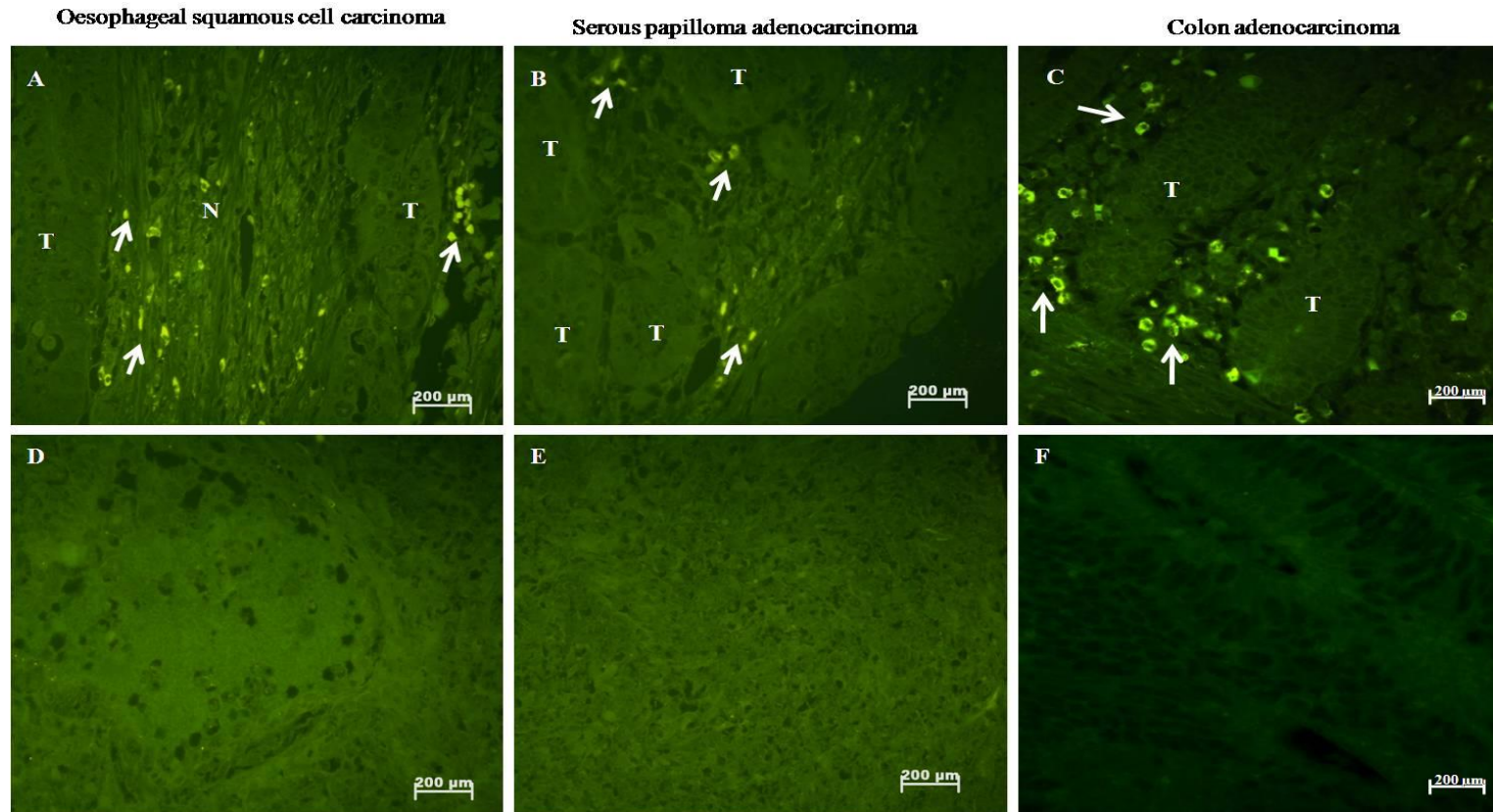


**Figure 5.5 – Localization of the DWNN-containing mRNAs (RBBP6 mRNA) in different carcinomas:** Fig 5.5A shows mRNA localization in oesophageal carcinoma with its negative control (sense probed) in fig 5.7D. White arrows point to positive cells for RBBP6 mRNAs in-between the islands of tumour cells (T). Fig 5.5B shows cells staining (white arrows) between the tumour islands (T) in ovarian cancer, in contrast to sense probed control ovarian cancer tissue (fig 5.5E). Fig 5.5C shows colon cancer cells within the tumour (T) staining negatively, compared to cancer associated tissue in-between the tumours. The sense probed control colon cancer tissue (5.5F) showed no labelling. **Magnification** 40X **Stain:** Fluorescein isothiocyanate.

### **5.4.5 Quantitative analysis of the expression of DWNN in human cancers**

In this study, the FISH technique showed reliability and sensitivity for the localization of the DWNN and RBBP6 mRNAs. The numbers of positively labelled cells in these tissue areas were counted from the tissue arrays sourced from both US Biomax Incl. and Cybrd Tissue Array Tech (USA). Mean averages were used from three independent experiments for the above listed cancers and their respective normal tissues. A minimum of three images for each tissue was taken under 40X objective and subsequently used for these quantifications (section 3.3.10.4).

In summary the pattern that was observed in all these cancers was: the absence of DWNN and RBBP6 mRNAs in the tumour islands, while the stromal tissue between the tumours showed labelling in the cytoplasm of these cells for these mRNAs. Interestingly, the tumour associated tissues had few cells staining positively for DWNN-containing RBBP6 mRNAs. Figure 5.6 shows the quantitative analysis of mRNA localization in the different tissues and in their respective tumours. Breast cancer was found to have down-regulated DWNN compared to normal breast tissue. The overall pattern that was observed in these tumours when FISH was used was a lack of DWNN mRNA expression in neoplastic cells.

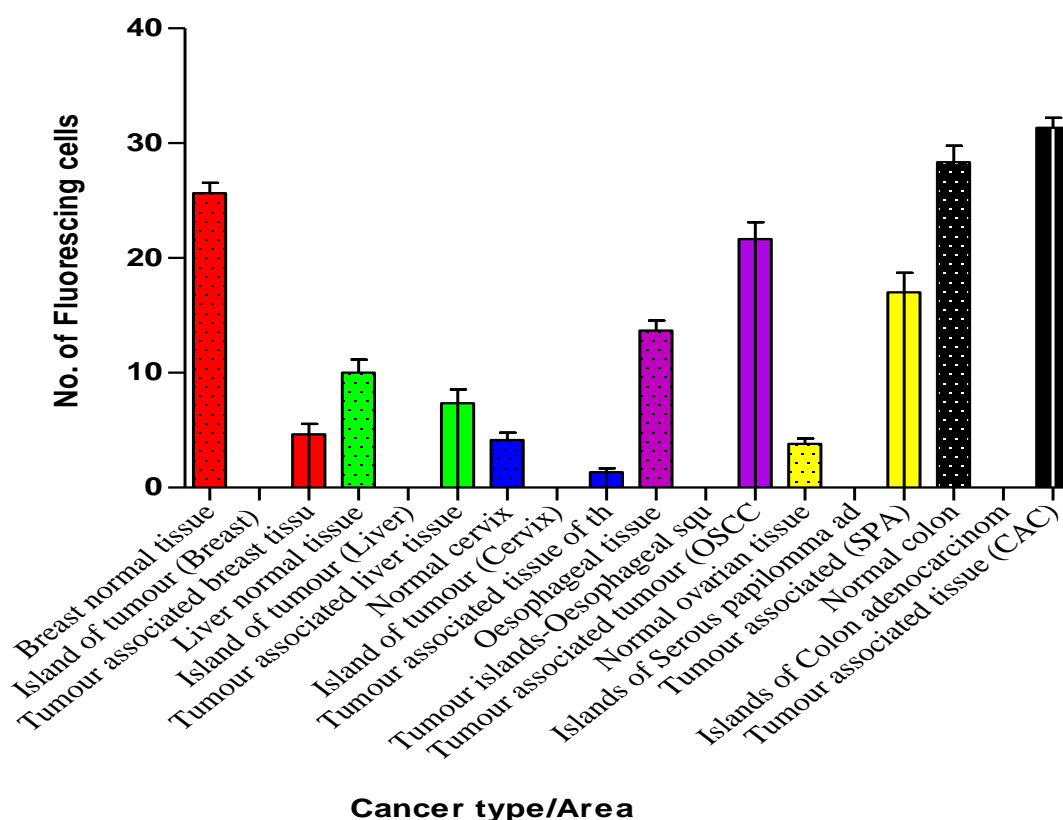


**Figure 5.6 – Analysis of FISH results for DWNN mRNA using GraphPad PRISM 5:** This graph was plotted using the statistical software, PRISM 5 showing the number of positive cells (y-axis) in different cancers (Red-Breast, Green-Liver, Blue-Cervix, Purple-Oesophagus, Yellow-Ovary and Black-Colon) and different areas within the cancer tissues (x-axis). The dotted bars show normal tissues and the striped bars showed the tumour associated tissue. The graph was plotted with mean  $\pm$ SE ( $P < 0.05$ ) from three independent experiments. At least 100 cells were counted in each field and this figure is accompanied by a column analysis (Appendix M).

### **5.5 DWNN-containing proteins in human cancers**

The correct localization of gene products or cellular molecules is crucial for cellular, biochemical and physiological functions of these molecules. One example documented by Wang et al. (2001) is that of the p53 protein where its nuclear localization is essential for its transcriptional activities that include p53-dependent cell cycle arrest and subsequent apoptosis. They illustrated that the confiscation of p53 by a cytomegalovirus to the cytoplasm after its translation negated its cell cycle arrest function (Wang et al., 2001). Essentially, the virus sequestered the p53 protein in the cytoplasm through its NLS I resulting in the inactivation of p53. This process is dependent on the stage of infection with the cytomegalovirus. At stage I and II, partial sequestration occurs while at stage III total sequestration occurs. pRb, another important tumour suppressor protein is also confiscated in a similar manner to that described for p53 in the same situation. It is normally secured by an A-type nuclear lamin to the nuclear matrix, where it facilitates its cell cycle control activities and other functions (Markiewicz et al., 2002). These examples demonstrate the importance of the appropriate localization of a protein to enable it to carry out its function.

It is therefore important to know the localization of the DWNN-containing RBBP6 proteins in order to be able to understand its cellular function/s. Different human carcinomas and normal tissue controls were examined for the localization of the RBBP6. Here, using the purified anti-human DWNN domain antibody, RBBP6 protein was found specifically within the cytoplasm of cancer cells.

### 5.5.1 RBBP6 proteins in breast carcinoma

In breast cancer, the DWNN domain-containing RBBP6 showed cytoplasmic accumulation while the normal breast tissue exhibited both cytoplasmic and nuclear localization. Figure 5.7 shows a comparison between the normal breast tissue section (5.7A) and a breast cancer tissue section (5.7B) where nuclear staining is seen in normal tissue (A) as opposed to cytoplasmic localization in breast cancer cells (B). The cells surrounding the breast tumour also show some nuclear localization.

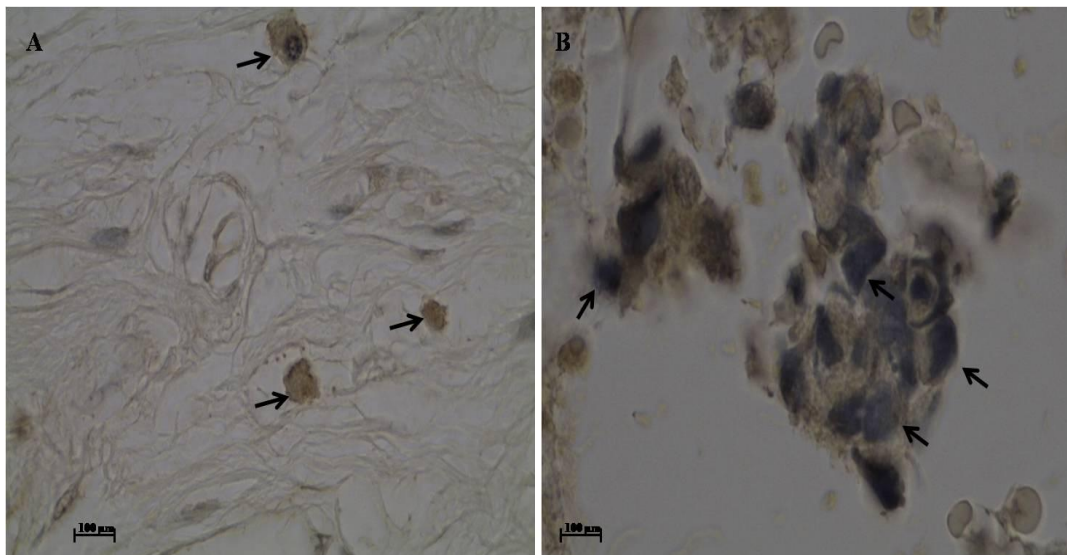


**Figure 5.7 - Micrographs showing localization of the DWNN domain-containing RBBP6 proteins in breast:** These micrographs show localization of the DWNN domain and its associated proteins in normal breast tissue (A) and in invasive breast carcinoma (B). In normal breast tissue (A), there is both cytoplasmic and nuclear localization of RBBP6 proteins as demonstrated by the presence of a dark brown precipitate (DAB) (black arrows), while this precipitate is confined only to the cytoplasm of the tumour cells (B) showing blue nuclei (arrows). **Magnification:** 100X **Stain:** diaminobenzidine (DAB); haematoxylin.

### 5.5.2 RBBP6 proteins in hepatocellular carcinoma (HCC)

Hepatocarcinogenesis involves a process where hepatic cells first change into intermediate cells that then evolve into HCC. The DWNN domain-containing RBBP6 proteins may contribute negatively towards this cancer phenotype either by its absence or its suppression. Figure 5.8 demonstrates that the RBBP6 is localized in both the nucleus and cytoplasm in normal hepatocytes (A) while the hepatocellular carcinoma cells (B) showed heavy localization in the cytoplasm.

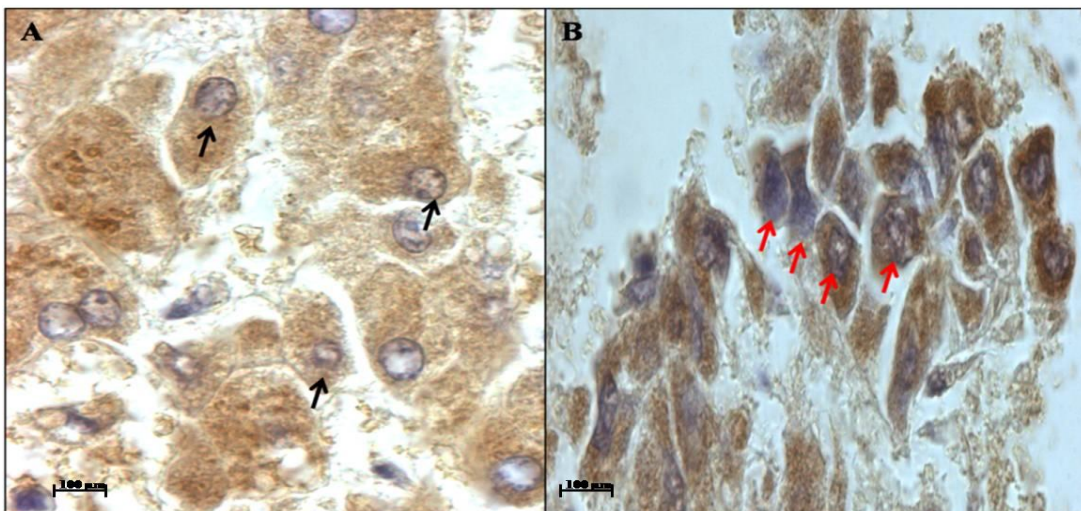


**Figure 5.8 - Micrographs showing RBBP6 proteins in normal and HCC tissues:** These micrographs show immunostaining of normal (A) and hepatocellular carcinoma (B) tissues with the DWNN antibody. The DWNN domain and associated protein products localized in both the nucleus and the cytoplasm (Black arrows) in normal liver tissues (A) while in hepatocellular carcinoma there was significant localization in the cytoplasm. The nuclei (blue) stain basophilically (red arrows) with haematoxylin counterstaining. **Magnification:** 100X **Stain:** DAB; haematoxylin.

### 5.5.3 RBBP6 proteins in cervical carcinoma

In a previous study conducted by Ledwaba (2005), RBBP6 showed little nuclear localization in normal cervix and no nuclear localization in cervical carcinoma (Ledwaba, 2005). In contrast, this study showed that little protein was localized in

the cervical cancer cell nuclei (figure 5.9B), when compared to normal cervix (figure 5.9A).

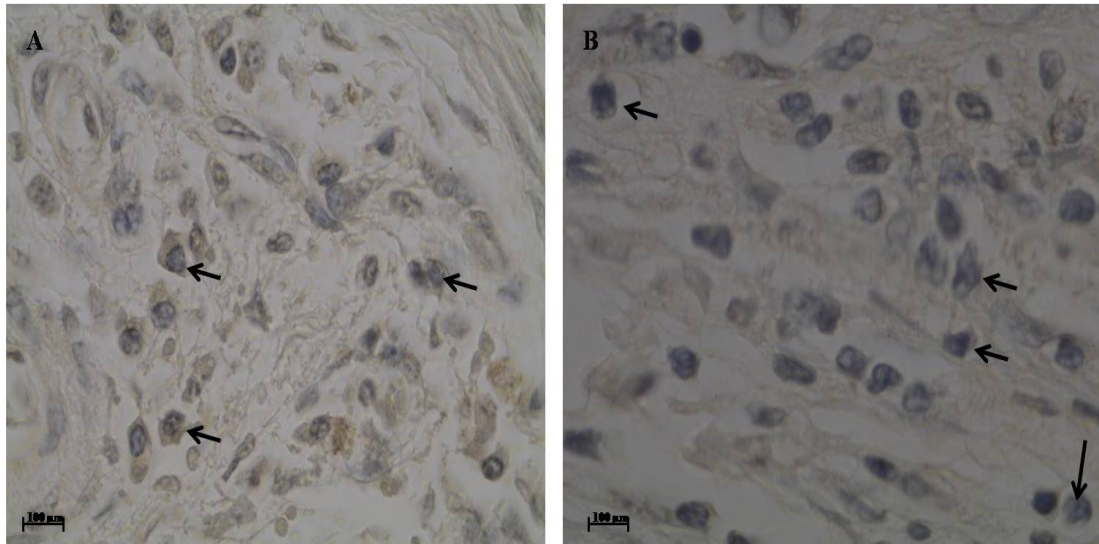


**Figure 5.9 - Micrographs showing localization of RBBP6 proteins in cervical carcinoma:** Normal cervical cells (A) show localization of the DWNN proteins in the nucleus compared to cervical carcinoma (B). The nuclei are stained with haematoxylin (Arrows) within the tumour island. **Magnification:** 100X **Stain:** DAB; haematoxylin.

#### **5.5.4 Localization of the RBBP6 proteins in other human cancers**

The pattern of localization of the DWNN-containing proteins appears to be similar in the different tumours examined, with the exceptions of ovarian carcinoma and its corresponding normal tissue; these displayed very little expression of RBBP6 proteins; and also kidney clear cell carcinoma that showed more cytoplasmic expression of the protein. Unlike other normal organs that showed nuclear localization of RBBP6 proteins (Figure 5.10A), the normal kidney tissue showed a few tubular cells where the cytoplasm stained positive for the RBBP6 proteins.

In the colon, rectal and stomach adenocarcinomas (Figure 5.10 A and B), there seemed to be a down-regulation of the RBBP6 proteins. This was accompanied by cytoplasmic accumulation of these proteins, this in contrast to both nuclear and cytoplasmic localization in normal tissues. Ovarian cancer (Figure 5.10C) displayed no localization of the DWNN and its related proteins. This is shown in figure 5.10 A, B and C where normal tissues and corresponding cancers are shown. These micrographs show the localization and expression of the DWNN domain-containing proteins in cancers and their corresponding normal tissues. Negative controls show no localization only the counterstain, haematoxylin. This figure shows less localization in the tumour tissues compared to the normal tissues. Figure 5.10A shows the localization of the DWNN protein in kidney clear carcinoma and stomach adenocarcinoma. Figure 5.10B shows localization of the DWNN in rectal and colon adenocarcinoma while 5.10C shows localization in ovarian tissues. The cancer cells show no nuclear localization.

Appendix G summarizes the localization of the RBBP6 gene product in different human tumours. The overall localization pattern of the DWNN and RBBP6 in human cancers was typified by the absence of these proteins in the tumour islands and the presence of these proteins in the cells adjacent to the tumours.

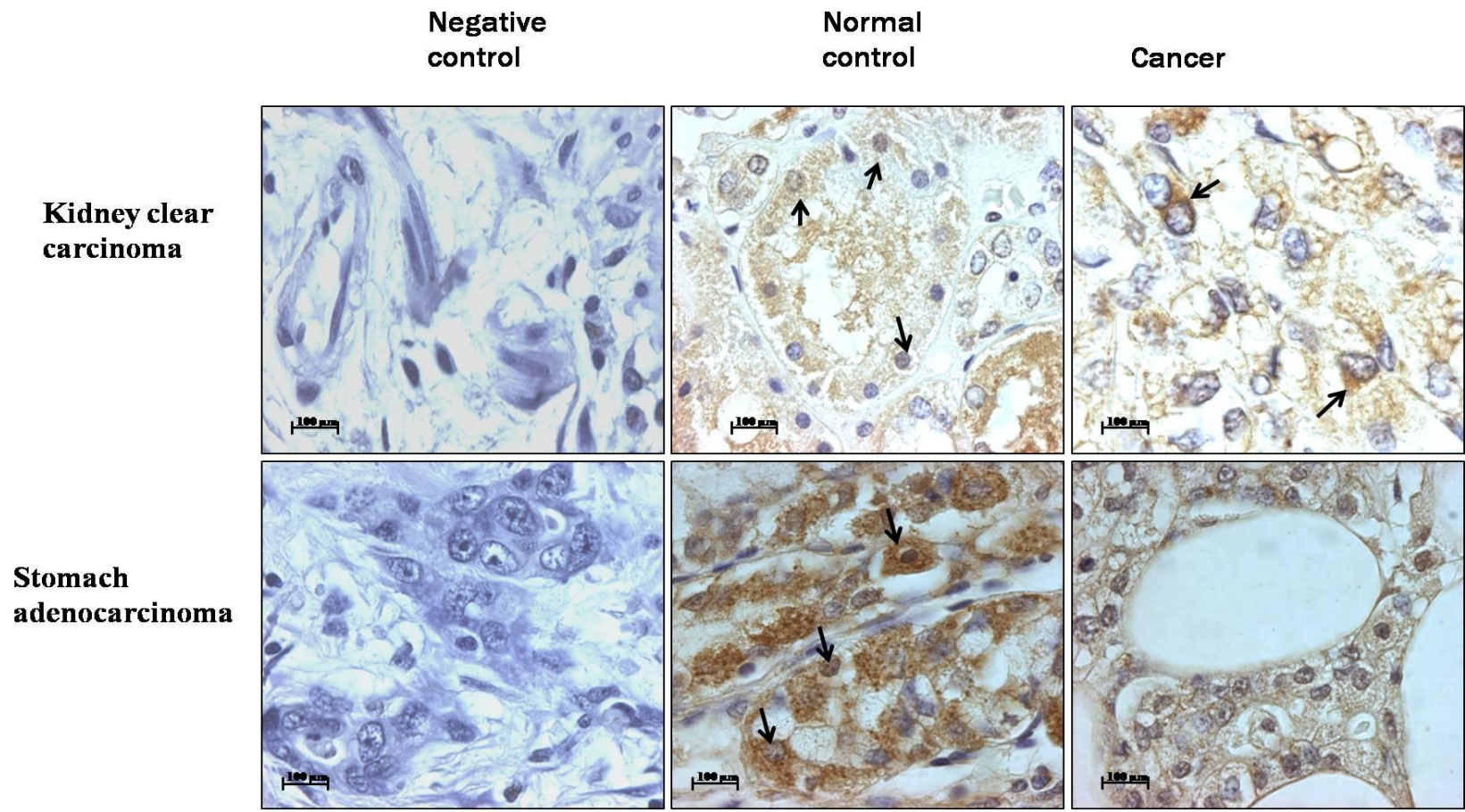


**Figure 5.10 A – Localization of DWNN proteins in different carcinomas:** Localization in kidney and stomach with their corresponding cancers and negative controls. **Magnification:** 100X **Stain:** DAB, Haematoxylin.

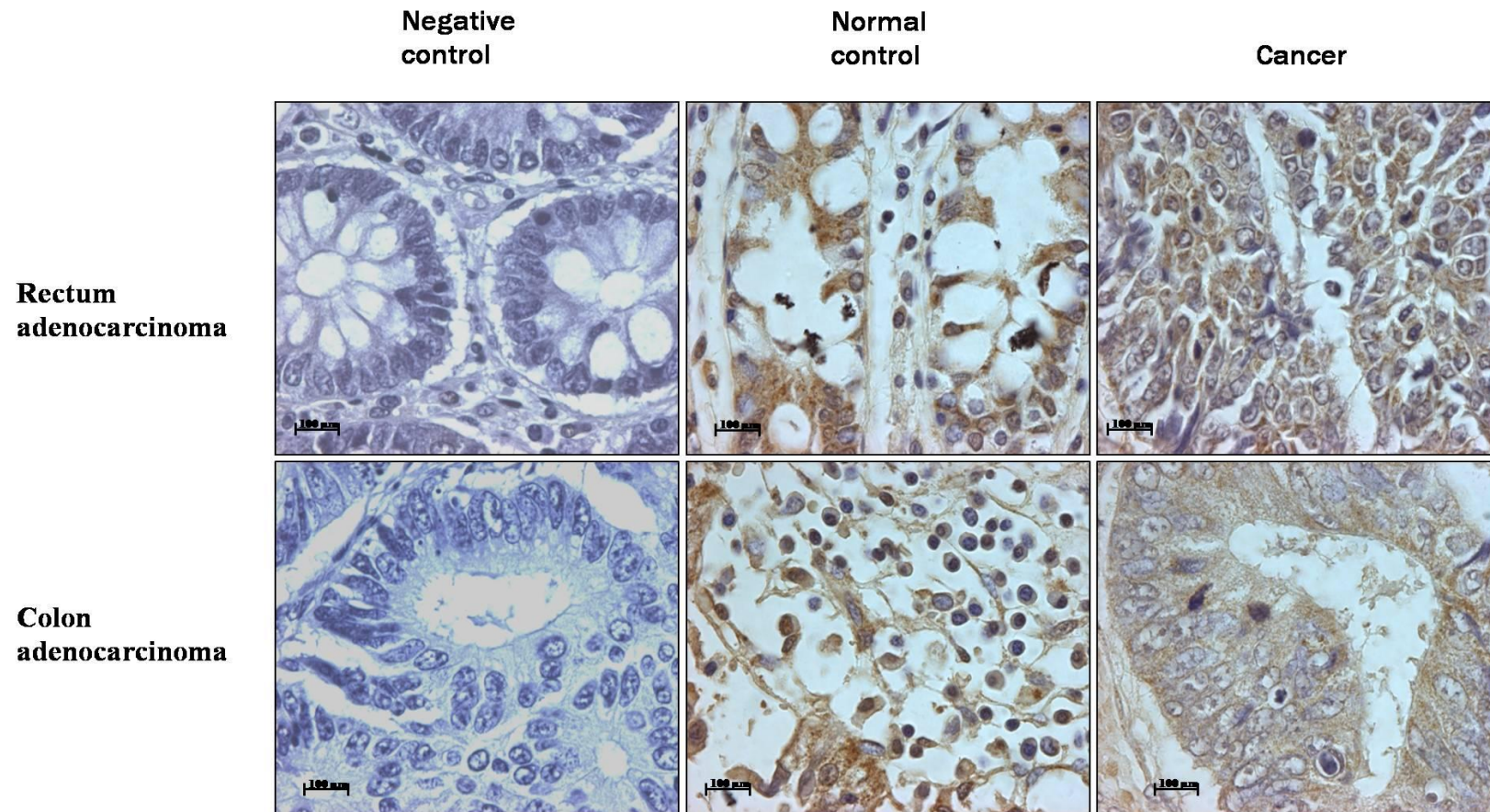


**Figure 5.10B - Localization of the DWNN in rectal and colon adenocarcinoma:** Localization of the DWNN in rectal and colon adenocarcinoma and their corresponding normal tissues and negative controls. **Magnification:** 100X **Stain:** DAB, Haematoxylin.

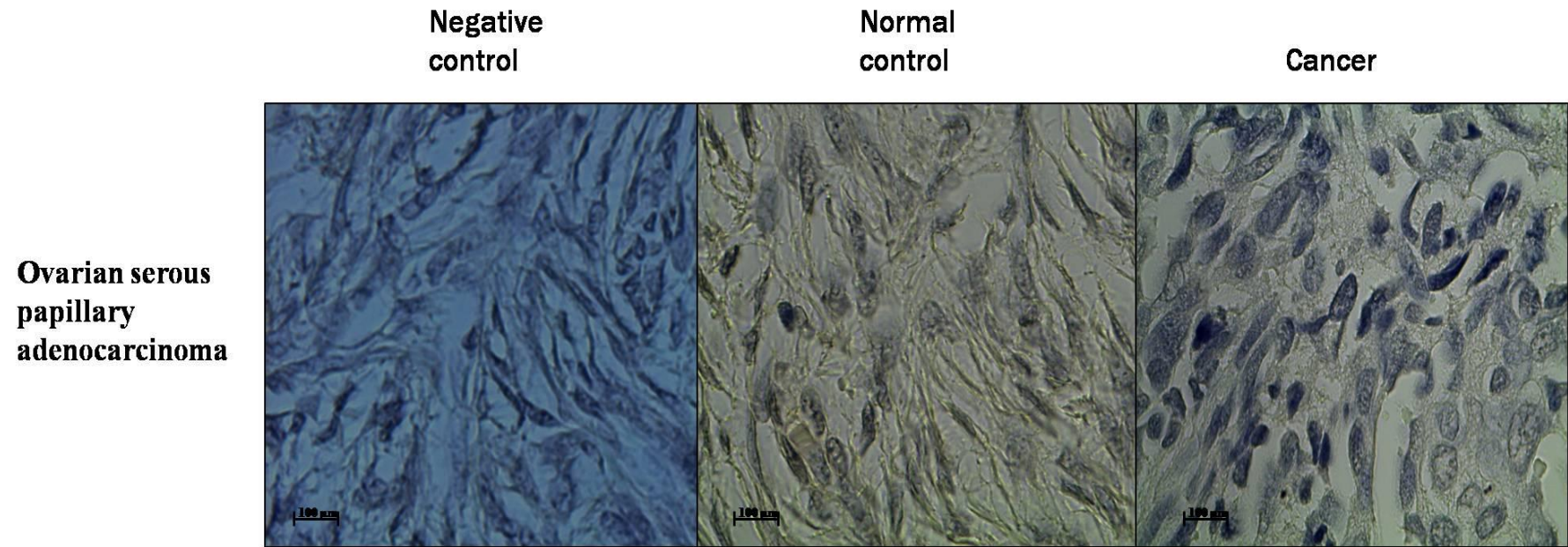


**Figure 5.10C - Localization of the DWNN proteins in ovarian papillary adenocarcinoma:** Localization of the DWNN in ovarian papillary adenocarcinoma and its corresponding normal tissue and negative control. **Magnification:** 100X **Stain:** DAB, Haematoxylin.

## **5.6 RBBP6 proteins in human cancer cell lines**

The DWNN domain was also localized using the same antibody used previously, in cell lines including, HepG2, HeLa, MCF-7, Hek 293 and CHO (Chinese Hamster Ovary) cell lines. The CHO cell line was used as a positive control because it is the original cell line that was used in the identification of the DWNN domain through promoter trap mutagenesis (Skepu, 2005). The cells were incubated with the anti-DWNN polyclonal primary antibody followed by a secondary antibody tagged with AlexaRed (3.3.9.2).

Antibody localization demonstrated that the DWNN domain-containing RBBP6 proteins are confined to the nucleus and cytoplasm of mitotic cells. Apoptotic cells also showed up-regulation of these proteins in the cytoplasm. Figures 5.11-5.15 demonstrate RBBP6 localization in different cell lines. Hek 293T cells are a non-cancerous cell line and showed a similar pattern of localization to the cancer cell lines (HeLa-cervical cancer, HepG2-hepatocellular carcinoma and MCF-7-breast cancer).

### **5.6.1 RBBP6 proteins in CHO cells**

Chinese Hamster Ovary (CHO) cells showed DWNN protein expression as expected (figure 5.11), since the DWNN was previously identified in the DWNN knock-downs of these cells through promoter-trap mutagenesis (George, 1995). This technique resulted in abrogation of apoptosis induced by staurosporine and CTL killing. (This was the initial link of this gene to apoptosis).

### **5.6.2 RBBP6 proteins in the HeLa cell line**

Cervical cancer (HeLa) cells do express the DWNN domain-containing RBBP6 gene products, at least at the mRNA level as demonstrated by FISH and RT-PCR (chapter 4). In this cell line RBBP6 exhibited both nuclear and cytoplasmic localization in mitotic cells (rearrangement of chromosomes as a marker for mitosis, with visible metaphase and anaphase) showing up-regulation of the RBBP6. Figures 5.12B and C show localization in the nucleus and the cytoplasm.

### **5.6.3 DWNN domain-containing proteins in MCF-7 cells**

The panel of DWNN localization in human cancer cells seems to follow a similar pattern with both nucleus and cytoplasm staining positive. Breast cancer (MCF-7) cells were no exception to this pattern as figure 5.13 shows. The localization was the same as with CHO cells and HeLa cells. In figure 5.13 it was observed that the mitotic cells (arrows) stained more for the DWNN proteins.

### **5.6.4 DWNN domain protein localization in HepG 2 cells**

The HepG2 cells showed a similar pattern to that of the other cells where there was both nuclear and cytoplasmic DWNN domain-containing RBBP6 accumulation. Figure 5.14 shows that the dying cells (black arrows) had more expression of the RBBP6 proteins. Note that cells that showed cell shrinkage and acquisition of a round small shape were regarded as dying cells and dead cells respectively; while those that showed mitotic cells (red arrows) and apoptotic bodies also showed higher expression levels of RBBP6 accumulation with apoptotic bodies (black arrows). Other cells showed no localization of the RBBP6 proteins and were regarded as negative (yellow arrows).

### **5.6.5 DWNN domain protein localization in Hek 293T cells**

The localization of the DWNN in Hek 293T cells showed a relatively higher expression of the DWNN proteins compared to other cell lines, that is, cancerous cells that showed more expression in dying or dividing cells. 293T cells showed higher intensity in most of the cells as figure 5.15 shows.

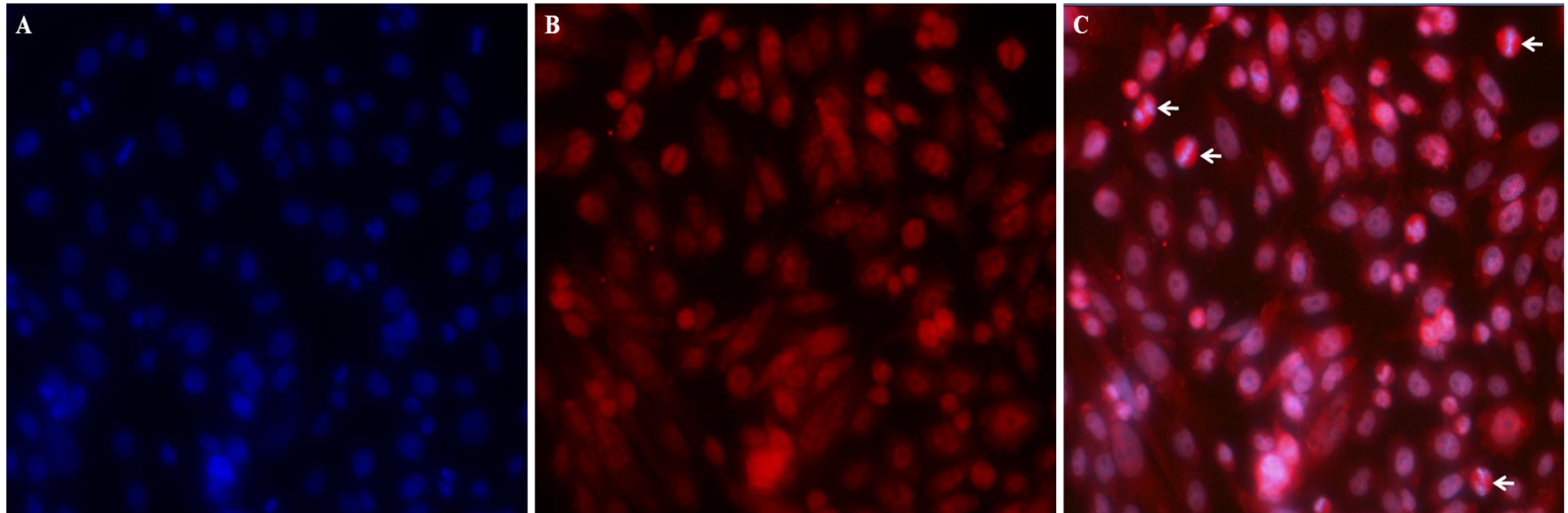


**Figure 5.11 - Localization of RBBP6 proteins in CHO cells:** These micrographs show staining of the CHO cells with anti-human DWNN antibody. Figure 5.11A shows DNA staining using DAPI. Figure 5.11B shows anti-human DWNN detected by Alexa Red and figure 5.11C shows an overlay of DAPI and anti-human DWNN. The white arrows indicate mitotic cells that show increased staining levels. **Magnification:** 40X **Stains:** Alexa Red and DAPI.

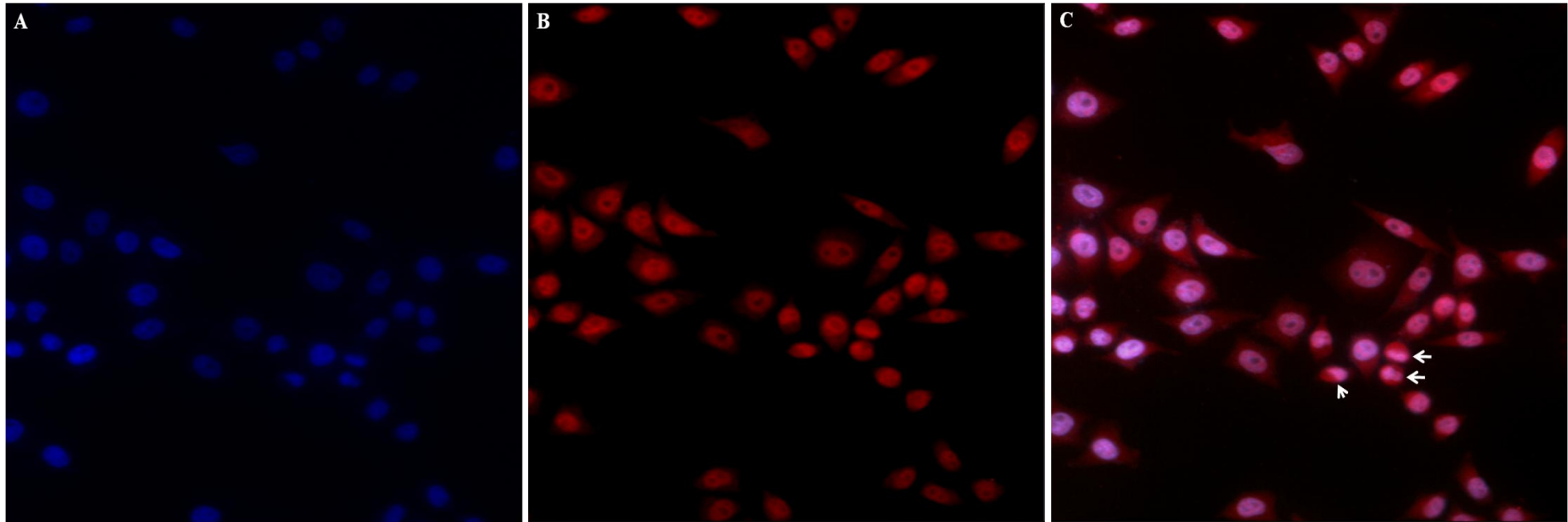


**Figure - 5.12 - Localization of DWNN-containing proteins in HeLa cells:** These micrographs show RBBP6 proteins *in situ* in HeLa cells. DAPI stain of the nuclei is shown by figure 5.12A. Figure 5.14B shows anti-human DWNN detected by Alexa Red and figure 5.12C shows an overlay of DAPI and the white arrows indicate mitotic cells at telophase showing increased labelling levels. **Magnification:** 40X **Stains:** Alexa Red and DAPI-nuclear stain.

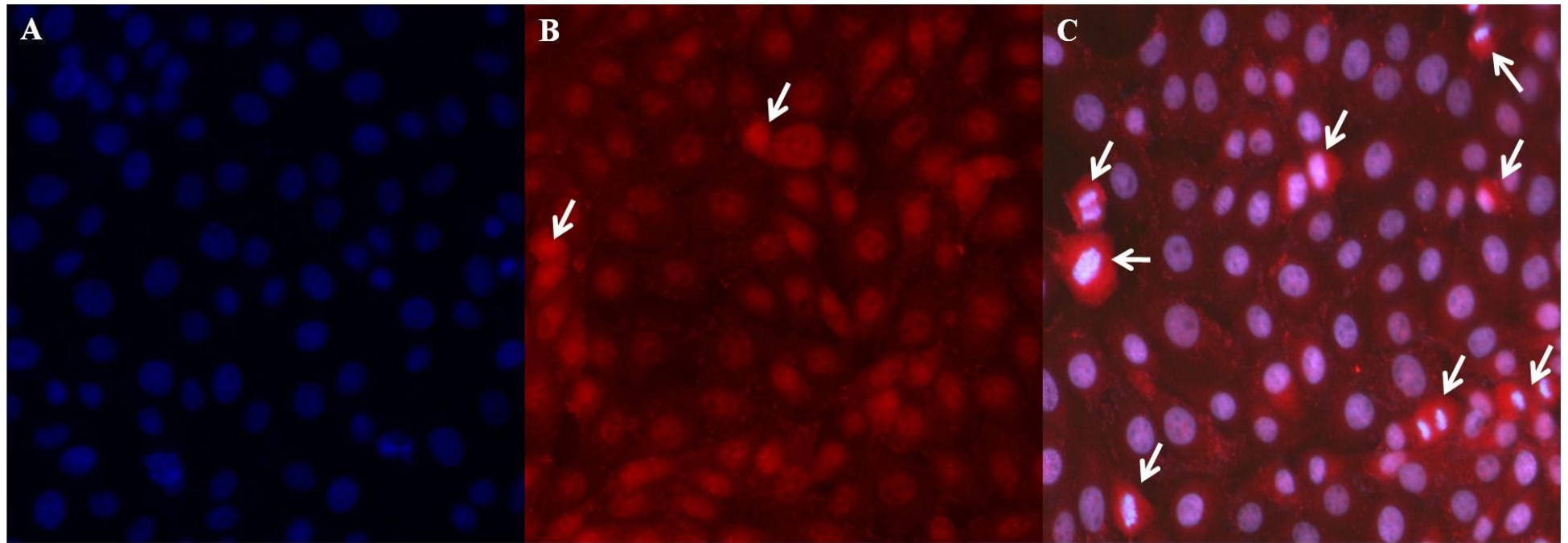


**Figure 5.13 - Nuclear and cytoplasmic localization of RBBP6 in MCF-7 cells:** Figure 5.13 shows a negative control (A), no labelling is seen. Micrographs B and C show positive DWNN staining in the nucleus and cytoplasm. White arrows point to mitotic cells with increased DWNN staining levels. **Magnification:** 40X **Stains:** Alexa Red and DAPI.

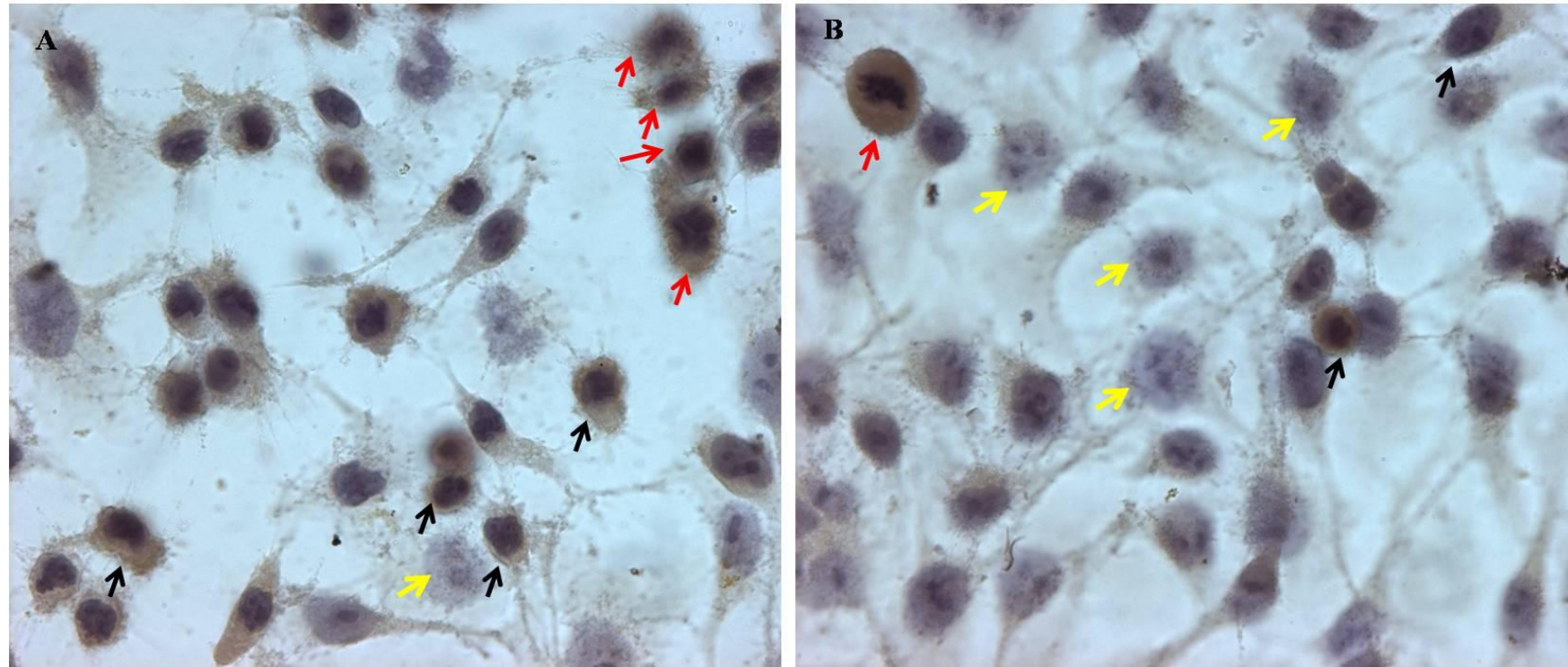


**Figure 5.14 - Immunostaining of the HepG2 cells with anti-human DWNN:** These micrographs show the DWNN domain and its related protein localization in HepG 2 cells. Cells lacking labelling are indicated by yellow arrows. Localization of the DWNN proteins was up-regulated in mitotic cells (red arrows) and dying cells (black arrows), while HepG 2 cells also show both nuclear and cytoplasmic localization. **Magnification: 40X Stains: DAB and Haematoxylin.**

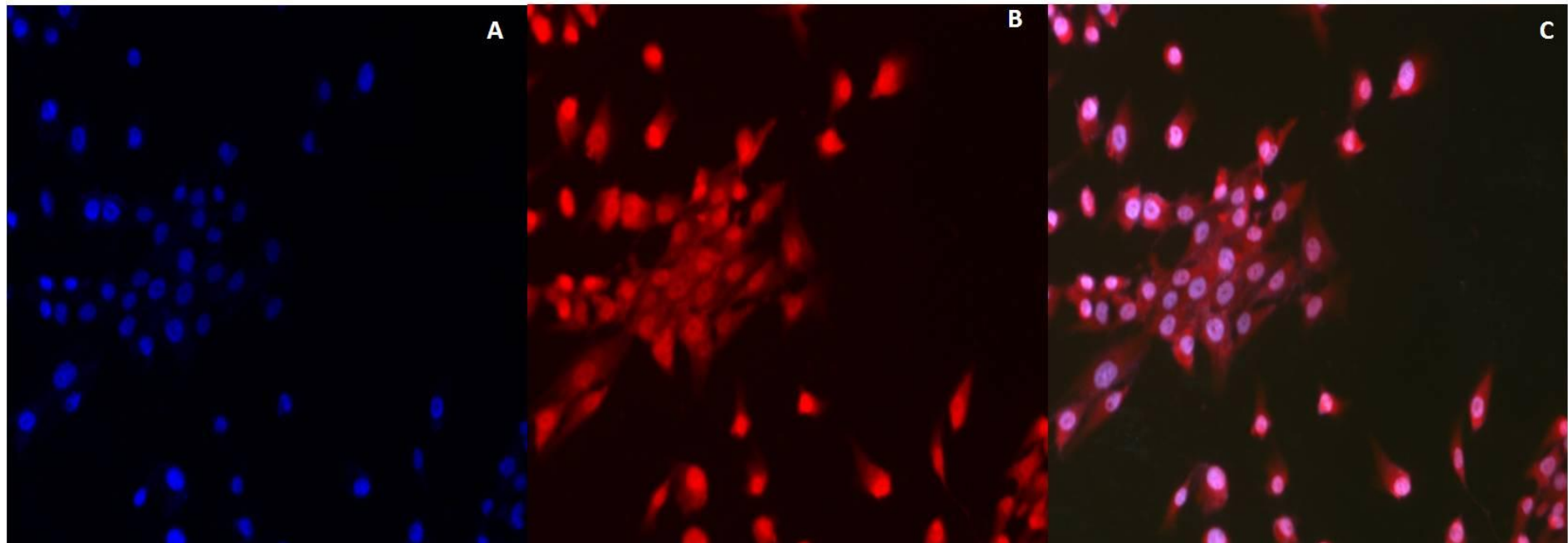


**Figure 5.15 – Micrograph showing localization of the DWNN in Hek 293T cells:** Micrograph (A), negative control. These micrographs (B and C) show RBBP6 staining positively in the nucleus and cytoplasm in Hek 293T cells. Micrograph B shows the labelling of these cells for DWNN proteins detected using an Alexa Red while micrograph C shows an overlay with DAPI. **Magnification:** 40X **Stains:** Alexa Red and DAPI.

## **Chapter Six: The role of the DWNN in apoptosis and cell cycle**

---

### **6.1 Introduction**

In chapters four and five, it was demonstrated that the RBBP6 gene is expressed at both mRNA and protein levels in both human tissues and human cancer cell lines. There was differential expression and localization of the RBBP6 mRNAs and proteins between cancer and normal cells/tissues. Localization studies using Fluorescent *In Situ* Hybridization and immunocytochemistry (chapter 5) revealed a differential expression of RBBP6 between normal and cancerous cells. It was found that RBBP6 is down-regulated in cancers, while normal cells showed nuclear localization of RBBP6 mRNA and proteins. When immunolocalized, RBBP6 proteins (chapter five) were found to be up-regulated in mitotic cells, as well as apoptotic cells and this prompted an investigation of RBBP6 in normal cells. RNA knock-down technology was chosen to further elucidate the function of RBBP6 in cell homeostasis and RNA interference (3.3.11) was used to further investigate the role of RBBP6.

### **6.2 Functional studies: summary of the methods**

This chapter addresses the following questions: (1) What would be the effect of RBBP6 knock-down in normal human cells (Hek 293T cells)? (2) What would be the effect of RBBP6 iso3 over-expression in human cancer cells that had been shown to have low expression of the RBBP6 isoforms 1 and 2 and 3? (3) Is there is a correlation between the expression of RBBP6, cell cycle and apoptosis induction in human cells?

### **6.3 The knock-down of the RBBP6 gene products**

The RNAi of the RBBP6 and the DWNN mRNAs showed that their proteins are required for both cell cycle control and apoptosis as previously suggested (Gao and Scott, 2002, Gao and Scott, 2003). The Hek 293T cells were used for the investigation of the role of the RBBP6 isoforms in human cells, as they were shown to express more RBBP6 family members than other cell types here. The RNAi constructs were confirmed by both PCR (figure 6.1A); RT-PCR (figure 6.1 B and C) and real-time PCR (figure 6.2).

The three RNAi constructs were shown to contain the cloned RNAi annealed oligos (Appendix D). Figure 6.1 shows the amplification of the annealed oligos and the vector control fragments. Lane 1 shows a molecular weight marker; lanes 2-4 are PCR products from RNAi plasmid DNA (targeting DWNN and RBBP6 transcripts 1 and 2) and lane 5 shows a PCR product from the vector, pEGFP-C1-U6, a control vector with random sequence that is not specific to any mRNA. The figure shows that the plasmid DNA contained inserts, while pU6GFP had only the cloning site and U6 promoter fragments. Lanes 2-4 were pEGFP-C1-U6-Rb1A/1B/3A PCR products amplified with RNAi colony PCR primers with a larger fragment than the EGFP-C1-U6 PCR product, amplified with the same primers in lane 5. A negative/Blank control in lane 6 was as expected, with no PCR product.

Amplification of the DWNN domain with Iso 3 primers (Appendix C1) showed that the RBBP6 variants were knocked down in cells transfected with Rb1A/B and Rb3A. Figure 6.1 B shows the efficacy of the RNA interference in knocking down

the *RBBP6* gene products. Both the *RBBP6* mRNA and proteins were successfully knocked down when mRNA and proteins extracted from Hek 293T cells transiently transfected with Rb3A and Rb1A that were designed to knock down *RBBP6* transcripts 3 and 1/2 respectively. Both the conventional PCR (figure 6.1A) and real-time PCR (figure 6.1B) showed that *RBBP6* mRNAs were significantly reduced in the knockdown cells compared to untransfected and vector control cells. In all three samples, that is, Rb3A, Rb1A and U6GFP there was an equivalent amplification of the *HPRT1* fragment. This figure demonstrates that equal amounts of cDNAs were used in the PCR setup. The real-time data was normalized with the *hHPRT1* house keeping gene. Western blotting analysis also showed reduced expression of *RBBP6* proteins (figure 6.1C). This result demonstrates that the *RBBP6* RNAi constructs were effective in silencing the respective *RBBP6* transcripts. Both Rb3A and Rb1A reduced the expression of the *RBBP6* at the mRNA level. Both the vector control or untransfected cells (negative control) showed no reduction in *RBBP6* transcript expression.

Figure 6.2 shows the efficiency of the transfections of Hek 293T cells using Metafectene Pro transfection reagent, by analysing the percentage of cells fluorescing green (transfected cells) compared to untransfected cells. The transient transfection with RNAi constructs targeting the *RBBP6* transcripts was shown to be effective and successful. Using the delta Ct value analysis, both DWNN and *RBBP6* variant 1/2 were knocked down (figure 6.1).

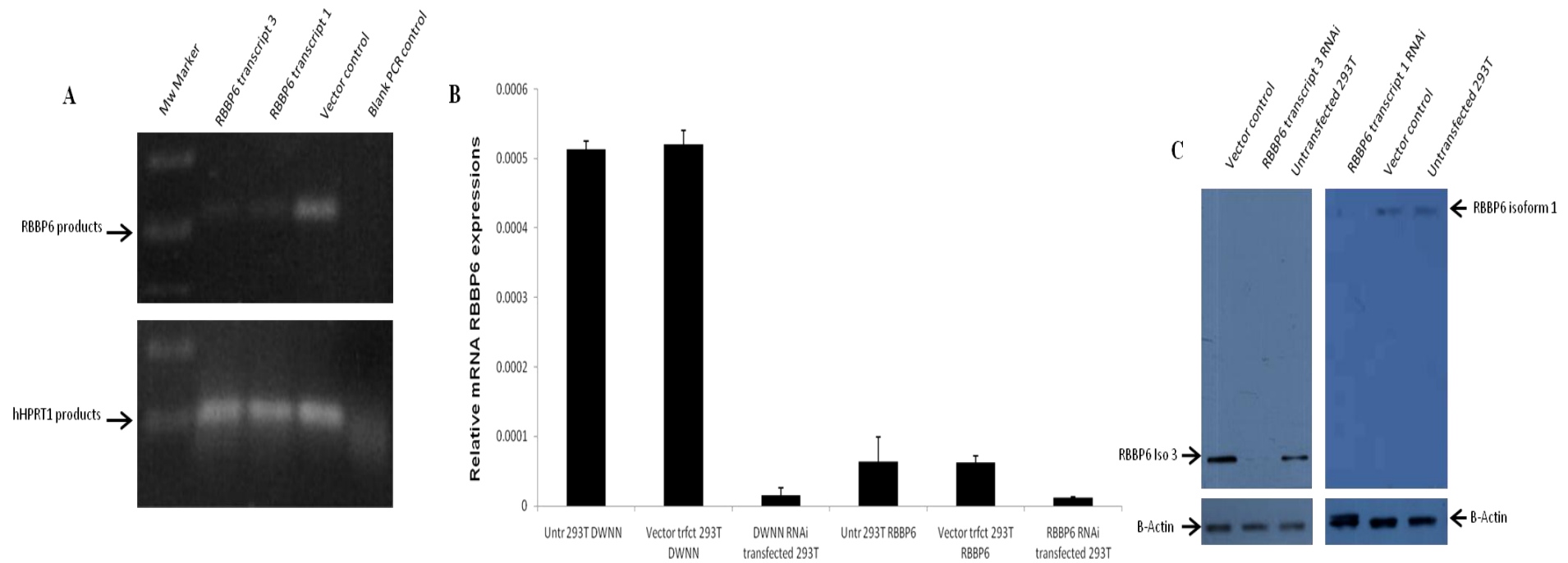


**Figure 6.1 – Confirmation of the DWNN and RBBP6 transcripts knockdown by RNAi:** Figures 6.1 A shows the efficacy of the RNAi constructs in knocking down the RBBP6 isoform 3 (Lane 2) and RBBP6 mRNA transcripts (lane3) compared to U6GFP/untransfected Hek 293T cells (Lane 5). Lane 1 shows a molecular weight marker while lane 5 shows a blank control (no template DNA). HPRT amplification shows a uniform amplification of HPRT1 fragment of approximately 100 bp from Rb3A (Lane 2) and Rb1A (Lane 3) knock-downs as well as from a vector control (Lane 4). The blank control was negative on lane 5. Figure 6.1B shows detection of RBBP6 mRNA transcripts by real-time PCR, showing significant reduction of both DWNN and RBBP6 mRNA from RNAi knockdown cells ( $P < 0.05$ ). Figure 6.1C confirms the reduced protein levels by Western blotting.

### **6.3 The effect of the RBBP6 knock-down in Hek 293T cells**

The RBBP6 gene products are down-regulated in MCF7; HeLa and HepG2 cells (see chapters four and five). The Hek 293T cells showed a higher expression than the other cells examined (figure 4.2 and 4.5). These cells were therefore suitable to study the knockdown of the DWNN domain (Isoform 3), while the MCF-7 cells were suitable for the analysis of the DWNN domain over-expression. Previously, the mouse RBBP6 homologue, P2P-R was shown to sensitize the MCF-7 cells to camptothecin-induced apoptosis (Gao and Scott, 2003) and it was important to investigate over-expression of the full RBBP6 isoform 1 and 3/DWNN in these breast cancer cells. The P2P-R that was introduced in the MCF-7 cells as reported in Gao and Scott study (2003), lacked the N-terminal DWNN domain, hence it was important to investigate this in the present study. In addition to the fore-mentioned suitability of Hek 293T cells, these cells were shown to be less sensitive to apoptosis induced by camptothecin (as demonstrated in figure 6.3). Hek 293T cells were therefore suitable for the knockdown and over-expression studies while the MCF-7 cells were only suitable for over-expression studies. Thus the question therefore is, could the DWNN knockdown or its over-expression sensitise these cells to apoptosis and affect cell cycle regulation?

The Hek 293T cells are resistant to G418 (observed in this study and suggested in online forums), hence stable transfections were not achieved for these cells and instead transient transfections were done. After 24 and 48 hrs, the transfected cells were induced to undergo apoptosis with camptothecin and staurosporine, left for a further 24 hrs and then analysed for apoptosis using the *APOPercentage* assay (section 3.3.13.2).

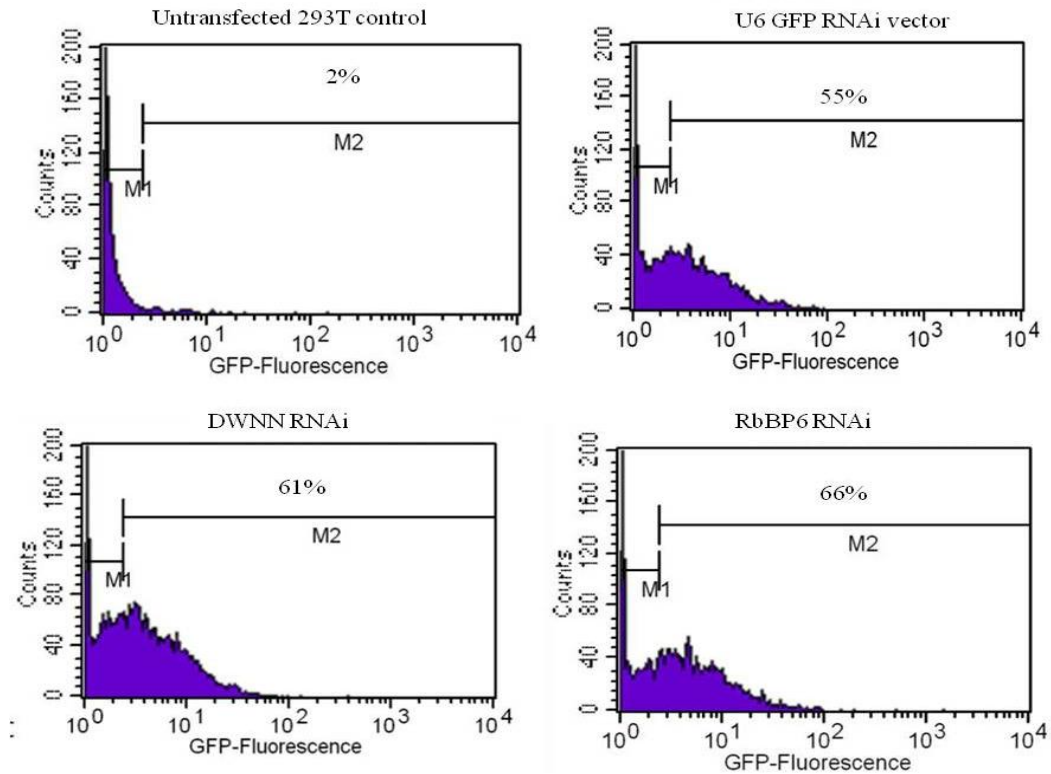


**Figure 6.2 – RNAi transfections and efficacy in Hek 293T cells:** Figure 6.2 shows the transfection of the RBBP6 RNAi constructs. The figure shows over 50% transfection efficiency for all the constructs (DWNN RNAi, RBBP6 RNAi and U6GFP vector).

Real-time PCR was used to analyse gene expression in knock-down cells; here, the increase in Ct values is interpreted as a decrease in the amount of the mRNA transcripts in such cells. The absence of the DWNN domain and RBBP6 were expected to show effects in cellular homeostasis processes, especially apoptosis, since the gene was originally identified as an apoptosis and cell cycle-related gene regulator.

The DWNN and RBBP6 mRNA reduction/knock-down did not sensitize these cells to camptothecin-induced apoptosis, nor did it enhance resistance to the

compound (figure 6.3). Even though there was an observable reduction in the staurosporine-induced apoptosis, especially in RBBP6 RNAi reduced/knock-down cells, the results was expected as the identification of the DWNN was initially through its knockout and resistance to staurosporine-induced apoptosis. It was noted here that the cells reached confluence faster than un-transfected and vector control cells. This result corroborated the results reported for cell labelling, as it was observed that the RBBP6 proteins were highly expressed in mitotic cells (figure 5.11-5.15), and this suggested that this gene might be involved in cell cycle arrest regulation, as its mouse homologue had been reported to play a role in cell cycle arrest (Scott and Gao, 2002). Arsenic trioxide had been reported to induce G2/M cell cycle arrest and apoptosis in human lung cancer cells (Ge-ping et al., 2009). The question therefore was, did the knock-down of the RBBP6 mRNAs have an effect on arsenic trioxide-induced apoptosis and cell cycle arrest? Figure 6.3 shows that the knockdown of the DWNN/RBBP6 did not sensitise the Hek 293T cells to apoptosis, but on the contrary reduced the cells' sensitivity to both staurosporine and arsenic trioxide-induced apoptosis. This result suggests that the absence or low expression of DWNN/RBBP6 favours the resistance to apoptosis and deregulation of cell cycle. It was thus important to study the role of the DWNN in the events of the cell cycle.

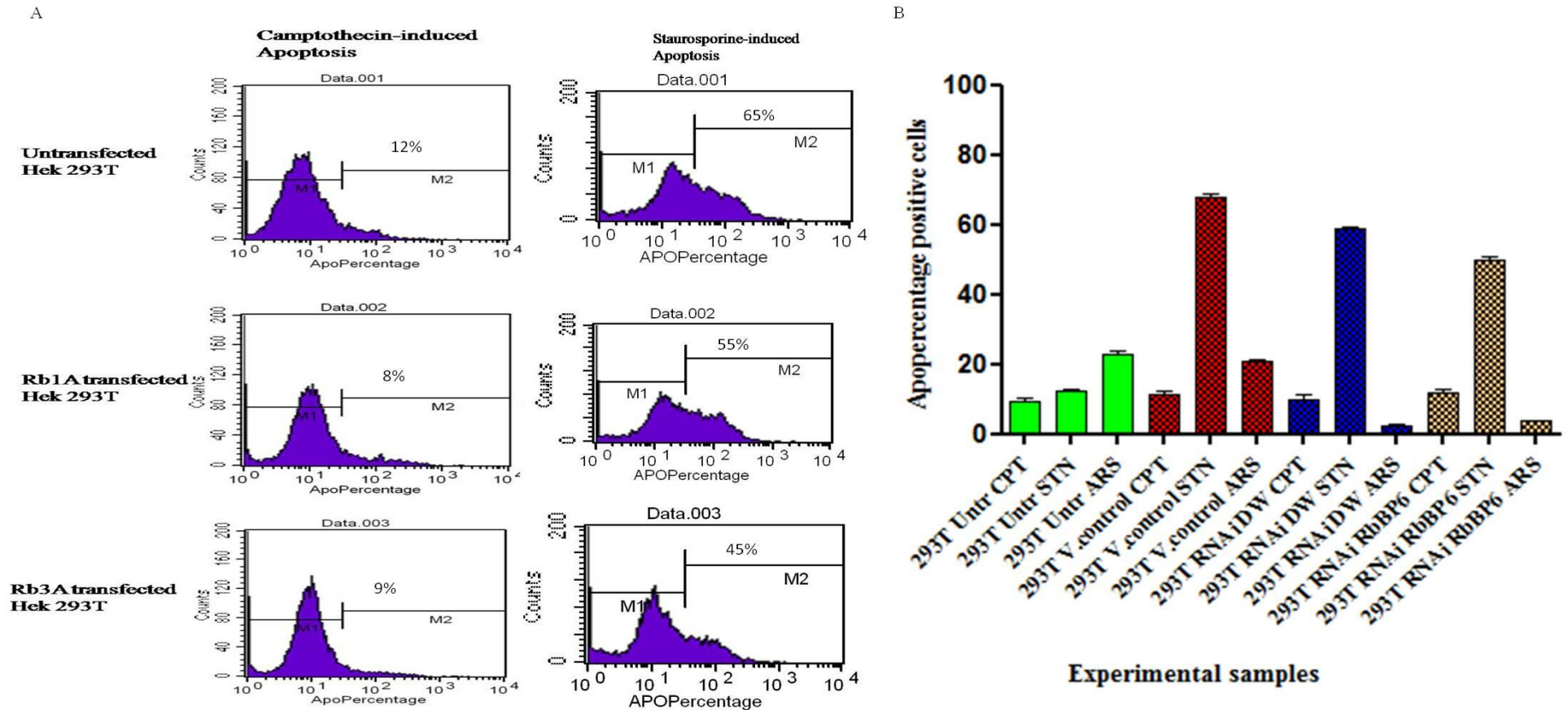


**Figure 6.3 – Effect of the RBBP6 knock-down in apoptosis:** Showing the RBBP6 RNAi effect on apoptosis in Hek293T cells. The figure shows apoptosis induced by camptothecin, staurosporine and arsenic trioxide, data presented as FACS histograms (A) and GraphPad Prism analyzed (B). Figure 6.3B shows that the apoptosis induced with arsenic trioxide was significantly reduced ( $P < 0.05$ ) when both DWNN and RBBP6 were knocked-down. Staurosporine-induced apoptosis was also reduced but not significantly.

#### **6.4 Cell cycle analysis of the DWNN domain in human cells**

In chapter five, cell labelling showed that the RBBP6 proteins are highly expressed at the G2/M phase of the cell cycle. Figure 6.4 confirms that the DWNN is a cell cycle regulator as the cell cycle analysis in Hek 293T cells showed that the expression of the DWNN is induced only in G2/M. Western blot analysis shows deglycosylation and/or dephosphorylation of the DWNN/Isoform 3, since this particular isoform was prominent after the cells have been arrested at the G2/M transition. This result suggests that the 13 kDa isoform 3 and its deglycosylation and dephosphorylation are required for the G2 cell cycle arrest. The treatment of Hek 293T cells with 12.5  $\mu$ M arsenic trioxide causes cell cycle arrest and so increased the population of cells that were in the G2 phase to 50% after 24 hours, while 3  $\mu$ M did not show an increase in the G2 cell population. In cells where the RNA knockdown of the DWNN/isoform 3 occurred, a significant decrease in the population of cells at G2/M phase was seen at both concentrations. Western blot analysis showed that this form of induced cell cycle arrest is accompanied with up-regulation of the DWNN domain and appearance of the 13 kDa DWNN domain that appears to be both deglycosylated and dephosphorylated.

RBBP6 seems likely to be a player in this pathway (Gao and Scott, 2002), the effects of the RBBP6 isoform 3/DWNN over-expression in Hek 293T cells on p53 was determined. Figure 6.5 showed that over-expression of DWNN (fig 6.5A) resulted in p53 stabilization (fig 6.5B). Figure 6.5C shows that the same quantity of lysates was loaded for both untransfected Hek 293T cells and transfected Hek

293T cells. This result suggests that DWNN cell arrest is likely to be in a p53-dependent manner.

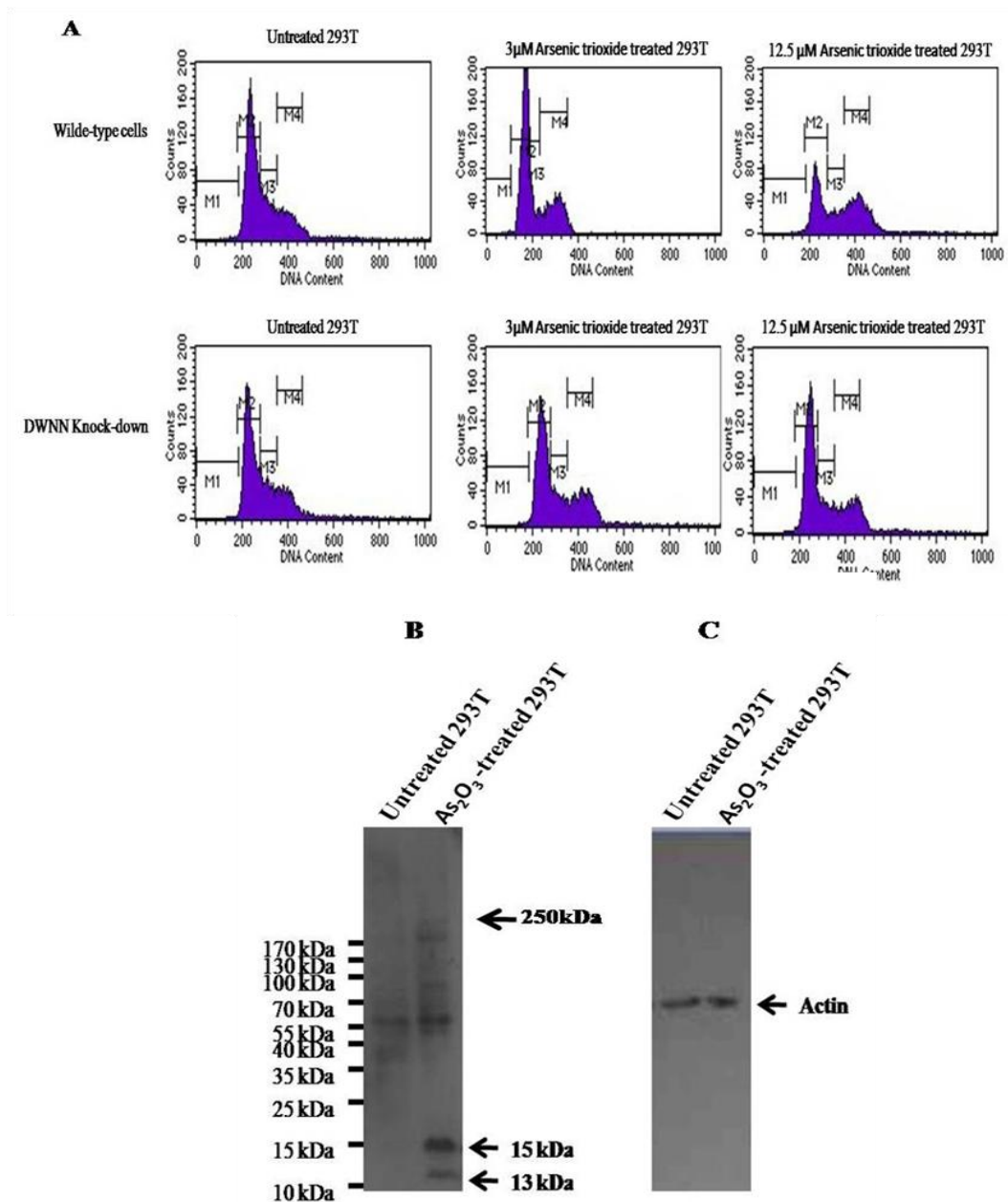


**Figure 6.4 – DWNN involvement in Cell cycle regulation:** This figure shows that arsenic trioxide-induced cell cycle arrest at G2 is dependent on the presence of the DWNN/Isoform 3. FACS data (A) shows that As<sub>2</sub>O<sub>3</sub> induces cell arrest at G2 at 12.5µM concentration and this arrest is DWNN dependent. DWNN knockdown decreased the As<sub>2</sub>O<sub>3</sub> effect. Figure 6.4B shows that As<sub>2</sub>O<sub>3</sub> up-regulated the DWNN/isoform 3 in wild type cells. Figure 6.4C shows a loading control (Actin).

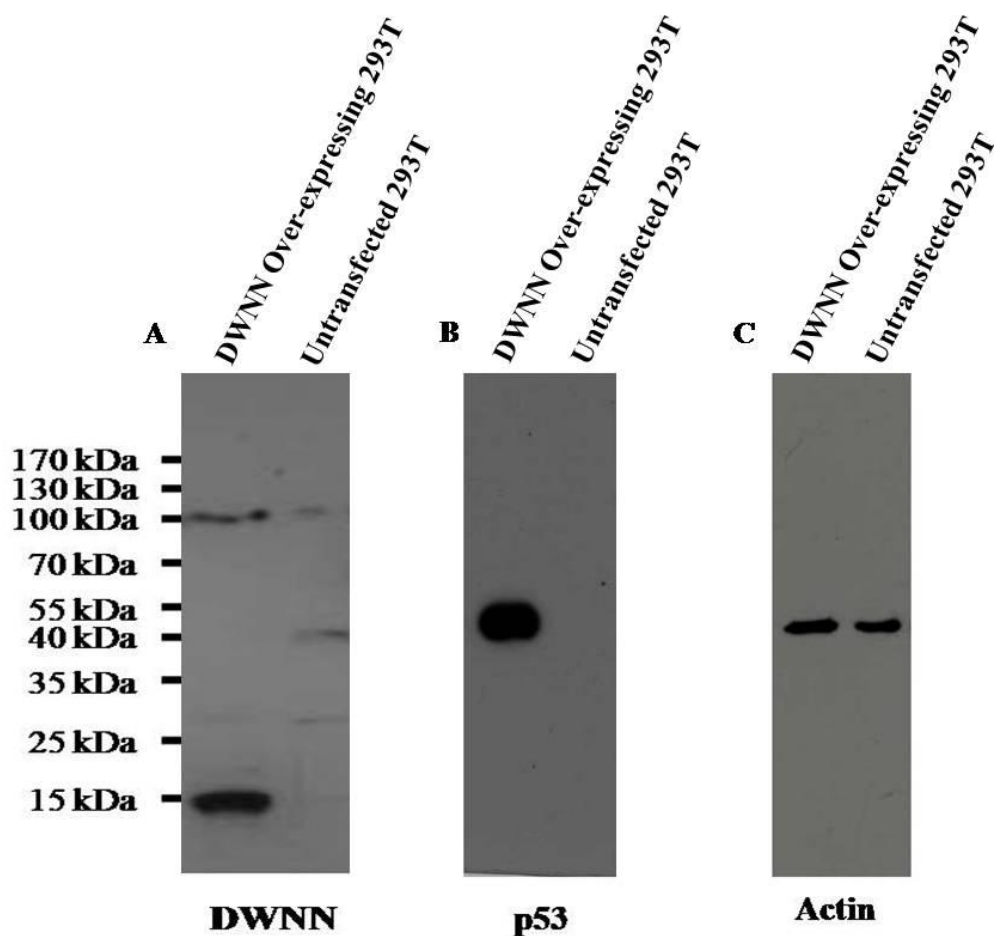


**Figure 6.5 – RBBP6 isoform 3, a p53 stabilizer:** This figure shows the over-expression of the DWNN in Hek 293 (A) and up-regulation of p53 in DWNN over-expressing cells (B). Figure 6.5C was an actin Western blot as a loading control.

### **6.5 Over-expression of the RBBP6 gene products in human cancer cells and related apoptosis**

In chapters three and four, the MCF-7 cells were demonstrated to express RBBP6 gene products at low levels. Solid tumour cells have previously been shown to respond to arsenic trioxide treatment and this toxic compound has been suggested as a potential drug for solid cancers (Jiang et al., 2010a, Siu et al., 2002, Zang et al., 1999, Zhou et al., 2008). Arsenic trioxide had been shown to cause cell cycle arrest in cancer cells at the G2/M phase and additionally induces apoptosis in a

cell cycle specific gene-dependent manner (Ling et al., 2002, Xie et al., 2002). Figure 6.4 showed that the DWNN domain is one of the cell cycle related gene products and DWNN is also induced by arsenic trioxide treatment. Figure 6.5 showed that the DWNN over-expression resulted in p53 stabilization.

Two stable MCF-7 cell lines expressing the DWNN domain and RBBP6 isoform 1 were established and analyzed for arsenic trioxide-induced cell cycle and apoptosis susceptibility using propidium iodide, MTT and *APOPercentage* assays. Figure 6.6 shows the over-expression of both the DWNN domain and RBBP6 isoform 1 in MCF-7 cells and the effect of these proteins in arsenic trioxide-induced-apoptosis using *APOPercentage* and cell viability using MTT and apoptosis.

The MTT assay (figure 6.7) showed that over-expression of the DWNN domain did not significantly decrease the percentage of viable cells compared to untransfected and vector control cells when treated with 50  $\mu$ M Camptothecin. The RBBP6 isoform 1 caused a significant decrease in the percentage of viable MCF-7 cells when treated with the same concentration of camptothecin compared to untransfected and vector control MCF-7 cells.

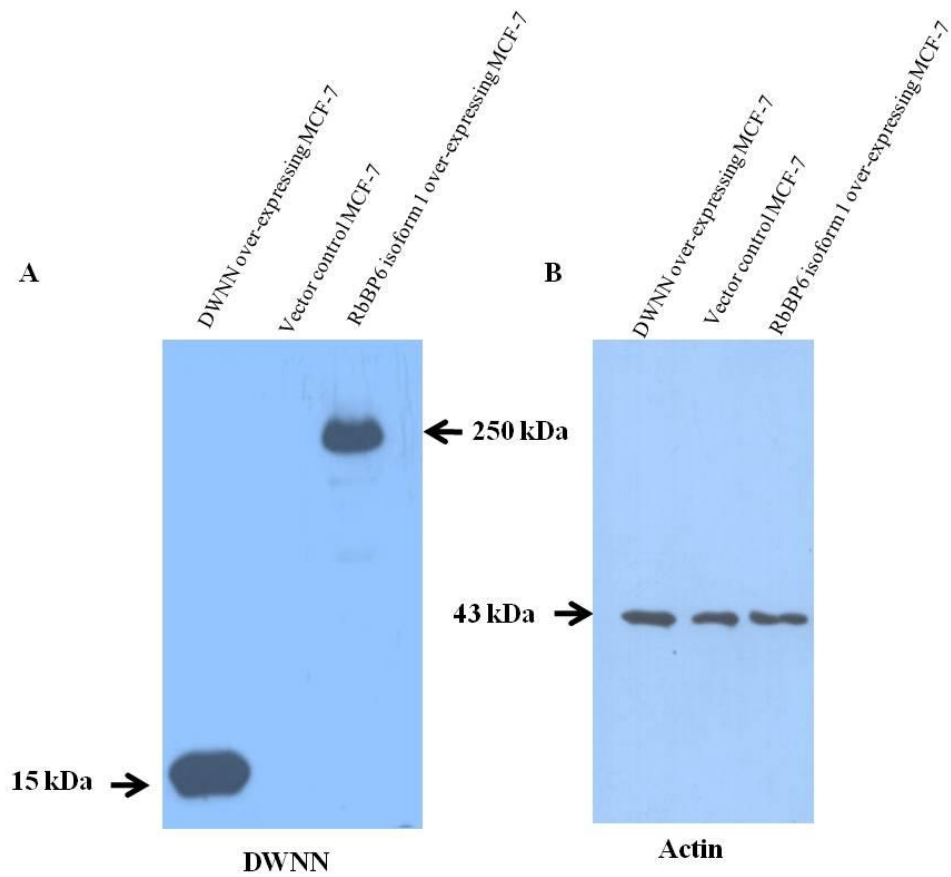


**Figure 6.6 – Over-expression of the DWNN/Isoform 3 and RBBP6 proteins in MCF-7 cells:** Two figures demonstrating over-expression of a 15 kDa DWNN domain and a 250 kDa RBBP6 isoform 1 proteins (A) in MCF-7 cells. The beta actin antibody (B) was used as a loading control.

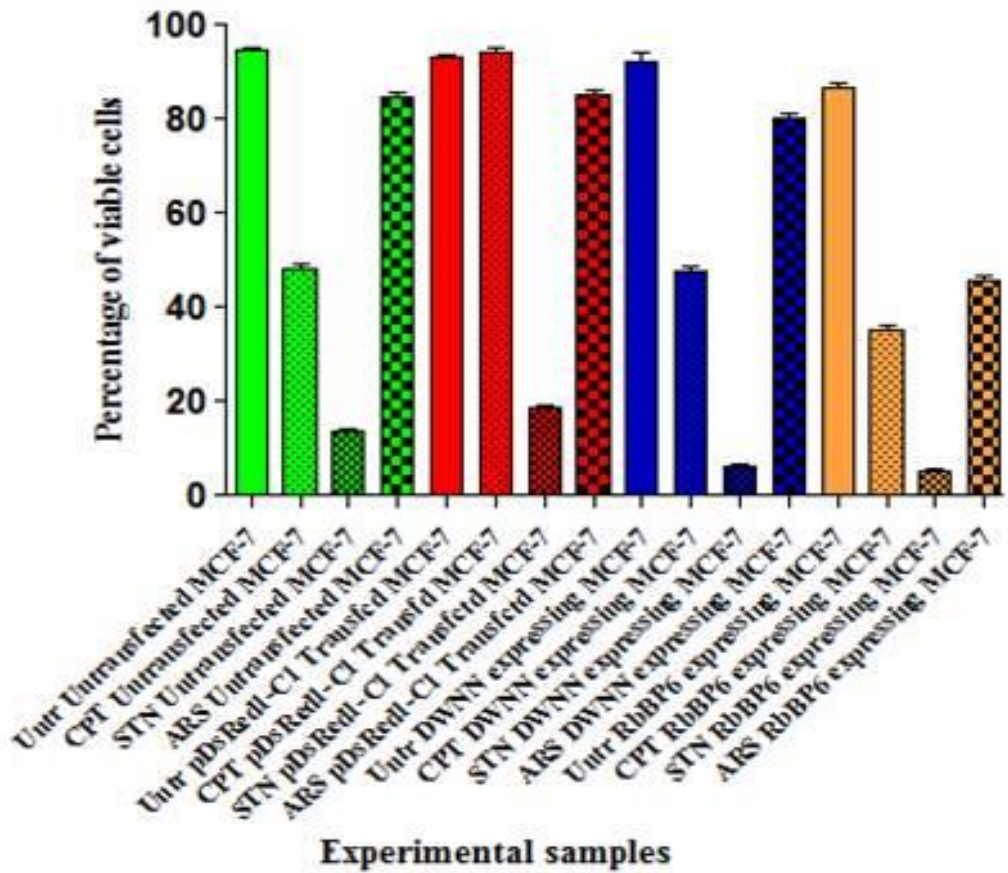


**Figure 6.7 – The MTT viability assay in DWNN/Isoform 3 and RBBP6 isoform 1 expressing MCF-7 cells:** This figure shows the MTT viability assay in MCF-7 cells over-expressing DWNN domain and RBBP6 isoform 1. The control cells (untransfected and vector transfected cells) were treated together with the transfected cells with arsenic trioxide, camptothecin and staurosporine. The graph was plotted with mean  $\pm$ SEM ( $P < 0.05$ ) from a mean of three independent experiments.

The treatment of the MCF-7 cells expressing DWNN/Isoform 3 and RBBP6 isoforms 1 with 3 $\mu$ M arsenic trioxide showed interesting results. The cells expressing the DWNN domain cells did show a decrease in viable cells but the cells over-expressing the RBBP6 bigger isoform 1 showed large decrease in the percentage of viable cells. This result was somewhat expected, as arsenic trioxide was shown here to induce G2/M cell cycle arrest and up-regulation of the DWNN

domain/isoform 3 (figure 6.4). This result suggests that the DWNN is indeed a G2/M cell cycle regulator while the RBBP6 isoform 1 and possibly isoform 2 are involved in the mitotic apoptosis in humans, as previously reported for the murine P2P-R (Gao and Scott, 2002, Gao and Scott, 2003).

Over-expression of both the DWNN/Isoform 3 and RBBP6 isoform 1 did not cause resistance to staurosporine-induced apoptosis, but rather showed a one-fold decrease of viable MCF-7 cells. This result suggested that these two molecules may both be involved in staurosporine-induced cell cycle regulation. The question that followed then was whether the DWNN/isoform 3 and RBBP6 isoform 1 sensitized MCF-7 breast cancer cells to apoptosis induced by these compounds. Camptothecin, arsenic trioxide and staurosporine were next used to treat the stable population of transfected MCF-7 cells and to assess them for apoptosis sensitivity using *APOPercentage* analysis. Figure 6.8 shows the effect of the over-expression of the DWNN/Isoform 3 and RBBP6 isoform 1 in MCF-7 in each of  $As_2O_3$ , camptothecin and staurosporine induced apoptosis, respectively.

The RBBP6 isoform 1 sensitized the MCF-7 cells to camptothecin- (figure 6.8A), staurosporine- (figure 6.8B) and  $As_2O_3$ -induced (figure 6.8C) apoptosis. The over-expression of the DWNN domain did not sensitize the MCF-7 cells to either camptothecin or staurosporine-induced apoptosis, but did significantly sensitize the MCF-7 cells to  $As_2O_3$ -induced apoptosis. The RBBP6 isoform 1 caused an over two-fold increase of apoptosis compared to control cells. Following this, the next question to be addressed was; whether  $As_2O_3$  causes induction of the DWNN

domain expression in HeLa and HepG2 cells, if these cells are sensitized to apoptosis.

Figure 6.9A shows that 3 $\mu$ M As<sub>2</sub>O<sub>3</sub> treatment induced an increase in the expression of the DWNN/Isoform 3 in the MCF-7, HeLa and HepG2 cells after 24 hours. Unlike the situation seen in normal Hek 293T cells, where the DWNN was dephosphorylated and/or deglycosylated (figure 6.4), in the above mentioned cancer cells the induced DWNN was phosphorylated and/or glycosylated. The difference between the DWNN concentrations in cancer and normal cells may partly determine the mechanisms of how cancer cells avoid cell cycle control. The induction of DWNN expression was not associated with increased apoptosis actively, but was associated rather with the G2/M cell cycle arrest that As<sub>2</sub>O<sub>3</sub> induces after 24 hours. Figure 6.9C showed that the population of apoptotic cells increased in all cancer cell lines after 48 hours of treatment with As<sub>2</sub>O<sub>3</sub>, when compared to apoptosis after 24 hours (figure 6.9B). These results further corroborate previous reports that documented the use of As<sub>2</sub>O<sub>3</sub> in cancer therapy (Lu et al., 2007, Shen et al., 1997). This data also suggests a use for the DWNN/Isoform 3 and RBBP6 isoform 1 in cancer treatment.

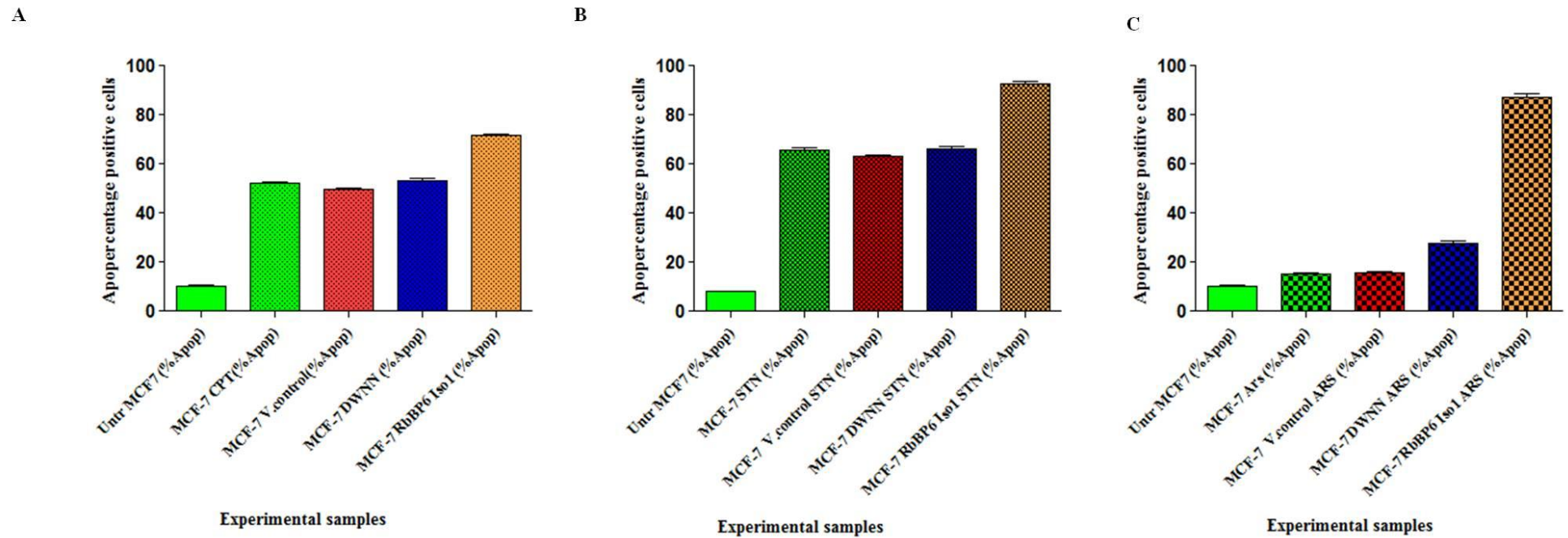


**Figure 6.8 – Apoptosis in the DWNN/Isoform 3 and RBBP6 isoform over-expressing MCF-7 cells:** These figures show apoptotic induction by Camptothecin (A), staurosporine (B) and  $As_2O_3$  (C) in MCF-7 cells that express the DWNN and RBBP6 isoform 1. The graph was plotted with mean  $\pm$ SEM ( $P < 0.05$ ) from a mean of three independent experiments for each compound. The DWNN domain does not show an apoptosis sensitizing effect in camptothecin and staurosporine-induced apoptosis. In arsenic trioxide-induced apoptosis both the DWNN and RBBP6 isoform 1 in MCF-7 cells resulted in a one fold and a threefold increase respectively.

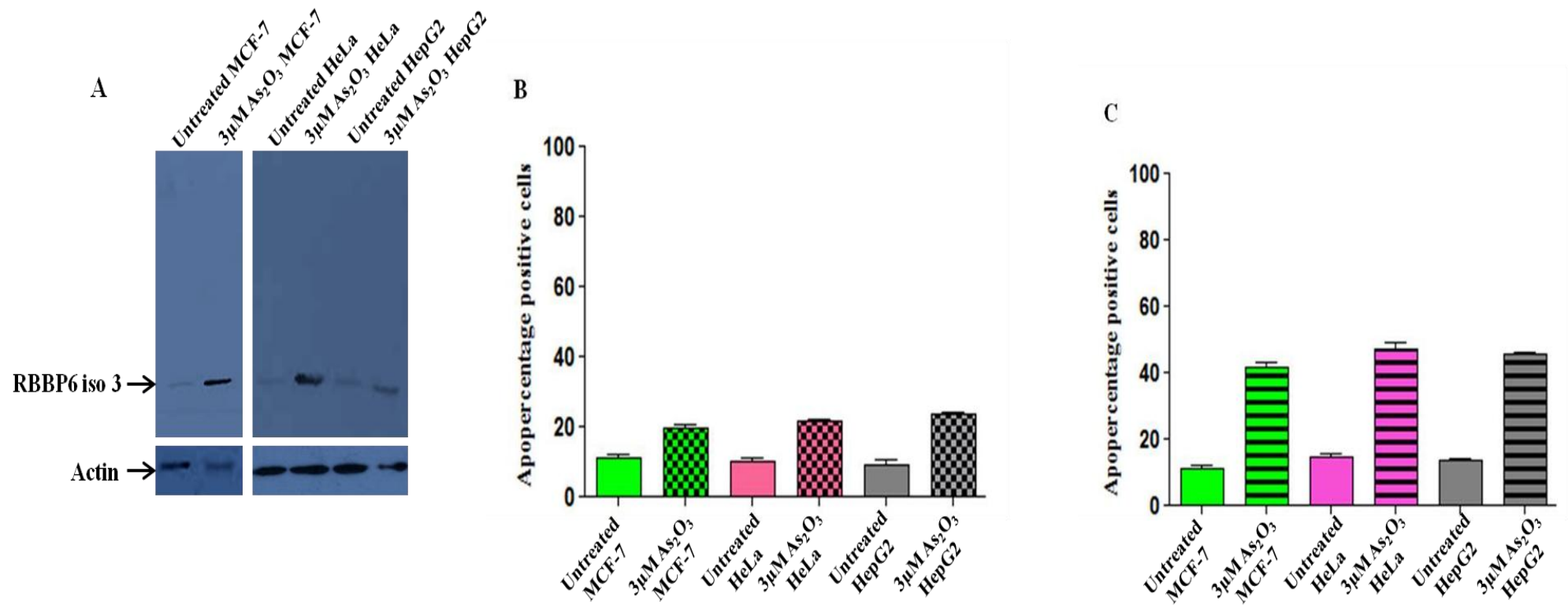


**Figure 6.9 - The induction of the DWNN domain/Isoform 3 expression and Arsenic trioxide-induced apoptosis:** These figures show the induced expression of the DWNN in MCF-7, HeLa and HepG2 cells (Figure 6.9A) after 24 hours (B) and 48 hours (C). Figures 6.9B and C show graphs with mean  $\pm$ SEM ( $P < 0.05$ ) from a mean of three independent experiments of arsenic trioxide in these cell lines. The percentage of apoptotic cells increased over 48 hour period but the DWNN expression was induced within the 24 hour periods.

## Chapter Seven: General discussion

---

### 7.1 Introduction

After many years subsequent to its discovery, DWNN has no defined function that can be stated conclusively. This study was directed at determining the role of this protein in mammalian cells by firstly examining the ubiquitin-like nature of the DWNN through the combined use of proteomics, Western blotting analysis and MALDI-TOF mass spectrometry. Additionally, DWNN was also localized in human cancers, specifically breast cancer, hepatocellular carcinoma and cervical carcinoma. Finally functional studies including RNA interference and over-expression were used here to elucidate the role(s) of DWNN in the cell cycle, apoptosis and carcinogenesis.

This study shows that in humans, RBBP6 multiple splice variants are involved in the suppression of cellular proliferation and are inactivated by cell cycle dependent phosphorylation. RBBP6 has been reported to interact with two tumour suppressors, p53 and pRb (Sakai et al., 1995, Simons et al., 1997) and this interaction suggests an involvement of this gene in cell homeostasis, since these two tumour suppressors play a role in cell turnover. Previous studies have attempted to decipher the role of the mouse RBBP6 homologues (Gao and Scott, 2002, Gao and Scott, 2003, Li et al., 2007a, Scott et al., 2003, Scott and Gao, 2002, Scott et al., 2005, Witte and Scott, 1997, Yoshitake et al., 2004), all reporting a role in the cell cycle and apoptosis regulation. Currently, while there is little information regarding the RBBP6 human counterpart, it would be logical to postulate a similar role for RBBP6 in humans as that for mice, wherein P2P-R is

involved in both apoptosis and cell cycle (Gao and Scott, 2002, Gao and Scott, 2003, Scott and Gao, 2002). Furthermore, the human RBBP6 was reported to have ubiquitin ligase activity through its RING finger domain (Chibi et al., 2008) and Yb-1, which has been reported to be a proliferation gene, at least in breast cancer cells (Basaki et al., 2010, Takahashi *et al.*, 2010, Yu et al., 2010), and was shown to be one of the RBBP6 targets for ubiquitination (Chibi et al., 2008). Similarly, the *Drosophila* counterpart SNAMA was also shown to possess E3 ubiquitin ligase activity through its RING finger domain and additionally proved to be an apoptosis suppressor (Mather et al., 2005).

Recently it was reported that the mouse homologue, P2P-R binds SRC-1 transcription co-regulatory factor (steroid receptor co-activator-1) wherein its over-expression represses oestrogen-induced transcription, while its knock-down increased oestrogen-mediated transcription (Peidis et al., 2010). It was reported that over-expression of SRC-1 contributes to cell growth of human cancer cells, for example, MCF-7, breast cancer cells and SCC, cells derived from squamous cell carcinoma, in an oestrogen (E2)-dependent manner and may thus be involved in breast cancer tumourigenesis (Hudelist et al., 2003, Ku and Crowe, 2007, Tai et al., 2000). In this regard, oestrogen was reported to induce tumourigenesis by targeting tumour suppressor genes, for example, Protein Tyrosine Phosphatase, PTPRO (Ramaswamy et al., 2009). This evidence further links RBBP6 involvement to tumourigenesis in humans. It should be mentioned that all of these reports present data concerning the larger RBBP6 products, with only very limited data concerning RBBP6 isoform 3 (DWNN), which has a ubiquitin-like fold (Pugh et al., 2006).

## **7.2 DWNN and its RBBP6 family relatives in human cancers**

### **7.2.1 RBBP6 transcripts**

In chapters four and five it was demonstrated that DWNN and RBBP6 gene products are down-regulated in human cancers. Figure 4.1 demonstrated that RBBP6 binding domains form part of the RBBP6 mRNA product and the amplification of a wild-type domain sequence suggested that this gene may not be the target of the mutagenesis that is often involved in cancer development. Previously it was shown that the two RBBP6 transcripts 1 and 2 (due to alternative splicing) are equally expressed in normal human cells (Mbita, 2004). In the present study however, using RT-PCR and real-time PCR (Figure 4.2), it was shown that human cancer cells generally have a low expression of the DWNN and RBBP6 transcripts, compared to non-cancerous cells. The exception to this was the high expression of the DWNN and RBBP6 transcripts seen in Jurkat cells. The reason for this result is unknown but this may imply that DWNN and RBBP6 play no role in the development of T cell leukaemia. It has previously been reported that DWNN is involved in CTL killing and its knock-down resulted in resistance to CTL killing and staurosporine-induced apoptosis (George, 1995). The low expression of the DWNN and RBBP6 reported here, with the exception of Jurkat cells, may facilitate the evasion of cell cycle control and subsequent apoptosis in cancer.

### **7.2.2 RBBP6 isoforms**

It was previously reported that the DWNN domain shared a 22 % similarity with ubiquitin and has a similar tertiary structure to that of ubiquitin (Pugh et al., 2006). Another important point is the presence of a highly conserved glycine

residue at the carboxyl terminus of the DWNN domain, analogous to that seen in ubiquitin. This conserved residue is required for covalent modification of targets for known modifiers but is not always the sole determinant (Wilkinson et al., 2004), further suggesting that the DWNN domain may be involved in ubiquitin-like modifications. It should be mentioned that ubiquitin-like proteins do not require a high sequence similarity to ubiquitin to possess ubiquitin like activities, for instance SUMO shares only 18 % sequence similarity (Buschmann et al., 2001), while DWNN shares 22% sequence similarity (Pugh et al., 2006).

The anti-human DWNN antibody used here detects two proteins, an approximately 250 kDa protein (isoform 1 and 2) and another protein of approximately 15 kDa (RBBP6 isoform3/DWNN domain). In the characterization of the anti-human DWNN polyclonal antibody, it was observed that the antibody reacted strongly with a protein of approximately 120 kDa (figures 4.3, 4.4 and 4.5). This could either be due to degradation of the 250 kDa RBBP6 protein products that also contain the DWNN domain, or that the DWNN domain is attached to a high molecular weight protein, or that this represent a truncated RBBP6 isoform 1 and/or 2 protein. The degradation theory seemed unlikely because gel electrophoresis and Western blot analysis (figures 4.3, 4.4 and 4.5) showed intact protein bands at 120 kDa with no evidence of degradation. Figure 4.1 suggested no evidence of truncating mutations in the sequenced RBBP6 domains. A polyclonal anti-PACT antibody had been reported to detect a full 250 kDa protein (Simons et al., 1997). This pointed to the second possibility that the DWNN domain is associated with a high molecular weight protein. This provides further credence for the nature of the DWNN domain as a modifier of other

proteins, binding to proteins and potentially facilitating the ubiquitination of these proteins. Two-dimensional Western blot analysis, using a purified antibody (see figure 4.9), suggests that DWNN may target more than one protein for modification.

Further to this, as Pugh et al. (2006) resolved the DWNN structure as a ubiquitin-like protein (UBL) [figure 7.1] and sequence similarity to ubiquitin, it was predicted that DWNN may be tagged to other proteins, as are many other UBL proteins (Kirkin and Dikic, 2007, Liao et al., 2010a). Indeed, in the present study the use of a polyclonal anti-human DWNN antibody confirmed that DWNN was attached to other proteins (figures 4.3 to figure 4.8) and could be described as “DWNNylation”. The Western blotting analysis using both 1D and 2D gel electrophoresis further implicated an association of DWNN with other proteins and moreover that DWNN is a likely UBL modifier, being able to target more than one protein for modification.

The low protein expression levels reported here reflects the aforementioned low transcript levels. High quantities of protein samples had to be loaded to allow for Western analysis and detection. Secondly, the DWNN domain is bound to other proteins, as urea extraction facilitated the detection of the DWNN domain as shown in figure 4.5 and figure 4.7 and could be detected on the 2D Western Blots. RBBP6 isoform 3 may therefore be considered as a ubiquitin-like domain protein (UDP), which may be responsible for either degradation of other proteins or their stabilization. The latter seemed more possible since the 120 kDa protein was a very stable and consistent protein product across all of the cell lines (figure 4.3 to

4.8). Several other UBL proteins have been described that are either for degradation or stabilization (see table 7.1 in the following page). These ubiquitin-like modifiers have a wide range of roles in cell homeostasis (table 7.2) and this study suggests a new ubiquitin-like modifier, DWNN to add to this list, which is a G2/M cell cycle regulator (chapter six). The DWNN may still have many substrates that require further characterization. From the additional results of the present study, especially analysis with MALDI-TOF Mass spectrometry, these substrates may include Recoverin and Hypothetical protein XP\_002342450 and possibly many more (Table 4.1). As already mentioned in earlier chapters (chapter two and six) the *RBBP6* gene encodes the DWNN and the two larger isoforms, 1 and 2. The latter two may be ubiquitin ligases and/or even ambitiously “DWNN” ligases, all of which would require further investigation.

**Table 7.1: Ubiquitin and ubiquitin-like proteins.**

(Kirkin and Dikic, 2007)

Ubiquitin family of small protein modifiers.		
Modifier	Functions	Ub-/Ubl-binding domains
Ubiquitin	Proteasomal and lysosomal degradation, endocytosis, DNA repair, transcription, chromatin structure	CUE, DUIM, GAT, GLUE, Jab1/MPN, MIU, NZF, PFU, UBA, Ubc, UBM, UBP, UBZ, UEV, UIM, ZnF_A20 Reviewed in [4].
SUMO1, 2, 3	Nuclear localization, transcriptional regulation, DNA repair, antagonizing ubiquitylation	SIM/SBD
NEDD8/Rub1	Regulation of E3 ligases, transcription, proteasomal degradation	UBA
FAT10	Proteasomal degradation, apoptosis	UBA
ISG15	IFN- $\alpha/\beta$ response	Uncharacterized
Urm1	Nutrient sensing, oxidative stress response	Uncharacterized
Ufm1	Unknown	Uncharacterized
FUB1	T-cell activation	Uncharacterized
Hub1/Ubl5	Pre-mRNA splicing	Uncharacterized
Atg8	Autophagy	Uncharacterized
Atg12	Autophagy	Uncharacterized

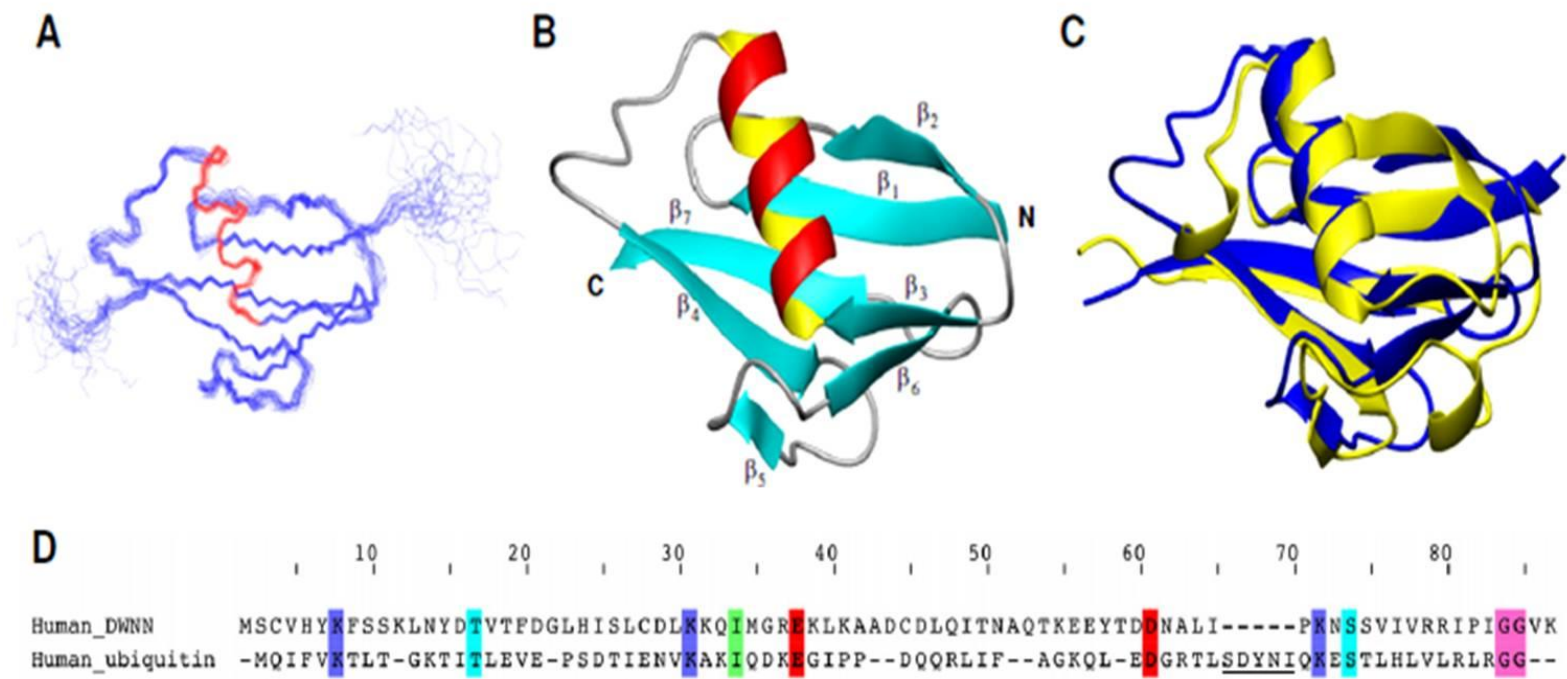


**Figure 7.1 – Structural and key amino acid similarities between ubiquitin and DWNN:** Figures 7.1 A and B show the determined structure of the DWNN while figure 7.1 C shows the structures of Ubiquitin (Blue) and DWNN super-positioned (Yellow). Figure 7.1D shows sequence alignment of the DWNN and ubiquitin showing the highlighted amino acid residues that are important for ubiquitination and possible “DWNNylation”. An extract from Pugh et al. , 2006.

**Table 7.2: Ubiquitin-like protein modifiers, substrates and their functions.**

(Herrmann et al., 2007)

Ubiquitin-Like Modifier	Ubiquitin Sequence Homology (%)	E1–E2–E3 Conjugating Enzymes Deconjugating Enzyme (DCE)	Substrates	Functions
ISG15 (UCRP) (2 ubiquitins)	29, 27	E1: UBE1L; E2: UBCH8	PLC-γ1, JAK1, STAT1, ERK1/2, serpin 2a	Positive regulator of IFN-related immune response, potentially involved in cell growth and differentiation
FUB1 (MNSFβ)	37	NA	TCR-α-like protein, Bcl-G	Negative regulator of leukocyte activation and proliferation
NEDD8 (Rub1)	58	E1: APPBP1-UBA3; E2: UBC12; E3: Roc1, Mdm2; DCE: DEN1/NEDP1, UCH-L1, UCH-L3, USP21, COP9	cullins, p53, Mdm2, synphilin-1	Positive regulator of ubiquitin E3s; directs to proteasomal degradation
FAT10 (2 ubiquitins)	29, 36	NA	MAD2	Cell cycle checkpoint for spindle assembly, directs to proteasomal degradation
SUMO-1 (SMT3C, GMP1, UBL1)	18	E1: SAE-1/-2 (AOS1-UBA2); E2: UBC9; E3: RanBP2, Pc2, PIAS superfamily; DCE: SENP-1 and -2 (Ulp-1 and -2), SUSP4	Glut1, Glut4, c-Jun, IκBα, p53, Mdm2, SOD-1, RXRα, NEMO, PML, Sam68, RanGAP1, RanBP2, ADAR1, PCNA, Drp1, STAT-1, Sp3, thymine-DNA glycosylase, topoisomerase II	Control of protein stability, function, and localization, antagonist to ubiquitin, overlap with SUMO-2/-3
SUMO-2 (SMT3B); SUMO-3 (SMT3A)	16	E1: SAE-1/-2; E2: UBC9; DCE: SENP-3 and -5	RanGAP1, C/EBPβ1, topoisomerase II, thymine-DNA glycosylase	Transcription regulation, cell cycle progression
Apg 8	10	E1: Apg7; E2: Apg3; DCE: Apg4	Phosphatidylethanolamine	Autophagy, cytoplasm-to-vacuole targeting
Apg 12	17	E1: Apg7; E2: Apg10	Apg 5	Autophagy, cytoplasm-to-vacuole targeting
Urm1	12	E1: Uba4	Ahp1	Potential role in oxidative stress response
UBL5 (Hub1)	25	NA	CLK4, Snu66, Sph1, Hbt1	Pre-mRNA splicing, appetite regulation
Ufm1	16	E1: Uba5; E2: Ufc1	NA	Potential role in endoplasmic stress response

In addition to the involvement of the DWNN in protein modifications, DWNN is itself posttranslationally modified, as shown in figures 4.7 and 4.8; here, the DWNN domain is present in both post-translationally modified and un-modified forms, these as such include both phosphorylation and glycosylation respectively. Figure 4.10 suggested that the other spots in 2D Western blotting analysis were GST related proteins, while the 2 spots in the 15 kDa region shown in figure 4.8, are likely to be DWNN domains. Bioinformatics analysis using ExPasy confidently predicted that these 2 spots are DWNN products with one being

posttranslationally modified and one un-modified DWNN respectively. Figure 4.9 showed that the DWNN domain had predicted phosphorylation sites when a NetPhos 2.0 server on ExPASy was used to predict this (Blom et al., 1999). Even though there are more phosphorylation (figure 4.9) than glycosylation sites (figure 4.10), figure 4.10 suggests that this variation may also be due to glycosylation. On 2D gel electrophoresis, phosphorylation of a particular protein results in protein spots that migrate horizontally at different levels, with no size difference, while glycosylation results in size differences. The two protein spots detected at 15 kDa are therefore most likely due to glycosylation of the DWNN domain in human cells. Transfection of MCF-7 cells with the wild-type DWNN domain, as well as mutant form in the post-translational site, can further increase the understanding of this novel domain protein in cell homeostasis and carcinogenesis. The use of arsenic trioxide resulted in the appearance of a 13 kDa protein (discussed in section 6.4) suggesting that a DWNN function is post-translationally regulated by both glycosylation and phosphorylation.

Using yeast-two-hybrid studies and immunoprecipitation Chibi et al. (2008) demonstrated that RBBP6 isoform 1 and 2 are E3 ubiquitin ligases by virtue of possessing a RING finger domain. They showed that RBBP6 ubiquitinated its target Yb1 (Chibi et al., 2008). The *Drosophila* RBBP6 homologue was shown to also have a ubiquitin ligase activity (Antunes, 2009, Mather et al., 2005), however the SNAMA DWNN domain is not a stand-alone protein domain as is its human counterpart. To date, this is the only work to our knowledge that has attempted to investigate the UBL nature of the DWNN.

Other factors associated with cell proliferation and survival are the Vav family of proteins (Madureira et al., 2005, Miller et al., 2005). RBBP6 has been involved with the ubiquitination of Vav2 and has thus been implicated in cancer cell signalling in pancreatic cancer cell lines (Thalappilly et al., 2008). The ubiquitin-like functions of DWNN may be implicated in the suppression of cancer initialization. The implication of RBBP6 in the ubiquitination of Vav proteins may also actually be DWNNylation of Vav2 by the RBBP6 E3 ligase.

The role of the DWNN and RBBP6 is more complex than initially thought. The RBBP6 isoforms 1 and 2 have previously been shown to induce or at least play a role in the intrinsic apoptotic pathway (Gao and Scott, 2002, Gao and Scott, 2003, Scott and Gao, 2002). Even though Pugh et al., (2006) demonstrated that the DWNN has a ubiquitin-like fold, there is to date no data showing that the DWNN behaves like ubiquitin in human cells (Pugh et al., 2006). The human DWNN is the only RBBP6 family protein that exists as a single domain protein. The Western blot analysis and MALDI-TOF mass spectrometry showed that the DWNN is associated with other proteins (Figures 4.11, 4.12 and table 4.1). The 100kDa spot (spot 1 in table 4.1) did not possess any DWNN peptides, but was identified as Amyotrophic lateral sclerosis 2 chromosomal region candidate gene 11 protein isoform 4. This result could not be explained since there were no associated DWNN peptide masses, likewise for the spot representing the T-cell receptor delta chain. However it cannot be ruled out that these are also targets for “DWNNylation”. Two proteins that were found to be associated with the RBBP6 isoform 3/DWNN peptides are Recoverin (Spot 6 in table 4.1) and Hypothetical protein XP\_002342450 (spot 3 in table 4.1). This result further implicates the

DWNN as a novel ubiquitin-like protein that interacts with Recoverin and Hypothetical protein XP\_002342450.

### **7.3 DWNN, a novel ubiquitin-like protein (UBL)**

This study has further strengthened the possibility that the DWNN domain is a ubiquitin-like protein that has a role in cell cycle regulation. It has been well documented that these ubiquitin-like proteins can either contribute to protein degradation or stabilization. In this study it was demonstrated that the DWNN is associated with other proteins (Table 4.1). Using Western blotting analysis, 2D gel electrophoresis and MALDI-TOF Mass Spectrometry this study showed that the DWNN may be conjugated to other proteins to either increase their stability or degradation or for other biological functions so far un-elucidated. Unfortunately there is no available information regarding the Hypothetical protein XP\_002342450, but the result showing that the DWNN is associated with Recoverin was very interesting.

#### **7.3.1 Recoverin**

Recoverin, a neuronal calcium binding protein is predominantly found in photoreceptor cells. Recoverin plays a role in the inhibition of rhodopsin kinase and is consequently involved in the regulation of rhodopsin phosphorylation (Sanada et al., 1996, Senin et al., 2004). As mentioned in this study DWNN, was found to be associated with this protein (Table 4.1) and is suggested to be a stabilizer of Recoverin. DWNN (in this study) and Recoverin have been shown to suppress cell proliferation, at least in the lung cancer cells, A549 cells (Maeda et al., 2000) and in gastric cells (Ohguro et al., 2004). The observed cell growth

inhibition by the DWNN (figure 6.7 to 6.9) may thus be associated with DWNN and Recoverin interactions. Additionally, over-expression of the DWNN in Hek 293T cells resulted in the stabilization of p53, with no p53 being detected in wild type cells (figure 6.5). This growth inhibition by the DWNN may be p53-dependent, involving Recoverin as well. Even though p53 was not identified as a target of possible “DWNNylation” in the MALDI-TOF mass spectrometry experiment, over-expression of the DWNN strongly suggests that the DWNN may be a p53 stabilizer. There may be more proteins that are DWNN targets since the anti-human DWNN antibody showed both laddering and scattering on 1D and 2D Western blot analysis respectively.

### **7.3.2 Immune system components**

As previously mentioned, DWNN was first identified through genetic screening aimed at identifying novel components of the antigen processing and presentation pathway via major histocompatibility class I (MHC class I) molecules (George, 1995). This initial study showed that somatic cell mutants lacking DWNN were resistant to cytotoxic T cell killing (George, 1995). A more recent study demonstrated that mutant Chinese Hamster Ovary (CHO) cells lacking the DWNN protein product were also resistant to staurosporine-induced apoptosis (Pretorius, 2007). These studies therefore demonstrated that the DWNN protein is important in cell death. The reaction of the anti-human DWNN antibody to protein spots identified using MALDI-TOF MS but lacking RBBP6 isoform 3 peptides, suggests that the DWNN may be targeting many proteins, or is itself targeted by many proteins. Reaction to Immunoglobulin heavy chain FW2-JH region may either be interpreted as non-specific, or alternatively the DWNN

forms complex with these immunoglobulins. Pull-down assays with the DWNN will help to resolve the understanding of these complex interactions.

This study has shown that the DWNN is expressed more by the T-lymphocytes, especially in the tumour stroma. This result further implicates the involvement of the DWNN in Cytotoxic lymphocyte induced cell killing and this corroborates the initial finding that the CHO cells lacking the DWNN were resistant to CTL killing. The high expression of the DWNN and its RBBP6 relatives in lymphocytes found in colon tissues (chapter five) further suggests the involvement of the *RBBP6* gene products in cytotoxic lymphocyte killing.

#### **7.4 Localization of the DWNN and RBBP6 gene products**

In chapter one and two it was mentioned that apoptosis is inhibited in the process of carcinogenesis and apoptosis regulators are deregulated in cancer cells. Since RBBP6 homologues from other organisms have been implicated in RNA processing (Vo et al., 2001), cell cycle regulation (Gao and Scott, 2002, Gao and Scott, 2003) and ubiquitin ligase activities (Pugh et al., 2006), RBBP6 may be a target of this deregulation in cancer progression, as its expression pattern changes in human cancers. Moreover, alterations of its expression in different cell states also argue well for its involvement in carcinogenesis and apoptosis.

Real-time PCR (chapter four) FISH, IHC and ICC (chapter five) all demonstrated that RBBP6 is down-regulated in human cancers at both mRNA and protein levels, respectively, especially in breast cancer. Down-regulation of this gene at both levels suggests that its impeded role favours carcinogenesis, or is at least pro-

cell survival and proliferation. This study found that RBBP6 gene products accumulate in the nucleus in normal tissues, while cancer tissues exhibit a somewhat consistent pattern of expression in which RBBP6 gene products either translocate to the cytoplasm, or are completely absent. Thus deregulated RBBP6 may be involved in carcinogenesis. Apoptosis is certain a gene-regulated mechanism and down-regulation and nuclear-cytoplasmic translocation of RBBP6 in human cancers suggests the RBBP6 product as being one of the gene products that is targeted in tumourigenesis.

RBBP6 protein products are nuclear proteins that are required for apoptosis and cell cycle regulation. Localization of the DWNN domain in cells revealed that the DWNN domain and its RBBP6 isoforms are localizing in the nucleus in viable human cells, while apoptotic and mitotic cells showed higher accretion of these proteins in both the cytoplasm and the nucleus. A mouse homologue of RBBP6, P2P-R has been reported to be involved in mitotic apoptosis and apoptosis in general (Gao and Scott, 2002, Gao et al., 2002). In all the human cell lines that were investigated in this study the RBBP6 was up-regulated in dividing cells and dying cells, thus pointing to its involvement in cell cycle regulation and apoptosis. It is suggested that RBBP6 products are likely involved in cell cycle check points and apoptosis that normally follows when the cells are damaged beyond repair.

Localization and cell staining for RBBP6 suggest involvement in carcinogenesis, cell cycle regulation and apoptosis. RBBP6 homologues have been previously implicated in mitosis and apoptosis (Scott and Gao, 2002). Therefore it is fitting to suggest that the DWNN domain and its RBBP6 isoforms are important in cell

homeostasis and cell regulation and are involved in the carcinogenesis in different organs and tissues. It was observed that at both mRNA and protein levels, MCF-7 cells had low expression of the gene and gene products. Recently, it was reported that the RBBP6 co-repress oestrogen receptor-alpha (ER- $\alpha$ ) in rat adipocytes and mouse eye tissues where oestrogen-induced transcription occurs (Peidis et al., 2010). In this study, the tissue that showed the highest expression of the DWNN mRNA was in normal adipose tissue, which suggests that this gene is also tissue specific. Cytoplasmic localization of the gene was expected to be similar to the reported murine P2P-R localization which showed heterogeneous nuclear ribonucleoprotein (hnRNP)-related protein (Witte and Scott, 1997) which is known to shuttle between the nucleus and the cytoplasm (Piñol-Roma and Dreyfuss, 1993). The identification of recoverin as a potential regulator of the DWNN or target for DWNNylation is very interesting and requires further analysis.

### **7.5 The role of the RBBP6 proteins in cell cycle and apoptosis**

In chapter six, the results of this study suggested that deglycosylation and dephosphorylation of the DWNN domain/RBBP6 isoform 3 may be required for G2/M cell cycle arrest. Two-dimensional gel electrophoresis and Western blotting showed that the DWNN domain is both glycosylated and phosphorylated, two post-translational modifications that may allow the cells to progress through the cell cycle. The abolition of both may result in increased cell cycle arrest and consequently, apoptosis.

RBBP6 isoforms 1 or 2 are possible tumour suppressors since over-expression of isoform 1 of the RBBP6 protein sensitized cancer cells (HepG2 and MCF-7) to apoptosis. Interestingly, isoform 1 also sensitized non-malignant cells, human embryonic 293T cells, to apoptosis induced by Camptothecin and arsenic trioxide. Gao and Scott (2003) showed that over-expression of the mouse P2P-R lacking the DWNN domain promoted Camptothecin-induced apoptosis in MCF-7 cells. Similarly, the use of the full human RBBP6 isoform 1 in this study had the same effect. This result further implies that the DWNN domain may not be necessary for apoptosis, but important for cell cycle regulation.

Arsenic trioxide induces G2/M cell cycle arrest and enhances Chk2/p53-mediated apoptosis (Yoda et al., 2008). Induced expression of the DWNN by arsenic trioxide further suggests the involvement of the DWNN in arsenic trioxide induced G2/M cell cycle arrest and possibly apoptosis in a p53-dependent and independent manners. In p53 compromised states, arsenic trioxide can cause cell abnormalities that may lead to carcinogenesis (Liao et al., 2010b).

### **7.5.1 Arsenic trioxide in phosphorylation and DWNN function**

Arsenic compounds can interfere with the phosphorylation and dephosphorylation processes by replacing the phosphate groups in the biochemical pathways (Xie et al., 2002). The treatment of the 293T cells with arsenic trioxide resulted in the up-regulation of the RBBP6 isoform 3 (DWNN) and dephosphorylation of the DWNN domain as observed by the existence of the 13 kDa DWNN in figure 6.4. This up-regulation was accompanied by the stabilization of the p53 tumour suppressor (figure 6.5). The DWNN may influence the cell cycle arrest in a p53-

dependent manner. The dephosphorylation was not observed in the human cancers (figure 6.9A) even though arsenic trioxide treatment resulted in the up-regulation of the DWNN. This suggests that the DWNN is de-regulated in human cancers, possibly through its post-translational modification. While the exact mechanism that  $As_2O_3$  uses to induce cell cycle arrest and apoptosis remains unclear, cell cycle and apoptosis regulators have nevertheless been reported to be regulated by this compound (Xie *et al.*, 2002). The DWNN domain can certainly be added to this list of cell homeostasis regulators.

Figure 5.4A showed that the knock-down of the DWNN domain resulted in the reduction of G2/M population after the arsenic trioxide treatment, indicating that the DWNN domain is required for the G2/M cell cycle arrest and may be important in p53 regulation. Casitas B-lineage Lymphoma (Cbl) has been shown to also play a role in regulation of the G2/M cell cycle arrest. Treatment of gastric cancer cells with arsenic trioxide up-regulated Cbl proteins and increased the G2/M cell populations (Li *et al.*, 2009d). This effect was reported to be due to PI3K/Akt inhibition by Cbl in a p53-dependant manner. These findings are similar to the findings of this study and raise a possible link of the DWNN in PI3K/Akt signalling pathway in cancer development. Arsenic trioxide has been reported to induce or up-regulate cell cycle and cytotoxic related functional genes (Zhao *et al.*, 2008). Arsenic trioxide induced DWNN up-regulation further substantiates the implication of DWNN as a cell cycle regulator.

## 7.6 Summary of the study

Using a real-time PCR technique in chapter 4, it was demonstrated that the breast cancer cell line, MCF-7 had low levels of DWNN expression at both the mRNA and protein levels. In chapter 5, using FISH, it was shown that the DWNN-containing mRNAs were not expressed in the islands of tumours, while the adjacent tumour associated tissues included cells that were positive for DWNN-containing mRNAs.

- There were no mutations or short nucleotide polymorphisms (SNPs) when different RBBP6 binding domains were investigated as a target for mutagenesis, a process that is often involved in carcinogenesis. Figure 4.1 showed that the RBBP6 transcripts are fully expressed in human cell lines even though the amplification of the RING finger, RbBD and p53BD required nested PCR before a PCR product could be observed in the human cancer cell lines.
- Hek 293T cell line and MCF-7 cell lines were found to be the best suited for the RNA interference and DWNN and RBBP6 isoform 1 over-expression studies respectively. This was investigated in chapter six.
- The anti-human DWNN antibody, after affinity purification was shown to detect the RBBP6 protein products including the DWNN domain under denaturing conditions. The data presented with this antibody corroborated with the RT-PCR and real-time PCR data in that the MCF-7 cells were the low expressers of the RBBP6 gene products. It would be very informative

if a non-cancerous breast cell line could be used for the comparison of the DWNN and RBBP6 expression.

The DWNN domain was found to be possibly a ubiquitin-like modifier of proteins that were tabulated in table 4.1, these being identified here using MALDI-TOF MS. One of the interesting proteins identified with MALDI-TOF was Recoverin, which has been implicated in human cancers. Reaction of the antibody to immunoglobulins suggests non-specificity or that the DWNN forms part of the immune system.

Figures 5.2-5.5 showed that the islands of breast, cervix, liver and other cancers lacked expression of the DWNN mRNAs. The corresponding normal tissues had few cells that were positive for RBBP6 gene products. Interestingly there were cells that were positive for this gene's mRNAs in the tissue associated with (surrounding) the tumours, which suggests that the gene may be a possible inhibitor of cell proliferation and carcinogenesis within the surrounding tissue. This result suggests possible functions for DWNN protein and gene products in the initialization of carcinogenesis and further indicates an involvement of the DWNN in tumourigenesis. As seen in figure 5.6, in all the cancers that were investigated, DWNN mRNAs were significantly reduced in the tumours ( $p < 0.05$ ). Since RBBP6 homologues from other organisms have been implicated in RNA processing (Vo et al., 2001), cell cycle regulation (Gao and Scott, 2002, Gao and Scott, 2003) and ubiquitin ligase activities (Pugh et al., 2006), RBBP6 may be deregulated in human cancers, especially as it had been reported that its murine homologue was found to be up-regulated in oesophageal cancer cells (Yoshitake

et al., 2004). In this chapter it was found that the DWNN mRNA was up-regulated in the tumour associated stromal tissue, but not in the islands of tumours. These results additionally suggest that the DWNN probe can be used as a diagnostic marker for cancer development and possibly staging, of these cancers at least. These results also affirm the sensitivity of FISH over chromogenic *in situ* hybridization.

In chapter three, the DWNN antibody was shown to detect many proteins, most likely because the DWNN has a ubiquitin-like-modifier. Cancer tissues stained positively for the DWNN-containing proteins, even in the tumour islands. The DWNN may thus be a stabilizing protein rather than a destructive protein, but also may stabilize undesired proteins. Some ubiquitin-like modifications are not ideal for cell homeostasis; Sumo1, for example, post-translationally modifies VHL through the action of the protein inhibitors of activated STAT  $\gamma$  (PIAS $\gamma$ ), a Sumo E3 ligase (Cai et al., 2010b). This modification negates the inhibitory function of the VHL tumour suppressor on tumour growth, migration and clonogenicity.

Immunohistochemical staining of human cancers with the anti-human DWNN antibody demonstrated discriminative staining between the cancers and their corresponding normal tissues. Figure 5.7A showed both nuclear and cytoplasmic staining in the normal breast tissue while the tumour tissue showed much increased cytoplasmic staining, this being restricted to the tumour island (Figure 5.7B). This result is in contrast to mRNA localization, which was absent in the tumour islands (Figure 5.6). Figure 5.8 A and B showed the same localization pattern in hepatocellular carcinoma where nuclei in the islands of tumours (figure

5.8 B) were negative compared to diffuse staining in the nuclei and cytoplasm of the normal tissues. Cervical cancer (figure 5.9), adenocarcinomas of the stomach, rectum and the colon (figure 5.10) also showed differential staining between the cancer tissue and their corresponding normal tissues. The kidney clear cell carcinoma displayed more staining than the normal kidney tissue and overall the ovarian tissues generally had a low expression DWNN-proteins over.

RBBP6 protein products are nuclear proteins that are required for apoptosis and cell cycle regulation. Cell staining (5.11-5.15) revealed that the DWNN domain and its RBBP6 isoforms are localized in the nucleus in viable human cells, with apoptotic and mitotic cells showing higher accretion of these proteins in both the cytoplasm and the nucleus. A mouse homologue of RBBP6, P2P-R has been reported to be involved in mitotic apoptosis and apoptosis in general (Scott and Gao, 2002). In all the human cell lines that were investigated in this study, the RBBP6 was up-regulated in dividing cells and dying cells and this points to its involvement in cell cycle regulation and apoptosis. RBBP6 products should be involved in cell cycle check points and apoptosis that normally follow when the cells are damaged beyond repair.

The localization and cell staining for RBBP6 suggest involvement in carcinogenesis, cell cycle regulation and apoptosis. RBBP6 homologues have been previously implicated in mitosis and apoptosis (Scott and Gao, 2002). Therefore it is fitting to suggest that the DWNN domain and its RBBP6 isoforms are important in cell homeostasis and cell regulation and are involved in the carcinogenesis in different organs and tissues.

The construction of RNAi molecules was successful and their effectiveness in the cells was also clearly demonstrated. The RBBP6 cloned RNAi molecules were found to be very specific to their targets and this provided a useful means of investigating the involvement of the DWNN domain and the RBBP6 transcripts, 1, and 3 in cell cycle control and apoptosis. RT-PCR and real-time PCR (figures 6.1 and 6.2) were used to show the knock-down of the RBBP6 variants by the RNAi constructs.

Transient transfection (+/-50%) of the Hek 293T cells with RNAi constructs did not sensitise these cells to camptothecin-induced apoptosis. As shown in Figure 6.3, the knock-down of the RBBP6 isoform three and isoform 1/2 favours an anti-apoptotic fate for the cells. This result suggests that cancerous cells might abolish the expression of this gene, if their excessive proliferation agenda is to be met. Figure 6.4 demonstrated that the DWNN is a G2/M cell cycle phase specific gene product. Figure 6.4 also demonstrates that arsenic trioxide, a cell cycle arrestor, induces the DWNN expression. The stabilization of p53 by the DWNN domain shown in figure 6.5, further suggests that this protein product will modify other proteins, thus suggesting that cell cycle arrest caused by DWNN is in a p53-dependent manner. RNAi of p53 or alternatively use of a p53 negative cell line will confirm this result.

This chapter also documented the establishment of the MCF-7 cells over-expressing DWNN domain and RBBP6 isoform 1 (figure 6.6). The MCF-7 cells over-expressing RBBP6 have been previously shown to be sensitized to

camptothecin-induced apoptosis (Gao and Scott, 2003). MCF-7 cells over-expressing RBBP6 were also shown in the present study to have been sensitized to camptothecin, staurosporine and arsenic trioxide-induced apoptosis (figure 5.7 and 6.8). The DWNN domain over-expressing MCF-7 cells were shown to have been sensitized to arsenic trioxide-induced apoptosis. This result further implicates the DWNN domain as a ubiquitin-like protein specific to cell cycle regulation. The DWNN domain was further shown to be a possible target during carcinogenesis since G2/M cell cycle arrest induced in non-carcinogenic cells, Hek 293T cells, was accompanied by dephosphorylation and deglycosylation of the DWNN, but not in the cancer cells tested (figure 6.9A), where this molecule remained phosphorylated and glycosylated. The induction of the DWNN expression in arsenic trioxide-treated cells was shown to be an early event (figure 6.9B) and increased levels of apoptosis (figure 6.9C) were not necessary for the DWNN domain induction.

The data presented in this study shows that the DWNN domain is a cell cycle regulator, while the RBBP6 isoforms 1 and 2 are probably key players in cell cycle-mediated apoptosis as previously shown for the murine RBBP6 homologue.

## **7.7 Conclusions**

- It is very important to note that the function of a gene may also be determined by the environment and species that the gene is expressed in. This is no exception for the RBBP6 gene: while in mice the evidence suggests a role as an anti-apoptotic gene, in humans, the data presented in this study suggests a pro-apoptotic function for this gene.

- Using RT-PCR and real-time PCR it was found that the DWNN and RBBP6 gene products are down-regulated in human cancer cells. This was corroborated by the Western blotting results, wherein human cancers preferentially lacked expression of the DWNN domain.
- Through the use of 1D and 2D gel electrophoresis and MALDI-TOF mass spectrometry, it was shown that the DWNN domain is a ubiquitin-like modifier that DWNNylates other proteins, in particular Recoverin and possibly p53, for purposes of stabilization.
- Cancer is characterized by the loss of cell cycle control and resistance to apoptosis. DWNN and RBBP6 gene products were found to be down-regulated in human tumours at least at the mRNA level. FISH, showed that DWNN and RBBP6 may be involved in carcinogenesis.
- Cell staining implicates a requirement for that the DWNN and RBBP6 proteins in cell cycle regulation in human cells. In this regard, the DWNN may be both hyperphosphorylated and hyperglycosylated to evade its effect of cell cycle regulation. Use of RNAi for knockdown of DWNN resulted in high proliferation rates; while conversely, over-expression of the DWNN resulted in inhibited growth. This was substantiated by the induced DWNN expression when cell growth was inhibited by arsenic trioxide treatment. It was previously thought that RBBP6 isoform 1 and 2 were responsible for RBBP6 cell cycle and apoptosis regulation. This study however showed that

the DWNN, the smallest RBBP6 family member, is responsible for the cell cycle regulation and may be a key cell cycle progression regulator in a p53-dependent manner.

## Chapter Eight: List of references

---

- ABE, Y., ODA-SATO, E., TOBIUME, K., KAWAUCHI, K., TAYA, Y., OKAMOTO, K., OREN, M. and TANAKA, N. 2008. Hedgehog signaling overrides p53-mediated tumor suppression by activating Mdm2. *Proceedings of the National Academy of Sciences*, 105, 4838.
- ACHANTA, G., PELICANO, H., FENG, L., PLUNKETT, W. and HUANG, P. 2001. Interaction of p53 and DNA-PK in Response to Nucleoside Analogues. *Cancer research*, 61, 8723-8729.
- ACQUAVIVA, J., CHEN, X. and REN, R. 2008. IRF-4 functions as a tumor suppressor in early B-cell development. *Blood*, 112, 3798.
- ADAMS, P. 2001. Regulation of the retinoblastoma tumor suppressor protein by cyclin/cdks. *BBA-Reviews on Cancer*, 1471, 123-133.
- AKERS, A. L., JOHNSON, E., STEINBERG, G. K., ZABRAMSKI, J. M. and MARCHUK, D. A. 2009. Biallelic somatic and germline mutations in cerebral cavernous malformations (CCMs): evidence for a two-hit mechanism of CCM pathogenesis. *Hum Mol Genet*, 18, 919-30.
- ALTSCHUL, S., MADDEN, T., SCHAFFER, A., ZHANG, J., ZHANG, Z., MILLER, W. and LIPMAN, D. 1997. Gapped Blast and Psi-Blast: A New Generation of Protein Database Search Programs. *Nucleic Acids Research*, 25, 3389-3402.
- AMATO, A., LENTINI, L., SCHILLACI, T., IOVINO, F. and DI LEONARDO, A. 2009. RNAi mediated acute depletion of retinoblastoma protein (pRb) promotes aneuploidy in human primary cells via micronuclei formation. *BMC Cell Biol*, 10, 79.
- AMBROSINI, G., SAMBOL, E. B., CARVAJAL, D., VASSILEV, L. T., SINGER, S. and SCHWARTZ, G. K. 2007. Mouse double minute antagonist Nutlin-3a enhances chemotherapy-induced apoptosis in cancer cells with mutant p53 by activating E2F1. *Oncogene*, 26, 3473-81.
- AMEMIYA, Y., AZMI, P. and SETH, A. 2008. Autoubiquitination of BCA2 RING E3 ligase regulates its own stability and affects cell migration. *Mol Cancer Res*, 6, 1385-96.
- AMRÁN, D., SÁNCHEZ, Y., FERNÁNDEZ, C., RAMOS, A., DE BLAS, E., BRÉARD, J., CALLE, C. and ALLER, P. 2007. Arsenic trioxide sensitizes promonocytic leukemia cells to TNF -induced apoptosis via p38-MAPK-regulated activation of both receptor-mediated and mitochondrial pathways. *BBA-Molecular Cell Research*, 1773, 1653-1663.
- ANTONSSON, A. and PERSSON, J. 2009. Induction of Apoptosis by Staurosporine Involves the Inhibition of Expression of the Major Cell Cycle Proteins at the G2/M Checkpoint Accompanied by Alterations in Erk and Akt Kinase Activities. *Anticancer research*, 29, 2893.
- ANTUNES, R. 2009. Characterization of the DWNN domain and ring finger-like motif within the DCM of the *Drosophila melanogaster* SNAMA protein. *University of the Witwatersrand*.
- ARAKAWA, T., YAMAMURA, T., HATTORI, T., HAYASHI, H., MORI, A., YOSHIDA, A., UCHIDA, C., KITAGAWA, M. and ONOZAKI, K. 2008. Contribution of extracellular signal-regulated kinases to the IL-1-induced

- growth inhibition of human melanoma cells A375. *Int Immunopharmacol*, 8, 80-9.
- ARAKAWA, Y., SAITO, S., YAMADA, H. and AIBA, K. 2009. Simultaneous treatment with camptothecin and valproic acid suppresses induction of Bcl-X(L) and promotes apoptosis of MCF-7 breast cancer cells. *Apoptosis*, 14, 1076-85.
- ARMES, J., LOURIE, R., DE SILVA, M., STAMARATIS, G., BOYD, A., KUMAR, B., PRICE, G., HYDE, S., ALLEN, D. and GRANT, P. 2005. Abnormalities of the RB1 pathway in ovarian serous papillary carcinoma as determined by overexpression of the p16 (INK4A) protein. *International Journal of Gynecologic Pathology*, 24, 363-368.
- ARORA, V., CHEUNG, H. H., PLENCHETTE, S., MICALI, O. C., LISTON, P. and KORNELUK, R. G. 2007. Degradation of survivin by the X-linked inhibitor of apoptosis (XIAP)-XAF1 complex. *J Biol Chem*, 282, 26202-9.
- ARUN, B., KILIC, G., YEN, C., FOSTER, B., YARDLEY, D., GAYNOR, R. and ASHFAQ, R. 2003. Correlation of Bcl-2 and p53 Expression in Primary Breast Tumors and Corresponding Metastatic Lymph Nodes. *Cancer*, 98, 2554-2559.
- ASHKENAZI, A. and DIXIT, V. 1998. Death receptors: signaling and modulation. *Science*, 281, 1305-1308.
- ASHKENAZI, A. and HERBST, R. 2008. To kill a tumor cell: the potential of proapoptotic receptor agonists. *The Journal of clinical investigation*, 118, 1979-1990.
- BAI, L., WEI, L., WANG, J., LI, X. and HE, P. 2006. Extended effects of human papillomavirus 16 E6-specific short hairpin RNA on cervical carcinoma cells. *Int J Gynecol Cancer*, 16, 718-29.
- BAI, X. M., JIANG, H., DING, J. X., PENG, T., MA, J., WANG, Y. H., ZHANG, L., ZHANG, H. and LENG, J. 2010. Prostaglandin E2 upregulates survivin expression via the EP1 receptor in hepatocellular carcinoma cells. *Life Sci*, 86, 214-23.
- BALASTIK, M., FERRAGUTI, F., PIRES-DA SILVA, A., LEE, T. H., ALVAREZ-BOLADO, G., LU, K. P. and GRUSS, P. 2008. Deficiency in ubiquitin ligase TRIM2 causes accumulation of neurofilament light chain and neurodegeneration. *Proc Natl Acad Sci U S A*, 105, 12016-21.
- BALTAZIAK, M., KODA, M., WINCEWICZ, A., SULKOWSKA, M., KANCZUGA-KODA, L. and SULKOWSKI, S. 2009. Relationships of P53 and Bak with EPO and EPOR in human colorectal cancer. *Anticancer Res*, 29, 4151-6.
- BASAKI, Y., TAGUCHI, K., IZUMI, H., MURAKAMI, Y., KUBO, T., HOSOI, F., WATARI, K., NAKANO, K., KAWAGUCHI, H. and OHNO, S. 2010. Y-box binding protein-1 (YB-1) promotes cell cycle progression through CDC6-dependent pathway in human cancer cells. *European Journal of Cancer*, 46, 954-965.
- BEDFORD, L., HAY, D., DEVOY, A., PAINE, S., POWE, D., SETH, R., GRAY, T., TOPHAM, I., FONE, K. and REZVANI, N. 2008. Depletion of 26S proteasomes in mouse brain neurons causes neurodegeneration and Lewy-like inclusions resembling human pale bodies. *Journal of Neuroscience*, 28, 8189-8198.

- BEITEL, L. K., ELHAJI, Y. A., LUMBROSO, R., WING, S. S., PANET-  
RAYMOND, V., GOTTLIEB, B., PINSKY, L. and TRIFIRO, M. A.  
2002. Cloning and characterization of an androgen receptor N-terminal-  
interacting protein with ubiquitin-protein ligase activity. *Journal of  
Molecular Endocrinology*, 29, 41-60.
- BELLET, V., DUVAL, R., DELEBASSEE, C., COOK-MOREAU, J. and  
BOSGIRAUD, C. 2004. AZT inhibits Vasa/maedi virus-induced  
apoptosis. *Arch Virol*, 149, 583-601.
- BELLSTEDT, D., HUMAN, P., ROWLAND, G. and VAN DER MERWE, K.  
1987. Acid-treated, naked bacteria as immune carriers for protein antigens.  
*J Immunol Methods*, 98, 249-55.
- BERGMAN, A., KARLSSON, P., BERGGREN, J., MARTINSSON, T.,  
BJORCK, K., NILSSON, S., WAHLSTROM, J., WALLGREN, A. and  
NORDLING, M. 2007. Genome-wide linkage scan for breast cancer  
susceptibility loci in Swedish hereditary non-BRCA1/2 families:  
suggestive linkage to 10q23.32-q25.3. *Genes Chromosomes Cancer*, 46,  
302-9.
- BERKE, S. and PAULSON, H. 2003. Protein aggregation and the ubiquitin  
proteasome pathway: gaining the UPPer hand on neurodegeneration.  
*Current Opinion in Genetics & Development*, 13, 253-261.
- BERLINGIERI, M., PALLANTE, P., GUIDA, M., NAPPI, C., MASCIULLO,  
V., SCAMBIA, G., FERRARO, A., LEONE, V., SBONER, A. and  
BARBARESCHI, M. 2006. UbcH10 expression may be a useful tool in  
the prognosis of ovarian carcinomas. *Oncogene*, 26, 2136-2140.
- BHUSHAN, S., MALIK, F., KUMAR, A., ISHER, H. K., KAUR, I. P., TANEJA,  
S. C. and SINGH, J. 2009. Activation of p53/p21/PUMA alliance and  
disruption of PI-3/Akt in multimodal targeting of apoptotic signaling  
cascades in cervical cancer cells by a pentacyclic triterpenediol from  
*Boswellia serrata*. *Mol Carcinog*, 48, 1093-108.
- BIAN, X., OPIPARI, A., RATANAPROEKSA, A., BOITANO, A., LUCAS, P.  
and CASTLE, V. 2002. Constitutively Active NF $\kappa$ B Is Required for the  
Survival of S-type Neuroblastoma. *Journal of Biological Chemistry*, 277,  
42144-42150.
- BIRBES, H., LUBERTO, C., YI-TE HSU, S., HANNUN, Y. and OBEID, L.  
2005. A mitochondrial pool of sphingomyelin is involved in TNF alpha-  
induced Bax translocation to mitochondria. *Biochemical Journal*, 386,  
445-451.
- BLOM, N., GAMMELTOFT, S. and BRUNAK, S. 1999. Sequence and structure-  
based prediction of eukaryotic protein phosphorylation sites. *Journal of  
Molecular Biology*, 294, 1351-1362.
- BOHSALI, A., ABDALLA, H., VELMURUGAN, K. and BRIKEN, V. 2010.  
The non-pathogenic mycobacteria *M. smegmatis* and *M. fortuitum* induce  
rapid host cell apoptosis via a caspase-3 and TNF dependent pathway.  
*BMC microbiology*, 10, 237.
- BORNSTEIN, G., GANOTH, D. and HERSHKO, A. 2006. Regulation of  
neddylation and deneddylation of cullin1 in SCF<sup>Skp2</sup> ubiquitin ligase by  
F-box protein and substrate. *Proceedings of the National Academy of  
Sciences*, 103, 11515-11520.

- BROMBERG, K., KLUGER, H., DELAUNAY, A., ABBAS, S., DIVITO, K., KRAJEWSKI, S. and RONAI, Z. 2007. Increased expression of the E3 ubiquitin ligase RNF5 is associated with decreased survival in breast cancer. *Cancer research*, 67, 8172-8179.
- BRUSTOVETSKY, T., ANTONSSON, B., JEMMERSON, R., DUBINSKY, J. and BRUSTOVETSKY, N. 2005. Activation of calcium-independent phospholipase A2 (iPLA2) in brain mitochondria and release of apoptogenic factors by BAX and truncated BID. *Journal of neurochemistry*, 94, 980-994.
- BURKHART, D., NGAI, L., ROAKE, C., VIATOUR, P., THANGAVEL, C., HO, V., KNUDSEN, E. and SAGE, J. 2010. Regulation of RB transcription in vivo by RB family members. *Molecular and Cellular Biology*.
- BUSCHMANN, T., LERNER, D., LEE, C. and RONAI, Z. 2001. The Mdm-2 Amino Terminus Is Required for Mdm2 Binding and SUMO-1 Conjugation by the E2 SUMO-1 Conjugating Enzyme Ubc9. *Journal of Biological Chemistry*, 276, 40389-40395.
- CAI, B. Z., MENG, F. Y., ZHU, S. L., ZHAO, J., LIU, J. Q., LIU, C. J., CHEN, N., YE, M. L., LI, Z. Y., AI, J., LU, Y. J. and YANG, B. F. 2010a. Arsenic trioxide induces the apoptosis in bone marrow mesenchymal stem cells by intracellular calcium signal and caspase-3 pathways. *Toxicol Lett*, 193, 173-178.
- CAI, Q., VERMA, S., KUMAR, P., MA, M., ROBERTSON, E. and JIN, D. 2010b. Hypoxia Inactivates the VHL Tumor Suppressor through PIASy-Mediated SUMO Modification. *PLoS ONE*, 5, e9720.
- CANDÉ, C., COHEN, I., DAUGAS, E., RAVAGNAN, L., LAROCLETTE, N., ZAMZAMI, N. and KROEMER, G. 2002. Apoptosis-inducing factor (AIF): a novel caspase-independent death effector released from mitochondria. *Biochimie*, 84, 215-222.
- CAO, X., WANG, A., WANG, C., MAO, D., LU, M., CUI, Y. and JIAO, R. 2009a. Surfactin induces apoptosis in human breast cancer MCF-7 cells through a ROS/JNK-mediated mitochondrial/caspase pathway. *Chemico-Biological Interactions*, 183, 357-362.
- CAO, X. H., WANG, A. H., JIAO, R. Z., WANG, C. L., MAO, D. Z., YAN, L. and ZENG, B. 2009b. Surfactin Induces Apoptosis and G(2)/M Arrest in Human Breast Cancer MCF-7 Cells Through Cell Cycle Factor Regulation. *Cell Biochemistry and Biophysics*, 55, 163-171.
- CARÉN, H., ERICHSEN, J., OLSSON, L., ENERBÄCK, C., SJÖBERG, R., ABRAHAMSSON, J., KOGNER, P. and MARTINSSON, T. 2008. High-resolution array copy number analyses for detection of deletion, gain, amplification and copy-neutral LOH in primary neuroblastoma tumors: Four cases of homozygous deletions of the CDKN 2 A gene. *BMC Genomics*, 9, 353.
- CARTER, B., GRONDA, M., WANG, Z., WELSH, K., PINILLA, C., ANDREEFF, M., SCHOBER, W., NEFZI, A., POND, G. and MAWJI, I. 2005. Small-molecule XIAP inhibitors derepress downstream effector caspases and induce apoptosis of acute myeloid leukemia cells. *Blood*, 105, 4043-4050.

- CARVAJAL, D., TOVAR, C., YANG, H., VU, B., HEIMBROOK, D. and VASSILEV, L. 2005. Activation of p53 by MDM2 antagonists can protect proliferating cells from mitotic inhibitors. *Cancer research*, 65, 1918-1924.
- CASTEDO, M., PERFETTINI, J., PIACENTINI, M. and KROEMER, G. 2005. p53—A pro-apoptotic signal transducer involved in AIDS. *Biochemical and Biophysical Research Communications*, 331, 701-706.
- CHANG, J., LIU, Y., ZHANG, D. D., ZHANG, D. J., WU, C. T., WANG, L. S. and CUI, C. P. 2010. Hepatopoietin Cn suppresses apoptosis of human hepatocellular carcinoma cells by up-regulating myeloid cell leukemia-1. *World J Gastroenterol*, 16, 193-200.
- CHANG, P. C., CHI, C. W., CHAU, G. Y., LI, F. Y., TSAI, Y. H., WU, J. C. and LEE, Y. H. W. 2006. DDX3, a DEAD box RNA helicase, is deregulated in hepatitis virus-associated hepatocellular carcinoma and is involved in cell growth control. *Oncogene*, 25, 1991-2003.
- CHARLOT, J., NICOLIER, M., PRÉTET, J. and MOUGIN, C. 2006. Modulation of p53 transcriptional activity by PRIMA-1 and Pifithrin-a on staurosporine-induced apoptosis of wild-type and mutated p53 epithelial cells. *Apoptosis*, 11, 813-827.
- CHATTERJEE, A., CHANG, X., SEN, T., RAVI, R., BEDI, A. and SIDRANSKY, D. 2010. Regulation of p53 family member isoform DeltaNp63alpha by the nuclear factor-kappaB targeting kinase IkappaB kinase beta. *Cancer Res*, 70, 1419-29.
- CHAUBE, S., PRASAD, P., THAKUR, S. and SHRIVASTAV, T. 2005. Hydrogen peroxide modulates meiotic cell cycle and induces morphological features characteristic of apoptosis in rat oocytes cultured in vitro. *Apoptosis*, 10, 863-874.
- CHEN, T. and WONG, Y. 2008a. Selenocystine induces apoptosis of A375 human melanoma cells by activating ROS-mediated mitochondrial pathway and p53 phosphorylation. *Cellular and Molecular Life Sciences (CMLS)*, 65, 2763-2775.
- CHEN, T. and WONG, Y. S. 2008b. In vitro antioxidant and antiproliferative activities of selenium-containing phycocyanin from selenium-enriched *Spirulina platensis*. *J Agric Food Chem*, 56, 4352-8.
- CHEN, T., WONG, Y. S. and ZHENG, W. 2009a. Induction of G1 cell cycle arrest and mitochondria-mediated apoptosis in MCF-7 human breast carcinoma cells by selenium-enriched *Spirulina* extract. *Biomed Pharmacother*.
- CHEN, Y., MA, D., HUANG, Q. L., ZHENG, W., ZHANG, J., SHEN, Y., LI, J., DONG, W., LU, M., WANG, J. and HUA, Z. C. 2009b. Expression, purification and characterization of C-FADD. *Cell Mol Immunol*, 6, 295-301.
- CHENG, F., LIU, J., ZHOU, S., WANG, X., CHEW, J. and DENG, L. 2008. RNA interference against mixed lineage leukemia 5 resulted in cell cycle arrest. *The International Journal of Biochemistry & Cell Biology*, 40, 2472-2481.
- CHENG, Q. and CHEN, J. 2010. Mechanism of p53 stabilization by ATM after DNA damage. *Cell cycle (Georgetown, Tex.)*, 9, 472-478.

- CHENG, Q., CHEN, L., LI, Z., LANE, W. and CHEN, J. 2009. ATM activates p53 by regulating MDM2 oligomerization and E3 processivity. *The EMBO journal*.
- CHEUNG, H. H., MAHONEY, D. J., LACASSE, E. C. and KORNELUK, R. G. 2009. Down-regulation of c-FLIP Enhances death of cancer cells by smac mimetic compound. *Cancer Res*, 69, 7729-38.
- CHEVALIER, F., HIRTZ, C., SOMMERER, N. and KELLY, A. L. 2009. Use of reducing/nonreducing two-dimensional electrophoresis for the study of disulfide-mediated interactions between proteins in raw and heated bovine milk. *Journal of agricultural and food chemistry*, 57, 5948-55.
- CHIBI, M., MEYER, M., SKEPU, A., G. REES, D., MOOLMAN-SMOOK, J. and PUGH, D. 2008. RBBP6 Interacts with Multifunctional Protein YB-1 through Its RING Finger Domain, Leading to Ubiquitination and Proteosomal Degradation of YB-1. *Journal of Molecular Biology*, 384, 908-916.
- CHITALIA, V., FOY, R., BACHSCHMID, M., ZENG, L., PANCHENKO, M., ZHOU, M., BHARTI, A., SELDIN, D., LECKER, S. and DOMINGUEZ, I. 2008. Jade-1 inhibits Wnt signalling by ubiquitylating -catenin and mediates Wnt pathway inhibition by pVHL. *Nature cell biology*, 10, 1208-1216.
- CHO, S. H., CHUNG, K. S., CHOI, J. H., KIM, D. H. and LEE, K. T. 2009. Compound K, a metabolite of ginseng saponin, induces apoptosis via caspase-8-dependent pathway in HL-60 human leukemia cells. *BMC Cancer*, 9, 449.
- CHOI, H., CHO, M., LEE, H. and YOON, D. 2010a. Indole-3-carbinol induces apoptosis through p53 and activation of caspase-8 pathway in lung cancer A549 cells. *Food and Chemical Toxicology*.
- CHOI, S., WRIGHT, J., GERBER, S. and COLE, M. 2010b. Myc protein is stabilized by suppression of a novel E3 ligase complex in cancer cells. *Genes & development*, 24, 1236.
- CHOW, J. Y., BAN, M., WU, H. L., NGUYEN, F., HUANG, M., CHUNG, H., DONG, H. and CARETHERS, J. M. 2010. TGF-beta downregulates PTEN via activation of NF-kappaB in pancreatic cancer cells. *Am J Physiol Gastrointest Liver Physiol*, 298, G275-82.
- CILLESSEN, S., REED, J., WELSH, K., PINILLA, C., HOUGHTEN, R., HOOIJBERG, E., DEURHOF, J., CASTRICUM, K., KORTMAN, P. and HESS, C. 2008. Small-molecule XIAP antagonist restores caspase-9 mediated apoptosis in XIAP-positive diffuse large B-cell lymphoma cells. *Blood*, 111, 369-375.
- COLLINS, K., JACKS, T. and PAVLETICH 1997. The cell cycle and cancer. *Proceedings of the National Academy of Sciences of the United States of America*, 94, 2776-2778.
- COPPÉ, J., PATIL, C., RODIER, F., SUN, Y., MUÑOZ, D., GOLDSTEIN, J., NELSON, P., DESPREZ, P. and CAMPISI, J. 2008. Senescence-associated secretory phenotypes reveal cell-nonautonomous functions of oncogenic RAS and the p53 tumor suppressor. *PLoS Biol*, 6, 2853-2868.
- COSTA, B. M., SMITH, J. S., CHEN, Y., CHEN, J., PHILLIPS, H. S., ALDAPE, K. D., ZARDO, G., NIGRO, J., JAMES, C. D., FRIDLYAND, J., REIS,

- R. M. and COSTELLO, J. F. 2010. Reversing HOXA9 oncogene activation by PI3K inhibition: epigenetic mechanism and prognostic significance in human glioblastoma. *Cancer Res*, 70, 453-62.
- CRNKOVIC-MERTENS, I., BULKESCHER, J., MENSGER, C., HOPPE-SEYLER, F. and HOPPE-SEYLER, K. 2010. Isolation of peptides blocking the function of anti-apoptotic Livin protein. *Cell Mol Life Sci*.
- CRNKOVIC-MERTENS, I., WAGENER, N., SEMZOW, J., GRONE, E. F., HAFERKAMP, A., HOHENFELLNER, M., BUTZ, K. and HOPPE-SEYLER, F. 2007. Targeted inhibition of Livin resensitizes renal cancer cells towards apoptosis. *Cell Mol Life Sci*, 64, 1137-44.
- CROSS, A. J., LEITZMANN, M. F., SUBAR, A. F., THOMPSON, F. E., HOLLENBECK, A. R. and SCHATZKIN, A. 2008. A prospective study of meat and fat intake in relation to small intestinal cancer. *Cancer Res*, 68, 9274-9.
- CUI, Q., YU, J., WU, J., TASHIRO, S., ONODERA, S., MINAMI, M. and IKEJAMA, T. 2007. p53-mediated cell cycle arrest and apoptosis through a caspase-3- independent, but caspase-9-dependent pathway in oridonin-treated MCF-7 human breast cancer cells. *Acta Pharmacol Sin*, 28, 1056-1066.
- DAS, R., MARIANO, J., TSAI, Y. C., KALATHUR, R. C., KOSTOVA, Z., LI, J., TARASOV, S. G., MCFEETERS, R. L., ALTIERI, A. S., JI, X., BYRD, R. A. and WEISSMAN, A. M. 2009. Allosteric activation of E2-RING finger-mediated ubiquitylation by a structurally defined specific E2-binding region of gp78. *Mol Cell*, 34, 674-85.
- DAUGAS, E., SUSIN, S., ZAMZAMI, N., FERRI, K., IRINOPOULOU, T., LAROCLETTE, N., PREVOST, M., LEBER, B., ANDREWS, D. and PENNINGER, J. 2000. Mitochondrio-nuclear translocation of AIF in apoptosis and necrosis. *The FASEB Journal*, 14, 729-739.
- DE FILIPPIS, R., GOODWIN, E., WU, L. and DIMAIO, D. 2003. Endogenous Human Papillomavirus E6 and E7 Proteins Differentially Regulate Proliferation, Senescence, and Apoptosis in HeLa Cervical Carcinoma Cells. *Journal of Virology*, 77, 1551-1563.
- DEBERNARDI, S., LILLINGTON, D. and YOUNG, B. 2004. Understanding cancer at the chromosome level: 40 years of progress. *European Journal of Cancer*, 40, 1960-1967.
- DEBRET, R., BRASSART-PASCO, S., LORIN, J., MARTORIATI, A., DESHORGUE, A., MAQUART, F., HORNEBECK, W., RAHMAN, I. and ANTONICELLI, F. 2008. Ceramide inhibition of MMP-2 expression and human cancer bronchial cell invasiveness involve decreased histone acetylation. *Biochimica et Biophysica Acta (BBA)-Molecular Cell Research*, 1783, 1718-1727.
- DEKEL, Y., KUGEL, V., LIVNE, P., GAL, R. and KOREN, R. 2004. DCC protein expression in clear cell renal cell carcinoma. *BJU International*, 93, 867-869.
- DENNY, L. 2006. Cervical cancer: the South African perspective. FIGO 6th Annual Report on the Results of Treatment in Gynecological Cancer. *Int J Gynaecol Obstet*, 95 Suppl 1, S211-4.

- DEVERAUX, Q., LEO, E., STENNICKE, H., WELSH, K., SALVESEN, G. and REED, J. 1999. Cleavage of human inhibitor of apoptosis protein XIAP results in fragments with distinct specificities for caspases. *The Embo Journal*, 18, 5242-5251.
- DI MARCOTULLIO, L., FERRETTI, E., GRECO, A., DE SMAELE, E., SCREPANTI, I. and GULINO, A. 2007. Multiple ubiquitin-dependent processing pathways regulate hedgehog/gli signaling: implications for cell development and tumorigenesis. *Cell Cycle*, 6, 390-3.
- DING, Q., XIA, W., HSU, J., CHEN, C., LI, L., LEE, D., YANG, J., XIE, X., LIU, J. and HUNG, M. 2007. Myeloid cell leukemia-1 inversely correlates with glycogen synthase kinase-3beta activity and associates with poor prognosis in human breast cancer. *Cancer Research*, 67, 4564-4571.
- DLAMINI, Z., MBITA, Z. and LEDWABA, T. 2005. Can targeting apoptosis resolve the cancer saga? *Future Oncol.*, 1, 339-349.
- DOONAN, F. and COTTER, T. G. 2008. Morphological assessment of apoptosis. *Methods*, 44, 200-4.
- DU, Z., FAN, M., KIM, J., ECKERLE, D., LOTHSTEIN, L., WEI, L. and PFEFFER, L. 2009. Interferon-resistant Daudi Cell Line with a Stat2 Defect Is Resistant to Apoptosis Induced by Chemotherapeutic Agents. *Journal of Biological Chemistry*, 284, 27808.
- DUAN, X.-X., OU, J.-S., LI, Y., SU, J.-J., OU, C., YANG, C., YUE, H.-F. and BAN, K.-C. 2005. Dynamic expression of apoptosis-related genes during development of laboratory hepatocellular carcinoma and its relation to apoptosis. *World J Gastroenterol*, 11, 4740-4744.
- DUPONT-VERSTEEGDEN, E. 2005. Apoptosis in muscle atrophy: relevance to sarcopenia. *Experimental gerontology*, 40, 473-481.
- EL-SERAG, H. B., ENGELS, E. A., LANDGREN, O., CHIAO, E., HENDERSON, L., AMARATUNGE, H. C. and GIORDANO, T. P. 2009. Risk of hepatobiliary and pancreatic cancers after hepatitis C virus infection: A population-based study of U.S. veterans. *Hepatology*, 49, 116-23.
- EL-SERAG, H. B. and RUDOLPH, K. L. 2007. Hepatocellular carcinoma: epidemiology and molecular carcinogenesis. *Gastroenterology*, 132, 2557-76.
- ELAYAT, G., SELIM, A. G. A. and WELLS, C. A. 2009. Alterations of the Cell Cycle Regulators Cyclin D1, Cyclin A, p27, p21, p16, and pRb in Apocrine Metaplasia of the Breast. *Breast Journal*, 15, 475-482.
- ENARI, M., OHMORI, K., KITABAYASHI, I. and TAYA, Y. 2006. Requirement of clathrin heavy chain for p53-mediated transcription. *Genes & development*, 20, 1087.
- ENGEL, T., CABALLERO-CABALLERO, A., SCHINDLER, C., PLESNILA, N., STRASSER, A., PREHN, J. and HENSHALL, D. 2010. The BH3-only protein Bid is dispensable for seizure-induced neuronal death and the associated nuclear accumulation of apoptosis-inducing factor (AIF). *Journal of neurochemistry*, 115, 92-101.
- ESSMANN, F., ENGELS, I., TOTZKE, G., SCHULZE-OSTHOFF, K. and JA'NICKE, R. 2004. Apoptosis Resistance of MCF-7 Breast Carcinoma Cells to Ionizing Radiation Is Independent of p53 and Cell Cycle Control

- but Caused by the Lack of Caspase-3 and a Caffeine-Inhibitable Event. *Cancer Research*, 64, 7065-7072.
- FADEEL, B. and ORRENIUS, S. 2005. Apoptosis: a basic biological phenomenon with wide-ranging implications in human disease. *Journal of Internal Medicine*, 258, 479-517.
- FENG, J., TAMASKOVIC, R., YANG, Z., BRAZIL, D., MERLO, A., HESS, D. and HEMMING, B. 2004. Stabilization of Mdm2 via Decreased Ubiquitination Is Mediated by Protein Kinase B/Akt-dependent Phosphorylation. *Journal of Biological Chemistry*, 279, 35510.
- FERENC, P., SOLAR, P., KLEBAN, J., MIKES, J. and FEDOROCKO, P. 2010. Down-regulation of Bcl-2 and Akt induced by combination of photoactivated hypericin and genistein in human breast cancer cells. *J Photochem Photobiol B*, 98, 25-34.
- FETZ, V., BIER, C., HABTEMICHAEL, N., SCHUON, R., SCHEITZER, A., KUNKEL, M., ENGELS, K., KOVACS, A., SCHNEIDER, S., MANN, W., STAUBER, R. and KNAUER, S. 2009. Inducible NO synthase confers chemoresistance in head and neck cancer by modulating survivin. *Int J Cancer*, 124, 2033-2041.
- FOO, R. S., CHAN, L. K., KITSIS, R. N. and BENNETT, M. R. 2007. Ubiquitination and degradation of the anti-apoptotic protein ARC by MDM2. *J Biol Chem*, 282, 5529-35.
- FRESE, S., SCHULLER, A., FRESE-SCHAPER, M., GUGGER, M. and SCHMID, R. A. 2009. Cytotoxic effects of camptothecin and cisplatin combined with tumor necrosis factor-related apoptosis-inducing ligand (Apo2L/TRAIL) in a model of primary culture of non-small cell lung cancer. *Anticancer Res*, 29, 2905-11.
- FRIEND, S., BERNARDS, R., ROGELJ, S., WEINBERG, R., RAPAPORT, J., ALBERT, D. and DRYJA, T. 1986. A human DNA segment with properties of the gene that predisposes to retinoblastoma and osteosarcoma. *Nature*, 323, 643-646.
- FULDA, S. 2009. Cell death in hematological tumors. *Apoptosis*.
- FURUKAWA, M., OHTA, T. and XIONG, Y. 2002. Activation of UBC5 Ubiquitin-conjugating Enzyme by the RING Finger of ROC1 and Assembly of Active Ubiquitin Ligases by All Cullins. *Journal of Biological Chemistry*, 277, 15758-15765.
- FURUKAWA, M. and XIONG, Y. 2005. BTB protein keap1 targets antioxidant transcription factor nrf2 for ubiquitination by the cullin 3-Roc1 ligase. *Molecular and Cellular Biology*, 25, 162-171.
- GADELHAK, N. A., GADELHAK, S. A., EL-MORSI, D. A., ABDELAZIZ, M. M., ABBAS, A. T. and EL-EMSHATY, H. M. 2009. Prognostic significance of three hepatitis markers (p53 antibodies, vascular endothelial growth factors and alpha fetoprotein) in patients with hepatocellular carcinoma. *Hepatogastroenterology*, 56, 1417-24.
- GAMA, V., GOMEZ, J., MAYO, L., JACKSON, M., DANIELPOUR, D., SONG, K., HAAS, A., LAUGHLIN, M. and MATSUYAMA, S. 2009. Hdm2 is a ubiquitin ligase of Ku70-Akt promotes cell survival by inhibiting Hdm2-dependent Ku70 destabilization. *Cell Death & Differentiation*, 16, 758-769.

- GAN, E. K. Y., LIU, X., ZHANG, J., ZHOU, T., YU, J., JIN, H. and SI, J. 2011. Homeobox D10 gene, a candidate tumor suppressor, is downregulated through promoter hypermethylation and associated with gastric carcinogenesis. *Molecular medicine (Cambridge, Mass.)*.
- GANZENMUELLER, T., MATTHAEI, M., MUENCH, P., SCHEIBLE, M., IFTNER, A., HILLER, T., LEIPRECHT, N., PROBST, S., STUBENRAUCH, F. and IFTNER, T. 2008. The E7 protein of the cottontail rabbit papillomavirus immortalizes normal rabbit keratinocytes and reduces pRb levels, while E6 cooperates in immortalization but neither degrades p53 nor binds E6AP. *Virology*, 372, 313-324.
- GAO, S. and SCOTT, R. 2002. P2P-R protein overexpression restricts mitotic progression at prometaphase and promotes mitotic apoptosis. *Journal of cellular physiology*, 193, 199-207.
- GAO, S. and SCOTT, R. 2003. Stable overexpression of specific segments of the P2P-R protein in human MCF-7 cells promotes camptothecin-induced apoptosis. *Journal of cellular physiology*, 197, 445-452.
- GAO, S., WITTE, M. and SCOTT, R. 2002. P 2 P-R protein localizes to the nucleolus of interphase cells and the periphery of chromosomes in mitotic cells which show maximum P 2 P-R immunoreactivity. *Journal of cellular physiology*, 191, 145-154.
- GAYM, A., MASHEGO, M., HARVEY, A., WALLDORF, J., FROHLICH, J. and KARIM, Q. 2007. High prevalence of abnormal Pap smears among young women co-infected with HIV in rural South Africa-implications for cervical cancer screening policies in high HIV prevalence populations. *South African Medical Journal*, 97, 130.
- GE-PING, Q., QING-YU, X., BING, L., YONG-AN, L. and LING-ZHEN, Z. 2009. Arsenic trioxide inhibits the growth of human lung cancer cell lines via cell cycle arrest and induction of apoptosis at both normoxia and hypoxia. *Toxicology and Industrial Health*, 25, 505.
- GEORGE, A. 1995. A new method for isolating genes involved in the processing and presentation of antigens to cytotoxic T cells. *University of Oxford (D.Phil. Thesis)*.
- GERMAIN, M., MILBURN, J. and DURONIO, V. 2008. MCL-1 inhibits BAX in the absence of MCL-1/BAX Interaction. *J Biol Chem*, 283, 6384-92.
- GHEE, M., MELKI, R., MICHOT, N. and MALLET, J. 2005. PA700, the regulatory complex of the 26S proteasome, interferes with a-synuclein assembly. *FEBS Journal*, 272, 4023-4033.
- GIRAO, H. and PEREIRA, P. 2007. The proteasome regulates the interaction between Cx43 and ZO 1. *Journal of cellular biochemistry*, 102, 719-728.
- GIRI, B., GOMES, A., DEBNATH, A., SAHA, A., BISWAS, A. and DASGUPTA, S. 2006. Antiproliferative, cytotoxic and apoptogenic activity of Indian toad (*Bufo melanostictus*, Schneider) skin extract on U937 and K562 cells. *Toxicon*, 48, 388-400.
- GLICKMAN, M. and CIECHANOVER, A. 2002. The Ubiquitin-Proteasome Proteolytic Pathway: Destruction for the Sake of Construction. *Physiological Reviews*, 82, 373-428.
- GLINSKII, A. B., GLINSKY, G. V., LIN, H. Y., TANG, H. Y., SUN, M., DAVIS, F. B., LUIDENS, M. K., MOUSA, S. A., HERCBERGS, A. H.

- and DAVIS, P. J. 2009. Modification of survival pathway gene expression in human breast cancer cells by tetraiodothyroacetic acid (tetrac). *Cell Cycle*, 8, 3554-62.
- GOBEIL, S., ZHU, X., DOILLON, C. and GREEN, M. 2008. A genome-wide shRNA screen identifies GAS1 as a novel melanoma metastasis suppressor gene. *Genes & development*, 22, 2932-2940.
- GOLAM SABBIR, M., ROY, A., MANDAL, S., DAM, A., ROYCHOUDHURY, S. and PANDA, C. 2006. Deletion mapping of chromosome 13q in head and neck squamous cell carcinoma in Indian patients: correlation with prognosis of the tumour. *International Journal of Experimental Pathology*, 87, 151-161.
- GRAS, E., CORTES, J., DIEZ, O., ALONSO, C., MATIAS-GUIU, X., BAIGET, M. and PRAT, J. 2001. Loss of heterozygosity on chromosome 13 q 12-q 14, BRCA-2 mutations and lack of BRCA-2 promoter hypermethylation in sporadic epithelial ovarian tumors. *Cancer*, 92, 787-795.
- GREGORY-BASS, R., OLATINWO, M., XU, W., MATTHEWS, R., STILES, J., THOMAS, K., LIU, D., TSANG, B. and THOMPSON, W. 2008. Prohibitin silencing reverses stabilization of mitochondrial integrity and chemoresistance in ovarian cancer cells by increasing their sensitivity to apoptosis. *International Journal of Cancer*, 122, 1923-1930.
- GUO, L. L., GAO, P., WU, Y. G., JIAN, W. C., HAO, C. Y., LI, H. and LIN, X. Y. 2007. Alteration of cyclin D1 in Chinese patients with breast carcinoma and its correlation with Ki-67, pRb, and p53. *Archives of Medical Research*, 38, 846-852.
- GUO, X., KEYES, W. M., PAPAZOGLU, C., ZUBER, J., LI, W., LOWE, S. W., VOGEL, H. and MILLS, A. A. 2009. TAp63 induces senescence and suppresses tumorigenesis in vivo. *Nat Cell Biol*, 11, 1451-7.
- HAHM, E. and SINGH, S. 2007. Honokiol causes G0-G1 phase cell cycle arrest in human prostate cancer cells in association with suppression of retinoblastoma protein level/phosphorylation and inhibition of E2F1 transcriptional activity. *Molecular cancer therapeutics*, 6, 2686-2695.
- HAN, J., GOLDSTEIN, L., GASTMAN, B., RABINOVITZ, A. and RABINOVITZ, H. 2005. Disruption of Mcl-1.Bim Complex in Granzyme B-mediated Mitochondrial Apoptosis. *Journal of Biological Chemistry*, 280, 16383-16392.
- HAN, S., WITT, R. M., SANTOS, T. M., POLIZZANO, C., SABATINI, B. L. and RAMESH, V. 2008. Pam (Protein associated with Myc) functions as an E3 Ubiquitin ligase and regulates TSC/mTOR signaling. *Cellular Signalling*, 20, 1084-1091.
- HAN, Y., WANG, Y., XU, H.-T., YANG, L.-H., WEI, Q., LIU, Y., ZHANG, Y., ZHAO, Y., DAI, S.-D., MIAO, Y., YU, J.-H., ZHANG, J.-Y., LI, G., YUAN, X.-M. and WANG, E.-H. 2009. X-radiation induces non-small-cell lung cancer apoptosis by upregulation of Axin expression. *International journal of radiation oncology, biology, physics*, 75, 518-26.
- HE, Y., WU, X., TANG, W., TIAN, D., LUO, C., YIN, Z. and DU, H. 2008. Impaired delta NP63 expression is associated with poor tumor development in transitional cell carcinoma of the bladder. *Journal of Korean medical science*, 23, 825-832.

- HEDAU, S., JAIN, N., HUSAIN, S. A., MANDAL, A. K., RAY, G., SHAHID, M., KANT, R., GUPTA, V., SHUKLA, N. K., DEO, S. S. V. and DAS, B. C. 2004. Novel germline mutations in breast cancer susceptibility genes BRCA1, BRCA2 and p53 gene in breast cancer patients from India. *Breast Cancer Research and Treatment*, 88, 177-186.
- HEMINGER, K., MARKEY, M., MPAGI, M. and BERBERICH, S. J. 2009. Alterations in gene expression and sensitivity to genotoxic stress following HdmX or Hdm2 knockdown in human tumor cells harboring wild-type p53. *Aging*, 1, 89-108.
- HENRIQUEZ-HERNANDEZ, L. A., ROSALES, A. M., GONZALEZ, A. H., DE LEON, A. C., DIAZ-CHICO, B. N., DE SANTIAGO, M. M. and PEREZ, L. F. 2009. Gene polymorphisms in TYMS, MTHFR, p53 and MDR1 as risk factors for breast cancer: A case-control study. *Oncology Reports*, 22, 1425-1433.
- HENSON, E., HU, X. and GIBSON, S. 2006. Herceptin Sensitizes ErbB2-Overexpressing Cells to Apoptosis by Reducing Antiapoptotic Mcl-1 Expression. *Clinical Cancer Research* 12, 845-854.
- HERIBERTO, B., PLINIO, F., LUCÍA, V., MARIE-PIERRE, P., DARREN, P., MARCO, C., SAMIA, M., FABIEN, C. and MÓNICA, M. 2010. Distinct expression patterns of the E3 ligase SIAH-1 and its partner Kid/KIF22 in normal tissues and in the breast tumoral processes. *Journal of Experimental & Clinical Cancer Research*, 29, 10.
- HERRMANN, J., LERMAN, L. and LERMAN, A. 2007. Ubiquitin and ubiquitin-like proteins in protein regulation. *Circulation research*, 100, 1276.
- HOEFNAGEL, J., DIJKMAN, R., BASSO, K., JANSEN, P., HALLERMANN, C., WILLEMZE, R., TENSEN, C. and VERMEER, M. 2005. Distinct types of primary cutaneous large B-cell lymphoma identified by gene expression profiling. *Blood*, 105, 3671-3681.
- HOLOWNIA, A., MROZ, R. M., KOZLOWSKI, M., CHYCZEWSKA, E., LAUDANSKI, J., CHYCZEWSKI, L. and BRASZKO, J. J. 2003. Therapy increases poly-ADP-ribose and p53-Ser392-P levels in recurrent squamous cell lung cancer. *Neoplasma*, 50, 266-71.
- HSU, J. L., CHIANG, P. C. and GUH, J. H. 2009. Tunicamycin induces resistance to camptothecin and etoposide in human hepatocellular carcinoma cells: role of cell-cycle arrest and GRP78. *Naunyn Schmiedebergs Arch Pharmacol*, 380, 373-82.
- HU, H. M., ZIELINSKA-KWIATKOWSKA, A., MUNRO, K., WILCOX, J., WU, D. Y., YANG, L. and CHANSKY, H. A. 2008. EWS/FLI1 suppresses retinoblastoma protein function and senescence in Ewing's sarcoma cells. *J Orthop Res*, 26, 886-93.
- HUANG, T., ZHU, Y., FANG, X., CHI, Y., KITAMURA, M. and YAO, J. 2009. Gap junctions sensitize cancer cells to proteasome inhibitor MG132-induced apoptosis. *Cancer Sci*.
- HUDELIST, G., CZERWENKA, K., KUBISTA, E., MARTON, E., PISCHINGER, K. and SINGER, C. 2003. Expression of sex steroid receptors and their co-factors in normal and malignant breast tissue: AIB1 is a carcinoma-specific co-activator. *Breast cancer research and treatment*, 78, 193-204.

- IJIMA, M., MOMOSE, I. and IKEDA, D. 2009. TP-110, a new proteasome inhibitor, down-regulates IAPs in human multiple myeloma cells. *Anticancer Res*, 29, 977-85.
- IMVRIOS, G., PAPANIKOLAOU, V., TSOULFAS, G., VASILIAKIS, T., KARDASSIS, D., PAPAGIANNIS, A., GOULIS, I., GIAKOUSTIDIS, D., ANTONIADIS, N., FOUZAS, I., PATSIAOURA, K., NTINAS, A., OUZOUNIDIS, N., VROCHIDES, D., KATSIKA, E., DIPLARIS, K., MISERLIS, G. and TAKOUDAS, D. 2008. The evolution of the role of liver transplantation in treating alcoholic cirrhosis in Greece. *Transplant Proc*, 40, 3189-90.
- ISMAIL, I., KANG, K., LEE, H., KIM, J. and SOHN, Y. 2007. Genistein-induced neuronal apoptosis and G2/M cell cycle arrest is associated with MDC1 up-regulation and PLK1 down-regulation. *European journal of pharmacology*, 575, 12-20.
- IVANTSIV, Y., KAPLUN, L., TZIRKIN-GOLDIN, R., SHABEK, N. and RAVEH, D. 2006. Unique role for the UbL-UbA protein Ddi1 in turnover of SCFUfo1 complexes. *Molecular and cellular biology*, 26, 1579.
- IWAI, A., MARUSAWA, H., KIUCHI, T., HIGASHITSUJI, H., TANAKA, K., FUJITA, J. and CHIBA, T. 2003. Role of a novel oncogenic protein, gankyrin, in hepatocyte proliferation. *J Gastroenterol*, 38, 751-8.
- JAKUPCIAK, J., MARAGH, S., MARKOWITZ, M., GREENBERG, A., HOQUE, M., MAITRA, A., BARKER, P., WAGNER, P., ROM, W. and SRIVASTAVA, S. 2008. Performance of mitochondrial DNA mutations detecting early stage cancer. *BMC Cancer*, 8, 285.
- JIANG, H., MA, Y., CHEN, X., PAN, S., SUN, B., KRISANSSEN, GW, and SUN, X. 2010a. Genistein synergizes with arsenic trioxide to suppress human hepatocellular carcinoma. *Cancer Science*, 101, 975-983.
- JIANG, L., BAO, Y., LUO, C., HU, G., HUANG, C., DING, X., SUN, K. and LU, Y. 2010b. Knockdown of ubiquitin-conjugating enzyme E2C/UbcH10 expression by RNA interference inhibits glioma cell proliferation and enhances cell apoptosis in vitro. *J Cancer Res Clin Oncol*, 136, 211-7.
- JIANG, L., HUANG, C., LU, Y., LUO, C., HU, G., LIU, H., CHEN, J. and HAN, H. 2008. Expression of ubiquitin-conjugating enzyme E2C/UbcH10 in astrocytic tumors. *Brain Research*, 1201, 161-166.
- JIMENEZ-LARA, A. M., ARANDA, A. and GRONEMEYER, H. 2010. Retinoic acid protects human breast cancer cells against etoposide-induced apoptosis by NF-kappaB-dependent but cIAP2-independent mechanisms. *Mol Cancer*, 9, 15.
- JIN, C., YANG, Y., ANVER, M., MORRIS, N., WANG, X. and ZHANG, Y. 2009. Smad ubiquitination regulatory factor 2 promotes metastasis of breast cancer cells by enhancing migration and invasiveness. *Cancer research*, 69, 735.
- JOSELIN, A., SCHULZE-OSTHOFF, K. and SCHWERK, C. 2006. Loss of Acinus inhibits oligonucleosomal DNA fragmentation but not chromatin condensation during apoptosis. *Journal of Biological Chemistry*, 281, 12475-12484.
- KANG, M. R., KIM, M. S., KIM, S. S., AHN, C. H., YOO, N. J. and LEE, S. H. 2009. NF-kappaB signalling proteins p50/p105, p52/p100, RelA, and

- IKKepsilon are over-expressed in oesophageal squamous cell carcinomas. *Pathology*, 41, 622-5.
- KANG, Y., LEE, K., RYU, C., LEE, H., LIM, J., PARK, S., PAIK, S. and YOON, D. 2006. Mitomycin C induces apoptosis via Fas/FasL dependent pathway and suppression of IL-18 in cervical carcinoma cells. *Cancer Letters*, 237, 33-44.
- KANG, Y. H. and LEE, S. J. 2008. Role of p38 MAPK and JNK in enhanced cervical cancer cell killing by the combination of arsenic trioxide and ionizing radiation. *Oncol Rep*, 20, 637-43.
- KATO, T., SUZUKI, K., OKADA, S., KAMIYAMA, H., MAEDA, T., SAITO, M., KOIZUMI, K., MIYAKI, Y. and KONISHI, F. 2012. Aberrant methylation of PSD disturbs Rac1-mediated immune responses governing neutrophil chemotaxis and apoptosis in ulcerative colitis-associated carcinogenesis. *International journal of oncology*, 40, 942-950.
- KAUR, S., WANG, F., VENKATRAMAN, M. and ARSURA, M. 2005. X-linked Inhibitor of Apoptosis (XIAP) Inhibits c-Jun N-terminal Kinase 1 (JNK1) Activation by Transforming Growth Factor {beta} 1 (TGF- $\beta$  1) through Ubiquitin-mediated Proteasomal Degradation of the TGF- $\beta$  1-activated Kinase 1 (TAK1). *Journal of Biological Chemistry*, 280, 38599.
- KAWAI, H., SUZUKI, T., KOBAYASHI, T., ISHII-WATABE, A., SAKURAI, H., OHATA, H., HONDA, K., MOMOSE, K., HAYAKAWA, T. and KAWANISHI, T. 2007. Caspase Cascade Proceeds Rapidly After Cytochrome c Release From Mitochondria in Tumor Necrosis Factor- $\alpha$ -Induced Cell Death. *Journal of Pharmacological Sciences*, 103, 159-167.
- KERR, J. 2002. History of the events leading to the formulation of the apoptosis concept. *Toxicology*, 181, 471-474.
- KERR, J., WYLLIE, A. and CURRIE, A. 1972. Apoptosis: a basic biological phenomenon with wide-ranging implications in tissue kinetics. *Br J Cancer*, 26, 239-57.
- KETER, F., KANYANDA, S., LYANTAGAYE, S., DARKWA, J., REES, D. and MEYER, M. 2008. In vitro evaluation of dichloro-bis (pyrazole) palladium (II) and dichloro-bis (pyrazole) platinum (II) complexes as anticancer agents. *Cancer chemotherapy and pharmacology*, 63, 127-138.
- KIM, E. J., LIM, S. S., PARK, S. Y., SHIN, H. K., KIM, J. S. and PARK, J. H. 2008. Apoptosis of DU145 human prostate cancer cells induced by dehydrocostus lactone isolated from the root of Saussurea lappa. *Food Chem Toxicol*, 46, 3651-8.
- KIM, H., KIM, K., LLEDIAS, F., KISSELEV, A., SCAGLIONE, K., SKOWYRA, D., GYGI, S. and GOLDBERG, A. 2007. Certain pairs of ubiquitin-conjugating enzymes (E2s) and ubiquitin-protein ligases (E3s) synthesize nondegradable forked ubiquitin chains containing all possible isopeptide linkages. *Journal of Biological Chemistry*, 282, 17375.
- KIM, S. S., AHN, C. H., KANG, M. R., KIM, Y. R., KIM, H. S., YOO, N. J. and LEE, S. H. 2010. Expression of CARD6, an NF-kappaB activator, in gastric, colorectal and oesophageal cancers. *Pathology*, 42, 50-3.
- KIM, W. and KAELIN, W. 2004. Role of VHL gene mutation in human cancer. *Journal of clinical oncology*, 22, 4991-5004.

- KIRCELLI, F., AKAY, C. and GAZITT, Y. 2007. Arsenic trioxide induces p53-dependent apoptotic signals in myeloma cells with SiRNA-silenced p53: MAP kinase pathway is preferentially activated in cells expressing inactivated p53. *Int J Oncol*, 30, 993-1001.
- KIRKIN, V. and DIKIC, I. 2007. Role of ubiquitin- and Ubl-binding proteins in cell signaling. *Curr Opin Cell Biol*, 19, 199-205.
- KLINGER, K. 1994. FISH: sensitivity and specificity on sorted and unsorted cells. *Annals of the New York Academy of Sciences*, 731, 48-56.
- KNUDSEN, E. and KNUDSEN, K. 2006. Retinoblastoma tumor suppressor: where cancer meets the cell cycle. *Experimental biology and medicine (Maywood, NJ)*, 231, 1271-1281.
- KO, S., KIM, H., JIN, D., BAE, H., KIM, S., PARK, C. and LEE, J. 2005. *Saussurea lappa* induces G2-growth arrest and apoptosis in AGS gastric cancer cells. *Cancer Letters*, 220, 11-19.
- KO, S., KOH, S., JUN, C., NAM, C., BAE, H. and SHIN, M. 2004. Induction of Apoptosis by *Saussurea lappa* and *Pharbitis nil* on AGS Gastric Cancer Cells. *Biological & Pharmaceutical Bulletin*, 27, 1604-1610.
- KOLIOPANOS, A., AVGERINOS, C., PARASKEVA, C., TOULOUMIS, Z., KELGIORGI, D., DERVENIS, C. and ATHENS, G. 2008. Molecular aspects of carcinogenesis in pancreatic cancer. *Hepatobiliary Pancreat Dis Int*, 7, 345-356.
- KOSTER, R., DI PIETRO, A., TIMMER-BOSSCHA, H., GIBCUS, J., VAN DEN BERG, A., SUURMEIJER, A., BISCHOFF, R., GIETEMA, J. and DE JONG, S. 2010. Cytoplasmic p21 expression levels determine cisplatin resistance in human testicular cancer. *J Clin Invest*.
- KOSTIC, M., MATT, T., MARTINEZ-YAMOUT, M. A., DYSON, H. J. and WRIGHT, P. E. 2006. Solution structure of the Hdm2 C2H2C4 RING, a domain critical for ubiquitination of p53. *Journal of Molecular Biology*, 363, 433-450.
- KOVACSOVICS, M., MARTINON, F., MICHEAU, O., BODMER, J., HOFMANN, K. and TSCHOPP, J. 2002. Overexpression of Helicard, a CARD-Containing Helicase Cleaved during Apoptosis, Accelerates DNA Degradation. *Current Biology*, 12, 838-843.
- KRANTIC, S., MECHAWAR, N., REIX, S. and QUIRION, R. 2007. Apoptosis-inducing factor: A matter of neuron life and death. *Progress in Neurobiology*, 81, 179-196.
- KRIEG, A., LE NEGRATE, G. and REED, J. C. 2009. RIP2-beta: a novel alternative mRNA splice variant of the receptor interacting protein kinase RIP2. *Mol Immunol*, 46, 1163-70.
- KU, T. K. and CROWE, D. L. 2007. Coactivator-mediated estrogen response in human squamous cell carcinoma lines. *J Endocrinol*, 193, 147-55.
- KUMAR, A., KUMAR, M., PARK, T.-Y., PARK, M.-H., TAKEMOTO, T., TERADO, T., KITANO, M. and KIMURA, H. 2009. Molecular mechanisms of ginsenoside R<sub>p1</sub>-mediated growth arrest and apoptosis. *International journal of molecular medicine*, 24, 381-6.
- KUMAR, A., MALIK, F., BHUSHAN, S., SETHI, V., SHAHI, A., KAUR, J., TANEJA, S., QAZI, G. and SINGH, J. 2008. An essential oil and its major constituent isointermedeol induce apoptosis by increased expression of

- mitochondrial cytochrome c and apical death receptors in human leukaemia HL-60 cells. *Chemico-Biological Interactions*, 171, 332-347.
- KUMAR, M., KUMAR, R., HISSAR, S., SARASWAT, M., SHARMA, B., SAKHUJA, P. and SARIN, S. 2007. Risk factors analysis for hepatocellular carcinoma in patients with and without cirrhosis: a case-control study of 213 hepatocellular carcinoma patients from India. *Journal of gastroenterology and hepatology*, 22, 1104-1111.
- KUO, P. C., TSAO, Y. P., CHANG, H. W., CHEN, P. H., HUANG, C. W., LIN, S. T., WENG, Y. T., TSAI, T. C., SHIEH, S. Y. and CHEN, S. L. 2009. Breast cancer amplified sequence 2, a novel negative regulator of the p53 tumor suppressor. *Cancer Res*, 69, 8877-85.
- KURIBAYASHI, K., MAYES, P. and EL-DEIRY, W. 2006. What are caspases 3 and 7 doing upstream of the mitochondria? *Cancer Biol Ther*, 5, 763-5.
- LANDSHAMER, S., HOEHN, M., BARTH, N., DUVEZIN-CAUBET, S., SCHWAKE, G., TOBABEN, S., KAZHDAN, I., BECCATTINI, B., ZAHLER, S., VOLLMAR, A., PELLECCIA, M., REICHERT, A., PLESNILA, N., WAGNER, E. and CULMSEE, C. 2008. Bid-induced release of AIF from mitochondria cause immediate neuronal cell death. *Cell Death Differ*, 15, 1553-63.
- LEDWABA, R. 2005. Characterisation of the DWNN gene in cervical carcinoma. *University of the Witwatersrand Masters Thesis*.
- LEE, K., LEUNG, A., TANG, M., CAI, D., SCHNEIDER, C., BRANCOLINI, C. and CHOW, P. 2001. Functions of the Growth Arrest Specific 1 Gene in the Development of the Mouse Embryo. *Developmental Biology*, 234, 188-203.
- LEE, M., SORN, S., BAEK, S., JANG, S. and KIM, S. 2009a. Antioxidant and apoptotic effects of korean white ginseng extracted with the same ratio of protopanaxadiol and protopanaxatriol saponins in human hepatoma HepG2 cells. *Ann N Y Acad Sci*, 1171, 217-27.
- LEE, S., KWON, J., CHOI, Y., EOM, H. and CHI, G. 2008. Induction of G2/M arrest and apoptosis by water extract of Strychni Semen in human gastric carcinoma AGS cells. *Phytotherapy Research*, 22, 752-758.
- LEE, S., LEE, S., JUNG, Y., XU, Y., KANG, H., HA, N. and PARK, B. 2009b. Blocking of p53-Snail binding, promoted by oncogenic K-Ras, recovers p53 expression and function. *Neoplasia (New York, NY)*, 11, 22-31.
- LEE, Y. M., LIM, J. H., CHUN, Y. S., MOON, H. E., LEE, M. K., HUANG, L. E. and PARK, J. W. 2009c. Nutlin-3, an Hdm2 antagonist, inhibits tumor adaptation to hypoxia by stimulating the FIH-mediated inactivation of HIF-1alpha. *Carcinogenesis*, 30, 1768-75.
- LEONG, S., CHRISTOPHERSON, R. and BAXTER, R. 2007. Profiling of apoptotic changes in human breast cancer cells using SELDI-TOF mass spectrometry. *Cell Physiol Biochem*, 20, 579-590.
- LI, H., ZHU, X., ZHANG, Y., XIANG, J. and CHEN, H. 2009a. Arsenic trioxide exerts synergistic effects with cisplatin on non-small cell lung cancer cells via apoptosis induction. *J Exp Clin Cancer Res*, 28, 110.
- LI, J., LI, Y., QIN, D., VON HARSDORF, R. and LI, P. 2010a. Mitochondrial fission leads to Smac/DIABLO release quenched by ARC. *Apoptosis*, 1-10.

- LI, J., PIAO, Y. F., JIANG, Z., CHEN, L. and SUN, H. B. 2009b. Silencing of signal transducer and activator of transcription 3 expression by RNA interference suppresses growth of human hepatocellular carcinoma in tumor-bearing nude mice. *World J Gastroenterol*, 15, 2602-8.
- LI, L., DENG, B., XING, G., TENG, Y., TIAN, C., CHENG, X., YIN, X., YANG, J., GAO, X. and ZHU, Y. 2007a. PACT is a negative regulator of p53 and essential for cell growth and embryonic development. *Proceedings of the National Academy of Sciences*, 104, 7951.
- LI, M., ZHANG, Z., HILL, D., WANG, H. and ZHANG, R. 2007b. Curcumin, a dietary component, has anticancer, chemosensitization, and radiosensitization effects by down-regulating the MDM2 oncogene through the PI3K/mTOR/ETS2 pathway. *Cancer research*, 67, 1988.
- LI, P., MAINES-BANDIERA, S., KUO, W. L., GUAN, Y., SUN, Y., HILLS, M., HUANG, G., COLLINS, C. C., LEUNG, P. C., GRAY, J. W. and AUERSPERG, N. 2007c. Multiple roles of the candidate oncogene ZNF217 in ovarian epithelial neoplastic progression. *Int J Cancer*, 120, 1863-73.
- LI, T., BRUSTOVETSKY, T., ANTONSSON, B. and BRUSTOVETSKY, N. 2008. Oligomeric BAX induces mitochondrial permeability transition and complete cytochrome c release without oxidative stress. *Biochimica et Biophysica Acta (BBA)-Bioenergetics*, 1777, 1409-1421.
- LI, Y., HE, K., HUANG, Y., ZHENG, D., GAO, C., CUI, L. and JIN, Y. 2010b. Betulin induces mitochondrial cytochrome c release associated apoptosis in human cancer cells. *Molecular Carcinogenesis*, 49, 630-640.
- LI, Y., LIU, L., ANDREWS, L. and TOLLEFSBOL, T. 2009c. Genistein depletes telomerase activity through cross-talk between genetic and epigenetic mechanisms. *International journal of cancer. Journal international du cancer*, 125, 289-296.
- LI, Y., QU, X., QU, J., ZHANG, Y., LIU, J., TENG, Y., HU, X., HOU, K. and LIU, Y. 2009d. Arsenic trioxide induces apoptosis and G2/M phase arrest by inducing Cbl to inhibit PI3K/Akt signaling and thereby regulate p53 activation. *Cancer Lett*, 284, 208-15.
- LIANG, F., CHEN, R., LIN, C., HUANG, K. and CHAN, S. 2006. Tuning the conformation properties of a peptide by glycosylation and phosphorylation. *Biochemical and biophysical research communications*, 342, 482-488.
- LIAO, S., WANG, T., FAN, K. and TU, X. 2010a. The small ubiquitin-like modifier (SUMO) is essential in cell cycle regulation in *Trypanosoma brucei*. *Experimental cell research*, 316, 704-715.
- LIAO, W. T., YU, H. S., LIN, P. and CHANG, L. W. 2010b. Arsenite promotes centrosome abnormalities under a p53 compromised status induced by 4-(methylnitrosamino)-1-(3-pyridyl)-1-butanone (NNK). *Toxicol Appl Pharmacol*, 243, 55-62.
- LIGGETT JR, W. and SIDRANSKY, D. 1998. Role of the p16 tumor suppressor gene in cancer. *Journal of Clinical Oncology*, 16, 1197.
- LIN, L., OZAKI, T., TAKADA, Y., KAGEYAMA, H., NAKAMURA, Y., HATA, A., ZHANG, J. H., SIMONDS, W. F., NAKAGAWARA, A. and KOSEKI, H. 2005. topors, a p53 and topoisomerase I-binding RING

- finger protein, is a coactivator of p53 in growth suppression induced by DNA damage. *Oncogene*, 24, 3385-3396.
- LIN, P. S., MCPHERSON, L. A., CHEN, A. Y., SAGE, J. and FORD, J. M. 2009. The role of the retinoblastoma/E2F1 tumor suppressor pathway in the lesion recognition step of nucleotide excision repair. *DNA Repair (Amst)*, 8, 795-802.
- LINEHAN, W., RUBIN, J. and BOTTARO, D. 2009. VHL loss of function and its impact on oncogenic signaling networks in clear cell renal cell carcinoma. *The International Journal of Biochemistry & Cell Biology*, 41, 753-756.
- LING, X., CALINSKI, D., CHANAN-KHAN, A., ZHOU, M. and LI, F. 2010a. Cancer cell sensitivity to bortezomib is associated with survivin and p 53 status but not cancer cell types. *Journal of Experimental & Clinical Cancer Research*, 29, 8.
- LING, Y., XU, X., HAO, J., LING, X., DU, X., LIU, X. and ZHAO, X. 2010b. Aberrant methylation of the THRB gene in tissue and plasma of breast cancer patients. *Cancer Genet Cytogenet*, 196, 140-5.
- LING, Y. H., JIANG, J. D., HOLLAND, J. F. and PEREZ-SOLER, R. 2002. Arsenic trioxide produces polymerization of microtubules and mitotic arrest before apoptosis in human tumor cell lines. *Molecular Pharmacology*, 62, 529-538.
- LIU, B., ZHANG, H., LUO, X., XIE, Y., HAO, J., DUAN, X. and ZHOU, Q. 2008. High-efficiency transfer and expression of AdCMV-p53 in human hepatocellular carcinoma cells induced by low-dose carbon-ion radiation. *Eur J Gastroenterol Hepatol*, 20, 860-4.
- LIU, B., ZHANG, H., ZHOU, G., XIE, Y., HAO, J., QIU, R., DUAN, X. and ZHOU, Q. 2007a. Adenovirus-mediated p53 gene transfer sensitizes hepatocellular carcinoma cells to heavy-ion radiation. *J Gastroenterol* 42, 140-145.
- LIU, H., CHANG, D. and YANG, X. 2005. Interdimer processing and linearity of procaspase-3 activation. *Journal of Biological Chemistry*, 280, 11578-11582.
- LIU, W., GREEN, N., SEYMOUR, L. and STEVENSON, M. 2009a. Paclitaxel combined with siRNA targeting HPV16 oncogenes improves cytotoxicity for cervical carcinoma. *Cancer Gene Therapy*, 16, 764-775.
- LIU, X., DISBROW, G. L., YUAN, H., TOMAIC, V. and SCHLEGEL, R. 2007b. Myc and human papillomavirus type 16 E7 genes cooperate to immortalize human keratinocytes. *J Virol*, 81, 12689-95.
- LIU, X. H., ZHENG, X. F. and WANG, Y. L. 2009b. Inhibitive effect of 3-bromopyruvic acid on human breast cancer MCF-7 cells involves cell cycle arrest and apoptotic induction. *Chin Med J (Engl)*, 122, 1681-5.
- LIVAK, K. and SCHMITTGEN, T. 2001. Analysis of relative gene expression data using real-time quantitative PCR and the 2 CT method. *Methods*, 25, 402-408.
- LO, C., LAI, T.-Y., YANG, J.-H., YANG, J.-S., MA, Y.-S., WENG, S.-W., CHEN, Y.-Y., LIN, J.-G. and CHUNG, J.-G. 2010. Gallic acid induces apoptosis in A375.S2 human melanoma cells through caspase-dependent and -independent pathways. *International journal of oncology*, 37, 377-85.

- LOPEZ SALON, M., MORELLI, L., CASTANO, E. M., SOTO, E. F. and PASQUINI, J. M. 2000. Defective ubiquitination of cerebral proteins in Alzheimer's disease. *J Neurosci Res*, 62, 302-10.
- LORENZO, H. and SUSIN, S. 2007. Therapeutic potential of AIF-mediated caspase-independent programmed cell death. *Drug Resistance Updates*, 10, 235-255.
- LOWE, J., CHA, H., YANG, Q. and FORNANCE, A. 2010. Nuclear factor-kappaB (NF-kappaB) is a novel positive transcriptional regulator of the oncogenic Wip1 phosphatase. *J Biol Chem*, 285, 5249-5257.
- LU, J., CHEW, E. and HOLMGREN, A. 2007. Targeting thioredoxin reductase is a basis for cancer therapy by arsenic trioxide. *Proceedings of the National Academy of Sciences*, 104, 12288.
- LU, J., TAN, M., HUANG, W. C., LI, P., GUO, H., TSENG, L. M., SU, X. H., YANG, W. T., TREEKITKARNMONGKOL, W., ANDREEFF, M., SYMMANS, F. and YU, D. 2009. Mitotic deregulation by survivin in ErbB2-overexpressing breast cancer cells contributes to Taxol resistance. *Clin Cancer Res*, 15, 1326-34.
- LUDVIGSEN, M., OSTERGAARD, M., VORUM, H., JACOBSEN, C. and HONORE, B. 2009. Identification and characterization of endonuclein binding proteins: evidence of modulatory effects on signal transduction and chaperone activity. *BMC biochemistry*, 10, 34.
- LUI PARK, H., SOOK KIM, M., YAMASHITA, K., WESTRA, W., LOPES CARVALHO, A., LEE, J., JIANG, W., HYEN BAEK, J., LIU, J. and OSADA, M. 2008. DCC promoter hypermethylation in esophageal squamous cell carcinoma. *International journal of cancer*, 122, 2498-2502.
- LUNGI, P., GIULIANI, N., MAZZERA, L., LOMBARDI, G., RICCA, M., CORRADI, A., CANTONI, A., SALVATORE, L., RICCIONI, R. and COSTANZO, A. 2008. Targeting MEK/MAPK signal transduction module potentiates ATO-induced apoptosis in multiple myeloma cells through multiple signaling pathways. *Blood*, 112, 2450.
- MACALUSO, M., MONTANARI, M., NOTO, P. B., GREGORIO, V., BRONNER, C. and GIORDANO, A. 2007. Epigenetic modulation of estrogen receptor-alpha by pRb family proteins: A novel mechanism in breast cancer. *Cancer Research*, 67, 7731-7737.
- MADUREIRA, P. A., MATOS, P., SOEIRO, I., DIXON, L. K., SIMAS, J. P. and LAM, E. W. 2005. Murine gamma-herpesvirus 68 latency protein M2 binds to Vav signaling proteins and inhibits B-cell receptor-induced cell cycle arrest and apoptosis in WEHI-231 B cells. *J Biol Chem*, 280, 37310-8.
- MAEDA, A., OHGURO, H., MAEDA, T., WADA, I., SATO, N., KUROKI, Y. and NAKAGAWA, T. 2000. Aberrant expression of photoreceptor-specific calcium-binding protein (recoverin) in cancer cell lines. *Cancer research*, 60, 1914-1920.
- MAHMUD, H., DÄLKEN, B. and WELS, W. 2009. Induction of programmed cell death in ErbB2/HER2-expressing cancer cells by targeted delivery of apoptosis-inducing factor. *Molecular cancer therapeutics*, 8, 1526.

- MAKISHIMA, H., CAZZOLLI, H., SZPURKA, H., DUNBAR, A., TIU, R., HUH, J., MURAMATSU, H., O'KEEFE, C., HSI, E., PAQUETTE, R. L., KOJIMA, S., LIST, A. F., SEKERES, M. A., MCDEVITT, M. A. and MACIEJEWSKI, J. P. 2009. Mutations of e3 ubiquitin ligase cbl family members constitute a novel common pathogenic lesion in myeloid malignancies. *J Clin Oncol*, 27, 6109-16.
- MAKKI, M., HEINZEL, T. and ENGLERT, C. 2008. TSA downregulates Wilms tumor gene 1 (Wt1) expression at multiple levels. *Nucleic Acids Research*, 36, 4067-78.
- MANCINI, F., DI CONZA, G., PELLEGRINO, M., RINALDO, C., PRODOSMO, A., GIGLIO, S., D'AGNANO, I., FLORENZANO, F., FELICIONI, L. and BUTTITTA, F. 2009. MDM4 (MDMX) localizes at the mitochondria and facilitates the p53-mediated intrinsic-apoptotic pathway. *The EMBO Journal*, 28, 1926-1939.
- MARKIEWICZ, E., DECHAT, T., FOISNER, R. and QUINLAN, R. 2002. Lamin A/C binding protein LAP2alpha is required for nuclear anchorage of retinoblastoma protein. *Molecular biology of the cell*, 13, 4401.
- MARTINEZ-NOEL, G., MULLER, U. and HARBERS, K. 2001. Identification of molecular determinants required for interaction of ubiquitin-conjugating enzymes and RING finger proteins. *European Journal of Biochemistry*, 268, 5912-5919.
- MASAMHA, C. and BENBROOK, D. 2009. Cyclin D1 Degradation Is Sufficient to Induce G1 Cell Cycle Arrest despite Constitutive Expression of Cyclin E2 in Ovarian Cancer Cells. *Cancer Research*, 69, 6565.
- MASTRANDREA, L., YOU, J., NILES, E. and PICKART, C. 1999. E2/E3-mediated assembly of lysine 29-linked polyubiquitin chains. *Journal of Biological Chemistry*, 274, 27299.
- MATALLANAS, D., ROMANO, D., YEE, K., MEISSEL, K., KUCEROVA, L., PIAZZOLLA, D., BACCARINI, M., VASS, J., KOLCH, W. and O'NEILL, E. 2007. RASSF1A elicits apoptosis through an MST2 pathway directing proapoptotic transcription by the p73 tumor suppressor protein. *Molecular Cell*, 27, 962-975.
- MATHER, A., RAKGOTHO, M. and NTWASA, M. 2005. SNAMA, a novel protein with a DWNN domain and a RING finger-like motif: A possible role in apoptosis. *BBA-Gene Structure and Expression*, 1727, 169-176.
- MATIC, I., VAN HAGEN, M., SCHIMMEL, J., MACEK, B., OGG, S., TATHAM, M., HAY, R., LAMOND, A., MANN, M. and VERTEGAAL, A. 2008. In vivo identification of human small ubiquitin-like modifier polymerization sites by high accuracy mass spectrometry and an in vitro to in vivo strategy. *Molecular & Cellular Proteomics*, 7, 132-144.
- MAZAN-MAMCZARZ, K., HAGNER, P., CORL, S., SRIKANTAN, S., WOOD, W., BECKER, K., GOROSPE, M., KEENE, J., LEVENSON, A. and GARTENHAUS, R. 2008. Post-transcriptional gene regulation by HuR promotes a more tumorigenic phenotype. *Oncogene*, 27, 6151-6163.
- MBITA, Z. 2004. Molecular Analysis of a Novel death-related gene, Domain With No Name (DWNN), in human parenchymal diseases *Wits MSc Thesis*.

- MCGAHREN-MURRAY, M., TERRY, N. and KEYOMARSI, K. 2006. The Differential Staurosporine-Mediated G1 Arrest in Normal versus Tumor Cells Is Dependent on the Retinoblastoma Protein. *Cancer Research*, 66, 9744.
- MCNAUGHT, K. and JENNER, P. 2001. Proteasomal function is impaired in substantia nigra in Parkinson's disease. *Neuroscience Letters*, 297, 191-194.
- MEI, Y., XIE, C., XIE, W., TIAN, X., LI, M. and WU, M. 2007. Noxa/Mcl-1 balance regulates susceptibility of cells to camptothecin-induced apoptosis. *Neoplasia (New York, NY)*, 9, 871-881.
- MERIC-BERNSTAM, F. 2007. Heterogenic loss of BRCA in breast cancer: the "two-hit" hypothesis takes a hit. *Ann Surg Oncol*, 14, 2428-9.
- MEYER, M., ESSACK, M., KANYANDA, S. and REES, J. 2008. A low-cost flow cytometric assay for the detection and quantification of apoptosis using an anionic halogenated fluorescein dye. *Biotechniques*, 45, 317-20.
- MILEO, A., ABBRUZZESE, C., MATTAROCCHI, S., BELLOCCHIO, E., PISANO, P., FEDERICO, A., MARESCA, V., PICARDO, M., GIORGI, A. and MARAS, B. 2009. Human papillomavirus-16 E7 interacts with glutathione S-transferase P1 and enhances its role in cell survival. *PiLoS One*, 4, e7254.
- MILLER, S. L., DEMARIA, J. E., FREIER, D. O., RIEGEL, A. M. and CLEVENGER, C. V. 2005. Novel association of Vav2 and Nek3 modulates signaling through the human prolactin receptor. *Molecular Endocrinology*, 19, 939-949.
- MIN, S. H., KIM, D. M., HEO, Y. S., KIM, H. M., KIM, I. C. and YOO, O. J. 2010. Downregulation of p53 by phosphatase of regenerating liver 3 is mediated by MDM2 and PIRH2. *Life Sciences*, 86, 66-72.
- MIN, S. H., KIM, D. M., HEO, Y. S., KIM, Y. I., KIM, H. M., KIM, J., HAN, Y. M., KIM, I. C. and YOO, O. J. 2009. New p53 target, phosphatase of regenerating liver 1 (PRL-1) downregulates p53. *Oncogene*, 28, 545-554.
- MING, Y.-L., GANG, S., CHEN, L.-H., ZHENG, Z.-Z., CHEN, Z.-Y., UOYANG, G.-L. and TONG, Q.-X. 2007. Anti-proliferation and apoptosis induced by a novel intestinal metabolite of ginseng saponin in human hepatocellular carcinoma cells. *Cell Biology International*, 31, 1265-1273.
- MORANDELL, D., ROSTEK, U., BOUVARD, V., CAMPO-FERNÁNDEZ, B., FIEDLER, M., JANSEN-DÜRR, P. and ZWERSCHKE, W. 2008. Human papillomavirus type 45 E7 is a transforming protein inducing retinoblastoma protein degradation and anchorage-independent cell cycle progression. *Virology*, 379, 20-29.
- MORIOKA, S., OMORI, E., KAJINO, T., KAJINO-SAKAMOTO, R., MATSUMOTO, K. and NINOMIYA-TSUJI, J. 2009. TAK1 kinase determines TRAIL sensitivity by modulating reactive oxygen species and cIAP. *Oncogene*, 28, 2257-65.
- MUKHERJEE, B., MCELLIN, B., CAMACHO, C., TOMIMATSU, N., SIRASANAGANDALA, S., NANNEPAGA, S., HATANPAA, K., MICKEY, B., MADDEN, C. and MAHER, E. 2009. EGFRvIII and DNA

- double-strand break repair: a molecular mechanism for radioresistance in glioblastoma. *Cancer Research*, 69, 4252.
- MUNOZ, M., SAUNDERS, D., HENDERSON, M., CLANCY, J., RUSSELL, A., LEHRBACH, G., MUSGROVE, E., WATTS, C. and SUTHERLAND, R. 2007. The E3 ubiquitin ligase EDD regulates S-phase and G (2)/M DNA damage checkpoints. *Cell Cycle*, 6, 3070-7.
- MUÑOZ, Ú., BARTOLOMÉ, F., BERMEJO, F. and MARTÍN-REQUERO, Á. 2008. Enhanced proteasome-dependent degradation of the CDK inhibitor p27kip1 in immortalized lymphocytes from Alzheimer's dementia patients. *Neurobiology of Aging*, 29, 1474-1484.
- MUPPIDI, J., LOBITO, A., RAMASWAMY, M., YANG, J., WANG, L., WU, H. and SIEGEL, R. 2006. Homotypic FADD interactions through a conserved RXDLL motif are required for death receptor-induced apoptosis. *Cell Death and Differentiation*, 13, 1641-1650.
- NADERI, A., LIU, J. and BENNETT, I. C. 2010. BEX2 regulates mitochondrial apoptosis and G1 cell cycle in breast cancer. *Int J Cancer*, 126, 1596-610.
- NAKAMURA-LÓPEZ, Y., SARMIENTO-SILVA, R., MORAN-ANDRADE, J. and GÓMEZ-GARCÍA, B. 2009. Staurosporine-induced apoptosis in P388D1 macrophages involves both extrinsic and intrinsic pathways. *Cell biology international*, 33, 1026-1031.
- NEES, M., GEOGHEGAN, J. M., MUNSON, P., PRABHU, V., LIU, Y., ANDROPHY, E. and WOODWORTH, C. D. 2000. Human papillomavirus type 16 E6 and E7 proteins inhibit differentiation-dependent expression of transforming growth factor-beta2 in cervical keratinocytes. *Cancer Res*, 60, 4289-98.
- NEIL, J., TIAN, M. and SCHIEMANN, W. 2009. X-linked inhibitor of apoptosis protein and its E3 ligase activity promote transforming growth factor- $\beta$ -mediated nuclear factor- $\kappa$ B activation during breast cancer progression. *Journal of Biological Chemistry*, 284, 21209.
- NICKELL, S., MIHALACHE, O., BECK, F., HEGERL, R., KORINEK, A. and BAUMEISTER, W. 2007. Structural analysis of the 26S proteasome by cryoelectron tomography. *Biochemical and Biophysical Research Communications*, 353, 115-120.
- NIKSERESHT, M., SEGHATOLESLAM, A., MONABATI, A., TALEI, A., GHALATI, F. and OWJI, A. 2010. Overexpression of the novel human gene, UBE2Q2, in breast cancer. *Cancer Genetics and Cytogenetics*, 197, 101-106.
- NOHARA, K., YOKOHAMA, Y. and KANO, K. 2007. The important role of caspase-10 in sodium butyrate-induced apoptosis. *Kobe J. Med. Sci*, 53, 265-273.
- OH, J., KIM, M., AHN, C., KIM, S., HAN, J., LEE, S. and YOO, N. 2010. Mutational analysis of CASP10 gene in colon, breast, lung and hepatocellular carcinomas. *Pathology*, 42, 73-76.
- OH, S., LEE, B. and LIM, S. 2004. Cadmium induces apoptotic cell death in WI 38 cells via caspase-dependent Bid cleavage and calpain-mediated mitochondrial Bax cleavage by Bcl-2-independent pathway. *Biochemical Pharmacology*, 68, 1845-1855.

- OHGURO, H., ODAGIRI, H., MIYAGAWA, Y., OHGURO, I., SASAKI, M. and NAKAZAWA, M. 2004. Clinicopathological features of gastric cancer cases and aberrantly expressed recoverin. *The Tohoku Journal of Experimental Medicine*, 202, 213-219.
- OKA, T., MAZACK, V. and SUDOL, M. 2008. Mst2 and Lats kinases regulate apoptotic function of Yes kinase-associated protein (YAP). *J Biol Chem*, 283, 27534-46.
- OKAMOTO, K., TAYA, Y. and NAKAGAMA, H. 2009. Mdmx enhances p53 ubiquitination by altering the substrate preference of the Mdm2 ubiquitin ligase. *FEBS Lett*, 583, 2710-4.
- OKAMOTO, Y., OZAKI, T., MIYAZAKI, K., AOYAMA, M., MIYAZAKI, M. and NAKAGAWARA, A. 2003. UbcH10 is the cancer-related E2 ubiquitin-conjugating enzyme. *Cancer research*, 63, 4167-4173.
- OUYANG, G., YAO, L., RUAN, K., SONG, G., MAO, Y. and BAO, S. 2009. Genistein induces G2/M cell cycle arrest and apoptosis of human ovarian cancer cells via activation of DNA damage checkpoint pathways. *Cell Biol Int*, 33, 1237-44.
- PALACIOS, C., LOPEZ-PEREZ, A. I. and LOPEZ-RIVAS, A. 2010. Down-regulation of RIP expression by 17-dimethylaminoethylamino-17-demethoxygeldanamycin promotes TRAIL-induced apoptosis in breast tumor cells. *Cancer Lett*, 287, 207-15.
- PANG, X., YI, Z., ZHANG, J., LU, B., SUNG, B., QU, W., AGGARWAL, B. and LIU, M. 2010. Celestrol Suppresses Angiogenesis-Mediated Tumor Growth through Inhibition of AKT/Mammalian Target of Rapamycin Pathway. *Cancer Research*, 70, 1951-1959.
- PARISI, T., BRONSON, R. and LEES, J. 2008. Inhibition of pituitary tumors in Rb mutant chimeras through E2f4 loss reveals a key suppressive role for the pRB/E2F pathway in urothelium and ganglionic carcinogenesis. *Oncogene*, 28, 500-508.
- PASCHEN, S., WEBER, A. and HACKER, G. 2007. Mitochondrial protein import: a matter of death? *Cell Cycle*, 6, 2434-9.
- PASTORINO, J., CHEN, S., TAFANI, M., SNYDER, J. and FARBER, J. 1998. The Overexpression of Bax Produces Cell Death upon Induction of the Mitochondrial Permeability Transition. *Journal of Biological Chemistry*, 273, 7770-7775.
- PASTORINO, J., TAFANI, M., ROTHMAN, R., MARCINKEVICIUTE, A., HOEK, J., FARBER, J. and MARCINEVICIUTE, A. 1999. Functional consequences of the sustained or transient activation by Bax of the mitochondrial permeability transition pore [published erratum appears in J Biol Chem 2000 Mar 17; 275 (11): 8262]. *J Biol Chem* 1999, 274, 31734-9.
- PEARSON, G. and HUNTER, T. 2009. PI-3 kinase activity is necessary for ERK1/2-induced disruption of mammary epithelial architecture. *Breast Cancer Research: BCR*, 11, R29.
- PEIDIS, P., GIANNAKOUROS, T., BUROW, M. E., WILLIAMS, R. W. and SCOTT, R. E. 2010. Systems genetics analyses predict a transcription role for P2P-R: molecular confirmation that P2P-R is a transcriptional co-repressor. *BMC Syst Biol*, 4, 14.

- PELLERITO, O., CALVARUSO, G., PORTANOVA, P., DE BLASIO, A., SANTULLI, A., VENTO, R., TESORIERE, G. and GIULIANO, M. 2010. The synthetic cannabinoid WIN sensitizes hepatocellular carcinoma cells to TRAIL-induced apoptosis by activating p8/CHOP/DR5 axis. *Mol Pharmacol*.
- PEREIRA, B., ZHOU, Y., GUPTA, A., LEONG, D., AUNG, K., LING, L., PHO, R., GALINDO, M., SALTO-TELLEZ, M. and STEIN, G. 2009. Runx2, p53, and pRB status as diagnostic parameters for deregulation of osteoblast growth and differentiation in a new pre-chemotherapeutic osteosarcoma cell line (OS1). *Journal of cellular Physiology*, 221, 778-780.
- PEROUKIDES, S., BRAVOU, V., ALEXOPOULOS, A., VARAKIS, J., KALOFONOS, H. and PAPADAKI, H. 2010. Survivin overexpression in HCC and liver cirrhosis differentially correlates with p-STAT3 and E-cadherin. *Histol Histopathol*, 25, 299-307.
- PETER, M., HEUFELDER, A. and HENGARTNER, M. 1997. Advances in apoptosis research. *Proceedings of the National Academy of Sciences of the United States of America*, 94, 12736-12737.
- PETITJEAN, A., MATHE, E., KATO, S., ISHIOKA, C., TAVTIGIAN, S. V., HAINAUT, P. and OLIVIER, M. 2007. Impact of mutant p53 functional properties on TP53 mutation patterns and tumor phenotype: lessons from recent developments in the IARC TP53 database. *Hum Mutat*, 28, 622-9.
- PIÑOL-ROMA, S. and DREYFUSS, G. 1993. hnRNP proteins: localization and transport between the nucleus and the cytoplasm. *Trends in Cell Biology*, 3, 151-155.
- PISANI, P., BRAY, F. and PARKIN, D. M. 2002. Estimates of the world-wide prevalence of cancer for 25 sites in the adult population. *Int J Cancer*, 97, 72-81.
- POLSER, B., BASANEZ, G., ETXEBARRIA, A., HARDWICK, J. and NICHOLLS, D. 2005. Calpain I induces cleavage and release of apoptosis factor from isolated mitochondria. *J Biol Chem*, 280, 6447-54.
- POLSKY, D., MASTORIDES, S., KIM, D., DUDAS, M., LEON, L., LEUNG, D., WOODRUFF, J., BRENNAN, M., OSMAN, I. and CORDON-CARDO, C. 2006. Altered patterns of RB expression define groups of soft tissue sarcoma patients with distinct biological and clinical behavior. *Histology and histopathology*, 21, 743-752.
- POULSEN, K. A., ANDERSEN, E. C., HANSEN, C. F., KLAUSEN, T. K., HOUGAARD, C., LAMBERT, I. H. and HOFFMANN, E. K. 2010. Deregulation of apoptotic volume decrease and ionic movements in multidrug-resistant tumor cells: role of chloride channels. *American Journal of Physiology-Cell Physiology*, 298, C14-C25.
- PRETORIUS, A. 2007. Functional analysis of the Mouse RbBP6 Gene Using Interference RNA. *University of the Western Cape (PhD Thesis)*.
- PRIVETTE, L., WEIER, J., NGUYEN, H., YU, X. and PETTY, E. 2008. Loss of CHFR in human mammary epithelial cells causes genomic instability by disrupting the mitotic spindle assembly checkpoint. *Neoplasia (New York, NY)*, 10, 643-652.

- PUCA, R., NARDINOCCHI, L., PISTRITTO, G. and D'ORAZI, G. 2008. Overexpression of HIPK2 circumvents the blockade of apoptosis in chemoresistant ovarian cancer cells. *Gynecol Oncol*, 109, 403-410.
- PUGH, D., AB, E., FARO, A., LUTYA, P., HOFFMANN, E. and REES, D. 2006. DWNN, a novel ubiquitin-like domain, implicates RBBP 6 in mRNA processing and ubiquitin-like pathways. *BMC Structural Biology*, 6, 1.
- QIU, W., WU, J., WALSH, E. M., ZHANG, Y., CHEN, C. Y., FUJITA, J. and XIAO, Z. X. 2008. Retinoblastoma protein modulates gankyrin-MDM2 in regulation of p53 stability and chemosensitivity in cancer cells. *Oncogene*, 27, 4034-43.
- RAJA, S., CHEN, S., YUE, P., ACKER, T., LEFKOVE, B., ARBISER, J., KHURI, F. and SUN, S. 2008. The natural product honokiol preferentially inhibits cellular FLICE-inhibitory protein and augments death receptor-induced apoptosis. *Molecular cancer therapeutics*, 7, 2212-2223.
- RAMASWAMY, B., MAJUMDER, S., ROY, S., GHOSHAL, K., KUTAY, H., DATTA, J., YOUNES, M., SHAPIRO, C. L., MOTIWALA, T. and JACOB, S. T. 2009. Estrogen-mediated suppression of the gene encoding protein tyrosine phosphatase PTPRO in human breast cancer: mechanism and role in tamoxifen sensitivity. *Molecular Endocrinology*, 23, 176-87.
- RAMZI, M., JACK, W., ASFAR, A., AMRO, A., ANGELA, S., SHERWIN, W., DAJUN, Y., SHAOMENG, W. and AYAD, A. 2009. An MDM2 antagonist (MI-319) restores p53 functions and increases the life span of orally treated follicular lymphoma bearing animals. *Molecular Cancer*, 8.
- REICH III, C. and PISETSKY, D. 2009. The content of DNA and RNA in microparticles released by Jurkat and HL-60 cells undergoing in vitro apoptosis. *Experimental cell research*, 315, 760-768.
- RIGGINS, G., THIAGALINGAM, S., ROZENBLUM, E., WEINSTEIN, C., KERN, S., HAMILTON, S., WILLSON, J., MARKOWITZ, S., KINZLER, K. and VOGELSTEIN, B. 1996. Mad-related genes in the human. *Nature Genetics*, 13, 347-349.
- ROSEN, K. M., MOUSSA, C. E., LEE, H. K., KUMAR, P., KITADA, T., QIN, G., FU, Q. and QUERFURTH, H. W. 2010. Parkin reverses intracellular beta-amyloid accumulation and its negative effects on proteasome function. *J Neurosci Res*, 88, 167-78.
- ROY, K. R., ARUNASREE, K. M., REDDY, N. P., DHEERAJ, B., REDDY, G. V. and REDDANNA, P. 2007. Alteration of mitochondrial membrane potential by Spirulina platensis C-phycocyanin induces apoptosis in the doxorubicinresistant human hepatocellular-carcinoma cell line HepG2. *Biotechnol Appl Biochem*, 47, 159-67.
- RUSAN, N. and PEIFER, M. 2008. Original CIN: reviewing roles for APC in chromosome instability. *The Journal of Cell Biology*, 181, 719-726.
- RYU, K., SINNAR, S., REINHOLDT, L., VACCARI, S., HALL, S., GARCIA, M., ZAITSEVA, T., BOULEY, D., BOEKELHEIDE, K. and HANDEL, M. 2008. The mouse polyubiquitin gene Ubb is essential for meiotic progression. *Molecular and cellular biology*, 28, 1136.
- SAIJO, M., SAKAI, Y., KISHINO, T., NIIKAWA, N., MATSUURA, Y., MORINO, K., TAMAI, K. and TAYA, Y. 1995. Molecular Cloning of a

- Human Protein That Binds to the Retinoblastoma Protein and Chromosomal Mapping. *Genomics*, 27, 511-519.
- SAKAI, Y., SAIJO, M., COELHO, K., KISHINO, T., NIKAWA, N. and TAYA, Y. 1995. cDNA sequence and chromosomal localization of a novel human protein, RBQ-1 (RBBP6), that binds to the retinoblastoma gene product. *Genomics*, 30, 98-101.
- SAL, G., COLLAVIN, L., RUARO, M., EDOMI, P., SACCONI, S., VALLE, G. and SCHNEIDER, C. 1994. Structure, Function, and Chromosome Mapping of the Growth-Suppressing Human Homologue of the Murine gas1 Gene. *Proceedings of the National Academy of Sciences*, 91, 1848-1852.
- SALVESEN, G. S. and DUCKETT, C. S. 2002. IAP proteins: blocking the road to death's door. *Nat Rev Mol Cell Biol*, 3, 401-10.
- SANADA, K., SHIMIZU, F., KAMEYAMA, K., HAGA, K., HAGA, T. and FUKADA, Y. 1996. Calcium-bound recoverin targets rhodopsin kinase to membranes to inhibit rhodopsin phosphorylation. *FEBS Lett*, 384, 227-30.
- SANTER, F., MOSER, B., SPODEN, G., JANSEN-DÜRR, P. and ZWERSCHKE, W. 2007. Human papillomavirus type 16 E7 oncoprotein inhibits apoptosis mediated by nuclear insulin-like growth factor-binding protein-3 by enhancing its ubiquitin/proteasome-dependent degradation. *Carcinogenesis*, 28, 2511-2520.
- SASAKI, Y., NEGISHI, H., KOYAMA, R., ANBO, N., OHORI, K., IDOGAWA, M., MITA, H., TOYOTA, M., IMAI, K. and SHINOMURA, Y. 2009. p53 family members regulate the expression of the apolipoprotein D gene. *Journal of Biological Chemistry*, 284, 872-883.
- SATO, Y., SAKAMOTO, K., SEI, M., EWIS, A. and NAKAHORI, Y. 2009. Proteasome subunits are regulated and expressed in comparable concentrations as a functional cluster. *Biochemical and Biophysical Research Communications*, 378, 795-8.
- SAUER, M. and ANDRULIS, I. 2005. Identification and characterization of missense alterations in the BRCA1 associated RING domain (BARD1) gene in breast and ovarian cancer. *Journal of medical genetics*, 42, 633-638.
- SCHARSTUHL, A., MUTSAERS, H., PENNINGS, S., RUSSEL, F. and WAGENER, F. 2009. Involvement of VDAC, Bax and ceramides in the efflux of AIF from mitochondria during curcumin-induced apoptosis. *PLoS One*, 4, e6688.
- SCHMIDT, F., KNOBBE, C., FRANK, B., WOLBURG, H. and WELLER, M. 2008. The topoisomerase II inhibitor, genistein, induces G2/M arrest and apoptosis in human malignant glioma cell lines. *Oncol Rep*, 19, 1061-6.
- SCHOLZ, C., RICHTER, A., LEHMANN, M., SCHULZE-OSTHOFF, K., DÖRKEN, B. and DANIEL, P. 2005. Arsenic trioxide induces regulated, death receptor-independent cell death through a Bcl-2-controlled pathway. *Oncogene*, 24, 7031-7042.
- SCHREINER, P., CHEN, X., HUSNJAK, K., RANGLES, L., ZHANG, N., ELSASSER, S., FINLEY, D., DIKIC, I., WALTERS, K. and GROLL, M. 2008. Ubiquitin docking at the proteasome through a novel pleckstrin-homology domain interaction. *Nature*, 453, 548-52.

- SCOTT, R., GIANNAKOUROS, T., GAO, S. and PEIDIS, P. 2003. Functional potential of P2P-R: A role in the cell cycle and cell differentiation related to its interactions with proteins that bind to matrix associated regions of DNA? *Journal of cellular biochemistry*, 90, 6-12.
- SCOTT, R. E. and GAO, S. 2002. P2P-R deficiency modifies nocodazole-induced mitotic arrest and UV-induced apoptosis. *Anticancer Res*, 22, 3837-42.
- SCOTT, R. E., WHITE-GRINDLEY, E., RULEY, H. E., CHESLER, E. J. and WILLIAMS, R. W. 2005. P2P-R expression is genetically coregulated with components of the translation machinery and with PUM2, a translational repressor that associates with the P2P-R mRNA. *Journal of cellular physiology*, 204, 99-105.
- SCULLY, R. 2000. Role of BRCA gene dysfunction in breast and ovarian cancer predisposition. *Breast Cancer Res*, 2, 324-330.
- SEGDITSAS, S., ROWAN, A. J., HOWARTH, K., JONES, A., LEEDHAM, S., WRIGHT, N. A., GORMAN, P., CHAMBERS, W., DOMINGO, E., ROYLANCE, R. R., SAWYER, E. J., SIEBER, O. M. and TOMLINSON, I. P. 2009. APC and the three-hit hypothesis. *Oncogene*, 28, 146-55.
- SEITZ, S., ROHDE, K., BENDER, E., NOTHNAGEL, A., KOELBLE, K., SCHLAG, P. and SCHERNECK, S. 1997. Strong indication for a breast cancer susceptibility gene on chromosome 8p12-p22: linkage analysis in German breast cancer families. *Oncogene*, 14, 741-743.
- SENIN, II, HOPPNER-HEITMANN, D., POLKOVNIKOVA, O. O., CHURUMOVA, V. A., TIKHOMIROVA, N. K., PHILIPPOV, P. P. and KOCH, K. W. 2004. Recoverin and rhodopsin kinase activity in detergent-resistant membrane rafts from rod outer segments. *J Biol Chem*, 279, 48647-53.
- SEOANE, M., IGLESIAS, P., GONZALEZ, T., DOMINGUEZ, F., FRAGA, M., ALISTE, C., FORTEZA, J. and COSTOYA, J. 2008. Retinoblastoma loss modulates DNA damage response favoring tumor progression. *PLoS One*, 3, 3632.
- SHAKYA, R., SZABOLCS, M., MCCARTHY, E., OSPINA, E., BASSO, K., NANDULA, S., MURTY, V., BAER, R. and LUDWIG, T. 2008. The basal-like mammary carcinomas induced by Brca1 or Bard1 inactivation implicate the BRCA1/BARD1 heterodimer in tumor suppression. *Proceedings of the National Academy of Sciences*, 105, 7040-7045.
- SHAN, Y. F., ZHOU, W. P., FU, X. Y., YAN, H. X., YANG, W., LIU, S. Q., CAO, H. F., KANG, B., WU, M. C. and WANG, H. Y. 2006. The role of p28GANK in rat oval cells activation and proliferation. *Liver Int*, 26, 240-7.
- SHANGARY, S., QIN, D., MCEACHERN, D., LIU, M., MILLER, R., QIU, S., NIKOLOVSKA-COLESKA, Z., DING, K., WANG, G. and CHEN, J. 2008. Temporal activation of p53 by a specific MDM2 inhibitor is selectively toxic to tumors and leads to complete tumor growth inhibition. *Proceedings of the National Academy of Sciences*, 105, 3933-3988.
- SHANKAR, E., SIVAPRASAD, U. and BASU, A. 2008. Protein kinase C epsilon confers resistance of MCF-7 cells to TRAIL by Akt-dependent activation of Hdm2 and downregulation of p53. *Oncogene*, 27, 3957-66.

- SHE, Q., CHANDARLAPATY, S., YE, Q., LOBO, J., HASKELL, K., LEANDER, K., DEFEO-JONES, D., HUBER, H. and ROSEN, N. 2008. Breast tumor cells with PI3K mutation or HER2 amplification are selectively addicted to Akt signaling. *PLoS One*, 3, 3065.
- SHEN, Z., CHEN, G., NI, J., LI, X., XIONG, S., QIU, Q., ZHU, J., TANG, W., SUN, G. and YANG, K. 1997. Use of arsenic trioxide (As<sub>2</sub>O<sub>3</sub>) in the treatment of acute promyelocytic leukemia (APL): II. Clinical efficacy and pharmacokinetics in relapsed patients. *Blood*, 89, 3354.
- SIDDIQA, A., LONG, L. M., LI, L., MARCINIAK, R. A. and KAZHDAN, I. 2008. Expression of HER-2 in MCF-7 breast cancer cells modulates anti-apoptotic proteins Survivin and Bcl-2 via the extracellular signal-related kinase (ERK) and phosphoinositide-3 kinase (PI3K) signalling pathways. *BMC Cancer*, 8, 129.
- SIMA, N., WANG, S., WANG, W., KONG, D., XU, Q., TIAN, X., LUO, A., ZHOU, J., XU, G., MENG, L., LU, Y. and MA, D. 2007. Antisense targeting human papillomavirus typ16 E6 and E7 genes contributes to apoptosis and senescence in SiHa cervical carcinoma cells. *Gynecologic Oncology*, 106, 299-304.
- SIMONS, A., MELAMED-BESSUDO, C., WOLKOWICZ, R., SPERLING, J., SPERLING, R., EISENBACH, L. and ROTTER, V. 1997. PACT: cloning and characterization of a cellular p53 binding protein that interacts with Rb. *Oncogene*, 14, 145-155.
- SINGH, M., SRIVASTAVA, S., SINGH, U., MATHUR, N. and SHUKLA, Y. 2009. Co-expression of p53 and Bcl-2 proteins in human papillomavirus-induced premalignant lesions of the uterine cervix: correlation with progression to malignancy. *Tumour Biol*, 30, 276-85.
- SINHA, R., CROSS, A. J., GRAUBARD, B. I., LEITZMANN, M. F. and SCHATZKIN, A. 2009. Meat intake and mortality: a prospective study of over half a million people. *Arch Intern Med*, 169, 562-71.
- SINHA, S., MALONIA, S., MITTAL, S., SINGH, K., KADREPPA, S., KAMAT, R., MUKHOPADHYAYA, R., PAL, J. and CHATTOPADHYAY, S. 2010. Coordinated regulation of p53 apoptotic targets BAX and PUMA by SMAR1 through an identical MAR element. *The EMBO Journal*.
- SIU, K., CHAN, J. and FUNG, K. 2002. Effects of Arsenic trioxide on human hepatocellular carcinoma HepG2 cells: Inhibition of proliferation and induction of apoptosis. *Life Sciences*, 71, 275-285.
- SIVARAJASINGHAM, N., CAWKWELL, L., BAKER, R., O'KANE, S., SMYTH, E., TILSED, J., WATSON, M., GREENMAN, J. and MONSON, J. 2006. Implication of the BRCA2 and Putative "BRCA3" Genes in Dukes' Stage C, Replication Error-Negative Colon Cancer. *Annals of surgical oncology*, 13, 881-886.
- SKEPU, A. 2005. Identification and characterisation of a novel gene, DWNN, isolated from promoter-trapped Chinese hamster ovary cells. *University of the Western Cape PhD Thesis*.
- SLEMMER, J., ZHU, C., LANDSHAMER, S., TRABOLD, R., GROHM, J., ARDESHIRI, A., WAGNER, E., SWEENEY, M., BLOMGREN, K., CULMSEE, C., WEBER, J. and PLESNILA, N. 2008. Causal role of

- apoptosis-inducing factor for neuronal cell death following traumatic brain injury. *Am J Pathol*, 173, 1795-1805.
- SOHN, D., SCHULZE-OSTHOFF, K. and JÄNICKE, R. 2005. Caspase-8 can be activated by interchain proteolysis without receptor-triggered dimerization during drug-induced apoptosis. *Journal of Biological Chemistry*, 280, 5267-5273.
- SONG, E., WERNER, S., NEUBAUER, J., STEGMEIER, F., ASPDEN, J., RIO, D., HARPER, J., ELLEDGE, S., KIRSCHNER, M. and RAPE, M. 2010. The Prp19 complex and the Usp4Sart3 deubiquitinating enzyme control reversible ubiquitination at the spliceosome. *Genes & development*, 24, 1434.
- SONG, G., CHEN, G. G., YUN, J. P. and LAI, P. B. 2009. Association of p53 with Bid induces cell death in response to etoposide treatment in hepatocellular carcinoma. *Curr Cancer Drug Targets*, 9, 871-80.
- STAMATAKI, P., PAPAZAFIROPOULOU, A., GIANNAKOPOULOU, M., BROKALAKI, H., APOSTOLOPOULOU, E., SARAFIS, P. and SAROGLU, G. 2010. Prevalence of HPV infection among Greek women attending a gynecological outpatient clinic. *BMC Infect Dis*, 10, 27.
- STEINBACH, J. and WELLER, M. 2004. Apoptosis in Gliomas: Molecular Mechanisms and Therapeutic Implications. *Journal of Neuro-Oncology*, 70, 245-254.
- STONE, S. L., HAUKSDOTTIR, H., TROY, A., HERSCHLEB, J., KRAFT, E. and CALLIS, J. 2005. Functional analysis of the RING-type ubiquitin ligase family of Arabidopsis. *Plant Physiology*, 137, 13-30.
- SUBAUSTE, M., VENTURA-HOLMAN, T., DU, L., SUBAUSTE, J., CHAN, S., YU, V. and MAHER, J. 2009. RACK1 downregulates levels of the pro-apoptotic protein Fem1b in apoptosis-resistant colon cancer cells. *Cancer biology & therapy*, 8, 2297-2305.
- SUN, M., MEARES, G., SONG, L. and JOPE, R. S. 2009. XIAP associates with GSK3 and inhibits the promotion of intrinsic apoptotic signaling by GSK3. *Cell Signal*, 21, 1857-65.
- TAFANI, M., KARPINICH, N., HURSTER, K., PASTORINO, J., SCHNEIDER, T., RUSSO, M. and FARBER, J. 2002. Cytochrome c Release upon Fas Receptor Activation Depends on Translocation of Full-length Bid and the Induction of the Mitochondrial Permeability Transition. *Journal of Biological Chemistry*, 277, 10073-10082.
- TAI, H., KUBOTA, N. and KATO, S. 2000. Involvement of nuclear receptor coactivator SRC-1 in estrogen-dependent cell growth of MCF-7 cells. *Biochem Biophys Res Commun*, 267, 311-6.
- TAKAHASHI, M., SHIMAJIRI, S., IZUMI, H., HIRANO, G., KASHIWAGI, E., YASUNIWA, Y., WU, Y., HAN, B., AKIYAMA, M. and NISHIZAWA, S. 2010. Y-box binding protein-1 is a novel molecular target for tumor vessels. *Cancer Science*, 101, 1367-1373.
- TAKAHASHI, R., DEVERAUX, Q., TAMM, I., WELSH, K., ASSA-MUNT, N., SALVESEN, G. and REED, J. 1998. A single BIR domain of XIAP sufficient for inhibiting caspases. *Journal of Biological Chemistry*, 273, 7787-7790.

- TAKEBA, Y., KUMAI, T., MATSUMOTO, N., NAKAYA, S. and TSUZUKI, Y. 2007a. Irinotecan Activates p53 With Its Active Metabolite, Resulting in Human Hepatocellular Carcinoma Apoptosis. *Journal of Pharmacological Sciences*, 104, 232-242.
- TAKEBA, Y., SEKINE, S., KUMAI, T., MATSUMOTO, N., NAKAYA, S., TSUZUKI, Y., YANAGIDA, Y., NAKANO, H., ASAKURA, T. and OHTSUBO, T. 2007b. Irinotecan-induced apoptosis is inhibited by increased P-glycoprotein expression and decreased p53 in human hepatocellular carcinoma cells. *Biological & pharmaceutical bulletin*, 30, 1400-1406.
- TAMM, I. 1998. IAP-family protein survivin inhibits caspase activity and apoptosis induced by Fas (CD95), Bax, caspases, and anticancer drugs. *Cancer Research*, 58, 5315-5320.
- TANG, D., LAHTI, J. and KIDD, V. 2000. Caspase-8 Activation and Bid Cleavage Contribute to MCF7 Cellular Execution in a Caspase-3-dependent Manner during Staurosporine-mediated Apoptosis. *Journal of Biological Chemistry*, 275, 9303-9307.
- TEOH, N., PYAKUREL, P., DAN, Y. Y., SWISSHELM, K., HOU, J., MITCHELL, C., FAUSTO, N., GU, Y. and FARRELL, G. 2009. Induction of p53 Renders ATM-Deficient Mice Refractory to Hepatocarcinogenesis. *Gastroenterology*.
- THAKAR, J., SCHLEINKOFER, K., BORNER, C. and DANDEKAR, T. 2006. RIP death domain structural interactions implicated in TNF-mediated proliferation and survival. *Proteins*, 63, 413-423.
- THALAPPILLY, S., SULIMAN, M., GAYET, O., SOUBEYRAN, P., HERMANT, A., LECINE, P., IOVANNA, J. and DUSETTI, N. 2008. Identification of multi-SH3 domain-containing protein interactome in pancreatic cancer: a yeast two-hybrid approach. *Proteomics*, 8, 3071.
- TOEGEL, S., HUANG, W., PIANA, C., UNGER, F., WIRTH, M., GOLDRING, M., GABOR, F. and VIERNSTEIN, H. 2007. Selection of reliable reference genes for qPCR studies on chondroprotective action. *BMC molecular biology*, 8, 13.
- TOMICIC, M. T., CHRISTMANN, M. and KAINA, B. 2010. Topotecan triggers apoptosis in p53-deficient cells by forcing degradation of XIAP and survivin thereby activating caspase-3-mediated Bid cleavage. *J Pharmacol Exp Ther*, 332, 316-25.
- TOMMASI, S., PILATO, B., PINTO, R., MONACO, A., BRUNO, M., CAMPANA, M., DIGENNARO, M., SCHITTULLI, F., LACALAMITA, R. and PARADISO, A. 2008. Molecular and in silico analysis of BRCA1 and BRCA2 variants. *Mutation Research/Fundamental and Molecular Mechanisms of Mutagenesis*, 644, 64-70.
- TORBETT, N. E., LUNA-MORAN, A., KNIGHT, Z. A., HOUK, A., MOASSER, M., WEISS, W., SHOKAT, K. M. and STOKOE, D. 2008. A chemical screen in diverse breast cancer cell lines reveals genetic enhancers and suppressors of sensitivity to PI3K isoform-selective inhibition. *Biochem J*, 415, 97-110.

- TOTH, A., NICKSON, P., QIN, L. and ERHARDT, P. 2006. Differential regulation of cardiomyocyte survival and hypertrophy by MDM2, an E3 ubiquitin ligase. *Journal of Biological Chemistry*, 281, 3679-3689.
- TOYOOKA, M. 1995. Somatic mutations of the adenomatous polyposis coli gene in gastroduodenal tumors from patients with familial adenomatous polyposis. *Cancer Research*, 55, 3165-3170.
- TSAO, C., TEH, B., JONASCH, E., SHREIBER-AGUS, N., EFSTATHIOU, E., HOANG, A., CZERNIAK, B., LOGOTHETIS, C. and CORN, P. 2008. Inhibition of Mx1 suppresses HIF-2 $\alpha$ -dependent renal cancer tumorigenesis. *Cancer biology & therapy*, 7, 1619-1627.
- TSENG, L. M., YIN, P. H., CHI, C. W., HSU, C. Y., WU, C. W., LEE, L. M., WEI, Y. H. and LEE, H. C. 2006. Mitochondrial DNA mutations and mitochondrial DNA depletion in breast cancer. *Genes Chromosomes Cancer*, 45, 629-38.
- UCHIDA, C., MIWA, S., ISOBE, T., KITAGAWA, K., HATTORI, T., ODA, T., YASUDA, H. and KITAGAWA, M. 2006. Effects of MdmX on Mdm2-mediated downregulation of pRB. *FEBS Lett*, 580, 1753-8.
- UCHIDA, K. 1996. Somatic in vivo alterations of the JV18-1 gene at 18q21 in human lung cancers. *Cancer Research*, 56, 5583-5585.
- UCHIKI, T., KIM, H., ZHAI, B., GYGI, S., JOHNSTON, J., O'BRYAN, J. and GOLDBERG, A. 2009. The Ubiquitin-interacting Motif Protein, S5a, Is Ubiquitinated by All Types of Ubiquitin Ligases by a Mechanism Different from Typical Substrate Recognition. *Journal of Biological Chemistry*, 284, 12622.
- UO, T., VEENSTRA, T. and MORRISON, R. 2009. Histone deacetylase inhibitors prevent p53-dependent and p53-independent Bax-mediated neuronal apoptosis through two distinct mechanisms. *Journal of Neuroscience*, 29, 2824.
- URIST, M., DI COMO, C., LU, M., CHARYTONOWICZ, E., VERBEL, D., CRUM, C., INCE, T., MCKEON, F. and CORDON-CARDO, C. 2002. Loss of p63 expression is associated with tumor progression in bladder cancer. *American Journal of Pathology*, 161, 1199-1206.
- VALLADARES, A., HERNENDEZ, N., GOMEZ, F., CURIEL-QUEZADA, E., MADRIGAL-BUJAJIDAR, E., VERGARA, M., MARTINEZ, M. and ARENAS ARANDA, D. 2006. Genetic expression profiles and chromosomal alterations in sporadic breast cancer in Mexican women. *Cancer Genetics and Cytogenetics*, 170, 147-151.
- VALLELEY, E., CORDERY, S. and BONTHRON, D. 2007. Tissue-specific imprinting of the ZAC/PLAGL1 tumour suppressor gene results from variable utilization of monoallelic and biallelic promoters. *Human molecular genetics*, 16, 972-981.
- VAN MAERKEN, T., FERDINANDE, L., TAILDEMAN, J., LAMBERTZ, I., YIGIT, N., VERCRUYSSSE, L., RIHANI, A., MICHAELIS, M., CINATL, J., JR., CUVELIER, C. A., MARINE, J. C., DE PAEPE, A., BRACKE, M., SPELEMAN, F. and VANDESOMPELE, J. 2009. Antitumor activity of the selective MDM2 antagonist nutlin-3 against chemoresistant neuroblastoma with wild-type p53. *J Natl Cancer Inst*, 101, 1562-74.

- VAN WIJK, S., DE VRIES, S., KEMMEREN, P., HUANG, A., BOELEN, R., BONVIN, A. and TIMMERS, H. 2009. A comprehensive framework of E2–RING E3 interactions of the human ubiquitin–proteasome system. *Molecular Systems Biology*, 5.
- VESTHEY, S., SEN, C., CALDER, C., PERKS, C., PIGNATELLI, M. and WINTERS, Z. 2005. Activated Akt expression in breast cancer: correlation with p53, Hdm2 and patient outcome. *European Journal of Cancer* 41, 1017-1025.
- VITTAR, N., AWRUCH, J., AZIZUDDIN, K. and RIVAROLA, V. 2010. Caspase-independent apoptosis, in human MCF-7c3 breast cancer cells, following photodynamic therapy, with a novel water-soluble phthalocyanine. *Int J Biochem Cell Biol*, 42, 1123-31.
- VO, L., MINET, M., SCHMITTER, J., LACROUTE, F. and WYERS, F. 2001. Mpe1, a Zinc Knuckle Protein, Is an Essential Component of Yeast Cleavage and Polyadenylation Factor Required for the Cleavage and Polyadenylation of mRNA. *Molecular and Cellular Biology*, 21, 8346-8356.
- WALLACE, D. C. 2005. A mitochondrial paradigm of metabolic and degenerative diseases, aging, and cancer: a dawn for evolutionary medicine. *Annu Rev Genet*, 39, 359-407.
- WANG, H., HAN, H. and VON HOFF, D. 2006a. Identification of an Agent Selectively Targeting DPC4 (Deleted in Pancreatic Cancer Locus 4)–Deficient Pancreatic Cancer Cells. *Cancer research*, 66, 9722-9730.
- WANG, H. J., ZHU, J. S., ZHANG, Q., GUO, H., DAI, Y. H. and XIONG, X. P. 2009a. RNAi-mediated silencing of ezrin gene reverses malignant behavior of human gastric cancer cell line SGC-7901. *J Dig Dis*, 10, 258-64.
- WANG, J., BELCHER, J. D., MARKER, P. H., WILCKEN, D. E., VERCELLOTTI, G. M. and WANG, X. L. 2001. Cytomegalovirus inhibits p53 nuclear localization signal function. *J Mol Med*, 78, 642-7.
- WANG, P., ZHANG, J., BELLAIL, A., JIANG, W., HUGH, J., KNETEMAN, N. M. and HAO, C. 2007. Inhibition of RIP and c-FLIP enhances TRAIL-induced apoptosis in pancreatic cancer cells. *Cell Signal*, 19, 2237-46.
- WANG, R., LI, B., WANG, X., LIN, F., GAO, P., CHENG, S. Y. and ZHANG, H. Z. 2009b. Inhibiting XIAP expression by RNAi to inhibit proliferation and enhance radiosensitivity in laryngeal cancer cell line. *Auris Nasus Larynx*, 36, 332-9.
- WANG, S., LIU, Q., ZHANG, Y., LIU, K., YU, P., LUAN, J., DUAN, H., LU, Z., WANG, F., WU, E., YAGASAKI, K. and ZHANG, G. 2009c. Suppression of growth, migration and invasion of highly-metastatic human breast cancer cells by berbamine and its molecular mechanisms of action. *Mol Cancer*, 8, 81.
- WANG, X., MATTA, R., SHEN, G., NELIN, L., PEI, D. and LIU, Y. 2006b. Mechanism of triptolide-induced apoptosis: effect on caspase activation and Bid cleavage and essentiality of the hydroxyl group of triptolide. *Journal of Molecular Medicine*, 84, 405-415.
- WANG, Y., SHNYRA, A., AFRICA, C., WARHOLIC, C. and MCARTHUR, C. 2009d. Activation of the extrinsic apoptotic pathway by TNF-[alpha] in

- Human Salivary Gland (HSG) cells in vitro, suggests a role for the TNF receptor (TNF-R) and Inter cellular Adhesion Molecule-1 (ICAM-1) in Sjögren's Syndrome-associated autoimmune sialadenitis. *Archives of Oral Biology*, 54, 986-996.
- WANG, Y., YANG, H., LIU, H., HUANG, J. and SONG, X. 2009e. Effect of staurosporine on the mobility and invasiveness of lung adenocarcinoma A549 cells: an in vitro study. *BMC Cancer*, 9, 174.
- WANG, Z., CUDDY, M., SAMUEL, T., WELSH, K., SCHIMMER, A., HANAI, F., HOUGHTEN, R., PINILLA, C. and REED, J. 2004. Cellular, biochemical, and genetic analysis of mechanism of small molecule IAP inhibitors. *Journal of Biological Chemistry*, 279, 48168-48176.
- WATABE, Y., NAZUKA, N., TEZUKA, M. and S, S. 2010. Aryl Hydrocarbon Receptor Functions as a Potent Coactivator of E2F1-dependent Transcription Activity. *Biol Pharm Bull*, 33, 389-3997.
- WAWRZYNOW, B., PETTERSSON, S., ZYLICZ, A., BRAMHAM, J., WORRALL, E., HUPP, T. R. and BALL, K. L. 2009. A Function for the RING Finger Domain in the Allosteric Control of MDM2 Conformation and Activity. *Journal of Biological Chemistry*, 284, 11517-11530.
- WEBER, A., BOGER, R., VICK, B., URBANIK, T., HAYBAECK, J., ZOLLER, S., TEUFEL, A., KRAMMER, P. H., OPFERMAN, J. T., GALLE, P. R., SCHUCHMANN, M., HEIKENWALDER, M. and SCHULZBERGKAMEN, H. 2009. Hepatocyte-specific deletion of the antiapoptotic protein myeloid cell leukemia-1 triggers proliferation and hepatocarcinogenesis in mice. *Hepatology*, 51.
- WEGER, S., HAMMER, E. and HEILBRONN, R. 2002. Topors, a p53 and topoisomerase I binding protein, interacts with the adeno-associated virus (AAV-2) Rep78/68 proteins and enhances AAV-2 gene expression. *Journal of General Virology*, 83, 511-516.
- WEGER, S., HAMMER, E. and HEILBRONN, R. 2005. Topors acts as a SUMO-1 E3 ligase for p53 in vitro and in vivo. *FEBS Letters*, 579, 5007-5012.
- WEIGEL, B. J., PIERPONT, M. E., YOUNG, T. L., MUTCHLER, S. B. and NEGLIA, J. P. 1998. Retinoblastoma and Hirschsprung disease in a patient with interstitial deletion of chromosome 13. *Am J Med Genet*, 77, 285-8.
- WHITTAKER, S., WALTON, M., GARRETT, M. and WORKMAN, P. 2004. The cyclin-dependent kinase inhibitor CYC202 (R-roscovitine) inhibits retinoblastoma protein phosphorylation, causes loss of cyclin D1, and activates the mitogen-activated protein kinase pathway. *Cancer research*, 64, 262-272.
- WICKSTROM, S. A., MASOUMI, K. C., KHOCHBIN, S., FASSLER, R. and MASSOUMI, R. 2010. CYLD negatively regulates cell-cycle progression by inactivating HDAC6 and increasing the levels of acetylated tubulin. *EMBO J*, 29, 131-44.
- WILKINSON, C., DITTMAR, G., OHI, M., UETZ, P., JONES, N. and FINLEY, D. 2004. Ubiquitin-like Protein Hub1 Is Required for Pre-mRNA Splicing and Localization of an Essential Splicing Factor in Fission Yeast. *Current Biology*, 14, 2283-2288.

- WINGO, S., GALLARDO, T., AKBAY, E., LIANG, M., CONTRERAS, C., BOREN, T., SHIMAMURA, T., MILLER, D., SHARPLESS, N., BARDEESY, N., KWIATKOWSKI, D., SCHORGE, J., WONG, K. and CASTRILLON, D. 2009. Somatic LKB1 mutations promote cervical cancer progression. *PLoS One*, 4, e5137.
- WITTE, M. and SCOTT, R. 1997. The proliferation potential protein-related (P2P-R) gene with domains encoding heterogeneous nuclear ribonucleoprotein association and Rb1 binding shows repressed expression during terminal differentiation. *Proceedings of the National Academy of Sciences of the United States of America*, 94, 1212-1217.
- WOO, R., JACK, M., XU, Y., BURMA, S., CHEN, D. and LEE, P. 2002. DNA damage-induced apoptosis requires the DNA-dependent protein kinase, and is mediated by the latent population of p53. *The EMBO Journal*, 21, 3000-3008.
- WU, L., WANG, Z., TSAN, J., SPILLMAN, M., PHUNG, A., XU, X., YANG, M., HWANG, L., BOWCOCK, A. and BAER, R. 1996. Identification of a RING protein that can interact in vivo with the BRCA1 gene product. *Nature Genetics*, 14, 430-440.
- WU, S., HANG, L., YANG, J., CHEN, H., LIN, H., CHIANG, J., LU, C., YANG, J., LAI, T. and KO, Y. 2010. Curcumin Induces Apoptosis in Human Non-small Cell Lung Cancer NCI-H460 Cells through ER Stress and Caspase Cascade-and Mitochondria-dependent Pathways. *Anticancer research*, 30, 2125.
- WU, S., NG, L. and LIN, C. 2005. Effects of antioxidants and caspase-3 inhibitor on the phenylethyl isothiocyanate-induced apoptotic signaling pathways in human PLC/PRF/5 cells. *European Journal of Pharmacology*, 518, 96-106.
- WU, Z., WU, L., LI, L., TASHIRO, S., ONODERA, S. and IKEJIMA, T. 2004. Shikonin regulates H e L a cell death via caspase-3 activation and blockage of DNA synthesis. *Journal of Asian Natural Products Research*, 6, 155-166.
- WULLAERT, A., HEYNINCK, K. and BEYAERT, R. 2006. Mechanisms of crosstalk between TNF-induced NF- $\kappa$ B and JNK activation in hepatocytes. *Biochemical Pharmacology*, 72, 1090-1101.
- XIAO, B., SPENCER, J., CLEMENTS, A., ALI-KHAN, N., MITTNACHT, S., BROCCEN, O, C., BURGHAMMER, M., PERRAKIS, A., MARMORSTEIN, R. and GAMBLIN, S. 2003. Crystal structure of the retinoblastoma tumor suppressor protein bound to E2F and the molecular basis of its regulation. *Proceedings of the National Academy of Sciences*, 100, 2363-2368.
- XIE, D., YIN, S., OU, Y., BAI, H., DING, F., WANG, X., LIU, Z., ZHOU, C. and WU, M. 2002. Arsenic trioxide (As<sub>2</sub>O<sub>3</sub>) induced apoptosis and its mechanisms in human esophageal squamous carcinoma cell line. *Chinese Medical Journal*, 115, 280-285.
- XU, L., ZHU, J., HU, X., ZHU, H., KIM, H., LABAER, J., GOLDBERG, A. and YUAN, J. 2007. c-IAP1 Cooperates with Myc by Acting as a Ubiquitin Ligase for Mad1. *Molecular Cell*, 28, 914-922.

- YAMADA, H., SHINMURA, K., OKUDELA, K., GOTO, M., SUZUKI, M., KURIKI, K., TSUNEYOSHI, T. and SUGIMURA, H. 2007. Identification and characterization of a novel germ line p53 mutation in familial gastric cancer in the Japanese population. *Carcinogenesis*, 28, 2013-2018.
- YAMAKOSHI, Y., LU, Y., HU, J., KIM, J., IWATA, T., KOBAYASHI, K., NAGANO, T., YAMAKOSHI, F., HU, Y. and FUKAE, M. 2008. Porcine dentin sialophosphoprotein: length polymorphisms, glycosylation, phosphorylation, and stability. *Journal of Biological Chemistry*, 283, 14835.
- YAN, H., WANG, Y. C., LI, D., WANG, Y., LIU, W., WU, Y. L. and CHEN, G. Q. 2007. Arsenic trioxide and proteasome inhibitor bortezomib synergistically induce apoptosis in leukemic cells: the role of protein kinase Cdelta. *Leukemia*, 21, 1488-95.
- YANG, S., ZHOU, Q. and YANG, X. 2007. Caspase-3 status is a determinant of the differential responses to genistein between MDA-MB-231 and MCF-7 breast cancer cells. *Biochimica et Biophysica Acta*, 1773, 903-911.
- YANG, W. and EL-DEIRY, W. 2007. CARPs are E3 ligases that target apical caspases and p53. *Cancer biology & therapy*, 6, 1676-1683.
- YEN, L., CAO, Z., WU, X., INGALLA, E., BARON, C., YOUNG, L., GREGG, J., CARDIFF, R., BOROWSKY, A. and SWEENEY, C. 2006. Loss of Nrdp1 Enhances ErbB2/ErbB3-Dependent Breast Tumor Cell Growth. *Cancer research*, 66, 11279-11286.
- YODA, A., TOYOSHIMA, K., WATANABE, Y., ONISHI, N., HAZAKA, Y., TSUKUDA, Y., TSUKADA, J., KONDO, T., TANAKA, Y. and MINAMI, Y. 2008. Arsenic trioxide augments Chk2/p53-mediated apoptosis by inhibiting oncogenic Wip1 phosphatase. *J Biol Chem*, 283, 18969-79.
- YOSHIDA, S., KAJITANI, N., SATSUKA, A., NAKAMURA, H. and SAKAI, H. 2008. Ras modifies proliferation and invasiveness of cells expressing human papillomavirus oncogenes. *J Virol*, 82, 8820-8827.
- YOSHITAKE, Y., NAKATSURA, T., MONJI, M., SENJU, S., MATSUYOSHI, H., TSUKAMOTO, H., HOSAKA, S., KOMORI, H., FUKUMA, D. and IKUTA, Y. 2004. Proliferation potential-related protein, an ideal esophageal cancer antigen for immunotherapy, identified using complementary DNA microarray analysis. *Clinical Cancer Research*, 10, 6437.
- YU, L., WU, W., LI, Z., WONG, H., TAI, E., LI, H., WU, Y. and CHO, C. 2008. E series of prostaglandin receptor 2-mediated activation of extracellular signal-regulated kinase/activator protein-1 signaling is required for the mitogenic action of prostaglandin E2 in esophageal squamous-cell carcinoma. *Journal of Pharmacology and Experimental Therapeutics*, 327, 258.
- YU, Y., YIP, G., TAN, P., THIKE, A., MATSUMOTO, K., TSUJIMOTO, M. and BAY, B. 2010. Y-box binding protein 1 is up-regulated in proliferative breast cancer and its inhibition deregulates the cell cycle. *International journal of oncology*, 37, 483.
- YUAN, L., YU, W., XU, M. and QU, C. 2005. SHP-2 phosphatase regulates DNA damage-induced apoptosis and G2/M arrest in catalytically

- dependent and independent manners, respectively. *Journal of Biological Chemistry*, 280, 42701.
- YUN, H., YOO, H., SHIN, D., HONG, S., KIM, J., CHO, C. and CHOI, Y. 2009. Apoptosis Induction of Human Lung Carcinoma Cells by Chan Su (Venenum Bufonis) Through Activation of Caspases. *Journal of Acupuncture and Meridian Studies*, 2, 210-217.
- ZAIDMAN, B.-Z., WASSER, S. P., NEVO, E. and MAHAJNA, J. 2007. Androgen receptor-dependent and -independent mechanisms mediate Ganoderma lucidum activities in LNCaP prostate cancer cells. *International journal of oncology*, 31, 959-67.
- ZANG, T., CAO, E., LI, J., MA, W. and QIN, J. 1999. Induction of Apoptosis and Inhibition of Gastric Cancer MGC-803 Cell Growth by Arsenic Trioxide. *European Journal of Cancer*, 35, 1258-1263.
- ZHANG, H. Y., DU, Z. X., LIU, B. Q., GAO, Y. Y., MENG, X., GUAN, Y., DENG, W. W. and WANG, H. Q. 2009a. Tunicamycin enhances TRAIL-induced apoptosis by inhibition of cyclin D1 and the subsequent downregulation of survivin. *Exp Mol Med*, 41, 362-9.
- ZHANG, J., GHIO, A., CHANG, W., KAMDAR, O., ROSEN, G. and UPADHYAY, D. 2007. Bim mediates mitochondria-regulated particulate matter-induced apoptosis in alveolar epithelial cells. *FEBS Letters*, 581, 4148-4152.
- ZHANG, P., SU, D.-M., LIANG, M. and FU, J. 2008. Chemoprevention agents induce programmed death-1 ligand-1 (PD-L1) surface expression in breast cancer cells and promote PD-L1-mediated T cell apoptosis. *Molecular Immunology*, 45, 1470-1476.
- ZHANG, S. X., GARCIA-GRAS, E., WYCUFF, D. R., MARRIOT, S. J., KADEER, N., YU, W., OLSON, E. N., GARRY, D. J., PARMACEK, M. S. and SCHWARTZ, R. J. 2005a. Identification of direct serum-response factor gene targets during Me2SO-induced P19 cardiac cell differentiation. *J Biol Chem*, 280, 19115-26.
- ZHANG, W., LI, J., KANGINAKUDRU, S., ZHAO, W., YU, X. and CHEN, J. J. 2010a. The human papillomavirus type 58 E7 oncoprotein modulates cell cycle regulatory proteins and abrogates cell cycle checkpoints. *Virology*, 397, 139-44.
- ZHANG, X., LIN, L., GUO, H., YANG, J., JONES, S., JOCHEMSEN, A. and LU, X. 2009b. Phosphorylation and Degradation of MdmX Is Inhibited by Wip1 Phosphatase in the DNA Damage Response. *Cancer Research*, 69, 7960.
- ZHANG, Y., HAN, T., ZHU, Q., ZHANG, W., BAO, W., FU, H., YANG, J., HUANG, X., WEI, J. and MENG, Y. 2009c. The proapoptotic activity of C-terminal domain of apoptosis-inducing factor (AIF) is separated from its N-terminal. *Biological Research*, 42, 249-260.
- ZHANG, Y., SHI, Y., LI, X., DU, W., LUO, G., GOU, Y., WANG, X., GUO, X., LIU, J. and DING, J. 2010b. Inhibition of the p53-MDM2 interaction by adenovirus delivery of ribosomal protein L23 stabilizes p53 and induces cell cycle arrest and apoptosis in gastric cancer. *The Journal of Gene Medicine*, 22, 147-156.

- ZHANG, Z., WANG, H., LI, M., RAYBURN, E. R., AGRAWAL, S. and ZHANG, R. W. 2005b. Stabilization of E2F1 protein by MDM2 through the E2F1 ubiquitination pathway. *Oncogene*, 24, 7238-7247.
- ZHANG, Z. and ZHANG, R. 2008. Proteasome activator PA28 regulates p53 by enhancing its MDM2-mediated degradation. *The EMBO journal*, 27, 852-864.
- ZHAO, D., ZHENG, H., ZHOU, Z. and CHEN, C. 2010. The Fbw7 Tumor Suppressor Targets KLF5 for Ubiquitin-Mediated Degradation and Suppresses Breast Cell Proliferation. *Cancer research*, 70, 4728.
- ZHAO, J., ZHOU, Q., WIEDMER, T. and SIMS, P. J. 1998. Level of expression of phospholipid scramblase regulates induced movement of phosphatidylserine to the cell surface. *J Biol Chem*, 273, 6603-6.
- ZHAO, S., ZHANG, J., ZHANG, X., DONG, X. and SUN, X. 2008. Arsenic trioxide induces different gene expression profiles of genes related to growth and apoptosis in glioma cells dependent on the p53 status. *Mol Biol Rep*, 35, 421-429.
- ZHOU, J., YE, J., ZHAO, X., LI, A. and ZHOU, J. 2008. JWA is required for arsenic trioxide induced apoptosis in HeLa and MCF-7 cells via oxygen species and mitochondria linked signal pathway. *Toxicology and Applied Pharmacology*, 230, 33-40.
- ZHOU, M., FOY, R., CHITALIA, V., ZHAO, J., PANCHENKO, M., WANG, H. and COHEN, H. 2005. Jade-1, a candidate renal tumor suppressor that promotes apoptosis. *Proceedings of the National Academy of Sciences*, 102, 11035-11040.
- ZHOU, R., WEN, H. and AO, S. 1999. Identification of a novel gene encoding a p53-associated protein. *Gene*, 235, 93-101.
- ZHOU, R., ZHANG, L. Z. and WANG, R. Z. 2010. Effect of celecoxib on proliferation, apoptosis, and survivin expression in human glioma cell line U251. 29, 294-299.
- ZHU, Q., WANI, G., YAO, J., PATNAIK, S., WANG, Q., EL-MAHDY, M., PRAETORIUS-IBBA, M. and WANI, A. 2007. The ubiquitin-proteasome system regulates p53-mediated transcription at p21waf1 promoter. *Oncogene*, 26, 4199-4208.
- ZHU, Z., LUO, Z., LI, Y., NI, C., LI, H. and ZHU, M. 2009. Human inhibitor of growth 1 inhibits hepatoma cell growth and influences p53 stability in a variant-dependent manner. *Hepatology*, 49, 504-12.
- ZIEGLER, D. S., WRIGHT, R. D., KESARI, S., LEMIEUX, M. E., TRAN, M. A., JAIN, M., ZAWEL, L. and KUNG, A. L. 2008. Resistance of human glioblastoma multiforme cells to growth factor inhibitors is overcome by blockade of inhibitor of apoptosis proteins. *Journal of Clinical Investigation*, 118, 3109-3122.
- ZUO, Z., ZHAO, M., LIU, J., GAO, G. and WU, X. 2006. Functional Analysis of Bladder Cancer-Related Protein Gene: A Putative Cervical Cancer Tumor Suppressor Gene in Cervical Carcinoma. *Tumor Biol*, 27, 221-226.

## Appendices

---

### Appendix A: Stock solutions recipes

**Note:** The working solutions were diluted down to the desired concentrations with DEPC-treated water or sterile distilled water. It was stated when a different solvent was used.

**10x TBE:** 0.9 M Tris, 0.89 M boric acid and 25 mM EDTA, pH 8.3. This stock solution was diluted 1/10 for the electrophoresis of agarose and polyacrylamide gels.

**10x TE:** 100 mM Tris-HCl (pH 7.5); 10 mM EDTA

**4x Stacking gel Buffer:** 0.5 M Tris-HCl, pH 6.8

**10x SDS Electrophoresis buffer:** 250 mM Tris, 10 % SDS and 1.92 M glycine, pH 8.3

**6x Glycerol BPB Gel-loading Buffer:** 30 % glycerol, 0.3 % Bromophenol blue and 0.3 % Xylene cyanol.

**12x Separating gel Buffer:** 1.5 M Tris-HCl, pH 8.8.

**10x MOPS:** 200 mM 3-[N-morpholinol] propane sulphuric acid (MOPS), 50 mM sodium acetate, 10 mM EDTA.

**0.5% Acetic Anhydride:** Dilute to 5% using 100 mM Tris pH 7.5, just before use.

**Ammonium persulphate:** A 10 % stock solution was prepared in deionised water. This solution was stored at 4 C.

**Ampicillin:** A 100 mg/ml stock solution was prepared in 70% ethanol and filter-sterilised using a 0.22 micron filter and stored at -20°C.

**Camptothecin Stock Solution:** A  $14.35 \times 10^3$   $\mu$ M stock solution was prepared in DMSO; filter-sterilized and stored at -20 °C in aliquots (0.5 ml).

**Coomassie Staining Solution:** 0.25% Coomassie Brilliant Blue R 250, 45 % methanol and 5 % acetic acid.

**0.1% v/v DEPC treated water:** Diethylpyrocarbonate (DEPC) was diluted in a litre of dH<sub>2</sub>O and incubated at 37°C with shaking and then autoclaved.

**Destaining Solution:** 30 % methanol and 10 % acetic acid in dH<sub>2</sub>O.

**DTT (Dithiothreitol):** A 1 M stock solution was prepared in 0.001 M Sodium acetate, pH 5.2. This solution was sterilised by filtration (0.22 $\mu$ m filter), aliquoted and stored at -20 °C.

**40% Dextran (w/v):** Dextran sulphate sodium salt was dissolved in DEPC water by heating in a 68°C water bath for 3-four hrs. This was filtered (0.2 $\mu$ M) and aliquoted and stored at 4°C.

**2D Equilibration Buffer:** 6 M Urea, 2% SDS, 0.05 M Tris pH 8.8 and 20% glycerol.

**Hybridisation buffer (ISH):** 2 X SSC, 10% Dextran, 0.2% SDS, 50% formamide and up to a required volume with DEPC water. Store as aliquots at -20°C.

**IPTG:** A 1 M stock solution was prepared in sterile deionised water. The solution was further sterilised by filtration; stored in aliquots at - 20 °C.

**Luria Broth:** 10 g/l Tryptone, 5 g/l Yeast extract and 5 g/l NaCl and 2 g/l glucose in distilled water.

**Lysis Buffer:** PBS containing 1 % Triton X-100 and protease inhibitor cocktail tablet (Roche Diagnostics, Germany).

**PBS, pH 7.4:** 137 mM NaCl, 2.7 mM KCl, 8 mM Na<sub>2</sub>HPO<sub>4</sub> and 1.5 mM KH<sub>2</sub>PO<sub>4</sub>, pH 7.4.

**PCR reaction buffer:** 50 mM Tris-HCL (pH 9.0), 50 mM NaCl and 5 mM MgCl<sub>2</sub>.

**0.2 M Phosphate buffer:** 23 mM Na<sub>2</sub>HPO<sub>4</sub> and 77 mM NaH<sub>2</sub>PO<sub>4</sub> in DEPC treated water.

**PI Master Mix:** 100 µg/ml RNase, 40 µg/ml propidium iodide in PBS.

**PMSF:** A 10 mM stock solution was prepared in isopropanol. The solution was aliquoted and stored at -20 °C.

**Propidium Iodide staining solution:** 1 mg/ml in 3.8 mM sodium citrate.

**Protein Elution Buffer:** 10 mM glutathione and 50 mM Tris-HCl, pH 8.0.

**10 mg/ml Proteinase K:** 10 mg Proteinase K was dissolved in DEPC treated water and stored in 100 µl aliquots.

**RIPA Buffer:** 50 mM Tris pH 7.4, 150 mM NaCl, 1 tablet of total protease inhibitors (Roche Diagnostics, Germany), 1% Triton X-100, 1% Sodium deoxycholate.

**2X Sample buffer:** 100 mM Tris pH 6.8, 25% glycerol, 2% SDS, 0.01% Bromophenol blue and 10 mM DTT.

**20x SSC:** 3 M NaCl and 0.3 M Tri-sodium Citrate in DEPC treated water. Adjust to pH 7.0 with HCl and autoclave.

**Staurosporine:** A 2 mM concentration was made in DMSO

**TBS:** 20 mM Tris-HCl and 150 mM NaCl, pH 7.4.

**TBS-MT:** 5% Low fat dried milk powder and 0.1% Tween 20 in TBS.

**TBS-T:** 0.1% Tween 20 in TBS.

**Tfb1 Buffer:** 30 mM Potassium acetate, 50 mM MnCl<sub>2</sub>, 0.1 M KCl, 6.7 mM CaCl<sub>2</sub> and 15% glycerol (v/v).

**Tfb2 Buffer:** 9 mM MOPS, 50 mM CaCl<sub>2</sub>, 10 mM KCl and 15% glycerol (v/v).

**Transfer Buffer:** 25 mM Tris, 192 mM glycine and 20 % methanol.

**TYM Broth:** 20 g/l Tryptone, 5 g/l Yeast extract 3.5 g/l NaCl and 2g / MgCl<sub>2</sub>

**Urea extraction buffer:** 9 M Urea, 2 M ThioUrea, 4% CHAPS.

## Appendix A2: Reagents

## Chemicals and suppliers

Absolute ethanol	Merck KGaA, Darmstadt, Germany
Acetic Anhydride	Reidel-de Haen, Seelze (Hanover), Germany
40% 37.5:1 Acrylamide:bis-acrylamide	BioRAD, Hercules CA, USA
Agarose	Promega, San Luis CA, USA
Ammonium persulphate	Merck KGaA, Darmstadt, Germany
Ampicillin	Fermentas, Maryland, USA
Bacteriological agar	Merck KGaA, Darmstadt, Germany
Boric acid	Merck KGaA, Darmstadt, Germany
Bovine serum albumin V	Roche, Mannheim, Germany
Bromophenol blue	Sigma, Munich, Germany
Camptothecin	Merck KGaA, Darmstadt, Germany
Chloroform	Merck KGaA, Darmstadt, Germany
Coomassie Brilliant Blue R 250	Sigma, Munich, Germany
DAPI (4', 6'-diamidino-2-phenylindole)	Sigma, Munich, Germany
DMSO (Dimethyl sulphoxide)	Sigma, Munich, Germany
Diethylpyrocarbonate	Sigma, Munich, Germany
DTT (Dithiothreitol)	Sigma, Munich, Germany
EDTA (Ethylene diamine tetra acetic acid)	Merck KGaA, Darmstadt, Germany
Entellan	Merck KGaA, Darmstadt, Germany
Ethidium bromide	Sigma, Munich, Germany
Glacial acetic acid	Merck KGaA, Darmstadt, Germany
Glucose	Merck KGaA, Darmstadt, Germany
Glycine	Sigma, Munich, Germany
Hydrochloric acid	Merck KGaA, Darmstadt, Germany
IPTG (Isopropyl $\beta$ -D-thiogalactopyranoside)	Fermentas, Maryland, USA
Methanol	Merck KGaA, Darmstadt, Germany
MOPS (4-Morpholine propanesulphonic acid)	Sigma, Munich, Germany
Paraformaldehyde	Sigma, Munich, Germany
PMSF (phenylmethylsulphonyl fluoride)	Roche, Mannheim, Germany
Poncheau S	Sigma, Munich, Germany
Premixed Protein marker	Fermentas, Maryland, USA
Proteinase K	Roche, Mannheim, Germany
PVDF (Polyvinylidene difluoride)membrane	Roche, Mannheim, Germany
SDS (Sodium dodecyl sulphate)	Sigma, Munich, Germany
Sodium hydroxide	Merck KGaA, Darmstadt, Germany
Staurosporine	Roche, Mannheim, Germany
TEMED ( <i>N, N, N', N'</i> -Tetra methylethylene-diamine)	Promega, San Luis CA, USA
Tris (Tris[hydroxymethyl] aminoethane)	Merck KGaA, Darmstadt, Germany
Tri-sodium Citrate	B&M Scientific cc., SA
Triton X-100 (iso-octylphenoxy-poly-ethoxyethanol)	Sigma, Munich, Germany
Trypsin	Invitrogen, Paisley, UK
Tryptone	Sigma, Munich, Germany
Tween 20 (Polyoxyethylene [20] sorbitan)	Sigma, Munich, Germany
Urea	Merck KGaA, Darmstadt, Germany
Xylene	Merck KGaA, Darmstadt, Germany
Xylene Cyanol	BDH, Leicestershire, UK

**Appendix A3: Equipment**

<b>Equipment</b>	<b>Manufacturer</b>
<b>Power Pac HC 300W</b>	<b>BioRAD, Hercules CA, USA</b>
<b>MiniOpticon</b>	<b>BioRAD, Hercules CA, USA</b>
<b>LightCycler 1.5</b>	<b>Roche, Mannheim, Germany</b>
<b>Thermocycler 2700</b>	<b>Applied Biosystems, Foster City CA, USA</b>
<b>Beckon Dickson Flow Cytometer</b>	<b>BD, Oxford, UK</b>
<b>Lab Rotator</b>	<b>Digisystems Laboratory Instruments Inc., Taipei Hsien, Taiwan</b>
<b>Labotec Laminar Flow</b>	<b>Labotec, Midrand, South Africa</b>
<b>Forma Range CO<sub>2</sub> Incubator</b>	<b>Forma Scientific, Marietta OH, USA</b>
<b>Thermo Fisher Incubator Shaker</b>	<b>Thermo Fisher Scientific Inc., Asheville NC, USA</b>
<b>NanoDrop ND1000</b>	<b>NanoDrop technologies, Wilmington DE, USA</b>
<b>BioRAD Gel Doc XR system</b>	<b>BioRAD, Hercules CA, USA</b>
<b>Eppendorf 5415D microfuge</b>	<b>Eppendorf, Cambridge, UK</b>
<b>Axio Scope Microscope</b>	<b>Carl Zeiss, Munich, Germany</b>
<b>Hybaid OmnSlide Flat Block</b>	<b>Hybaid Ltd., Cambridge, UK</b>
<b>IEF Focusing Machine</b>	<b>BioRAD, Hercules CA, USA</b>

**Appendix B: Ethics clearance certificate**

**UNIVERSITY OF THE WITWATERSRAND, JOHANNESBURG**

Division of the Deputy Registrar (Research)

**HUMAN RESEARCH ETHICS COMMITTEE (MEDICAL)**

R14/49 Mbita

**CLEARANCE CERTIFICATE**

**PROTOCOL NUMBER M040531**

**PROJECT**  
cancers

Molecular analysis of the DWNN gene in human

**INVESTIGATORS**

Mr Z Mbita

**DEPARTMENT**

Genetics & Dev. biology

**DATE CONSIDERED**

04.05.28

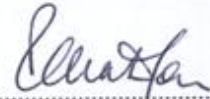
**DECISION OF THE COMMITTEE\***

Approved unconditionally

**Unless otherwise specified this ethical clearance is valid for 5 years and may be renewed upon application.**

**DATE** 04.06.25

**CHAIRPERSON** .....



(Professor PE Cleaton-Jones)

\*Guidelines for written 'informed consent' attached where applicable

cc: Supervisor : Dr Z Dlamini

---

---

**DECLARATION OF INVESTIGATOR(S)**

To be completed in duplicate and **ONE COPY** returned to the Secretary at Room 10005, 10th Floor, Senate House, University.

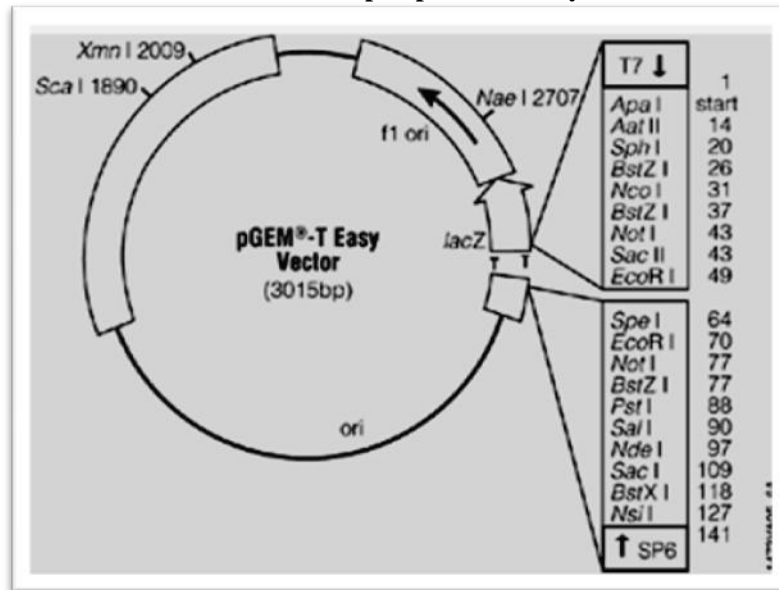
I/We fully understand the conditions under which I am/we are authorized to carry out the abovementioned research and I/we guarantee to ensure compliance with these conditions. Should any departure to be contemplated from the research procedure as approved I/we undertake to resubmit the protocol to the Committee. **I agree to a completion of a yearly progress report.**

PLEASE QUOTE THE PROTOCOL NUMBER IN ALL ENQUIRIES

Appendix C, primer sets 1-6: Different primer sets, sequences, product sizes and pGEM T Easy vector

PRIMER SETS		PRIMER SEQUENCES	AMPLICON	PRODUCT SIZE
1	Iso3 Forward: Iso3 Reverse or RT-RBBP6 F RT-RBBP6 R	5'GGTCCTTCGGTGTCTTTG 3' 5'AGGTGACGGTATCATAGTTG 3' 5'GCATTATCATCAGTATATTCTTCTTTTCG 3' 5' GGCTCCACATCTCCCTCTG 3'	DWNN Fragment	128 bp 200 bp
2	Iso2&1 Forward Iso2&1 Reverse	5TTGGACCGTCTGAATGAAC 3' 5'TGGAAC TTGAATACTCTCTGG 3'	RBBP6 Transcripts 1 and 2 fragments	200bp
3	RING F RING R	5GCTGGATCCCCTCCCTTCTTACCAGAG 3' 5GCTCTCGAGTCATTACTGTTTTTCGTAGTCTTTTTG 3'	RBBP6 RING FINGER	300bp
4	RbBD F RbBD R	5'GAGGCGGGATCCACAGGTGTTGAAGAAAATAAACAGAC 3' 5GAGGCGCTCGAGTTATCATTTGACATCTTTGGAATAGTCCTTCTT 3'	RBBP6 RbBD	500bp
5	ABI F ABI R	5GAGGCGGGATCCAGCACTCAGCCAGAGAAAGAGAGT 3' 5GAGGCGCTCGAGTTATCAGCTGTCCTGACTTTCTGCTGAGCT 3'	RBBP6 p53BD	914bp
6	Fc primer Rc primer	5'CTGCGTTATCCCCTGATTCTGTG 3' 5' GTAACGCGGAACTCCATATGG 3'	RNAi Vector primers	517bp
7	hHPRT1 F hHPRT1 R	5'TGACACTGGCAAAACAATGCA 3' 5'GGTCCTTTTACCAGCAAGCT 3'	Housekeeping gene primers	200bp

Vector map 1: pGEM-T Easy



**pGEM-T Easy vector:** This pGEM-T Easy vector map shows the different restriction endonucleases cut/digest sites in the pGEM-T Easy multiple cloning sites (MCS). This vector was used for the insertion/cloning of PCR products of the RBBP6 domains for sequencing. This vector map was obtained from Promega, USA, ([www.promega.com](http://www.promega.com)).

## Appendix D: A table showing different RBBP6 RNAi oligos, annealing of oligos and RNAi vector

Table 1: RBBP6 RNAi oligos

Oligos	Oligo sequence
Rb1AF	<i>Bgl</i> II 5' <u>GAT</u> CCCTCAAGACTTGGTTCAACACGTTCAAGAGACGTGTTGAACCAGATCTTGATTTTTGG AAA 3'
Rb1AR	<i>Hind</i> III 5' <u>AGC</u> TTTTCCAAAAA TCAAGATCTGGTTCAACACGTCCTTGAACGTGTTGAACCAGATCTTGAGGG 3'
Rb1BF	<i>Bgl</i> II 5' <u>GAT</u> CCCTCTCCCTATAGTGGTTCTTCGTATTCAAGAGATACGAAGAACCAGTATAGGGAGATTTTTGGAAA 3'
Rb1BR	<i>Hind</i> III 5' <u>AGC</u> TTTTCCAAAAA TCTCCCTATAGTGGTTCTTCGTATCTTGAATACGAAGAACCAGTATAGGGAGAGGG 3'
Rb3AF	<i>Bgl</i> II 5' <u>GAT</u> CCC CTC TCA CAC TTT TTC TAC ACA TTG CTT CAA GAG AGC AAT GTG TAG AAA AAG TGT GAG ATT TTT GGA AA 3'
Rb3AR	<i>Hind</i> III 5' <u>AGC</u> TTT TCC AAA AAT CTC ACA CTT TTT CTA CAC ATT GCT CTC TTGAAG CAA TGT GTA GAA AAA GTG TGA GAG GG 3'

Table showing the different RBBP6 RNAi oligos where different regions are coloured with different colours, sense target sequence (red); loop region (blue) and antisense target sequence (green).

### RNAi oligo designing

RNAi oligos were designed using Ambion search engine:

[http://www.ambion.com/techlib/misc/siRNA\\_finder.html](http://www.ambion.com/techlib/misc/siRNA_finder.html). The following parameters were set when searching for the silencing fragments:

1. Standard start with two AA residues/nucleotides on the 5' end.  
Standard ends with two TT residues/nucleotides on the 3' end.
2. Length should be 19 to 25 bp
3. Avoid stretches of TT or AAs nucleotides longer than two.
4. GC content between 30 and 70% (Preferably between 40 and 60)
5. Choose 3 or more targets
6. Search for a pattern: AA-[N]<sub>19</sub>-TT.
7. Insert cloning restriction sites (*Hind* III and *Bgl* II were used).

The resultant hits were blasted against NCBI database:

(<http://blast.ncbi.nlm.nih.gov/Blast.cgi>) to confirm the targeted sequences.

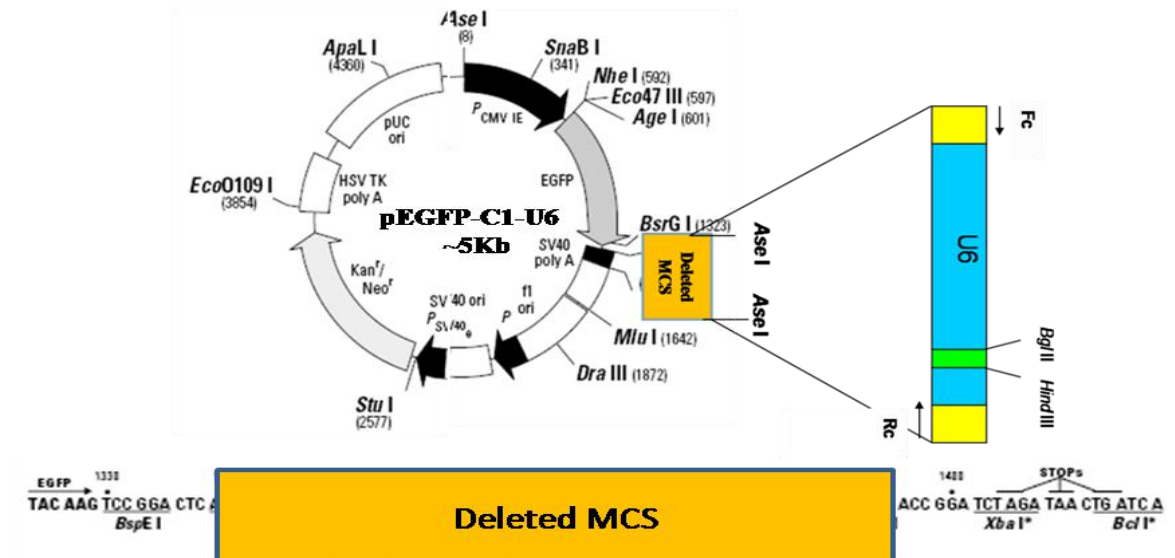
**Table 2: Cloning of the annealed RNAi oligos.**

Reaction component	Final Quantity
RNAi vector	10ng
RNAi annealed oligos	10pmol of each
2X Ligation buffer (Promega)	1X
T4 Ligase	3u

A summary of the steps required for the cloning of the annealed oligos.

**NOTE:** RNAi vector was pEGFP-C1-U6 vector as shown in vector map 2 below. The cloned RNAi constructs were sent for sequencing to Inqaba Biotech, Pretoria, and SA.

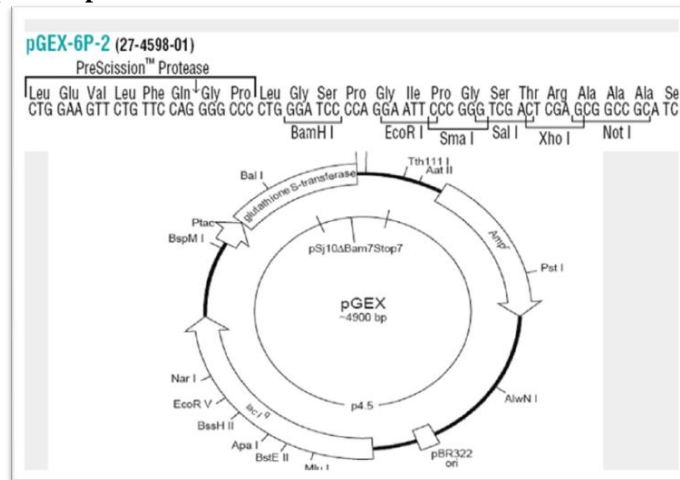
**Vector map 2: pEGFP-C1-U6 vector**



**pEGFP-C1-U6 vector:** The MCS was replaced with the U6 promoter containing with *Bgl* II and *Hind* III sites flanking a random a random sequence for cloning of the annealed RNAi oligos downstream the U6 promoter. The random sequence in-between the two cloning sites was used as a control. Fc/Rc primer sites are also available for colony PCR screening. This map was obtained from Pretorius *et al.* (2007).

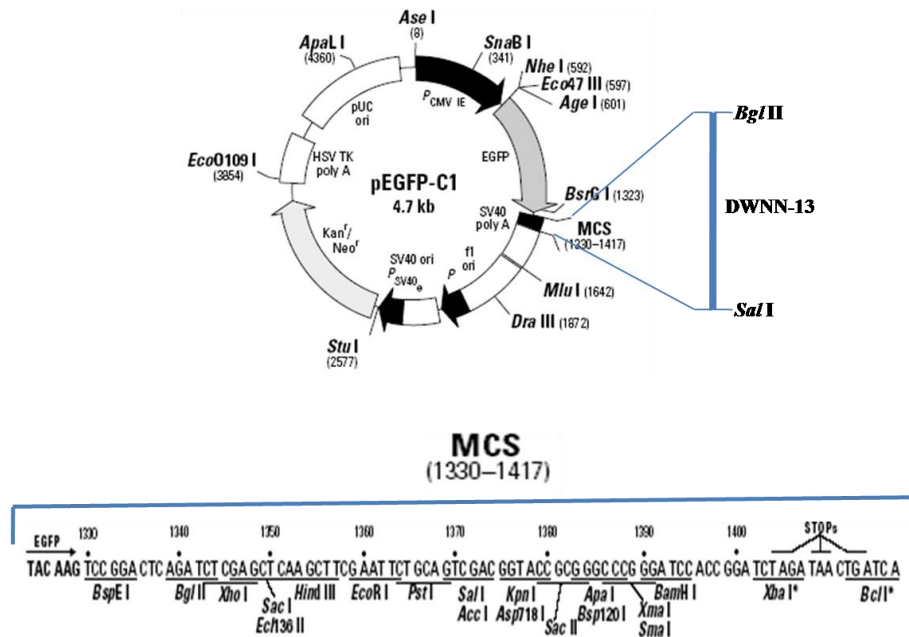
### Appendix E: Vector maps 3-5

#### Vector map 3: pGEX 6p-2 vector



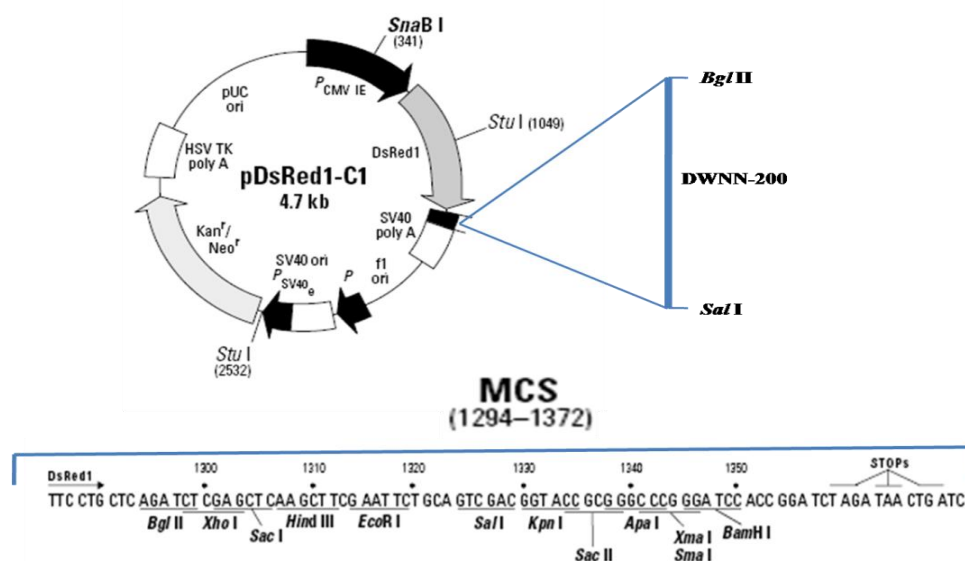
**pGEX 6p-2 vector:** The pGEX-6p-2 vector is characterized by its PreScission Protease recognition site for the cleavage of the GST tag from the fused protein fragment or domain. The multiple cloning sites facilitate the cloning of the fragment to be recombinantly expressed. This vector map was obtained from [www.gelifsciences.com](http://www.gelifsciences.com).

#### Vector map 4: pGFP-DWNN-13



**pGFP-DWNN-13:** This vector shows a DWNN-13 fragment cloned between *Bgl* II and *Sal* I sites in the multiple cloning sites of the pGFP-C1 vector. This expression is under the CMV promoter that is downstream of the GFP. This vector map is a modification of a map obtained from [www.clontech.com](http://www.clontech.com).

Vector map 5: pDsRed1-C1-DWNN-200



**pDsRed1-C1-DWNN-200:** This figure shows the DWNN-200/RBBP6 isoform 1 cloned between the *Bgl* II and *Sal* I sites of the MCS and the expression is driven by a CMV promoter. DWNN-200 is RBBP6 isoform 1 and not 2. This vector map is a modification of a map obtained from [www.clontech.com](http://www.clontech.com).

#### Appendix F: Supporting tables

**Table 3: Template preparation for reverse transcription.**

Total RNA	1 µg
Oligo dT <sub>15</sub>	0.5 µg
Nuclease free H <sub>2</sub> O	Up to 5 µl
<b>Final reaction volume</b>	<b>5 µl</b>

**Table 4: Cocktail of the reverse transcription (RT) mix.**

	Volume	Final concentration
5x Improm II reaction buffer	4 µl	1x
Magnesium chloride (25 mM)	5 µl	5 mM
dNTP mix	1 µl	0.5 mM each dNTP
Recombinant RNAsin (40 u/µl)	0.5 µl	20 u
Nuclease free water	-	Up to 15 µl
Improm II Reverse transcriptase (1 u/µl)	1.0 µl	1 u
<b>Final Volume</b>	<b>15 µl</b>	

**Table 5: Cocktail for Polymerase Chain Reaction.**

Reagent	Volume	Final Conc.
Master Mix (2X) Promega, USA	12.5 µl	1X
Forward primer (10 pmoles)	1.0 µl	0.4 pmoles
Reverse primer (10 pmoles)	1.0 µl	0.4 pmoles
MgCl <sub>2</sub> (25 mM)	2.0 µl	2 mM
Nuclease free water	7.5 µl	-
Template DNA/colony mix	1.0 µl	-
<b>Total Volume</b>	<b>25.0 µl</b>	-

**Table 6: Restriction digestion for *EcoR*I, *Pst* I and *Apa*I.**

Components	<i>EcoR</i> I digest	<i>Pst</i> I digest	<i>Apa</i> I digest	Final concentration
pGEM-T-Easy plasmid (50 ng/µl)	10.0 µl	10.0 µl	10.0 µl	500 ng
Buffer B 10X	5.0 µl	5.0 µl	5.0 µl	
<i>EcoR</i> I (3u/ µl)	1.0 µl			1 u
<i>Pst</i> (3u/ µl)		1.0 µl		1 u
<i>Apa</i> I (3u/ µl)			1.0 µl	1 u
Sterile distilled Water	34 µl	34 µl	34 µl	-
<b>Total volume</b>	<b>50 µl</b>	<b>50 µl</b>	<b>50 µl</b>	-

**Table 7: Real-time PCR setup.**

Component	Quantity	Final Concentration
Sybr Green (5X)	2 µl	1X
Forward primer (10 pmoles)	0.5 µl	0.5 pmoles
Reverse primer (10 pmoles)	0.5 µl	1-5 pmoles
sdH <sub>2</sub> O	5 µl	Up to 10 µl
cDNA (1 µg)	2 µl	200 ng
<b>Final reaction volume</b>	<b>10 µl</b>	-

**Table 8: Typical real-time conditions.**

Analysis Mode	Cycles	Segment	Target Temperature <sup>1)</sup>	Hold Time	Acquisition Mode
<b>Pre-Incubation</b>					
None	1		95°C	10 min <sup>4)</sup>	none
<b>Amplification</b>					
Quantification	45	Denaturation	95°C	10 s	none
		Annealing	primer dependent <sup>2)</sup>	0 - 10 s <sup>5)</sup>	none
		Extension	72°C <sup>3)</sup>	= (amplicon [bp]/25) s <sup>6)</sup>	single
<b>Melting Curve</b>					
Melting Curves	1	Denaturation	95°C	0 s	none
		Annealing	65°C	15 s	none
		Melting	95°C slope = 0.1°C/sec <sup>1)</sup>	0 s	continuous
<b>Cooling</b>					
None	1		40°C	30 s	none

From [Roche](#) applied Science

**Table 9: Linearization of pGEM-T Easy-DWNN plasmid DNA.**

Components	Volume	Final concentrations
pGEM-T Easy-DWNN plasmid DNA (100 ng/μl)	10 μl	1 μg
Buffer O [Fermentas] (10X)	2 μl	1X
<i>Pst</i> I/ <i>Apa</i> I (10 u/μl)	2 μl	20 u
Sterile dH <sub>2</sub> O	16 μl	-
<b>Total Volume</b>	<b>30 μl</b>	-

**Table 10: PCR mix for DIG labelling.**

Reagents	Antisense RNA	Sense RNA	Control RNA	Final concentrations	
DWNN cDNA- <i>Pst</i> I/ <i>Apa</i> I digested (40 ng/μl).	25.0 μl	25.0 μl	-	1 μg	
Control DNA PSPT 18-Neo/PvuII (125 ng/μl)	-	-	8.0 μl	1 μg	
10X NTP labelling mix	4.0 μl	4.0 μl	4.0 μl	1X	
10X Transcription buffer	4.0 μl	4.0 μl	4.0 μl	1X	
T7 RNA polymerase 20 u/μl	2.0 μl	-	-	40 u	
Sp6 RNA polymerase 20 u/μl	-	2.0 μl	4.0 μl	40 u	80 u
DEPC-treated water	5 μl	5 μl	20.0 μl	-	
Total volume	40.0 μl	40.0 μl	40.0 μl	-	

**Table 11: Dilutions for the estimation of the probes.**

<b>Dilution</b>	<b>DIG-labelled cRNA</b>	<b>DIG labelled cRNA to control DNA-Pspt-18-Neo</b>	<b>DWNN probe (Antisense &amp; sense)</b>
Initial conc.	0.1 µg/µl	0.005 µg/µl	~ 0.2 µg/µl
Dilution 1	1:5 (0.02µg/µl)		1:10 (0.02 µg/µl)
Dilution 2	1:20 (0.001µg/µl)	1:5 (0.001 µg/µl)	1:20 (0.001 µg/µl)
Dilution 3	1:10 (0.0001 µg/µl)	1:10 (0.0001 µg/µl)	1:10 (0.0001 µg/µl)
Dilution 4	1:10 (0.00001 µg/µl)	1:10 (0.00001 µg/µl)	1:10 (0.00001 µg/µl)
Dilution 5	1:10 (0.000001 µg/µl)	1:10 (0.000001 µg/µl)	1:10 (0.000001 µg/µl)
Dilution 6	1:10 (0.0000001 µg/µl)	1:10 (0.0000001 µg/µl)	1:10 (0.0000001 µg/µl)
Dilution 7	1:10 (0.00000001 µg/µl)	1:10 (0.0000001 µg/µl)	1:10 (0.0000001 µg/µl)

**Table 12: Preparation of the transfection mix.**

<b>Tube 1</b>	<b>DNA Tube</b>	<b>DNA Tube</b>	<b>DNA Tube</b>	<b>DNA Tube</b>
Component	Rb1A	Rb1B	Rb3A	U6GFP
siRNA	2 µg	2 µg	2 µg	2 µg
1XPBS	Up to 100 µl			
<b>Tube 2</b>	<b>Transfection Reagent Tube</b>	<b>Transfection Reagent Tube</b>	<b>Transfection Reagent Tube</b>	<b>Transfection Reagent Tube</b>
Metafectene Pro	12 µl	12 µl	12 µl	12 µl
1XPBS	88 µl	88 µl	88 µl	88 µl

**NOTE:** The control included the RNAi vector with no insert and this was used to assess whether the GFP protein expression had an effect on the cells and additionally to monitor the GFP expression. Another control was Metafectene Pro without a DNA molecule to assess the toxicity of the transfection.

**Table 13: Preparation of protein standards for the Bradford Assay.**

[STD] $\mu\text{g}/\mu\text{l}$	Volume Stock Standard ( $\mu\text{l}$ ) 5 mg/ $\mu\text{l}$	Volume of the Extraction Buffer	0.1M HCL ( $\mu\text{l}$ )	dH <sub>2</sub> O ( $\mu\text{l}$ )
0	0	10	10	80
5	1	9	10	80
10	2	8	10	80
20	4	6	10	80
40	8	2	10	80
50	10	0	10	80

In each tube, 900  $\mu\text{l}$  of the Bradford Reagent was added and mixed well. The samples' concentrations were determined by preparing the sample reaction as tabulated in table 14. The samples were done in triplicates and the absorbance readings were taken using a spectrophotometer at 595nm. The mean value (of 3) was used to plot a standard curve on Microsoft excel 2007.

**Table 14: Sample preparation for a Bradford Assay.**

Volume of Sample ( $\mu\text{l}$ )	Volume of Extraction Buffer	0.1M HCL ( $\mu\text{l}$ )	dH <sub>2</sub> O ( $\mu\text{l}$ )	Bradford Reagent ( $\mu\text{l}$ )
5	5	10	80	900

The samples were also measured in a spectrophotometer at 595nm and the concentrations were extrapolated from the linear equation of the standard curve. The concentration obtained was  $\mu\text{g}/5\mu\text{l}$ ; therefore the value was divided by 5 to obtain the concentration in  $\mu\text{g}/\mu\text{l}$ .

## Appendix G: RBBP6 quantitative assessment of tissues on arrays

## Cybrdi Tissue Array (CC00-11-001)

Organ	Pathology Diagnosis	Sex	Age	Grade	Labelling intensity	Stromal staining
Oesophagus	Squamous cell carcinoma	M	62	III	+	Yes
Oesophagus	Squamous cell carcinoma	M	56	III	+	Yes
Oesophagus	Squamous cell carcinoma	M	48	III	+	Yes
Stomach	Inflammatory tissue	F	55	-	+	-
Stomach	Adenocarcinoma	M	57	III	-	Yes
Stomach	Adenocarcinoma	M	74	III	-	Yes
Colon	Adenocarcinoma	M	37	II	-	Yes
Colon	Adenocarcinoma	M	62	II	-	Yes
Colon	Adenocarcinoma	M	58	II	-	Yes
Oesophagus	Inflammatory tissue	M	62	-	++	-
Oesophagus	Normal tissue	F	72	-	+	-
Oesophagus	Inflammatory tissue	M	54	-	+	-
Stomach	Normal tissue	F	55	-	++	-
Stomach	Normal tissue	M	57	-	++	-
Stomach	Normal tissue	M	66	-	++	-
Colon	Normal tissue	F	56	-	++	-
Colon	Inflammatory tissue	M	62	-	++	-
Colon	Inflammatory tissue	M	58	-	++	-
Rectum	Adenocarcinoma	M	55	I	-	Yes
Rectum	Adenocarcinoma	M	67	I	-	Yes
Rectum	Adenocarcinoma	F	55	I	-	Yes
Liver	Hepatocellular carcinoma	F	32	II	+	Yes
Liver	Hepatocellular carcinoma	M	39	II	+	Yes
Liver	Hepatocellular carcinoma	F	55	II	+	Yes
Lung	Squamous cell carcinoma	M	66	II	++	Yes
Lung	Squamous cell carcinoma	F	59	II	++	Yes
Lung	Squamous cell carcinoma	M	55	II	++	Yes
Colon	Normal tissue	M	68	-	+++	-
Rectum	Normal tissue	F	58	-	+++	-
Rectum	Fatty tissue	M	67	-	+++	-
Liver	Liver fatty degeneration	M	63	-	+	-
Liver	Inflammatory tissue	F	66	-	+	-
Liver	Inflammatory tissue	M	48	-	+	-
Lung	Normal tissue	F	69	-	+++	-
Lung	Normal tissue	F	43	-	+++	-
Lung	Normal tissue	M	65	-	+++	-
Kidney	Transitional cell carcinoma	M	72	I	++	-
Kidney	Transitional cell	M	50	I	++	-

	carcinoma					
Kidney	Transitional cell carcinoma	M	54	I	++	-
Breast	Adenosis	F	29	-	+	Yes
Breast	Infiltrating duct carcinoma	F	45	-	+	Yes
Breast	Infiltrating duct carcinoma	F	52	-	+	Yes
Uterine Cervix	Transitional cell carcinoma	F	76	-	++	Yes
Uterine Cervix	Transitional cell carcinoma	F	47	-	++	Yes
Uterine Cervix	Transitional cell carcinoma	F	42	-	++	Yes
Kidney	Normal tissue	M	54	-	++	-
Kidney	Normal tissue	F	61	-	++	-
Kidney	Normal tissue	F	47	-	++	-
Breast	Fibrofatty tissue	F	43	-	++	-
Breast	Normal tissue	F	39	-	++	-
Breast	Adenosis	F	54	-	+	-
Breast	Normal tissue	F	73	-	++	-
Breast	Normal tissue	F	50	-	++	-
Breast	Normal tissue	F	43	-	++	-
Ovary	Serous papillary adenocarcinoma	F	56	III	-	Yes
Ovary	Serous papillary adenocarcinoma	F	49	III	-	Yes
Ovary	Serous papillary adenocarcinoma	F	24	III	-	Yes
Ovary	Normal tissue	F	40	-	+	-
Ovary	Normal tissue	F	39	-	+	-
Ovary	Smooth muscle	F	31	-	+	-

**Biomax.us Tissue array (BC001111)**

<b>Organ</b>	<b>Pathology Diagnosis</b>	<b>Sex</b>	<b>Age</b>	<b>Grade</b>	<b>Labelling intensity</b>	<b>Stromal staining</b>
Oesophagus	Squamous cell carcinoma	M	62	II	++	Yes
Oesophagus	Squamous cell carcinoma	M	56	III	+	Yes
Oesophagus	Squamous cell carcinoma	F	72	-	++	Yes
Stomach	Adenocarcinoma	F	55	III	-	Yes
Stomach	Adenocarcinoma	M	56	II	+	Yes
Stomach	Adenocarcinoma	M	74	III	-	Yes
Colon	Adenocarcinoma	M	37	-	-	Yes
Colon	Adenocarcinoma	M	82	I	-	Yes
Colon	Adenocarcinoma	M	58	I	-	Yes
Oesophagus	Normal mucosa of the oesophagus	M	38	-	+	Yes
Oesophagus	Normal mucosa of the oesophagus	F	72	-	+	Yes
Oesophagus	Normal mucosa of the oesophagus	M	53	-	+	Yes
Stomach	Normal mucosa of the stomach	M	54	-	++	-
Stomach	Normal mucosa of the stomach	M	54	-	++	-
Stomach	Normal mucosa of the stomach	M	66	-	++	-
Colon	Normal mucosa of the colon	F	56	-	+++	-
Colon	Normal mucosa of the colon	M	62	-	+++	-
Colon	Normal mucosa of the colon	M	58	-	+++	-
Rectum	Adenocarcinoma	M	55	II	-	Yes
Rectum	Adenocarcinoma	M	67	II	-	Yes
Rectum	Adenocarcinoma	F	55	II	-	Yes
Liver	Hepatocellular carcinoma	F	32	II	+	
Liver	Hepatocellular carcinoma	M	39	III	-	Yes
Liver	Hepatocellular carcinoma	F	55	II	+	Yes
Lung	Squamous cell carcinoma	M	66	II	++	Yes
Lung	Squamous cell carcinoma	F	59	III	++	Yes
Lung	Chronic inflammation of lung	M	55	-	++	-
Rectum	Normal mucosa of the rectum	F	43	-	+++	-
Rectum	Normal mucosa of the rectum	M	33	-	+++	-
Rectum	Normal mucosa of the rectum	M	67	-	+++	-

Liver	Normal tissue	M	63	-	+	-
Liver	Normal tissue	F	66	-	+	-
Liver	Normal tissue	F	48	-	+	-
Kidney	Clear carcinoma cell	M	72	-	++	-
Kidney	Clear carcinoma cell	M	50	-	++	-
Kidney	Clear carcinoma cell	M	54	-	++	-
Breast	Intraductal carcinoma	F	29	-	+	Yes
Breast	Infiltrating carcinoma duct	F	45	-	+	Yes
Breast	Malignant fatty tissue	F	52	-	-	Yes
Uterine cervix	Squamous carcinoma cell	F	76	II	+	Yes
Uterine cervix	Squamous carcinoma cell	F	47	II	+	Yes
Uterine cervix	Squamous carcinoma cell	F	42	III	-	-
Kidney	Normal tissue	M	54	-	++	-
Kidney	Normal tissue	F	61	-	++	-
Kidney	Normal tissue	F	47	-	++	-
Breast	Normal tissue	F	43	-	++	-
Breast	Normal tissue	F	48	-	++	-
Breast	Normal tissue	F	41	-	++	-
Breast	Normal tissue	F	37	-	++	-
Breast	Normal tissue	F	50	-	++	-
Breast	Normal tissue	F	43	-	++	-
Ovary	Serous papillary adenocarcinoma	F	56	III	-	Yes
Ovary	Serous papillary adenocarcinoma	F	49	III	-	Yes
Ovary	Serous papillary adenocarcinoma	F	39	I	-	Yes
Ovary	Normal tissue	F	40	-	+	-
Ovary	Normal tissue	F	39	-	+	-
Ovary	Normal tissue	F	31	-	+	-

**Appendix H: Method schedules****Schedule 1: Plasmid DNA Miniprep (Promega kit)**

1. Grow a single colony containing a plasmid of interest in 6 ml LB overnight.
2. Collect the cells by centrifugation at 12 000 rpm for 5 min. Discard the supernatant.
3. Resuspend the cell pellet in 250 µl Resuspension Solution (Promega Corp., USA)
4. Lyse the cells in 250 µl Cell Lysis Solution (Promega Corp., USA) and mix by inverting the tube 4-5 times.
5. Add 10 µl Alkaline Phosphatase Solution (Promega Corp., USA), mix by inverting 4-5 times and incubate for 5 min at room temperature.
6. Add 350 µl Neutralization Solution (Promega Corp., USA) to precipitate chromosomal DNA and proteins. Mix by inverting 4-5 times.
7. Centrifuge at 9676 x g at room temperature for 10 min.
8. Decant the supernatant into a collection/collection tubes assemble and incubate for 1 min at room temperature.
9. Centrifuge at 9676 x g at room temperature for 1 min.
10. Discard the flow through and reassemble the column/collection tubes assemble.
11. Wash the column with 750 µl Wash Solution (Promega Corp., USA) and centrifuge at 9676 x g at room temperature for 1 min.
12. Repeat the wash with 250 µl Wash Solution (Promega Corp., USA) at 9676 x g for 2 min.
13. Transfer the column to a 1.5 ml micro-centrifuge tube.
14. Elute the plasmid DNA by adding 100 µl 1XTE and centrifuge at 11 709 x g for 1 min.
15. Store the DNA at -20°C for further use.

**Schedule 2: Immunohistochemical staining**

1. Dewax the tissue arrays in xylene for 20 min (2 changes of 10 min each) at room temperature.
2. Rehydrate the slides in 100% ethanol for 10 min (2 changes of 5 min each).
3. Quench endogenous peroxidases by immersing the tissue arrays in 100% methanol for 20 min at room temperature.
4. Rehydrate the slides in 95% ethanol for 8 min (2 changes of 4 min) at room temperature.
5. Rehydration in 70% ethanol at room temperature for 3 min.
6. Perform antigen retrieval in 0.1M Sodium citrate (pH 6.0) at 80°C for 2 min at a high microwave setting and for 5 min at a low microwave setting.
7. Wash the slides with 1XTBST1%BSA for 2 min at room temperature.
8. Block the endogenous peroxidases in TBST3%H <sub>2</sub> O <sub>2</sub> for 20 min at room temperature.
9. Wash the slides in TBST1%BSA for 2 min at room temperature.
10. Incubate the slides in anti-human DWNN dilution 1:4000 (Optimised) prepared in TBST3%BSA. Incubate at 4°C overnight in a humid chamber (Hybaid Ltd., UK).
11. Wash the slides in TBST1%BSA for 2 min.
12. Apply a biotinylated antibody linker (DAKO, Denmark) on each slide and incubate for 15 min at room temperature.

13. Wash the slides in TBST1%BSA for 2 min room temperature.
14. Apply the secondary anti-rabbit IgG-conjugated with horse radish peroxidase (HRP) [DAKO, Denmark] and incubate at room temperature for 15 min.
15. Wash the slides with TBST1%BSA for 5 min.
16. Prepare the chromogen substrate according to the manufacturer's instructions (DAKO, Denmark). Apply the chromogen preparation on each slide.
17. Allow a colour change to develop for approximately 30 seconds and immediately immerse in water.
18. Counterstain the slides with Mayer's haematoxylin for 10 min and wash in tap for 5 min.
19. Dehydrate the slides in 70%, 95% and 100% ethanol for 1 min in each.
20. Clear the slides in xylene for 1 min X2.
21. Mount the slides in Entellan (Merck, USA) and allow to completely dry.
22. Examine the slides under the Axioplan 2 imaging system (Zeiss, Germany)
23. Store the mounted slides in the dark for further referencing.

**Schedule 3: Promega SV DNA gel purification kit**

1. Perform 0.8% agarose gel electrophoresis on the linearized clone.
2. Cut the linearized DNA with a sterile blade and transfer it into a 1.5 ml micro-centrifuge tube.
3. Dissolve the gel slice in Membrane Binding Solution (Promega Corp., USA) [10µl Membrane Binding Solution for each 10 mg of the gel slice].
4. Incubate the gel slice in Membrane Binding Solution at 65°C for 10 min with occasional mixing until the gel has completely dissolved.
5. Transfer the dissolved gel mix onto the SV mini-column-collection tube assemble (Promega Corp., USA) and incubate at room temperature for 1 min.
6. Centrifuge at 4480 x g for 1 min. Remove the mini-column and discard the flow through. Re-assemble the SV mini-column-collection tubes assemble.
7. Wash the SV mini-column with 700 µl Membrane Wash Solution (Promega Corp., USA). Centrifuge at 4480 x g for 1 min.
8. Repeat the wash with 500 µl Membrane Binding Solution and centrifuge at 4480 x g for 5 min.
9. Transfer the mini-column carefully to a 1.5 ml micro-centrifuge tube.
10. Add 65 µl Nuclease-free DEPC treated water onto the centre of the mini-column. Incubate for 1 min.
11. Centrifuge at room temperature at 4480 x g for 1 min.
12. Discard the SV mini-column and quantify the DNA spectrophotometrically and store for labelling a later stage.

**Schedule 4: Estimation of the concentration of the probes**

1. Mark the spot points light with pencil on the nylon membrane (Hybond, Amersham, USA).
2. Spot 1 µl of each dilution onto the membrane and allow to dry for 10 min.
3. Fix the probes on the membrane by placing the membrane under UV light for 5 min.
4. Wash the membrane with 1X Washing Buffer (Roche Diagnostics, Germany) on a shaker for 5 min.
5. Incubate the membrane in 1X Blocking Buffer (Roche Diagnostics, Germany) while shaking for 30 min.
6. Incubate the membrane in Anti-DIG-Alkaline Phosphatase (Roche Diagnostics, Germany) diluted 1:10 000 in 1X Blocking Buffer for 30 min. Make sure that the membrane is covered.
7. Wash twice with 1X Washing buffer while shaking for 15 min each.
8. Immerse the membrane in 1X Detection buffer (Roche Diagnostics, Germany) for 2 min while shaking.
9. Immerse the membrane in NBT/BCIP (Roche Diagnostics, Germany) diluted 1:50 and develop in the dark overnight.
10. Terminate the reaction in 1X TE buffer (pH 8.0) for 5 min while shaking.
11. Air-dry the membrane and estimate the probe concentrations from the known DIG-labelled control RNA probe concentrations by comparing the intensities of the developed colour spots on the membrane.

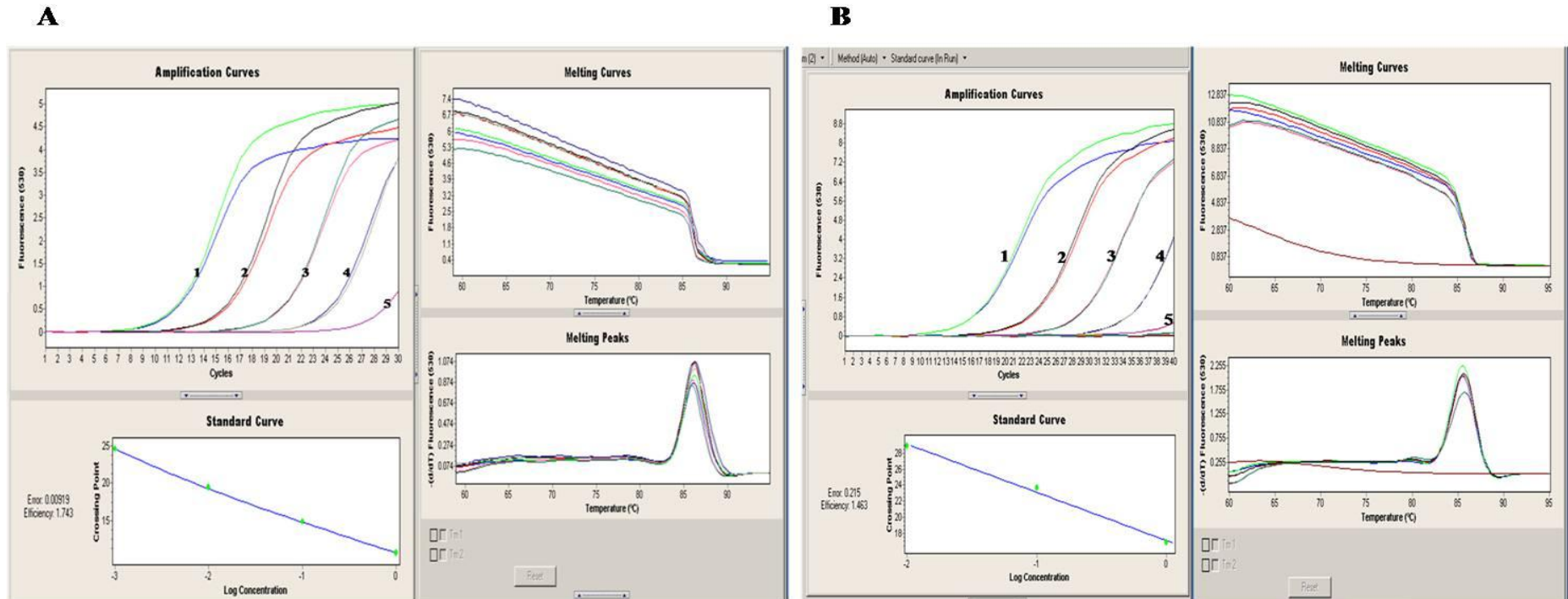
**Schedule 5: *In situ* hybridization treatments: Pre-hybridization treatment**

1. Dewax the tissue array slides in clean xylene (Merck) for 30 min (3 changes of 10 min).
2. Rehydrate the tissues in fresh absolute ethanol for 6 min (2 changes of 3 min each) at room temperature (RT).
3. Further rehydrate the tissues in 90%, 70%, 50% and DEPC treated water for 3 min in each solution at RT.
4. Fix the tissues in freshly prepared 4% paraformaldehyde for 20 min at RT.
5. Denature the proteins in 0.1M HCl for 10 min at RT.
6. Rinse three times in fresh TBS for 1 min at RT.
7. Limit non-specific labelling with freshly prepared 0.5% Acetic anhydride in 100 mM Tris pH 8.0 for 10 min at RT.
8. Rinse in TBS three time for 1 min for each rinse.
9. Permeabilize the cell membranes using 20 µg/µl Proteinase K (Roche Diagnostics, Germany) prepared in TBS for 20 min at RT
10. Rinse the tissues for 1 min 3 times in TBS.
11. Terminate the Proteinase K activity by immersing the slides in chilled TBS for 5 min at 4 °C.
12. Dehydrate the tissues in 50%, 70%, and 90% ethanol for 1 min in each solution.
13. Dehydrate the tissues in 100% ethanol for 2 min (2 changes of 1 min each).
14. Dry the tissues in chloroform for 10 min on the fume hood.
15. Tissues can be stored in a dust-free slide box in the dark and probed at a convenient time or probed immediately.

**Schedule 6: Post-hybridization washes and detection of bound probes**

1. After hybridization, remove the slides from the human chamber and discard the excess probe.
2. Wash off the un-bound probe in 2X SSC for 30 min at 37 °C in the hybridization oven (Biosystems, USA)
3. Wash in 2X SSC, 1X SSC, 0.1X SSC at 55 °C for 20 min in each.
4. Rinse the slides in TBS for 3 min (3 changes of 1 min each) at RT.
5. Block non-specific binding using 1X blocking buffer (Roche Diagnostics) in the humid chamber for 2 hours.
6. Incubate the slides with anti-DIG IgG conjugated with alkaline phosphatase (Roche Diagnostics, Germany) diluted 1:500 in 1X blocking buffer. Incubate for 1 hour at RT.
7. Rinse the slides in TBS for 3 min (3 changes of 1 min each) at RT.
8. Incubate the slides with the chromogen; NBT/BCIP (Roche Diagnostics, Germany) diluted 1:50 in detection buffer (Roche Diagnostics, Germany).
9. Develop in the dark humid chamber overnight at RT.
10. Stop the reaction in 1XTE for 5 min at RT.
11. Wash the slides in tap water for 5 min at RT.
12. Counterstain with Mayer's Haematoxylin at RT for 5 min.
13. Wash the slides in tap water for 10 min.
14. Mount the slides with permanent aqueous mounting medium (Serotec, UK).
15. Dry the mounted-slides and view them under the light microscope.

Appendix I: hHPRT1 and DWNN standard curve constructed with dilutions made from a Hek 293T cDNA



**hHPRT1 and DWNN standard curve constructed with dilutions made from a Hek 293T cDNA:** Appendix I demonstrates a good PCR amplification by the house-keeping genes, in this case a hHPRT1 primer pair. The Hek 293T cDNA was diluted (1 is 1:10, 2 is 1:100, 3 is 1:1000, 4 is 1:10000 and 5 is 1:100000) to construct the hHPRT1 standard curve. The melting curves on the right show that only one product was amplified. Figure 6.5B shows the efficiency and the melting point of the DWNN primers. Different dilutions (1-1:10; 2-1:100; 3-1:1000; 4-1:10000 and 5-1:100000) were made from the Hek 293T cDNA.

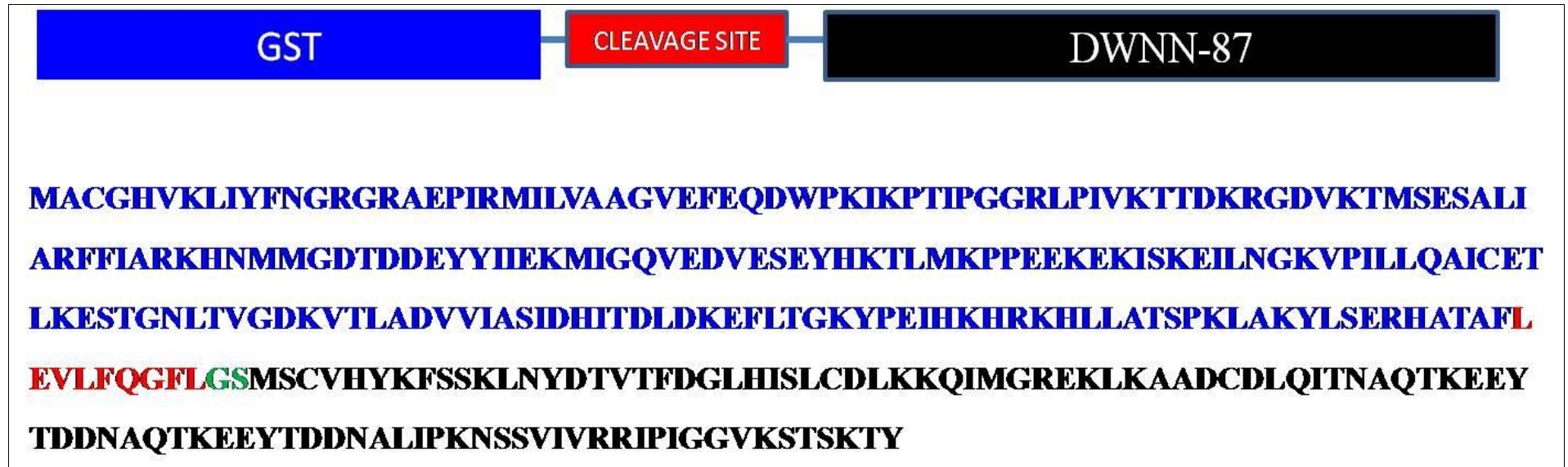
**Table 15: Relative expression of DWNN normalized using hHPRT1.**

Cell lines	DWNN Av Ct	hHPRT1 Av Ct	Delta Ct	Relative expression
Hek 293T	23	15	-8	0.0039
MCF-7	35	15	-20	$9.5 \times 10^{-7}$
HeLa	31	14	-17	$7.6 \times 10^{-6}$
HepG2	30	14	-16	$1.53 \times 10^{-5}$
Jurkats	18	15	-3	0.125
WHCO	30	15	-14	$1.53 \times 10^{-5}$

**Table 16: Relative expression of RBBP6 normalized using hHPRT1.**

Cell lines	RBBP6 Av Ct	hHPRT1 Av Ct	Delta Ct	Relative expression
Hek 293T	33	15	-18	$3.8 \times 10^{-6}$
MCF-7	42	15	-27	$7.5 \times 10^{-9}$
HeLa	40	14	-26	$1.4 \times 10^{-8}$
HepG2	40	14	-26	$1.4 \times 10^{-8}$
Jurkats	28	15	-13	$1.2 \times 10^{-4}$
WHCO	40	15	-25	$2.9 \times 10^{-8}$

Appendix J: The GST-DWNN construct, an antigen for the generation of Anti-human DWNN antibody



The GST-DWNN construct, an antigen for the generation of anti-Human DWNN antibody: This figure shows the antigen that was used for immunization for anti-Human DWNN antibody production. The GST (Blue) can be cleaved from the DWNN -87 (Black) by using a 3C protease recognition site (Red) between the two proteins.

**Appendix K: Sequence alignment of RBBP6 domains versus reference sequence (NM006910)**

**RING finger T7**

Score = 556 bits (301), Expect = 1e-155  
 Identities = 301/301 (100%), Gaps = 0/301 (0%)  
 Strand=Plus/Minus

```

Query 96  ACTGTTTTCGTAGTCTTTTGTATAGCCAGTTTCATTTTTGAAGTTATTTACAGCCTGTC 155
          |||
Sbjct 2046 ACTGTTTTCGTAGTCTTTTGTATAGCCAGTTTCATTTTTGAAGTTATTTACAGCCTGTC 1987

Query 156  GTAAAAATTTATTGGCAATTAAGCATCAGGAGAAACATCATTTTGATGACACGTCGGAC 215
          |||
Sbjct 1986  GTAAAAATTTATTGGCAATTAAGCATCAGGAGAAACATCATTTTGATGACACGTCGGAC 1927

Query 216  ATGTGTGCTCATCTGATTCAGGAGTGTCTTCTTATACATTCATCACAGTAACTGTTTC 275
          |||
Sbjct 1926  ATGTGTGCTCATCTGATTCAGGAGTGTCTTCTTATACATTCATCACAGTAACTGTTTC 1867

Query 276  CACAGCAGGGAATCACAAACAGCATCAGTCATAATATCCTTGCAGATGAGACACAACAATT 335
          |||
Sbjct 1866  CACAGCAGGGAATCACAAACAGCATCAGTCATAATATCCTTGCAGATGAGACACAACAATT 1807

Query 336  CATCTGGGATAGGATCATCTTCTTCTGAGGAAGAAGATGGCTCCTCTGTTAAGAAGGGAG 395
          |||
Sbjct 1806  CATCTGGGATAGGATCATCTTCTTCTGAGGAAGAAGATGGCTCCTCTGTTAAGAAGGGAG 1747

Query 396  G 396
          |
Sbjct 1746  G 1746
    
```

**RING finger Sp6**

Score = 556 bits (301), Expect = 6e-156  
 Identities = 301/301 (100%), Gaps = 0/301 (0%)  
 Strand=Plus/Plus

```

Query 87  CCTCCCTTCTTACCAGAGGAGCCATCTTCTCCTCAGAAGAAGATGATCCTATCCCAGAT 146
          |||
Sbjct 1746  CCTCCCTTCTTACCAGAGGAGCCATCTTCTCCTCAGAAGAAGATGATCCTATCCCAGAT 1805

Query 147  GAATTGTTGTGTCATCTGCAAGGATATTATGACTGATGCTGTTGTGATTCCCTGCTGT 206
          |||
Sbjct 1806  GAATTGTTGTGTCATCTGCAAGGATATTATGACTGATGCTGTTGTGATTCCCTGCTGT 1865

Query 207  GGAAACAGTTACTGTGATGAATGTATAAGAACAGCACTCCTGGAATCAGATGAGCACACA 266
          |||
Sbjct 1866  GGAAACAGTTACTGTGATGAATGTATAAGAACAGCACTCCTGGAATCAGATGAGCACACA 1925

Query 267  TGTCCGACGTGTCATCAAATGATGTTTCTCCTGATGCTTTAATTGCCAATAAATTTTTA 326
          |||
Sbjct 1926  TGTCCGACGTGTCATCAAATGATGTTTCTCCTGATGCTTTAATTGCCAATAAATTTTTA 1985

Query 327  CGACAGGCTGTAATAACTTCAAAAATGAACTGGCTATACAAAAAGACTACGAAAACAG 386
          |||
Sbjct 1986  CGACAGGCTGTAATAACTTCAAAAATGAACTGGCTATACAAAAAGACTACGAAAACAG 2045

Query 387  T 387
          |
Sbjct 2046  T 2046
    
```

This sequence alignments of the T7/Sp6 generated sequences from MCF-7 against the reference sequence for the sequenced RING finger domain coding region of the RbBP6 gene. It is a representation of the RING finger domain sequences from the human cancer cell lines.



**p53BD Sp6**

Score = 1243 bits (673), Expect = 0.0  
 Identities = 673/673 (100%), Gaps = 0/673 (0%)  
 Strand=Plus/Plus

Query	88	CAGCACCTCAGCCAGAGAAAAGAGAGTAATTTGGACCGCTCTGAATGAACAAGGAAATTTTAA	147
Sbjct	5201	CAGCACCTCAGCCAGAGAAAAGAGAGTAATTTGGACCGCTCTGAATGAACAAGGAAATTTTAA	5260
Query	148	AAGTCTGTCTCAATCTTCCAAAGAGGCTAGAACGTCAGATAAACATGATTCCTACTCGTGC	207
Sbjct	5261	AAGTCTGTCTCAATCTTCCAAAGAGGCTAGAACGTCAGATAAACATGATTCCTACTCGTGC	5320
Query	208	TTCTCAAATAAAGACTTCACTCCCAATGAGACAAAAAACTGACTATGACACCAGAGA	267
Sbjct	5321	TTCTCAAATAAAGACTTCACTCCCAATGAGACAAAAAACTGACTATGACACCAGAGA	5380
Query	268	GTATTCAAAGTTCCAAACGTAGAGATGAAAAGAAATGAATTAACAAGACGAAAAGACTCTCC	327
Sbjct	5381	GTATTCAAAGTTCCAAACGTAGAGATGAAAAGAAATGAATTAACAAGACGAAAAGACTCTCC	5440
Query	328	TTCTCGGAATAAAGATTCTGCATCTGGACAGAAAAATAAACCAAGGGAAGAGAGAGATTT	387
Sbjct	5441	TTCTCGGAATAAAGATTCTGCATCTGGACAGAAAAATAAACCAAGGGAAGAGAGAGATTT	5500
Query	388	GCCTAAAAAGGAAACAGGAGATTCCAAAAAAGTAATTC TAGTCCCTCAAGAGACAGAAA	447
Sbjct	5501	GCCTAAAAAGGAAACAGGAGATTCCAAAAAAGTAATTC TAGTCCCTCAAGAGACAGAAA	5560
Query	448	ACCTCATGATCACAAAGCCACTTATGATACTAAACGGCCAAATGAAGAGACAAAACTGT	507
Sbjct	5561	ACCTCATGATCACAAAGCCACTTATGATACTAAACGGCCAAATGAAGAGACAAAACTGT	5620
Query	508	AGATAAAAATCCTTGTAGGATCGTGAGAAGCATGTATTAGAAGCAAGGAACAATAAAGA	567
Sbjct	5621	AGATAAAAATCCTTGTAGGATCGTGAGAAGCATGTATTAGAAGCAAGGAACAATAAAGA	5680
Query	568	GTCAAAGTGGCAATAAACTACTTTATATACTTAAACCCACCAGAGACACAGGTTGAAAAAGA	627
Sbjct	5681	GTCAAAGTGGCAATAAACTACTTTATATACTTAAACCCACCAGAGACACAGGTTGAAAAAGA	5740
Query	628	GCAAATTAAGTGGGCAAAATTGACAAGAGTACTGTCAAGCCTAAACCCAGTTAAGTCATTC	687
Sbjct	5741	GCAAATTAAGTGGGCAAAATTGACAAGAGTACTGTCAAGCCTAAACCCAGTTAAGTCATTC	5800
Query	688	CTCTAGACTTTCCCTCTGACTTAACTAGAGAAACTGATGAAGCTGCTTTTGAACCAGACTA	747
Sbjct	5801	CTCTAGACTTTCCCTCTGACTTAACTAGAGAAACTGATGAAGCTGCTTTTGAACCAGACTA	5860
Query	748	TAATGAAAGTGAC 760	
Sbjct	5861	TAATGAAAGTGAC 5873	

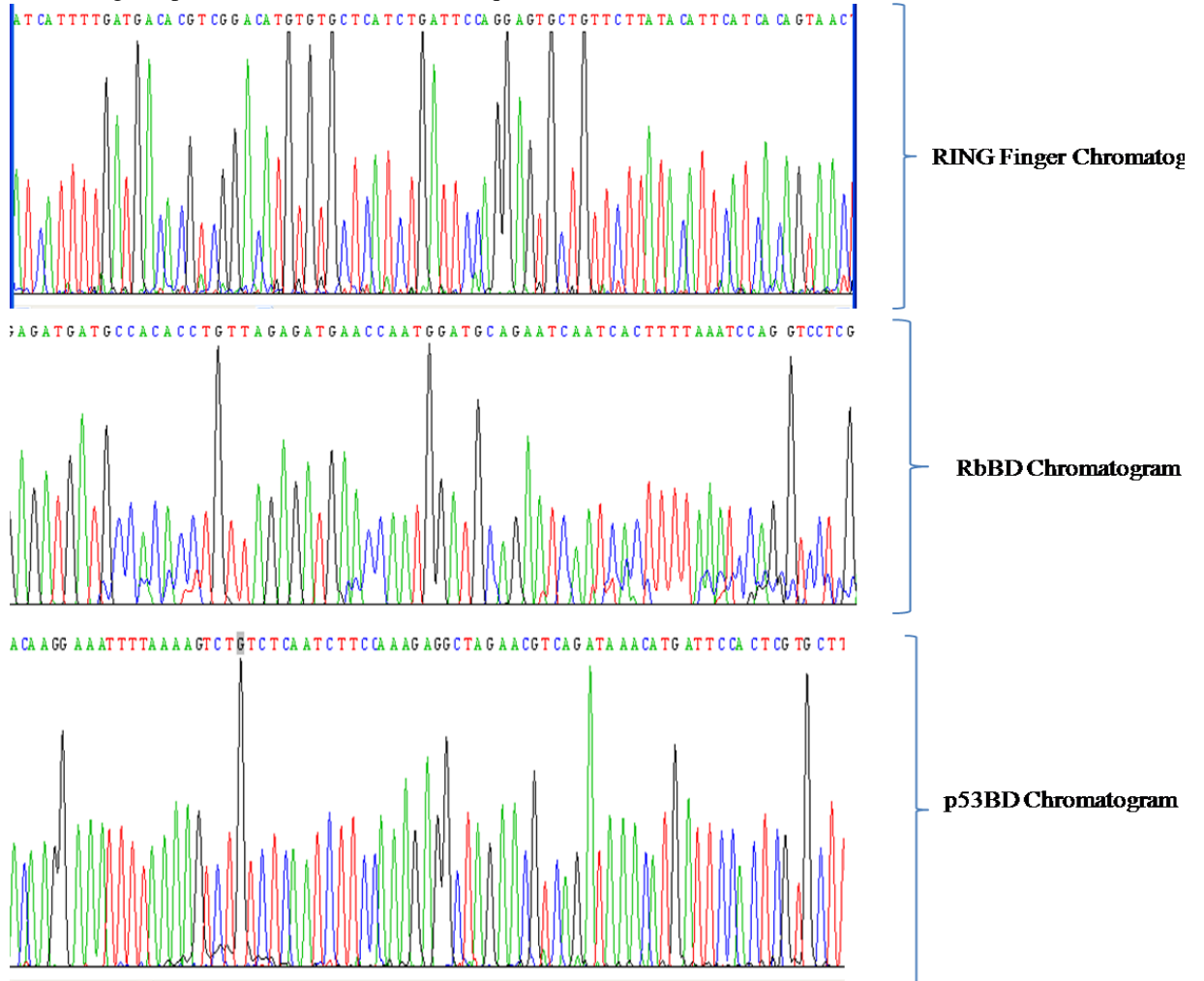
**p53BDT7**

Score = 1240 bits (671), Expect = 0.0  
 Identities = 673/674 (99%), Gaps = 0/674 (0%)  
 Strand=Plus/Minus

Query	66	GCTGTCCTGACTTTCTGCTGAGCTGGCACTGCTACTGTGGCTTCGGGCTTCGGCTTCCAGA	125
Sbjct	6116	GCTGTCCTGACTTTCTGCTGAGCTGGCACTGCTACTGTGGCTTCGGGCTTCGGCTTCCAGA	6057
Query	126	AGGACTGTGGCTTCTGCTGGGGCTGACCGCTGGGGCTGCTGTGGCTCTGATTCCTGCTTAT	185
Sbjct	6056	AGGACTGTGGCTTCTGCTGGGGCTGACCGCTGGGGCTGCTGTGGCTCTGATTCCTGCTTAT	5997
Query	186	GCCCACCTGGACAACCTGCTGCTGTGTCCAGGCTCTCTTTTCGCTTTCTCCACTATTTTATC	245
Sbjct	5996	GCCCACCTGGACAACCTGCTGCTGTGTCCAGGCTCTCTTTTCGCTTTCTCCACTATTTTATC	5937
Query	246	TTTCAGGTCCTTAGAAAATGTTTCTGAAAGATTCTCTTTTACAGAAACATTACTTTC	305
Sbjct	5936	TTTCAGGTCCTTAGAAAATGTTTCTGAAAGATTCTCTTTTACAGAAACATTACTTTC	5877
Query	306	ACTGTCACCTTTCATTATAGTCTGGTTCAAAAGCAGCTTCATCAGTTTCTCTAGTAAAGTC	365
Sbjct	5876	ACTGTCACCTTTCATTATAGTCTGGTTCAAAAGCAGCTTCATCAGTTTCTCTAGTAAAGTC	5817
Query	366	AGAGGAAAGTCTAGAGGAATGACTTAACTGGGGTTTAGGCTTGACAGTACTCTTGTCAT	425
Sbjct	5816	AGAGGAAAGTCTAGAGGAATGACTTAACTGGGGTTTAGGCTTGACAGTACTCTTGTCAT	5757
Query	426	TTGCCAGTAATTTGCTCTTTTCAACCTGTCTCTGGTGGGTAAAGTATATAAAGTAG	485
Sbjct	5756	TTGCCAGTAATTTGCTCTTTTCAACCTGTCTCTGGTGGGTAAAGTATATAAAGTAG	5697
Query	486	TTTATTGCCACTTGACTCTTTATTGTTCCTTGCTTCTAATACATGCTTCTCACGATCCTT	545
Sbjct	5696	TTTATTGCCACTTGACTCTTTATTGTTCCTTGCTTCTAATACATGCTTCTCACGATCCTT	5637
Query	546	ACAAGGATTTTTATCTACAGATTTTGTCTCTTCATTGGCCGTTTAGTATCATAAGTGGC	605
Sbjct	5636	ACAAGGATTTTTATCTACAGATTTTGTCTCTTCATTGGCCGTTTAGTATCATAAGTGGC	5577
Query	606	TTTGTGATCATGAGGTTTCTGTCTCTTGAGGGACTAGAATTACTTTTTTTGGAATCTCC	665
Sbjct	5576	TTTGTGATCATGAGGTTTCTGTCTCTTGAGGGACTAGAATTACTTTTTTTGGAATCTCC	5517
Query	666	TGTTCCTTTTTAGGCAAACTCTCTCTTCCCTTGTTTATTTTCTGTCCAGATGCAGA	725
Sbjct	5516	TGTTCCTTTTTAGGCAAACTCTCTCTTCCCTTGTTTATTTTCTGTCCAGATGCAGA	5457
Query	726	ATCTTTATTCCGAG 739	
Sbjct	5456	ATCTTTATTCCGAG 5443	

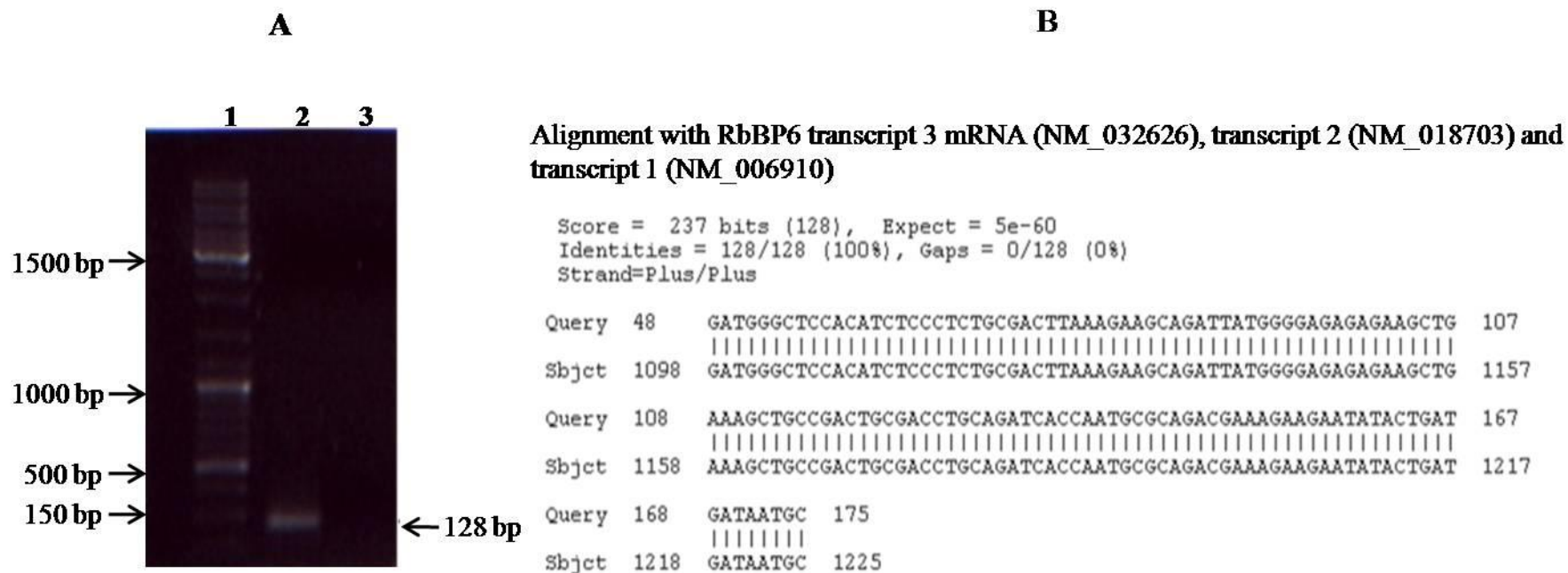
This sequence alignments of the T7/Sp6 generated sequences from MCF-7 against the reference sequence for the sequenced p53BD domain coding region of the RbBP6 gene. It is a representation of the p53BD domain sequences from the human cancer cell lines.

Chromatogram presentation of the resultant sequences



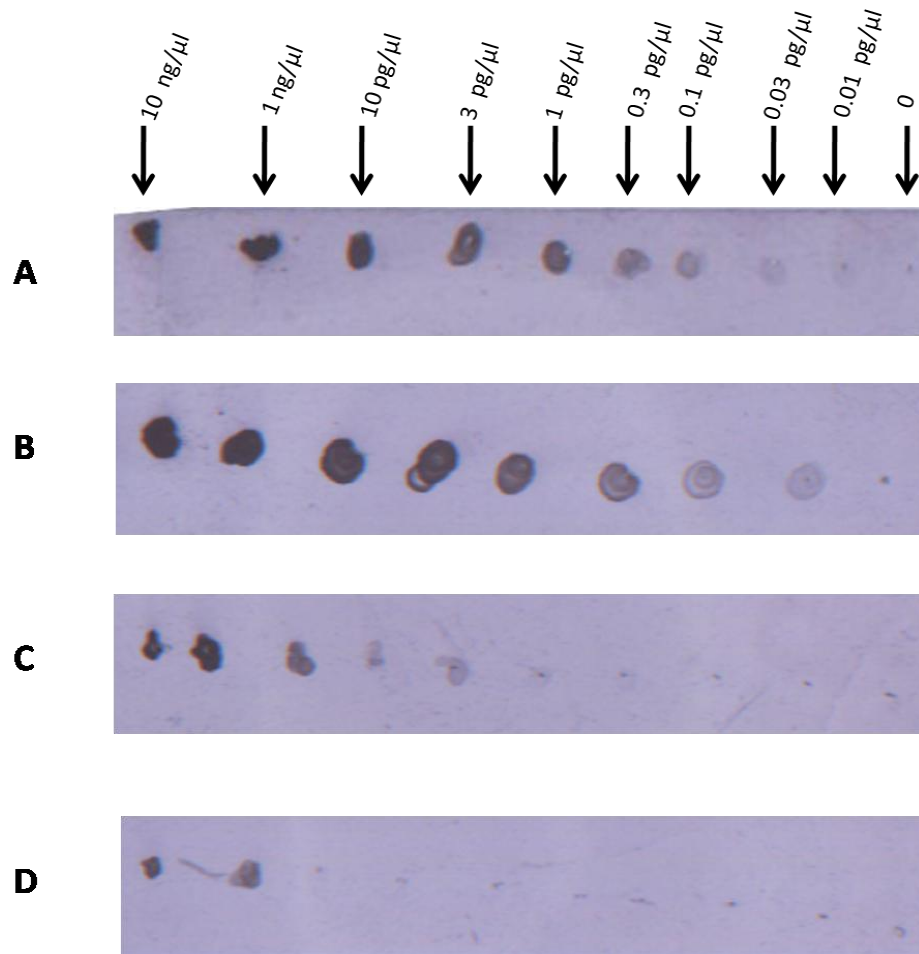
**Chromatograms from sequences of different RBBP6 domains:** The sequences obtained were edited according to chromatographic picks (e.g. G was not called and was added in the p53BD sequence) and the final sequence was then used to determine any alterations in the clones from different cancers.

Appendix L1 An amplified DWNN fragment for probe labelling and sequence analysis



**An amplified DWNN fragment for probe labelling and sequence analysis:** (A) shows a fragment that was amplified for probe synthesis. A 128 bp fragment was amplified (lane 2), cloned and sequenced before labelling. Lane 3 represents a negative control (reaction with no template DNA). The obtained sequence gave 100% identity to all RBBP6 transcripts (B).

**Appendix L2 - Dot plots for the estimation of the labelled probe concentrations**

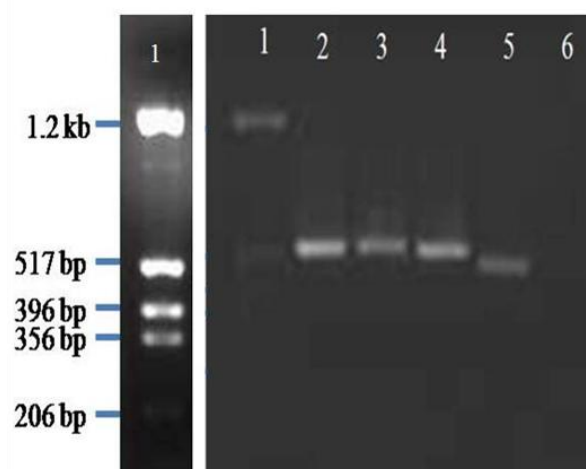


**Dot plots for the estimation of the labelled probe concentrations:** The figure shows the control labelled RNA of known concentrations (Panel A) used for estimating the concentration of labelled probes. The figure demonstrates successful labelling of the RNA probe (B-labelled control RNA; C-labelled DWNN antisense RNA probe and D- labelled DWNN sense RNA probe).

Panel A shows a comparison of the labelled RNA (Roche Diagnostic, Germany) to labelled control RNA (Panel B), the DWNN antisense probe (Panel C) and sense probe (Panel D). The lowest dilution of the antisense probe that could be detected was found to be 0.1 pg/μl when compared to the labelled RNA, while the lowest dilution for the sense probe was determined to be 0.3 pg/μl. This figure also demonstrates that the labelling was successful.

**Appendix M: Summary of the results for the Column Analysis**

Table Analyzed	Data 1		
Repeated Measures ANOVA			
P value	P<0.0001		
P value summary	***		
Are means signif. different? (P < 0.05)	Yes		
Number of groups	18		
F	146.2		
R squared	0.9865		
Was the pairing significantly effective?			
R squared	0.00001817		
F	0.02288		
P value	0.9774		
P value summary	ns		
Is there significant matching? (P < 0.05)	No		
ANOVA Table			
	SS	df	MS
Treatment (between columns)	6034	17	354.9
Individual (between rows)	0.1111	2	0.05556
Residual (random)	82.56	34	2.428
Total	6116	53	
Post test for linear trend			
Slope	0.2822		
R squared	0.07573		
P value	P<0.0001		
P value summary	***		
Is linear trend significant (P < 0.05)?	Yes		
Column analysis showed significance for mean differences (P<0.0001) and linear trend in Post test linear test (P<0.05).			

**Appendix O: Real-time PCR analysis**

Confirmation of RNAi constructs by PCR. These constructs were also sequenced to further confirm their identities. Figure shows PCR products of 517 bp fragments from the amplification of RNAi plasmid DNA inserts (Lanes 2-4), a smaller PCR fragment for from the RNAi vector only control (pU6GFP) [Lane 5] and a negative control (PCR reaction with no template DNA, replaced with sterile distilled water) [lane 6].

**Table 17: Relative knockdown of RBBP6 mRNAs normalized to hHPRT1 expression.**

Untransfected 293T (DWNN primers)	0.000513±1.2X10 <sup>-5</sup>
Vector transfected 293T (DWNN primers)	0.00052±2X10 <sup>-5</sup>
DWNN RNAi transfected 293T (DWNN primers)	0.0000157±1X10 <sup>-5</sup>
Untransfected 293T (RBBP6 primers)	0.000064±3.52X10 <sup>-5</sup>
Vector transfected 293T (RBBP6 primers)	0.000061±9.0310 <sup>-6</sup>
RBBP6 RNAi transfected 293T (RBBP6 primers)	0.000012±1X10 <sup>-6</sup>